The Development of Smart-Bandage Technologies

Duncan Sharp

A thesis submitted in partial fulfilment of the requirements of Nottingham Trent University for the degree of Doctor of Philosophy

November 2009

Declaration

Acknowledgements

I would like to take this opportunity to thank all the people who have provided help and support throughout the duration of my studies at Nottingham Trent University. I express my gratitude to my project supervisor Dr James Davis for his continual support, expertise, inspiration and guidance. I also thank my second supervisor Prof. Stephen Forsythe for his guidance and supervision. I would like to thank the members of the research group, Maria Marti Villalba and Laura Newton, and Dr Robert Smith for their help, support and friendship. Finally, I wish to express my sincere thanks to my parents, brother, friends and everyone close to me for their relentless belief, support and encouragement.

Abstract

Healthcare associated infections of wound sites are a complex problem with substantial effects on patient morbidity and financial ramifications to healthcare bodies. The increasing interest in novel diagnostic strategies and preventing infections have led to an incursion of research into the topic. Whilst most emphasis has been placed on preventing wound infections, the bacterial flora is an ever present risk to the compromised host. In contrast with the majority of research developing antibacterial smart-dressings, the research detailed within describes the development of *in-situ* electrochemical sensor assemblies suitable for incorporation within traditional or 'smart' wound dressings. Sensor developments have led to prototype construction of a multitude of sensing substrates capable of quantitative analyses for the identification of infection. The key developments contained within highlight both generic and organism-specific sensors which can reliably monitor key chemical components of a wound exudate to allow sampling-free infection diagnostics. The target biomarkers of pH, urate and pyocyanin have been chosen and measurements attained using novel, small and flexible carbon-based substrates to form chemical-free electrodes - thereby removing the risk of chemical leaching into the wound environment. The ability to monitor pH using chemical-free carbon miniaturized electrodes is both innovative and of widespread commercial interest within woundcare and therefore subject to patent approval. Novel sensors to detect pyocyanin, produced specifically by *Ps. aeruginosa* have allowed accurate and precise measurements of pyocyanin at physiologically relevant concentrations and are suggested for the specific diagnosis of *Ps. aeruginosa* wound infections. To enable the reliable use of these sensing systems *in situ* advances in antibacterial sensor coatings have also been targeted, culminating in the development of electrodes coated with a polymer of the natural product plumbagin. These are proven to aid the catalytic reduction of molecular oxygen to reactive intermediates with bactericidal activity. Developments contained within have made a substantial contribution to the scientific community, not only to sensor materials and interfaces, but also towards the real-life applicability of the sensing technologies as highlighted by the list of publications and conference presentations (**Appendices 1** and **2**, respectively).

Contents

Abbreviations

AA	Ascorbic Acid
AFM	Atomic Force Microscopy
ATP	Adenosine triphosphate
BPPG	Basal Plane Pyrolytic Graphite
BR	Britton-Robinson buffer
BSA	Bovine Serum Albumin
CA	Cellulose Acetate
cAMP	Cyclic adenosine monophosphate
CBF	Ciliary Beat Frequency
CE	Counter / Auxiliary electrode
CF	Carbon Fibre
CFib	Cystic Fibrosis
CSF	Cerebrospinal fluid
C_V	Coefficient of Variance
CV	Cyclic Voltammetry
DCM	Dichloromethane
DNA	Deoxyribonucleic acid#
DoH	Department of Health
DPBF	1,3-diphenylisobenzofuran
EPPG	Edge Plane Pyrolytic Graphite
FrT4	Free Thyroxine
FT3	Free Thiiodothyronine
GCE	Gassy Carbon Electrode
GC-MS	Gas Chromatography – Mass Spectrometry
GMP	Guanosine Monophosphate
GTP	Guanosine Triphosphate
HAI	Healthcare Associated Infection
HMDE	Hanging Mercury Drop Electrode
HOPG	Highly Orientated Pyrolytic Graphite
HPA	Health Protection Agency
HPLC	High Performance Liquid Chromatography
HSA	Human Serum Albumin
IEM	Inborn Error of Metabolism
IMP	Inositol Triphosphate
LSV	Linear Sweep Voltammetry
MRSA	Methicillin-Resistant Staphylococcus Aureus
NAD(P)H	Nicotinamide Adenine Dinucleotide Phosphate
NHS	National Health Service
NHS	National Health Service
PBS	Phosphate Buffered Saline
PCR	Polymerase-chain reaction
PDMA	Polymer of N-N-dimethylaniline

PKU	Phenylketonuria
PMS	Phenazine Methosulfate
PNP	Purin-Nucleosid-Phosphorylase
PoCT	Point of Care Testing
Poly-Trp	Polymeric deposit of Tryptophan oxidation
PPE	Pad Printed Electrode
PVP	Poly(4-vinylpyridine)
Pyo	Pyocyanin
QS	Quorum sensing
RBC	Red Blood Cells
RE	Reference Electrode
RNA	Ribonucleic acid
SAD	Seasonal Affective Disorder
SD	Standard Deviation
SEM	Scanning Electron Microscopy
SPE	Screen Printed Electrode
SqWV	Square Wave Voltammetry
SSI	Surgical Site Infection
TLC	Thin Layer Chromatography
TPP	Tetraphenyl porphyrin
Trp	Tryptophan
TSA	Tryptic Soya Agar
TSB	Tryptic Soya Broth
TSH	Thyroid Stimulating Hormone
Tyr	Tyrosine
UA	Uric Acid
UTI	Urinary Tract Infection
WE	Working Electrode
WHO	World Health Organisation
XMP	Xanthosine Monophosphate

Chapter 1

Why Smart Bandages?

Abstract

The prevalence of wound infections within healthcare environments has driven the necessity for technological advancements. This chapter introduces the problem of healthcare associated infections and those affecting wound sites. Key ramifications of such complications have instigated innovative approaches towards intelligent wound management through dressings to prevent and detect bacterial incursion. A variety of organisms are capable of causing the wound infections and the mechanisms of transformation from contamination to invasive colonization are detailed. This is of importance to fully understand the wound environment and metabolic processes to enable the development of sensor arrays that have real clinical benefits. Understanding the physiological changes anticipated during bacterial colonization has led to the identification of novel markers to be evaluated. The relevant and challenging advancements of wound dressing technology in modern medicine are assessed and the rationale for the novel use of electrochemical sensors for smart-bandage applications established.

1.0 *Introduction to Healthcare Associated Infections*

Healthcare associated infections (HAI) are typically defined as infections acquired whilst in hospital or as a result of medical interventions and are an ever present problem in modern healthcare. The surveillance and prevention of HAI is a key focus of many government bodies: Department of Health (DoH), Health Protection Agency (HPA) and World Health Organisation (WHO). There are substantial implications for healthcare providers and there is a near continuous revision and updating of guidelines and regulations in an effort to reduce the impact, both on morbidity and bottom line financial costs. Standard guidelines issued by the health regulatory bodies outline the essential, good practice, principles to be followed by healthcare staff to help reduce the occurrence of HAI. Four distinct interventions have been described involving: hospital environment hygiene, hand hygiene, the use of personal protective equipment and the use and disposal of sharps [1]. It has been estimated by the DoH and the European Centre for Disease Prevention and Control that with intensive hand and environmental hygiene that up to 30% of HAI could be preventable. While this is of key importance, hygienic governance can only go so far in protecting patients from infection.

A substantial factor in the prevention of HAI is that the sources of infection can be exogenous or endogenous in origin. Exogenous sources include those attributed to cross-infection, whereby the source is another person, and environmental infections, from e.g. contaminated equipment. It is these exogenous sources that form much of the preventable causes of infection. Endogenous sources result from self-contamination - typically from the presence of adventitious microbes on the patients own skin or from gastrointestinal or upper-respiratory flora. While bacteria from these sources may be carried by healthy individuals without causing infection, the compromised nature of most hospitalised patients may allow the progression from contamination to colonisation, thereby causing infection. As so many infections are caused by ‘non-preventable’ means, the early diagnosis and treatment of infections is key, not only regarding patient health and financial costs, but minimising the development of antibiotic resistant strains. The trends within HAI show an alarming increase in resistant strains and with the widespread use of antibiotics - this is expected to keep increasing until new therapies and technological approaches are established. HAI can affect many different sites of the body, typically the urinary

tract, respiratory tract, gastrointestinal tract and wound sites are described. Certain infection sites can be associated with specific medical procedures e.g. urinary tract infections (UTI) from urethral catheterisation, however the causes of many are less distinct.

1.1 Wound Infections

The rate of HAI relating to surgical wound management is currently around 10% [2,3]. The complications of infections not only affect patient mortality but are also an increasing financial burden, with costs to the UK NHS alone within the billion pound region [4]. In many cases, the origin is simply the colonisation of the wound by adventitious opportunistic bacteria such as *Pseudomonas aeruginosa* or *Staphylococcus aureus* [5-7] as a consequence of wound contamination. In the 1997-2005 Surgical Site Infection (SSI) study, 53% of SSIs were caused by *Staphylococcus aureus* and a staggering 64% of these infections were caused by methicillin-resistant *Staphylococcus aureus* (MRSA) strains [8]. Irrespective of the origin, there is a need for more intelligent approaches to wound management which can alert the clinical staff to the onset of bacterial colonisation of wound surfaces. Wounds can be differentiated into acute and chronic wound categories. An acute wound is typically classified as a direct and more immediate injury to the skin, and these may be in the form of a surgical incision, an accidental graze, puncture or cut or as a result of a thermal injury. Chronic and slow/non-healing wounds (e.g. diabetic ulcers and bed-sores) are at risk of infection due to their prolonged healing and account for some 10% of MRSA bacteriaemas [9]. However, any high surface area wound, especially within a compromised host, can facilitate the development of severe infections with potentially life-threatening complications. The moist, exudate-rich environment of a typical burn wound will also provide all the nutritional requirements for infection and further exacerbates the propensity for infection

Burn patients are especially susceptible to infection due to subsequent physiological changes leading to a compromised host. A burn induces increased microvascular permeability which allows fluid and protein to leak into the interstitial space which forms the wound exudate. This can cause potentially fatal hypovolaemia and associated hypotension, therefore large resuscitation fluid volumes of isotonic crystalloid solution are required to compensate for this fluid loss from the circulation

into the oedema as well as fluid loss though the wound and to combat the reduced tissue perfusion [10]. The wound may be debrided and topical antimicrobial treatments applied. Once the patient is stable, the wound may be excised and / or grafted to aid rapid healing [11]. The insufficient peripheral perfusion observed in burns is sufficient to alter cellular dynamics, during the aggressive fluid resuscitation this perfusion returns. This may be essential to cell survival but the reperfusion induces ROS generation which causes cellular damage associated with oxidative stress [11]. Due to the multitude of physiological stresses and the large surface area of wounds, burn patients are in effect ideal hosts for infection and so have become the primary target for the smart bandage development detailed in the subsequent chapters. It could be anticipated that the production of a ‘smart-bandage’ capable of monitoring and / or controlling bacterial colonisation would be ideal for the management of burns patients as after the initial resuscitation, up to 75% of mortality in burns patients is related to infection [12].

1.2 Current Diagnosis

The diagnosis of wound infections is a major problem for effective healthcare. While the existence of infection can often become obvious - identification of the main protagonist remains problematic. There is also the issues that while wound appearance can indicate an infection (yellow-pus or inflammation and redness around the wound), it only arises when an infection has become established and therefore such indicators are unsuitable for early infection diagnosis. Swabs and biopsies from the wound may be collected and sent to a centralised microbiology department for microbial analysis, primarily microscopy, culture and antibiotic sensitivity testing. This is far from ideal due to the necessary incubation time required to grow the organism(s) and will result in either guesswork by the clinician or the application of broad spectrum antibiotics in the intervening analysis time. The move towards molecular based techniques with analysers using PCR (Polymerase chain reaction) allows faster identification of certain organisms and although advances in both cost-effective and ward-based analysers are progressing they are liable to be prohibitively expensive for mainstream application. Even if such diagnostics become readily available, it does not address the problem that the wound would still need to be redressed and induces an extra wound procedure. The redressing of the wound not only offer an opportunity for yet further

wound contamination, but the disruption of the healing process. Moreover, it could be assumed that such in-ward diagnostics would only be suitable for inpatients and not outpatients or elderly patients under the care of care-home/hospice or district nurses. In addition, they only represent the actual area tested and therefore may not be able to differentiate between contamination and the more serious colonisation until the clinical features of an infection are observed. There is a distinct need to be able to determine the onset of colonisation and, ideally, permit direct *in situ* intervention that inhibits bacterial growth. This is the core rationale that underpins the current drive to develop smart bandage materials.

1.3 Bacterial Characteristics

Wound infections can be caused by a multitude of organisms but it is widely accepted that the majority of those arise due to opportunistic bacterial pathogens commonly found on the skin, but which can cause serious infections especially in a compromised host. The skin is essentially the first line of defence against bacteria but once the integrity of the barrier has been damaged, bacterial contamination can occur rapidly leading to infection and, if left unhindered, could ultimately lead to sepsis. Bacteria are principally classified into Gram positive and Gram negative organisms depending on their Gram staining properties. Gram positive bacteria stain purple as a result of the thick peptidoglycan cell wall retaining the crystal violet as indicated in **Figure 1.1**. The organisms are subsequently rinsed with an alcohol/acetone mixture that removes unbound stain, the near absence of the peptidoglycan layer in Gram negative cells prevents them from retaining the purple stain. They can however be counterstained pink/red, commonly by Safinin due to the extra outer membrane. Other cellular differences exist between the two Gram categories, but these are not important regarding their classification characteristics.

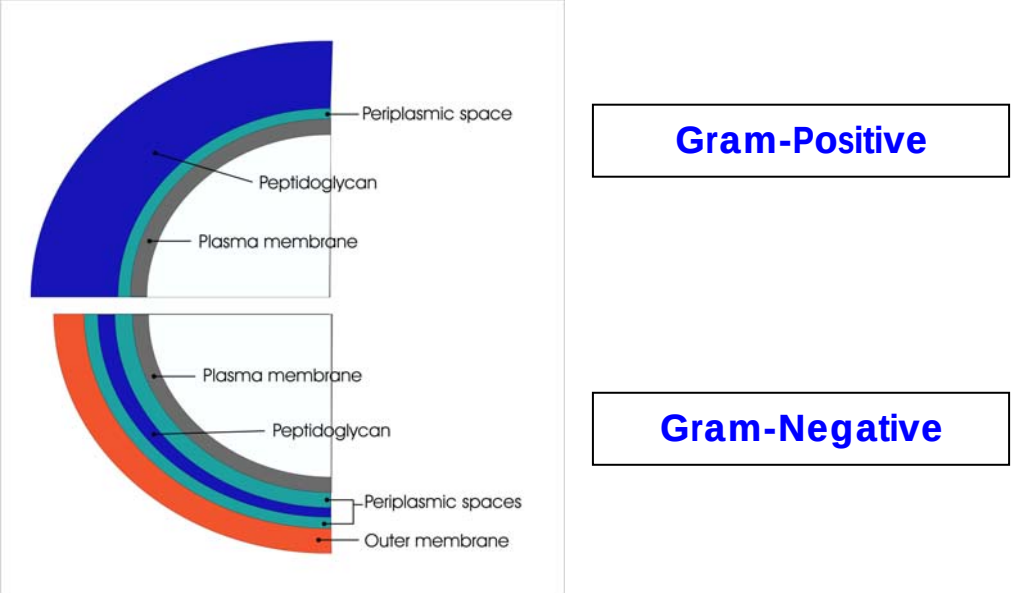

Figure 1.1. Cellular structure of Gram positive and negative bacteria

While HAI can be caused by a mixture of both Gram positive and Gram negative groups, the latter tend to be the predominant players. Examples of common pathogenic species include: *Staphylococcus aureus* (Gram positive) and *Escherichia coli*, *Pseudomonas aeruginosa* and *Klebsiella pneumonia* which are all Gram negatives. These can be responsible for wound infections with antibiotic resistant strains causing widespread problems in healthcare. Pathogenic *Ps. aeruginosa* is the most prolific cause of burns infection [13] and is of major concern given the increasing ability of such species to develop resistance to many chemotherapeutic drugs. As a consequence of the frequent complication of antibiotic resistant, *Ps. aeruginosa* strains can rapidly spread throughout a burns unit [14]. Other common infectants of burns and superficial wounds include: streptococci, staphylococci and *E. coli* [12,13].

The skin provides the main barrier against infectious organisms so when the integrity of this barrier is compromised, it exposes the body to bacterial threats. Due to the abundance of microorganisms present on the skin, damage to this physical defence is likely to introduce bacteria (either immediately or through wound redressing) to the underlying tissue i.e. contamination. The immune system is capable of moping up small numbers of contaminant in a healthy individual but the compromised nature and potential severity of wound depth and size can limit the

efficiency, especially considering the vascular disruption in major traumas. The unsuccessful neutralisation of the contaminants within a nutritious and warm environment allows the bacterial to attach and grow to form stable colonies.

One of the initial signs of infection is inflammation, the body's response to trauma, whether physical, chemical or by infectious agents. The local release of inflammatory mediators (e.g. histamine, cytokines, leukotrienes) leads to inflammation, primarily by vasodilation, increased vascular permeability and cellular infiltration. This typically presents as redness, swelling, pain and heat, the immune system response to bacterial infiltration sequesters a multitude of leucocytes (importantly, neutrophils and macrophages) and the inflammation allows an enhanced supply of these to combat local infections. If the infection is not halted in time, either by the immune system or antibacterial therapeutics, a major problem can arise as the bacterial infection becomes invasive (dictated by the pathogenicity of the organism) and thereby spreads from a local environment to deeper tissue and the circulatory system, which may facilitate the potentially fatal systemic infection and inflammation associated with sepsis. As bacteria grow in a biofilm they are encapsulated in an exopolysaccharide, this enables them to stay adhered to the surface but also protects them from the external environment. They remain encapsulated until sufficient numbers are present - at which point some of the bacteria are released and disperse allowing the cycle to restart in more locations. The formation of a stable biofilm develops through five sequential steps [1]: 1. Initial attachment (via van der Waal forces), 2. Irreversible attachment (surface attachment by pili), 3. Maturation I, 4. Maturation II and 5. Dispersion, as highlighted in **Figure 1.2**:

Figure 1.2 Lifecycle of bacterial biofilm development

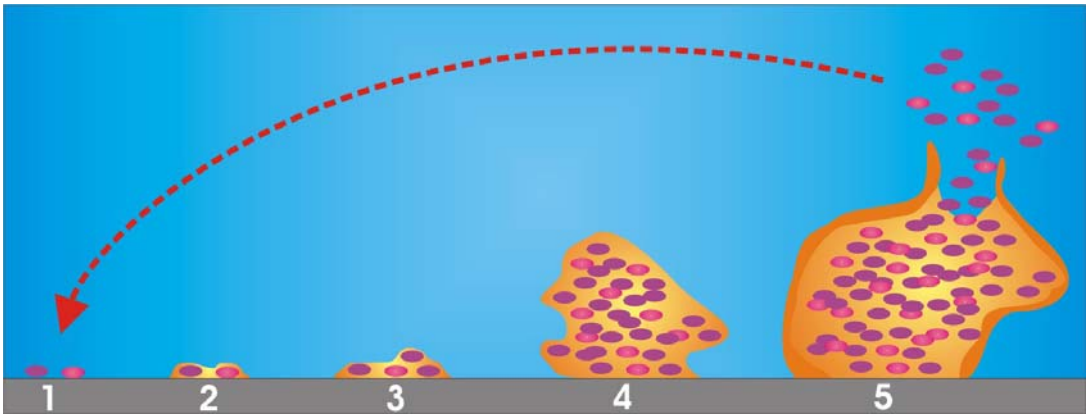

1.4 Advances in Wound Dressing Technologies

While current infection control drives and guidelines from government bodies are vital, technology has a vital part to play and there is a need for a more intelligent approach toward wound management. Recent advances in nano-particle science have seen the development of antibacterial dressings - frequently Silver based [16,17]. Nevertheless, the inherent adaptability of micro-organisms means that there remains a need for a failsafe system that can alert either the patient or healthcare professional to the advent of a potential infection. The detection of wound infections may be missed due to the short hospitalisation period following surgery and the increasing use of outpatient surgery, with the ability of the patient to identify a wound infection having been questioned [18]. This highlights an additional use for intelligent wound management in outpatient care and could potentially permit shorter hospital stays if improved patient care could be provided by more accurate wound monitoring and effective management for outpatients.

1.5 Intelligent Wound Management

The development of smart wound dressings and Point of Care Testing (PoCT) diagnostics for the identification of wound infections are of key concern within industry, with millions of pounds invested by companies, including: NanoEurope, D3 Technologies Ltd / ITI Techmedia [20-22]. Intelligent wound devices have been established to monitor the size and healing progression of a chronic wound but there has been very little published on the *in situ* detection of infection within wound environments. It could be envisaged that the development of an intelligent wound dressing encompassing sensors capable of accurately monitoring the wound conditions and which possesses the ability to actually detect the transition from harmless contamination to potentially fatal colonization would be of considerable clinical benefit for both ward application and decentralised use.

The ill-defined term ‘smart-bandage’ is continually evolving, but at present, can be regarded as a bandage which can assist wound healing, either directly or through providing information regarding the wound and/or health status of the patient. There are several types of ‘smart-bandage’ under development and include functions such as:

1. monitoring healing progression via size of the wound, particularly aimed towards chronic and non-healing wounds;
2. removing excessive constituents e.g. a bandage which removes excess elastase which hinders healing;
3. the detection of bacterial infection, currently by directly detecting bacteria [19] and
4. dressings that can deliver drugs, growth factors etc as required to aid healing.

However, the purpose of the present project was to develop analytical technologies to principally aid diagnosis of bacterial wound infection by detection of bacterial compounds and / or the subsequent wound biochemical factors. The majority of the progress in smart-bandage development over the past 5 years has focused upon chronic and non-healing wounds e.g. diabetic ulcers and bedsores and on other large surface area wounds e.g. burns wounds. As mentioned previously, these wounds have a high risk of infection due to their very nature and, as such, represent a major problem area for current health care practice and should be one in which the advent of smart-bandage technologies could play a vital role.

At the commencement of this research project the leading smart-bandage development to date centred on a system for detecting bacteria directly using molecular probes on Silicon microcavity technology allowing the identification of Gram negative bacteria via Lipid A molecules on the surface of the bacteria. In this instance – the binding interaction of specific bacteria with the silicon particles alters the optical properties of the latter (**Figure 1.3**) resulting in a luminescent colour shift which can be electronically detected [19]. The molecular probes and properties of the silicon beads are to be modified to allow the specific identification of key bacterial pathogens.

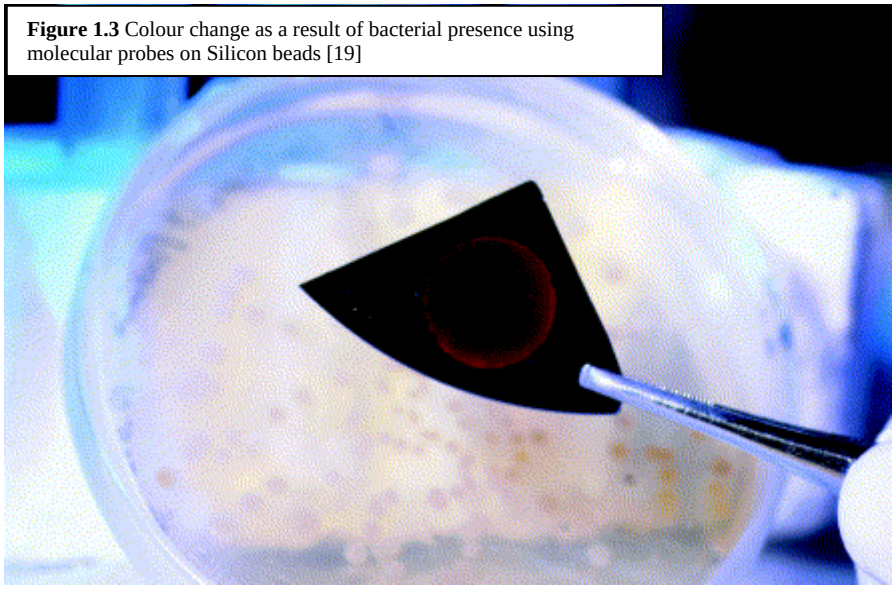

Figure 1.3 Colour change as a result of bacterial presence using molecular probes on Silicon beads [19]

As no quantitative capabilities have been outlined it could be anticipated that its application is very limited – all the more so given the need for laser illumination. It could be difficult to expect deployment of such technologies within a point of care context where non specialist staff are in attendance. There remains a need to monitor and differentiate between simple contamination and colonization / infection. The rationale adopted in this project rely on the sensitivity and inherent quantitative nature of electrochemistry to allow bacterial presence and growth monitoring. Importantly, these may allow the *in situ* assessment of the response to treatment, a crucial factor with the rapid and perturbing development of antibiotic resistant strains of two common wounds infectants: *S. aureus* and *Ps. aeruginosa*.

Electroanalytical techniques have a long history in facilitating biological monitoring both *in vivo* and *in vitro*. Ironically, early work involving electrochemistry and microbes sought to harness the metabolism of the latter as versatile sensors for a multitude of environmental agents [23-25]. Now, research has focused on targeting the byproduct of microbial metabolism as indicators of their presence. A recent approach has to target the volatile products of bacterial metabolism emanating from an infected would using various polymer coated interdigitated gold electrodes [26]. Although the idea of detecting such volatile compounds (e.g. ammonia, ethanol, butyric acid, dimethylsulfide) with regards wound infection is an established one (typically using laboratory based GC-MS, gas chromatography-mass spectrometry),

the *in situ* approach is novel. These two approaches highlight the core options available – direct detection of the bacteria or indirect detection through characteristic biochemical changes in the wound environment as a consequence of bacterial growth.

While the aforementioned devices are aimed at infection diagnostics, others have focused on monitoring the healing of a wound environment. These are particularly important for chronic and non-healing wounds. The moisture levels within a wound healing environment can have important influences on wound healing and a prototype bioimpedance based sensor array allowing moisture mapping inside a wound dressing has been developed [27]. Another approach has been to develop an immunosensor to allow the wound healing process to be monitored based on pH changes and the concentration of inflammatory proteins. In this instance, optical measurements are utilized as the diagnostic handle and recorded using a miniaturized spectrometer. This allowed the measurement of pH between 6 and 8 and C-reactive protein (an inflammatory response biomarker) from 1 to 100 μg/mL [28]. The biochemical approach towards wound assessment has also been studied through the measurement of total protein and albumin in chronic wound exudates as an indicator of wound healing [29] but relies upon sending the samples to a central clinical laboratory and uses conventional biochemical tests.

1.6 Biomedical Electrochemistry / Medical Implants

The use of electrochemistry for wound sensors is considered to be one of the more feasible methods due to the versatility of the sensor materials and the large variety of modifications and detection strategies available. In general, most biomedical devices utilizing electroanalytical detection rely upon a combination of modified electrode substrates and substrate selective catalysts to overcome the generic nature of bare / unmodified electrodes. This is typified by the glucose meters which almost invariably employ the enzyme glucose oxidase for specificity. In terms of Point of Care Testing (PoCT) diagnostics, this is an ideal approach to enhance the limited selectivity of many substrates in biological matrices. The use of such modified electrodes within a wound, at borderline *in vivo* level is a more challenging prospect due to the possible consequences that could arise upon device failure where leaching of the sensor components could occur (either with time or through electrode

mishandling/damage) and could have a potentially worse effect than the contamination it was originally designed to detect. The same is true for chemically modified electrodes, the chemicals must not leach or interact with host physiology and would be required to form a very stable polymer on the surface. Due to these factors the bio-compatibility of the sensor systems developed in the course of the project was a primary concern, therefore the analytical developments were limited to physical modification of the substrates so as to reduce the degradatory or inhibitory effects on systemic or local wound physiology of exogenous chemicals.

It is little surprise to find that the choice of sensor substrate is of major significance. The use of carbon substrates for working electrodes (e.g. glassy carbon electrodes and screen printed electrodes) are widespread throughout electrochemistry. The associated costs and preparative difficulty make many of these unsuitable for use in the cheap, disposable electrode-assembly sought. Carbon fibre matting or tow has been largely used throughout this research due to its low-cost, flexibility and easy manipulation. Moreover, carbon fibre electrodes have found a variety of uses within biomedical applications and include the detection of: uric acid [30,31], nitric oxide [32], lactate [33], perphenazine [34], haemoglobin [35], ascorbate, catechol and indole [36] and chloramphenicol [37]. The use of carbon sensors are not limited to *in-vitro* diagnostics, single fibre electrodes are commonly used *in-vivo* for the intra-cranial detection of acetylcholine and choline [38], dopamine [39-41], acetaminophen [42], nitric oxide [43] and glucose [44].

1.7 Project Aims and Objectives

Figure 1.4. Prototype smart-bandage manufactured using pad-printed sensor technology

The development and characterisation of the sensors capable of providing qualitative and quantitative data on both bacterial contamination and critical wound parameters were sought. The principal target was wound infections in which *Ps. aeruginosa* and *S. aureus* are likely to be the main protagonists. The specific chemical targets chosen included pH, urate and pyocyanin and each biomarker is considered in turn in the following chapters. The measurement of pH has been suggested as a useful marker for both wound infection but also for assessing healing physiology. A number of novel approaches to the development of *in situ* pH sensors have been developed (patents-pending) which allow the simple and cheap measurement of wound exudate pH using a small and flexible electrochemical sensor as highlighted in **Figure 1.4**.

The second approach was to exploit the activity of the enzyme uricase. This is absent from human biophysiology but is expressed by a wide range of wound pathogens (e.g. *Ps. aeruginosa*). Thus, it could be expected that the presence of bacteria and thereby the enzyme would result in fluctuations of *in vivo* urate concentration at the wound surface. Hence monitoring the latter as a biomarker could form the basis of a sensing strategy that could potentially allow the early detection of wound infection.

The final strategy was to investigate the detection of a bacterial metabolite characteristic of a given bacterial species – thereby allowing the possibility of identification as well as quantification of potential population. Pyocyanin is produced specifically by *Ps. aeruginosa* and is produced as a virulence factor during colonisation. This could serve as an ideal indicator for the early detection of the transition from contamination to colonisation by the organism.

As mentioned previously – it was anticipated that chemical modification of the sensing surface needed to be kept to a minimum and thus a more rapid and automatable approach to sensor construction and activation was sought through the

novel use of laser ablation of the sensor surfaces. Due to the commonly encountered problem of biofouling of sensor surfaces by bacterial biofilm formation (e.g. that of *S. aureus*), new antibacterial electrode coatings were briefly investigated as a means through which to improve the long term periodical monitoring stability. Through the surface modification of the sensor window – catalytic species capable of facilitating the reduction of oxygen to antibacterial reactive oxygen species (ROS) is enhanced. It was hoped these modifications would serve as a means of controlling biofilm formation but ultimately could lead the way forward to devices that not only detect microbial contamination but could actively minimise or inhibit the progression to colonisation. As a consequence of these investigations and the need to identify the nature of the ROS produced, a new electrochemical method for the detection of singlet oxygen was developed.

The overall target is the development of an array of sensors which can be incorporated within a wound dressing to allow a combination of generic and specific sensors to the common and more serious causes of wound infection. It could be envisaged that an array of sensors would represent the more ideal format as it has been shown that more than one species of bacteria was found in 27% of surgical site infected wounds when bacteria were isolated [8]. Through monitoring wound physiology and incursion of infection via a smart-bandage, it could be anticipated that there would be reduction in the need for wound redressing and sample collection (swabs or biopsies). This would not only save healthcare staff time and resources, but the redressing of wounds has the potential to disrupt wound healing and allow contamination of the wound.

1.8 References

1. Pratt RJ, Pellowe C, Loveday HP, Robinson N, Smith GW. The epic project: developing national evidence-based guidelines for preventing healthcare associated infection. *Journal of Hospital Infection* 2001;47:S1-46
2. Wilson J. *Infection Control in Clinical Practice* 2001, Elsevier Science, London.
3. Surveillance of Surgical Site Infection in English Hospitals: a national surveillance and quality improvement programme. Health Protection Agency-NINSS, 2002.
4. Plowman R. The socioeconomic burden of hospital acquired infection. *Eurosurveillance* 2000;5:49-50
5. Mousa HAL. Aerobic, anaerobic and fungal burn wound infections. *Journal of Hospital Infection* 1997;37:317-23
6. Chai J, Sheng Z, Yang H, Diao L, Li L. Successful treatment of invasive burn wound infection with sepsis in patients with major burns. *Chinese Medical Journal* 2000;113:1142-6
7. Vidhani S, Mehndiratta PL, Mathur MD. Study of methicillin resistant S. aureus (MRSA) isolates from high riskpatients. *Indian Journal of Medical Microbiology* 2001;19(2):87-90
8. Surveillance of Surgical Site Infection in England October 1997-September 2005. *Health Protection Agency* 2006.
9. Reducing the risk of chronic wound-related bloodstream infections. *Department of Health*: London 2007.
10. Horton JW. Free radicals and lipid peroxidation mediated injury in burn trauma: the role of antioxidant therapy *Toxicology* 2003*;*189:75-88.
11. Craft B, Kagan RJ. Current management of burns. *Medical update for psychiatrists* 1998;3(2):53–7.
12. Ansermino M, Hemsley C. ABC of burns - Intensive care management and control of infection. *British Medical Journal* 2004;329(7459):220-3
13. Estahbanati HK, Kashani PP, Ghanaatpisheh F. Frequency of Pseudomonas aeruginosa serotypes in burn wound infections and their resistance to antibiotics. *Burns* 2002;28(4):340-8
14. Douglas MW, Mulholland K, Denyer V, Gottlieb T. Multi-drug resistant Pseudomonas aeruginosa outbreak in a burns unit - an infection control study. *Burns* 2001;**27**(2):131-5.
15. Moseley R, Hilton JR, Waddington RJ, Harding KG, Stephens P, Thomas DW Comparison of oxidative stress biomarker profiles between acute and chronic wound environments. *Wound Repair and Regeneration* 2004;**12**(4):419-29.
16. Atiyeh BS, Costagiola M, Hayek SN, Dibo SA. Effect of silver on burn wound infection control and healing: Review of literature. *Burns* 2007;33:139-48
17. Rujitanaroj P, Pimpha N, Supaphol P. Wound-dressing materials with antibacterial activity from electrospun gelatine fiber mats containing silver nanoparticles. *Polymer* 2008;49;4723-32

18. Whitby M, McLaws ML, Collopy B, Looke DFL, Doidge S, Henderson B, Selvey L, Gardner G, Stackelroth J, Sartor A.Post-discharge surveillance: can patients reliably diagnose surgical wound infections? *Journal of Hospital Infection* 2002;52:155-60
19. Whelan J. Smart Bandages diagnose wound infection. *Drug Discovery Today* 2002;7:9-10
20. Smart wound dressings open up new perspectives in patient care. *NanoEurope: Media Release:* July 4 2008
21. D3 Technologies provides R&D to aid chronic wound care, *D3 Technologies Ltd. News release*, April 2009.
22. ITI Techmedia invests £7.9m in R&D programme to aid chronic wound care: new Technology set to improve patient care, *News Release* 28 April 2009, ITI-Techmedia.
23. Peter J, Hutter W, Stillinberger W, Hampel W. Detection of chlorinated and brominated hydrocarbons by an ion sensitive whole cell biosensor. *Biosensors & Bioelectronics* 1996;11:1215-9
24. Naessens M, Tran-Minh C. Whole-cell biosensors for direct determination of solvent vapours. *Biosensors & Bioelectronics* 1998;13:341-6
25. Dubey RS, Upadhyay SN. Microbial corrosion monitoring by an amperometric microbial biosensor developed using whole cell of *Pseudomonas* sp. *Biosensors & Bioelectronics* 2001;16:995-1000
26. Bailey ALPS, Pisanelli A.M, Persaud KC. Development of conducting polymer sensor arrays for wound monitoring. *Sensors and Actuators B* 2008;131:5-9
27. McColl D, Cartlidge B, Connolly P. Real-time monitoring of moisture levels in wound dressings *in vitro*: an experimental study. *International Journal of Surgery* 2007;5:316-22
28. Pasche S, Angeloni S, Ischer R, Liley M, Luprano J, Voirin A. Wearable Biosensors for Monitoring Wound Healing. *Advances in Science and Technology* 2008;57:80-7
29. James TJ, Hughes MA, Cherry GW, Taylor RP. Simple biochemical markers to assess chronic wounds. *Wound Repair and Regeneration* 2001;8(4):264-9
30. Dutt JSN, Cardosi MF, Wilkins S, Livingstone C, Davis J. Characterisation of carbon fibre composites for decentralised biomedical testing. *Materials Chemistry and Physics* 2006;97:267-72
31. Sharp D, Forsythe S, Davis, J. Carbon Fibre Composites: Integrated Electrochemical Sensors for Wounds Management. *Journal of Biochemistry* 2008;144:87-93
32. Katrlic J, Zaleskova, P. Nitric oxide determination by amperometric carbon fibre microelectrode. *Bioelectrochemistry* 2002;56:73-6
33. Ju HX, Doug L, Chen, HY. Amperometric determination of lactate dehydrogenase based on a carbon fibre microcylinder electrode modified covalently by Toluidine Blue 0 by acylation. *Talanta* 1996;43:1177-83
34. Liu D, Jin W. Amperometric detection of perphenazione at a carbon fibre microbundle electrode by capillary zone electrophoresis. *Journal of Chromatography B* 2003;789:411-5
35. Ju H, Sun H, Chen H. Properties of poly-B-aminoanthraquinonemodified carbon fibre electrode as a basis for haemoglobin biosensor. *Analytica Chimica Acta* 1996;327:125-32

36. Crespi F. Carbon fibre micro-electrode and *in vitro* or in brain slinces voltammetric measurement of ascorbate, catechol and indole oxidation signals: influence of temperature and physiological media. *Biosensors and Bioelectronics* 1996;11:743-9
37. Agui L, Guzman A, Yanez-Sedeno P, Pingarron JM. Voltammetric determination of chloramphenicol in milk at electrochemically activated carbon fibre microelectrodes. *Analytica Chimica Acta* 2002;461:65-73
38. Schuvailo ON, Dzyadevych SV, El'skaya AV, Gautier-Sauvigne S, Csoregi E, Cespuglio R, Soldatkin AP. Carbon fibre-based microbiosensors for in vivo measurements of acetylcholine and choline. *Biosensors and Bioelectronics* 2005;21:87-94
39. Suard-Chagny MF. In vivo monitoring of dopamine overflow in the central nervous system by amperometric techniques combined with carbon fibre electrodes. *Methods* 2004;33:322-9
40. Yavich L, Tiiohonen J. In vivo voltammetry with removable carbon fibre electrodes in freely-moving mice: dopamine release during intracranial self-stimulation. *Journal of Neuroscience Methods* 2000;104:55-63
41. Dressman SF, Peters JL, Michael AC. Carbon fibre microelectrodes with multiple sensing elements for in vivo voltammetry. *Journal of Neuroscience Methods* 2002;119:75-81
42. Logman MJ, Budygim EA, Gainetdinov RR, Wightman RM. Quantification of in vivo measurements with carbon fibre microelectrodes. *Journal of Neuroscience Methods* 2000;95:95-102
43. Park JK, Tran PH, Chao JKT, Ghodadra R, Rangarajan R, Thakor NV. In vivo nitric oxide sensor using non-conducting polymer-modified carbon fibre. *Biosensors and Bioelectronics* 1998;13:1187-95
44. Netchiporouk LI, Shram NF, Jaffrezic-Renault N, Martelet C, Cespuglio R. In vivo brain glucose measurements: Differential normal pulse voltammetry with enzyme-modified carbon fibre microelectrodes. *Analytical Chemistry* 1996;68:4358-64

Chapter 2

Experimental Details and Methodology

Abstract

Electrochemical methods are amongst the most abundant techniques used for point of care and many ward-based diagnostics. Electrochemistry has been used throughout due to the versatility and compact sensing interface facilitated by this technology. The development and functional characterisation of the sensor interface has been of utmost importance in the development of sensitive and specific electrodes. The difficulty of this is heightened by the miniaturisation of sensor substrates and the complexity of the wound exudate matrices. Developments of new sensor substrates have led to accurate and precise measurements of select markers within biofluids and simulated wound environments. To allow bacterial testing of sensor prototypes appropriate applications of bacterial pathogens are required to allow an accurate assessment, the culture methods and conditions are evaluated. Finally, the construction methods of the prototype sensors have been detailed at length and will be referred back to in subsequent chapters.

2.1 Electrochemistry

Electrochemistry is the study of chemical species through their capacity to interact with an electrode interface i.e. to donate or withdraw electrons. Electrochemistry has been used throughout the project both for quantitative analyses and qualitative studies of biochemical interactions [1]. Analytical electrochemistry was largely used to enable the identification/quantification of key electrochemically active biomolecules and can be achieved through the oxidation and/or reduction at specified potentials characteristic to both the species under investigation, the solution conditions and the nature of the electrode substrate. Physical or chemical modification of the working electrode is usually necessary to achieve speciation in complex biofluids due to the variety of electrochemically-active species present. Electrochemical sensors have widespread applications including: environmental, industrial and biomedical remits and this versatility and adaptability of electrochemical techniques have lead to its success.

2.2 Electrodes

2.2.1. Reference Electrodes

Within an electrochemical system, the reference electrode is used to provide a stable potential through which to control the magnitude of the potential at the working electrode. For most of the research performed, a silver-silver chloride half cell reference electrode was used which was comprised of a silver wire coated with silver chloride in a glass sheath filled with 3M NaCl solution. A porous frit at the bottom allows a very slow outflow of the NaCl and thus enable electrical conduction with the test solution.

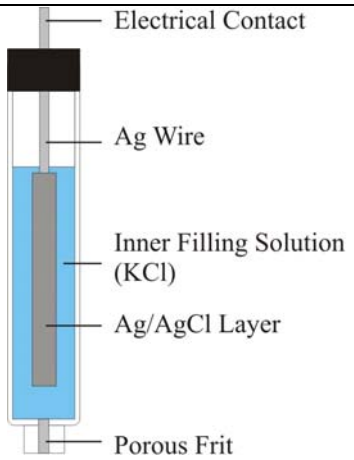

$Cl^-_{(aq)}|\ AgCl_{(s)}, Ag_{(s)}$

$AgCl_{(s)} + e \Leftrightarrow Ag_{(s)} + Cl^-_{(aq)}\quad E^o = +0.222\ V$

Figure 2.1. Commercial reference electrode and corresponding electrode process

The overall chemical reaction, taking place into the cell can be described by the means of two processes – oxidation and reduction. The difference in potential between two of them is the electromotive force (emf) of the cell. The electrochemical process taking place in the cell can be described by the Nernst equation:

$$aOx + n\bar{e} \leftrightarrow b\,\mathrm{Re}\,d$$

$$E = E^o - \frac{RT}{nF}\ln\frac{a_{red}^{\ b}}{a_{ox}^{\ a}}, \text{ where}$$

E is a electrode potential;

E^o is a standard electrode potential;

R is the gas constant 8.314 $JK^{-1}mol^{-1}$;

T is temperature in Kelvin;

n is the number of electrons transferred to the electrode during reaction;

F is Faraday constant $9.649x10^4$ C mol^{-1}

a_{ox} *and* a_{red} are activities of oxidized and reduced species.

In the case of the silver / silver chloride reference system – the activities of the Ag metal and AgCl solid are both unity and hence the potential of the reference electrode is dictated by the activity of chloride ion. In the design of the bandage sensors – the glass half cell was replaced simply by the chloridised silver wire. In these cases the concentration of chloride was maintained at a constant value within the buffer solution to ensure comparability between experiments.

Manipulation of the Nernst equation allows for the electrochemical potential shift [2] derived from a log change in hydrogen ion concentration (i.e. 1 pH unit) to be calculated (B). Therefore it could be anticipated in a Nernstian relationship, the potential shift anticipated by a change of 1 pH unit would be 29.58 mV for a 2-electron transfer reaction and 59.16 mV for a 1-electrode reaction. This electrochemical characteristic is the fundamental base for the pH sensing technology developed in Chapters 4 and 5.

2.2.2 Working Electrodes

The working electrode is where the electrochemical reaction of interest takes place. The potentials set by the user in an electrochemical system are effectively applied here with the current flow through this electrode (to the counter) measured. A huge range of substrates can be used as working electrodes depending on application. The most common of which are carbon, platinum and gold and are selected on the basis of the relative chemical inertness. Due to the expense of gold and platinum electrode and the issues over the reproducibility of oxide layers, commercially available vitreous (glassy) carbon electrodes have been used throughout this research as an initial starting point for all investigations. The electrode surface is polished prior to experiments on nanoparticle alumina (50 nm diameter) and ultrasonically cleaned in deionised water. This produces a fresh, smooth and hence reproducible and reliable electrode surface. Alternative carbon based substrates have been used for the development of disposable wound sensors, both laminated carbon fibre electrodes and pad-printed carbon electrodes, the specific details of which are provided in the individual chapters.

2.2.3 Auxiliary / Counter Electrodes

The counter electrode is used to complete the circuit from the working electrode and to avoid passing current through the reference electrode. A platinum wire counter electrode was used throughout unless otherwise stated, due to its high conductivity and inert nature.

2.3 Buffer Solution

In most cases, the background solution typically consisted of a solvent with dissolved salts (or acids) essential to allow sufficient electrical current to flow through the solution and hence to perform the electrochemical measurements. Britton-Robinson buffer was used throughout most of the initial investigations and electrode developments. Britton-Robinson is comprised of three acids (acetic, boric and phosphoric) each at 0.04M. The pH was adjusted through the addition of sodium hydroxide. In later experiments, alternative broth media were used to provide specific conditions necessary for optimal bacterial growth and are detailed in the appropriate chapter. Solutions were prepared in deionised water from an Elgastat (Elga, UK) water system.

2.4 Mass Transport

Since electrochemical measurements are performed at the electrode-solution interface and that the molecules are chemically altered by the measurement process, the modes of molecular movement are important within analytical electrochemistry. There are three principle methods of molecule transport in solution:

- *Diffusion* is the natural movement of molecules through moving from areas of high concentrations to areas of low concentration to minimise concentration gradients.

- *Convection* is the physical movements of molecules within solution and can arise either naturally, due to density gradients, or mechanically by the use of stirred or flowing solutions.

- *Migration* is a result of electrostatic-attraction and electrostatic-repulsion of charge molecules.

2.5 Voltammetry

Voltammetry is a commonly used electrochemical technique, whereby the potential (voltage) between the working and reference electrode is varied and the current flow (amps) is measured and displayed in relation to the potential forming a voltammogram. Different wave forms can be used depending on the desired application, the most sensitive waveform for chemical detection and quantification is square wave voltammetry, due to its nature of two step forward-measure, one step back-measure. In contrast to conventional voltammetry, squarewave pauses immediately after the step pulse to allow the capacitance component of the current to dissipate thereby leaving the Faradaic component. The latter is attributed solely to the electrode process of interest and provide not only a more reproducible signal but the removal of the capacitance background provides better signal to noise discrimination allowing more sensitive determination. The inherent background correction allows for very sensitive measurement, compared to e.g. a linear sweep, when the potential is ramped from x to y linearly and the whole current measured. The advantages of this technique however are the electrical design simplicity and as such it could be more suitable to low cost device development than technologies associated with either spectroscopic or chromatographic analysis.

2.5.1 Cyclic Voltammetry

Cyclic voltammetry (CV) is a widely used electrochemical technique, which although able to provide quantitative data is more often used to aid the understanding of

the underlying electrochemical processes that the target species undergo. This method was used for initial biomarker testing for redox potential comparison and in later chapters as an initial test for finding the redox potentials and understanding the electrochemical transformations. CV relies on linear scanning using a triangular waveform (**Figure 2.2A**) in an unstirred solution. Multiple cycles of this triangular potential waveform can be performed to provide additional information about the target species and the electrochemical products of analysis. A typical cyclic voltammogram is shown in **Figure 2.2B**, with the key oxidation and reduction transformations given.

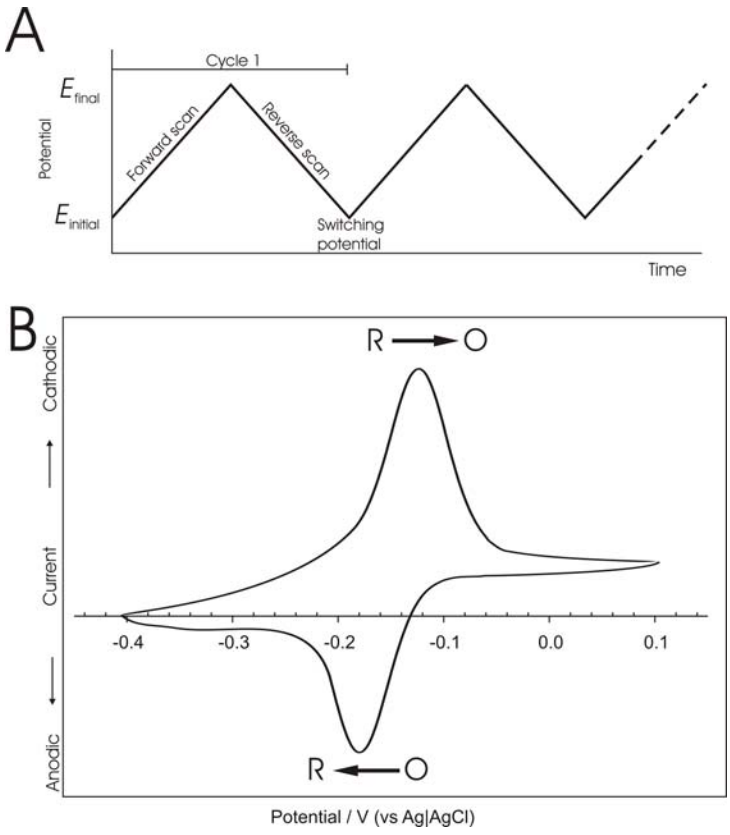

Figure 2.2. A. Waveform used in cyclic voltammetry, B. An example cyclic voltammogram showing reversible redox peaks.

2.5.2 Linear Sweep Voltammetry

Linear Sweep Voltammetry (LSV) is the simplest form of quantitative voltammetry and is essentially one half of a cyclic voltammogram as shown in **Figure 2.3A**. a linear potential ramp is used, which produces a linear sweep voltammogram (**Figure 2.3B**). Linear sweep voltammetry was solely used for the development of pH sensors due to the analytical ease required in a commercial device, despite the decrease in peak magnitude and sharpness that can be observed.

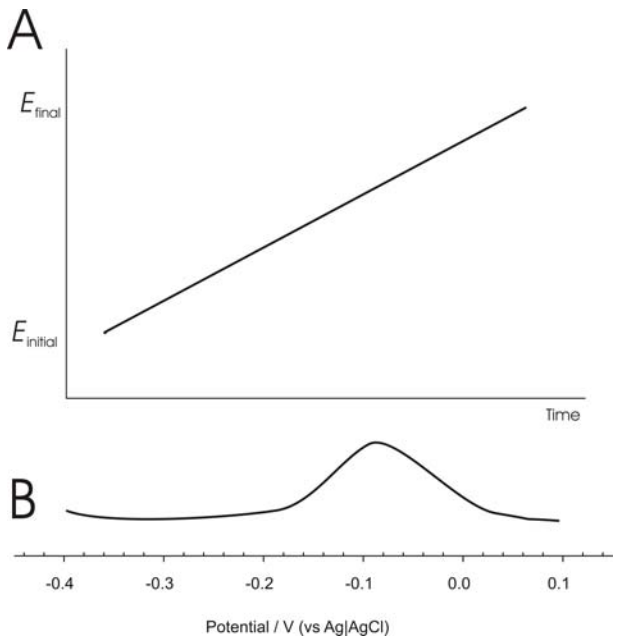

Figure 2.3. A) Voltage ramp applied in linear sweep voltammetry, B). Example linear sweep voltammogram.

2.5.3 Square Wave Voltammetry

Square Wave Voltammetry (SqWV) was used widely throughout this project for the more sensitive quantification as alluded to in the opening summary of this section. The inherent background correction achieved through the step-forward measure, step-back measure allowed for greater ease of peak current measurements and sharper redox

peaks. **Figures 2.4A** and **2.4B** detail the nature of the waveform and the key variables that may be changed for optimisation. In **Figure 2.4A** the two measurement points are highlighted for: the high (H) and low (L) current measurements, respectively, it is the difference between these two values which is plotted in a square wave voltammogram, as shown in **Figure 2.4C**. The exact values for each of the parameters are given in the experimental section of each chapter.

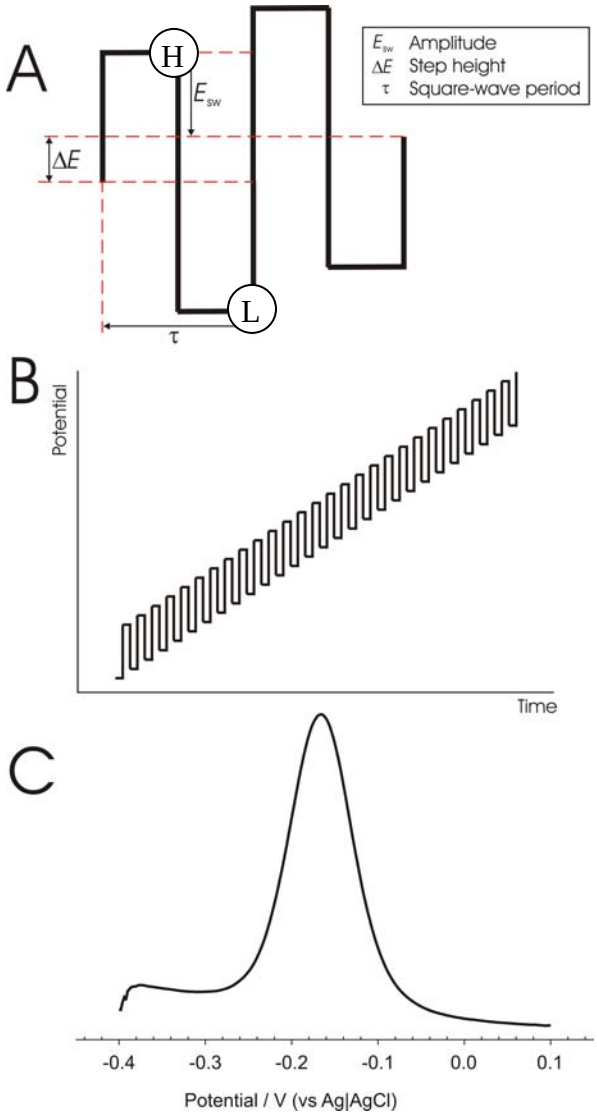

Figure 2.4. A). Detailed waveform and parameters used in square wave voltammetry, B).Example of full square wave scan profile. C). Example square wave voltammogram.

2.6 Bacteriology

The bacteria assessed throughout this research were:

Gram positive:

Staphylococcus aureus National Collection of Type Cultures (NCTC) 10788

Gram negative:

Pseudomonas aeruginosa National Collection of Type Cultures (NCTC) 6749

Pseudomonas aeruginosa National Collection of Type Cultures (NCTC) 8060

Pseudomonas aeruginosa National Collection of Type Cultures (NCTC) 8602

Klebsiella pneumoniae National Collection of Industrial Food and Marine Bacteria (NCIMB) 10341

Escherichia coli National Collection of Industrial Food and Marine Bacteria (NCIMB) 10214

2.6.1 Bacterial Cultures

Bacteria can have the ability to replicate very rapidly and thus to enable the study of organisms and importantly the rapid identification of bacteria (e.g. in a healthcare environment) a huge array of culturing techniques have been developed. Whilst certain extremophilic bacteria thrive in harsh conditions e.g. temperature or pH, the organisms in medical microbiology have a much smaller tolerance of extremes. Many of the growing conditions are used to replicate the *in vivo* environment and, as such, growth media will typically have a pH within physiological ranges (e.g. pH 6-8) and be grown at ~37°C. For successful bacterial growth, both the physical and chemical environments need to be suitable. In the advancement of medical microbiology, different growth conditions have been used to preferentially grow an organism either of research interest or confirmation of identity in suspected causes of infection.

2.6.2 Culture Media

In general, the culture media must provide the essentials for bacterial life to allow *in vitro* growth and subsequent studies of the bacterial colonies. Due to the multitude of bacterial types and a multitude of reasons for studying them, a huge array of culture

media have been developed which can be split into nutrient, minimal and selective media [3, 4]. All media contain the basic necessities for bacterial growth: water, salts and a carbon source, commonly glucose. Other components can also be added to the basic composition to enhance or inhibit the growth of particular species.

2.6.3. Nutrient Media

Nutrient media contain a complex and undefined mixture of amino acids as nitrogen source, commonly from plant, yeast or animal extracts. Nutrient media effectively simulates the conditions found in wounds where most causes of HAI are found and are used in the present project to promote the general growth of cultures due to their non-specific nature.

2.6.4 Minimal Media

In this case the exact composition of the media is known and typically contains the absolute minimum requirements to enable growth of the target strains. In order to allow sufficient construction of necessary proteins and nucleic acids, sources of nitrogen, magnesium, phosphate and sulphur may be added in the form of salts.

2.6.5 Selective Media

In addition to the nutritional requirements, culture media may contain selective agents, to allow the growth of antibiotic resistant strains (e.g. MRSA, methicillin resistant *Staphylococcus aureus*) or only certain species (e.g. *Ps. aeruginosa*). These are used for identification of bacteria or to isolate / purify certain organisms from a mixed culture to allow further studies e.g. into resistance mechanisms.

2.6.6 Agar Plates and Broth Media

Culture media are generally used in two forms: broths and agar plates. Broths are liquid culture media of the desired composition to allow the mass growth of organisms in solution. For optimal growth of bacteria in broth cultures, the cultures require orbital mixing to prevent the organisms from clumping and to allow a fresh supply of nutrient and to prevent local accumulation of by-products. Agar is a polysaccharide extract of seaweed which is indigestible by bacteria and acts as a solidifying agent. Other solidification agents have been used e.g. gelatine or egg albumin, but agar is most widespread. When poured into Petri dishes as a warm molten culture media and then cooled, the agar forms a semi-solid gel. Inoculating the cultures onto the surface of this nutrient gel can allow the phenotypic study and the separation of pure colonies from a mixed inoculum if a sufficiently low population density is used, allowing isolation of pure cultures. Nutrient media was used throughout for the initial growth and for culture maintenance. Tryptic Soy Agar (TSA, MERCK 1.05458) and Tryptic Soy Broth (TSB, MERCK 1.05459) were used unless otherwise stated. Various minimal and nutrient media were used throughout this research for specific tests and or cultures, the details are included in the experimental section of the appropriate chapters.

2.6.7 Presence of Oxygen

While there are many anaerobic bacteria that prefer or require the absence of oxygen to grow, the majority of wound infecting organisms are aerobic and therefore thrive in the presence of oxygen. *Ps. aeruginosa* is a facultative anaerobe [5], allowing it to grow in the presence or absence of oxygen, but will utilise oxygen if present. As such all of the bacterial cultures were incubated in normal aerobic conditions.

2.7 Sensor Construction

2.7.1 Laminated Working Electrodes

The majority of the working electrodes used throughout this research were constructed from laminated carbon-substrates. The exact carbon substrates and sensor sizes are detailed within the experimental section of each chapter. Laminated carbon–substrate prototypes were prepared by thermally sandwiching carbon-substrate between sleeves of a commercial 75μm resin-polyester lamination pouch (Rexel, UK), **Figure 2.5A,** using a commercially available office laminator. The polyester laminate were either pre-etched or etched after lamination with the sensing window, depending on the requirements, using a 25W CO_2 Computer Controlled Laser Cutter (CadCam Technology Ltd, UK). Laser etching allows the rapid and accurate patterning of individual components. Electrical connection to the carbon film was made through the presence of a strip of 100μm thick copper shielding tape, **Figure 2.5B**. The electrodes were baked at 100°C for 16 hours in order to ensure the complete permeation of the resin to the carbon substrate surface within the laminate. This is necessary to ensure the mechanical integrity and coherence of the seal between the sensing fibre layer and the insulating polyester sheath such that no solvent creep or de-

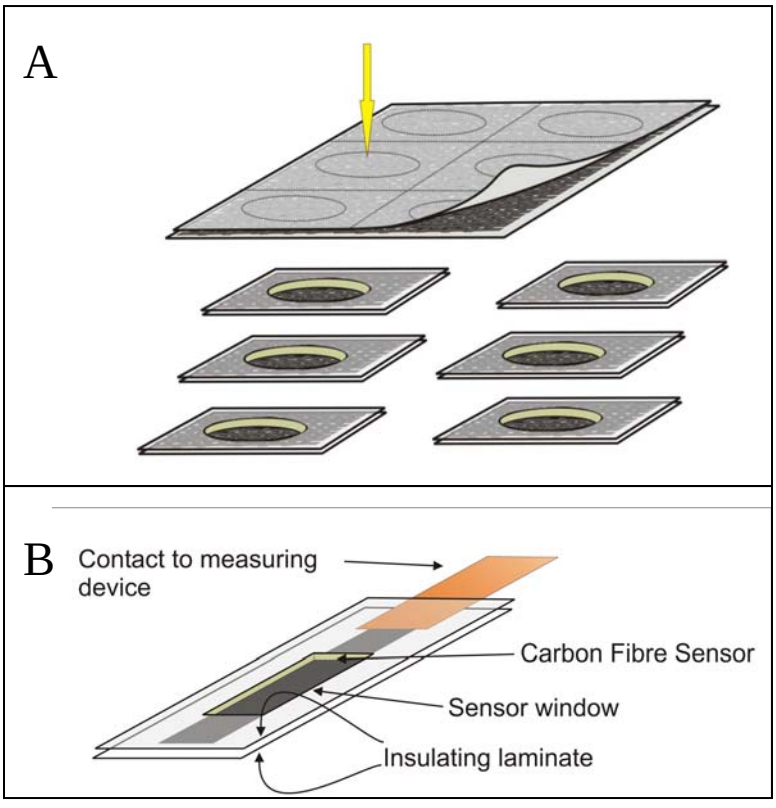

Figure 2.5. A) Schematic of the lamination process and B) Detailed diagram of completed carbon-substrate working electrode.

lamination would occur during extended monitoring periods, especially when using complex 3-D structured sensor substrates.

The two major carbon substrates used throughout this research are referred to as carbon matting and carbon tow. Carbon fibre matting is a commercially available pressed carbon matting (Toray carbon fibre cloth), available from E-Tek Inc (USA). Carbon fibre tow is a commercially available bundle (typically containing 3000 individual fibres) of un-woven 10μm diameter carbon fibre (Goodfellow, UK). The two differing carbon fibre substrates were used for different applications. The carbon fibre tow is more flexible and less prone to damage whilst handling, but suffers from less sensitive measurements than the high surface area matting. Whilst the two forms differ, they are essentially the same sensing elements, but possess different macroscopic structures. The different morphologies are illustrated in the scanning electron micrographs detailed in Figure 2.6A and B for the tow and matting respectively.

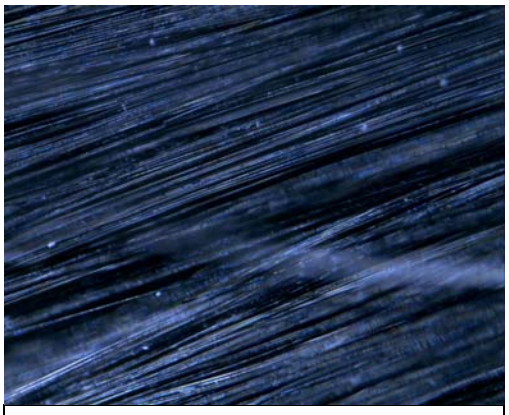

Figure 2.6A. Image of Carbon fibre tow at x600 magnification showing the 10μm diameter smooth fibre

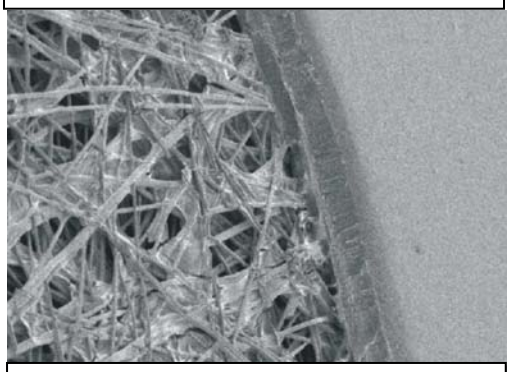

Figure 2.6B. SEM of the carbon fibre matting shows the complex, 3-D structure

2.7.2 Pad Printed Working Electrodes

Pad printed electrodes offer advantages over the laminated carbon-substrate electrodes due to greater mass-producibility and versatility of printing onto a wide variety of substrate media. The pad-printed carbon electrodes were printed using a PE-4C pad-printing machine (Pad Printer Eng. Co. Ltd., supplied by Pad Print UK, Stevenage, UK) from an etched stainless steel plate/closed cup arrangement containing a silver-free carbon ink. The basic printing process is highlighted in **Figure 2.7**. The electrodes were comprised of 20 print layers deposited on a flexible wound dressing backing material (Brightwake Ltd, UK). The printed sensors were baked at 100°C for 12 hour to complete polymerisation of the carbon ink.

Figure 2.7. Pad printing process used for electrode manufacture

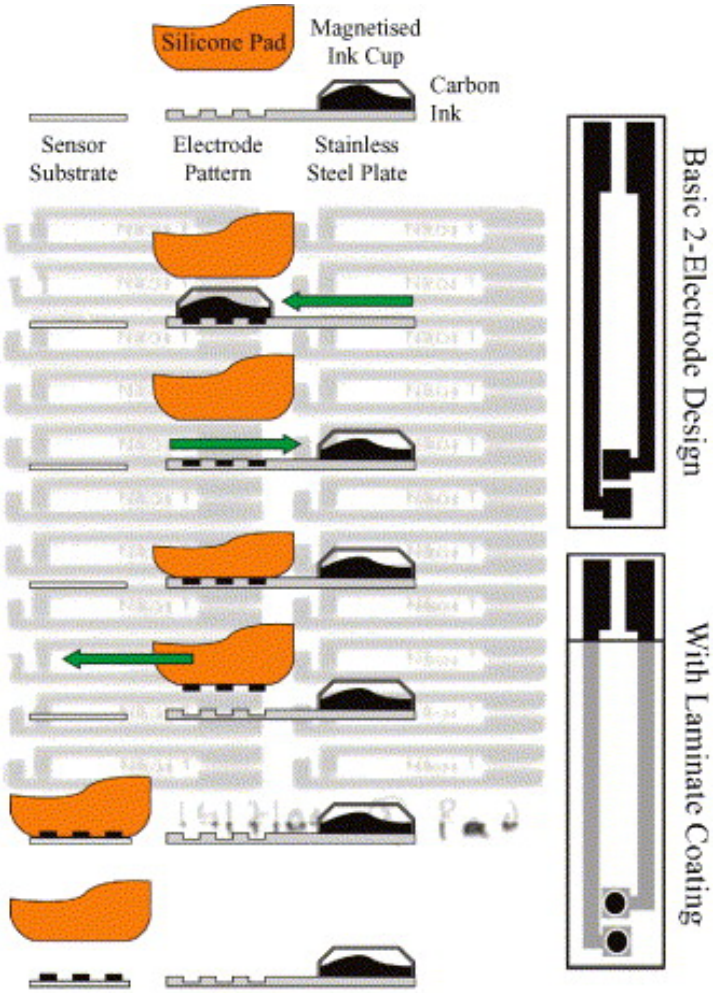

2.8 References

1. Brett CMA, Brett AMO. Electroanalysis. Oxford University Press, Oxford UK 1998.
2. Wang J. Analytical Electrochemistry 3rd Edition. Wiley-VCH, New Jersey USA 2006
3. Greenwood D, Slack RCB, Peutherer JF eds. Medical Microbiology 16th Edition, Churchill Livingston, Elsevier Science Limited, London UK 2002.
4. Atlas RM. Handbook of Microbiological Media. CRC-Press, London UK 1993.
5. Mahon CR, Lehman DC, Manuselis G. Textbook of Diagnostic Microbiology, Saunders Elsevier, Missouri USA 2007.

Chapter 3

Characterisation of Biomolecules Endogenous to Wound Physiology

Abstract

The ability to monitor pH in wound fluids is of clear benefit to a range of healthcare scenarios in terms of direct clinical and patient led wound management. Changes in pH have been associated with many important changes within the wound environment, prominently through healing progression or due to bacterial infections. Due to the Nernst equation detailed in the earlier experimental section, the ability to monitor pH through the peak shifting of redox interactions is investigated as a novel sensing system. To allow the reliable function a specific biomarker must be used, the main electroactive components of biofluids are investigated to aid the identification of specific target for further evaluations. The thorough evaluation of the electrochemical activities of these key biomarkers have been assessed and subsequently compared to allow a more rigorous selection process. The key species of urate and the polymeric deposit of tryptophan oxidation are selected as suitable candidates and therefore are highlighted for further testing for the development of novel pH sensing systems.

3.1 Introduction

The problem of wound associated HAI clearly prompts the need for technological advancements to facilitate improved patient care. It has been established in Chapter 1 that the early *in situ* identification of infected wounds would provide major benefits through reducing hospitalisation times and freeing up hospital beds, helping mortality and reducing the substantial costs associated with the follow up treatment of wound / HAI infections. It has been found that the wound exudate pH may change with bacterial load of certain important organisms: the pH of wound exudate was found to be pH 6.7 or lower when the loads of *E. coli* or *S. aureus* is over 10^7 cells/gm of granulating tissue and pH 8.0 with 10^8 cells/gm granular tissue of *Ps. aeruginosa* [1]. Thus, it could be envisaged that monitoring the change in pH of the wound environment may give a diagnostic handle on the potential for bacterial colonisation.

The use of pH measurements within the wound environment is not however limited solely to an infection diagnostic role, it has also been suggested that such measurements could be a useful tool in monitoring the healing progression of both acute and chronic wounds. It was also suggested that there is a need for a better understanding of the pH requirements under different wound circumstances [2]. Shukla *et al.* have shown that the baseline pH value of most wounds was greater than pH 8.5, with the pH decreasing with wound healing [3] and therefore monitoring this change would clearly be advantageous. Mildly acidic conditions may be beneficial [4] and the results of Chai *et al.* [1] show that pH 7.2 - 7.5 is optimal for tissue granulation in the healing process. Therefore the availability of a sensor capable of monitoring pH may be of value in alerting healthcare staff and / or the patient to the conditions that may be sub-optimal or inhibitory on wound healing thus enabling appropriate remedial treatment(s).

One problem in pursuing the development of such a device is the ambiguities of what the responses actually mean as the fluctuations in the pH response could be representative of the natural wound physiology or, alternatively, could be a product of bacterial contamination. There is little doubt that being able to monitor wound pH is adventitious and more studies would be required to ascertain the actual diagnostic merit – it is for this reason that the development of an *in situ* pH sensor was continued.

Moreover, the design characteristics represent a considerable challenge and it was likely that the material developments would be of more generic benefit to sensor construction irrespective of target. In this instance, the pH range targeted for this development focused on a range of pH 4 to 10. It is worthwhile to note that the range of pH 5.45 to 8.65 has been observed in a large study of chronic wounds [5] and thus the range selected for the present study should be of relevance to a number of studies. While a pH sensor may not be able to definitively differentiate between these two causative mechanisms of pH change (infection and healing progression), the ability to monitor the pH remotely may nevertheless be of advantage to improving patient healthcare through providing the clinicians with information more readily, allowing earlier evaluation and monitoring of wound problems. Given the importance of pH measurements with regards to both primary aspects, measurements common rely upon the visually subjective litmus paper [3] or the use of conventional large glass pH probes. The aim of the work presented in this chapter was to develop sensors that would have greater accuracy and incur less wound disruption than these methods.

In situ pH sensors need to meet certain criteria to be of widespread use: the sensors need to be cheap, reliable, non-hazardous, small, flexible and essentially disposable. As such the core design must be suitable for mass production such that the economics are viable. A survey of the literature has found no competing technology that adequately meets all of these criteria. While there are many designs and analytical strategies that can provide a pH measurement, most tend to fall foul of the exacting demands needed to produce a clinically acceptable wound sensor.

Conventional pH sensors take several forms: they are either the relatively large lab based design containing the glass bulb or based on ion selective field effect transistors. They may also be based on a voltammetric methodology containing an immobilised chemical layer that responds to changes in the pH environment. Recent developments in pH sensors have enabled the production of small pH sensors. These rely upon polymerisation or impregnation of chemicals onto the electrode surface (e.g. tetraphenylborate, quinones, anthracenes and ferrocene combinations [6,7]). While these may be suitable for environmental pH monitoring, they are not applicable to *in-vivo*

wound sensors due to the potential problems with surface components leaching from the electrode or the electrode becoming damaged.

3.2 Proposed Methodology

Voltammetric methodologies rely upon the fact that the potential at which most organic molecules will be dependent strongly on the pH of the local environment. They typically immobilise a redox species onto the electrode surface and then scan a potential range. The peak position associated with either the reduction or oxidation of the immobilised component can then be related to the pH through the Nernst equation outlined in Chapter 2. There is typically a shift of 59/n mV/pH unit – where n is the number of electrons associated with the given electrode process. Thus as the pH is lowered the peak position will shift towards more positive (or less negative depending on the probe chosen) potentials. In order to exploit this as the basis of an analytical signal it requires the peak to be easily measurable in terms of magnitude and resolution. The first criterion is easy to fulfil if the redox probe is immobilised on the surface of the electrode. The second depends on the choice of the probe such that the peak is capable of being interrogated in region where there are no competing electrode processes due to the matrix constituents. Even assuming both requirements are met there will always be the issue of potential leakage. In many cases the redox probes are organic molecules which possess toxicological properties that are incompatible with direct exposure to a wound interface.

A novel approach was proposed whereby it was envisaged that if all that is needed is an organic molecules that is pH responsive then why not make use of the compounds that may well be present naturally within the wound environment. The use of an endogenous compound obviates the need for electrode modification and the hazards that such procedures can bring. The main question however was the identification of a suitable “natural” probe – again remembering that it would have to give a clear, unambiguous signal – moreover it would have to be ubiquitous within wound fluids.

The biomolecules typically encountered within a wound environment were initially screened to identify those that would possess electrochemical properties accessible to carbon electrodes. Most molecules are electrochemically invisible and while

they can be oxidised or reduced, the potentials required to achieve such are beyond the analytical window available within an aqueous environment. The application of potentials sufficient to reduce a carboxylic acid group for example would be too negative and would incur the reduction of water as a competing process. Hence the current would provide no meaningful analytical signal. It is important that the target redox probe be capable of oxidation and/or reduction within the limits of the potential window such that the current observed is solely attributed to the electrode process of the target and not the decomposition of the solvent.

The first screen eliminated most compounds but there is a core of electroactive species that meet the criterion of being present in the majority of wounds fluids reported to date. Their electrochemical suitability however remained open to question and were therefore assessed. The intention was, in essence, to create a library of their electrochemical characteristics which could then serve as a useful reference for oxidation and reduction potentials for the compounds most likely to be electrochemically detected within biofluids. Even if they were found to be unsuitable as probe their presence could nevertheless hinder the electroanalytical measurement if their peak processes overlapped with the chosen probe. The work presented in this chapter focused primarily on the identification of those endogenous molecules that could be exploited either directly or indirectly as a probe through which to measure pH.

3.3 Experimental Details

Materials. Stock solutions of uric acid, xanthine and guanine (typically 5mM) were prepared in 0.1M NaOH. All other solutions were prepared using pH 7 BR buffer. Electrochemical measurements were conducted using a μAutolab type III computer controlled potentiostat (Eco-Chemie, Utrecht, The Netherlands) using a standard three electrode configuration consisting of the Glassy Carbon working electrode (GC, 0.07 cm^2, BAS Technicol, UK), a Ag|AgCl reference electrode and a Pt wire counter electrode. The Glassy Carbon Electrode was polished using Aluminium Oxide nanopowder (Sigma-Aldrich) prior to thorough rinsing with deionised water and

ultrasonicated in deionised water. Measurements were performed in 10ml BR buffer (with required analyte addition).

3.4 Results and Discussion

The following subsections describe the main properties of those molecules which passed the preliminary screening of wound biomolecules and were deemed to possess electrochemical properties that could either be harnessed or were in need of careful evaluation in the event that may be a potential interferent. A description of the biomolecule common roles, how it is normally detected and the reference range is provided. The electrochemical properties were assessed using cyclic voltammetry to determine the relative peak position and to critically compare the sensitivity and to identify potential issues relating to their adoption as a viable pH probe.

3.4.1 **Ascorbic Acid (Vitamin C)**

Ascorbic acid (AA), Figure 3.1, is irreversibly oxidised to dehydroascorbic acid which may subsequently be oxidised to 2,3-diketo-L-gluonic acid [8]. Plants and most animals can produce their own AA from glucose; however humans are unable to do this due to a lack of L-gluconolactone oxidase. Therefore vitamin C (ascorbic acid) is an essential part of the diet. The best sources of this include citrus fruits, tomatoes, raw cabbage and leafy green vegetables [9]. The most important functions of AA are as a cofactor for protocollagen hydroxylase and to serve as an antioxidant [10]. This is essential for the production of collagen and related proteins, which form cartilage, dentin and bone. AA is also involved in tyrosine metabolism, drug metabolism, synthesis of epinephrine and anti-inflammatory steroids by the adrenals, folic acid metabolism and leukocyte functions. AA has a half life of approximately 16 days in humans and the recommended daily allowance for adults is 60mg [9]. Deficiency may lead to scurvy, which initially has some or all of the following

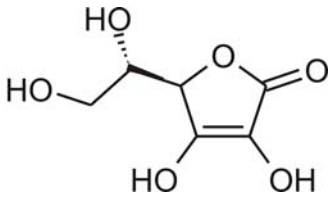

Figure 3.1 Ascorbic Acid

symptoms: fatigue, swollen and bleeding gums, follicular hyperkeratosis, muscular aches and pains and emotional changes [11].

When handling samples for AA measurement consideration have to be taken due to its instability in aqueous solutions as it is very rapidly oxidised to dehydroascorbic acid. Experiments have shown that AA in whole blood is sufficiently stable at room temperature for 8 hours. However when separated to plasma it is very rapidly oxidised at room temperature and must therefore be stored frozen at -70^{o}C [12]. Ascorbic acid can be measured by HPLC (high performance liquid chromatography), fluorimetry and UV spectrophotometry [8,9] . The nutritional status of AA is usually assessed in plasma. However it has been suggested that the leukocyte AA concentration is a better indicator of tissue stores. It may also be measured in the urine although no reference ranges are available. Reference ranges for adults: Plasma: 0.4 – 1.5 mg/dL (23 – 85 μmol/L), Leukocytes: 20 – 53 μg/10^{8} leukocytes (1.14 – 3.01 fmol/leukocyte)

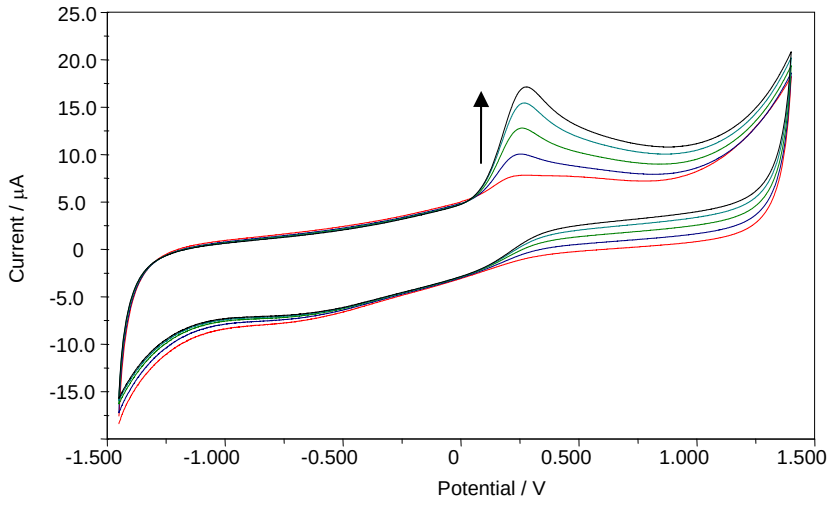

Figure 3.2. Cyclic voltammograms of increasing concentrations of ascorbic acid (100 to 500 μM) recorded at a glassy carbon electrode in pH 7 buffer. Scan Rate: 50mV/s

It can be seen from the cyclic voltammograms detailed in Figure 3.2 that the oxidation of AA gives rise to a single, broad oxidation peak at +0.29V as the AA is electrochemically oxidised to dehydroascorbic acid. No reverse / reduction peak is observed as the oxidation product cannot be electrochemically reduced back to the AA at a GCE and is consistent with the previously reported irreversibility of the system. A very

slight reduction peak at -0.75V is derived solely from the reduction of molecular oxygen in the solution. The height of the ascorbate oxidation peak heights was found to increase linearly in response to increasing concentrations (100 to 500μM) of the biomolecule.

3.4.2 **Folic Acid**

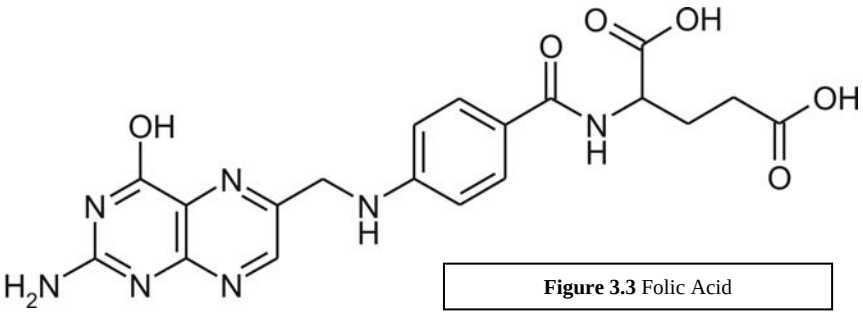

Figure 3.3 Folic Acid

The folates, Figure 3.3, are a family of compounds related to pteroic acid and are readily absorbed from the diet. Naturally, folates are found in green leafy vegetables [9], however many breakfast cereals and bread are fortified with folic acid (FA), a topic of current debate. Folate is required by the body for DNA replication and for cell production and maintenance. The body requires 50 μg per day, which is generally far exceeded by the average daily intake of 500 μg. FA deficiency generally arise in patients with diets low in folate, gut sterilisation, poor intestinal absorption, liver disease, malignancies or excessive demand e.g. pregnancy [9]. A clinical deficiency of FA may result in megaloblastic anaemia and sometimes sensory neuropathy or neuropsychiatric changes [9]. However folate deficiencies have also been associated with Alzheimer's dementia, osteoporosis, cancer and coronary heart disease, either directly from the deficiency or through an associated condition [13]. FA deficiency during pregnancy increases the chances of neural tube defects e.g. spina bifida. Taking folic acid supplements for 3 months pre-conception and throughout pregnancy can help reduce this by 50%[14]. However recent studies have shown that taking these high dose folic acid supplements may actually increase the risk of breast cancer in older life [15]. Therefore the fortification of products is creating much debate and controversy. Measurement of folic acid in clinical laboratories is routinely performed by immunoassay e.g. chemiluminescence, used to measure either the serum/plasma folate or the Red Blood Cell (RBC) folate, in which case the RBCs are lysed releasing the contained folate. Folate has previously been measured by competitive radio-immunoassay [16]. Reference ranges: serum, 7-48 nmol/L, red cell, 317-1422 nmol/L [17]

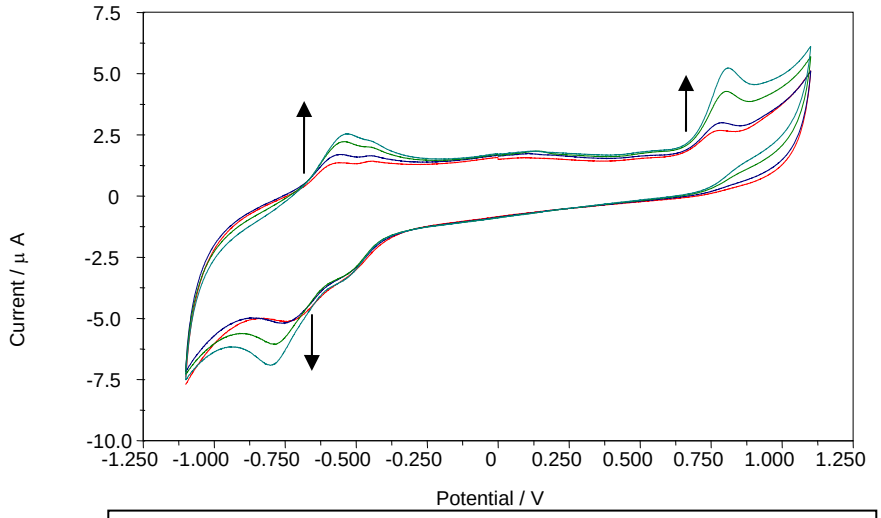

Figure 3.4. Cyclic voltammograms of increasing concentrations of folic acid (100 to 400 µM) at a glassy carbon electrode in pH 7 buffer. Scan Rate: 50mV/s

Cyclic voltammograms obtained for folate leads to a fairly complex voltammogram, the primary oxidation of folate occurs at +0.85V, with no corresponding reduction peaks. This can be attributed to the oxidation of the central aromatic amine which can be expected to possess some aniline type properties. However, other peaks are derived, with a quasi reversible redox system also identified at -0.50/-0.55V and -0.80/-0.60V. The latter is ascribed to the heterocyclic ring structure (Figure 3.4). It is important to note that, while there are a number of redox signatures, both sets are located near the extremes of the potential window. One benefit of this is that it provides an expansive middle section free from interference.

3.4.3. **Guanine (Guanosine and Deoxyguanosine)**

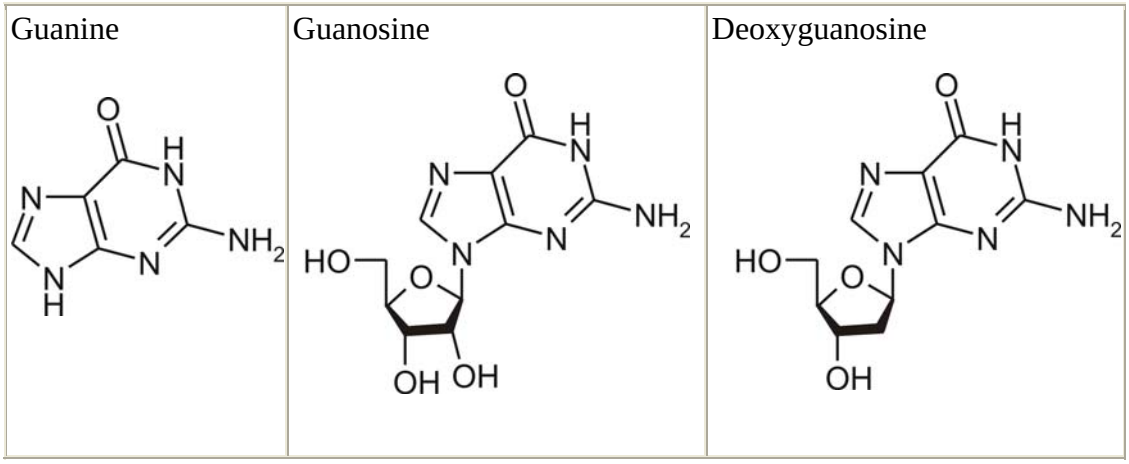

Figure 3.5. Structure of guanine, guanosine and deoxyguanosine

Guanine (via guanine nucleotides, Figure 3.5) is part of both DNA and RNA, in which it is bound to cytosine residues through three hydrogen bonds. In DNA and RNA, the guanine tends to undergo more reactions than the other 4 bases [18] and, as such, its oxidative modification has been ascribed as a major cause of genetic mutations in both eukaryotic and prokaryotic cells, in mammals this has been associated with cancer [19]. However, guanine has many other physiological roles aside that of a nucleic acid; in guanosine triphosphate (GTP) as an energy source for metabolic reactions and also as a regulatory molecule for cellular processes [20]. Guanine is produced in the human body in the purine metabolism pathways and its synthesis is regulated by p53 conversion of inositol triphosphate (IMP) to xanthosine monophosphate (XMP) (prior to GMP) and forms the rate limiting step in guanine synthesis [21]. The detection and quantification of guanine is most commonly used in the investigation of Inborn Error of Metabolism (IEM) where the urinary concentration is measured. The identification of high levels of urinary guanine may be indicative of the deficiency of PNP (Purine-Nucleosid-phosphorylase) [22]. The most commonly used method of analysis is after HPLC whereby guanine can be measured spectrophotometrically, it is difficult to measure guanine directly in biological fluids, therefore the samples are commonly separated by HPLC or electrophoresis [23,24] prior to quantification. However it is also possible to detect guanine using pre-treated glassy-carbon electrodes, fluorometric dyes or UV

colorimetry [25,26] and may be assessed relative to other amino acids. The guanosine reference ranges are method specific, urine reference ranges were described by *Vidotto et al* in 2003 [22], 10.7 ± 10.0 (Mean ± Standard deviation in μmol/mmol creatinine)

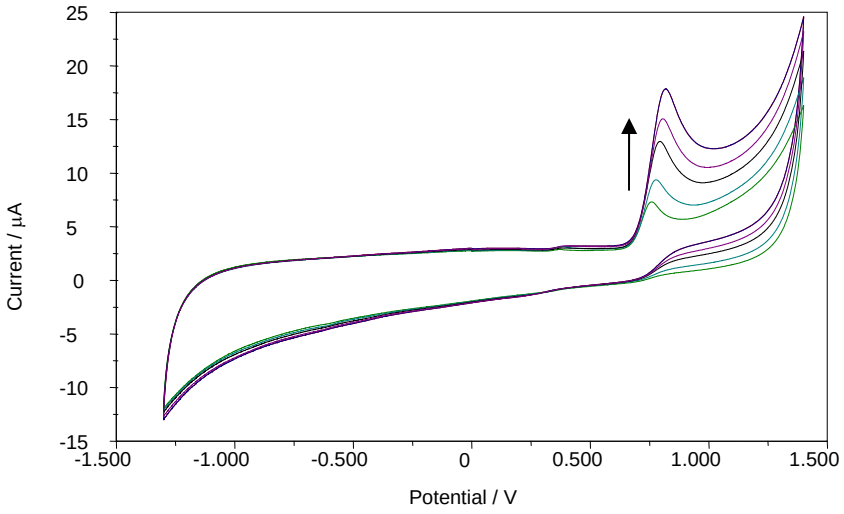

Figure 3.6. Cyclic voltammograms of increasing concentrations of guanine (100 to 500 μM) recorded at a glassy carbon electrode in pH 7 buffer. Scan Rate: 50mV/s

The cyclic voltammograms of guanine, detailed in Figure 3.6, highlight a sharp oxidation peak at +0.65V, the oxidised guanine is typically not reduced, hence the absence of a reduction peak. At very high concentrations a very small back peak is observed, but only at concentration far in excess of physiological concentrations. The peak height increases proportionally to concentration (100 to 500μM). The oxidation peak is again near the extreme of the anodic potential range and given that expected concentrations are liable to be low – the electrochemical characteristics would suggest that it represents neither a viable biomarker nor a substantive interferent.

3.4.4. **Iodide (I^-)**

Iodide is the reduced form of iodine. The main biological role of iodide / iodine in humans is for the synthesis of thyroid hormones Triiodothyronine (T3) and Tyroxine (T4). These are generally protein carried through the body in the serum [9]. It is the free

form of these hormones (FT3 and FrT4), which are biologically active and which are generally measured for the determination of thyroid function, along with Thyroid Stimulating Hormone (TSH). Iodide is an essential part of the thyroid hormones, which control the rate of metabolism. The recommended daily allowance of iodide is very low, 150 μg per day [9]. Despite iodine being present in most tap water [20], throughout the western world iodine is commonly added to milk or salt to help prevent iodine deficiency as this may lead to cretinism in children [28]. Iodine deficiency is still a large problem for developing countries. The symptoms of iodine deficiency include goitre (enlarged thyroid) and hypothyroidism (insufficient production of the thyroid hormones) and are primarily caused by inadequate iodine in the diet [28].

The plasma iodide is enzymatically trapped and incorporated into the thyroid where it is utilized in the synthesis of the thyroid hormones [9]. Therefore before exposure to radioactive iodine, (commonly used in medical imaging) the patient will take an excess of iodide (typically in the salt form e.g. sodium iodide) to prevent the radioactive form being taken into the thyroid, which would increase the risk of thyroidal cancer [9]. Iodine and iodide are not commonly measured in biological fluids. However it can be measured in urine (preferably 24 hour collection) and serum. The following methods may be used for iodine measurement: iodine selective electrodes [9], micellar electrokinetic capillary chromatography [29], atomic absorption spectroscopy [27], energy dispersive x-ray fluorescence spectrometry [27] and dry / wet ashing [30]

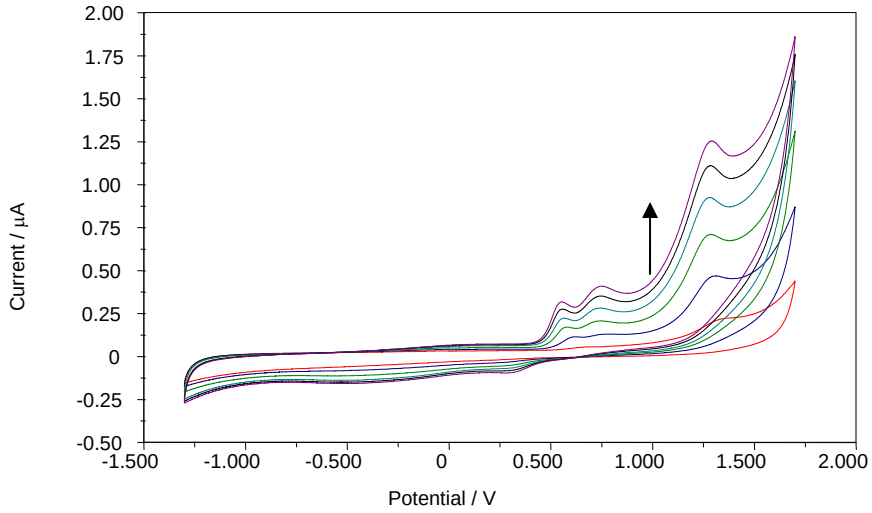

Figure 3.7. Cyclic voltammograms of increasing concentrations of potassium iodide (100 to 500 μM) recorded at a glassy carbon electrode in pH 7 buffer. Scan Rate: 50mV/s

The electrochemistry of iodine/iodide leads to a very complex voltammetric profile. Three clear oxidation peaks arise (0.55, 0.72 and 1.51V) through the sequential oxidation of iodide to triiodide, triiodide to iodine and iodine to iodic acid, respectively. Many problems are encountered to detect iodide electrochemically due to the extremely low free-concentrations of the iodine ions, the relatively small oxidation (and reduction) potentials, coupled with the complexity of the voltammograms. Again, it is clear that iodide does not represent a viable marker given the complex nature of the analysis profile. Fortunately, the relative low concentration of free iodide within biological fluids also means that it is unlikely to represent a major interferent in the analysis process.

3.4.5 **Nitrites and Nitrates (NO_2^- and NO_3^-)**

Nitrite and nitrate ions are final metabolic products of nitric oxide degradation [31]. Nitrite can be detected and measured in a variety of biological fluids including: saliva, urine, blood, plasma and serum [31]. The detection of nitrite in urine is indicative of an infection as bacteria convert nitrate into nitrites. This test can be used to assess whether a patient is likely to have or not have a urinary tract infection (UTI) [9]. The detection of nitrite is usually semi-quantitative using urine dipsticks. In nitrite dipsticks the nitrite in the urine reacts with arsanilic acid to produce diazonium salt, this couples with a quinolol to produce a pink colour. The test typically has a detection limit of 13 to 22 μmol/L and is intended for the detection of infections caused by at least 10^5 bacteria per mL [9]. Nitrites in the blood act as nitric oxide stores, but as this compound is toxic, elevated levels can lead to infantile methaemaglobulinaemia and carcinogenesis [31,32].

The measurement of nitrites in blood requires a greater preparation due to the short half life and rapid oxidation of nitrites in blood by heme proteins e.g. haemoglobin, therefore it may be necessary to perform an extensive extraction protocol immediately after phlebotomy [25]. Commonly used methods for the quantification of nitrite in biological samples are; HPLC, GC-MS, Griess assay, capillary electrophoresis and chemiluminescence. [32,33,34] Concentrations of nitrite in blood, serum and plasma are very low in normal subjects, one study suggested a serum normal range of 15-70μM [26].

However another has reported 282-328 nmol/L as a range of results obtained from normal subjects [34], therefore the aforementioned problems with collection, storage and measurement appear to have caused conflicting results. From a literature search it becomes apparent that there is a need for more reliable and reproducible methods of sample preservation or treatment and analysis to provide the accurate results required.

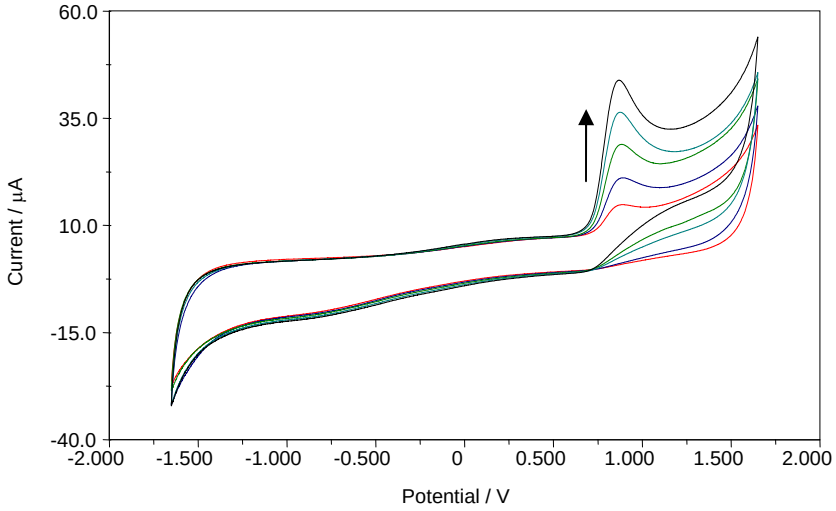

Figure 3.8. Cyclic voltammograms of increasing concentrations of sodium nitrite (100 to 500 µM) recorded at a glassy carbon electrode in pH 7. Scan Rate: 50mV/s

The voltammograms recorded for (sodium) nitrite are detailed in Figure 3.8 and lead to an oxidation peak at +0.74V due to the electrochemical conversion from the nitrite to the nitrate. The oxidation product can not be reduced back to nitrite at a plain glassy carbon electrode (GCE) and, as such, no reduction peak is observed. The oxidation peak increases proportionally with the increasing concentration. The response to increasing nitrite is qualitatively good but again suffers in terms of it exploitation as probe in that the position of the oxidation peak is observed at a relatively large anodic potential and its use would be questionable.

3.4.6 **Tryptophan**

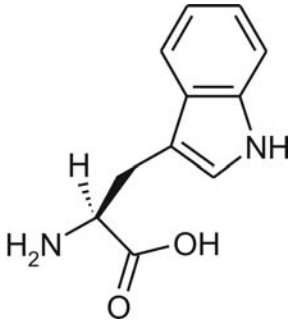

Figure 3.9. Tryptophan

Tryptophan (Trp), Figure 3.9, is an essential amino acid with a variety of roles within the human body - primarily in the synthesis and maintenance of proteins but is also important in the nitrogen balance [9, 35, 36]. Trp is a precursor for three main compounds: serotonin, melatonin and niacin, and has the ability to cross the blood brain barrier by specific carriers for neutral amino acids. It may subsequently be converted to serotonin by tryptophan hydroxylase [37]. Serotonin is involved in the control of mood and emotion and food behaviour [38]. Tryptophan may also be metabolised into melatonin, which is released at or after dusk and is continuously released throughout the night until dawn [39]. As well as being involved in the control of sleep, melatonin is also involved in seasonal cycles. Abnormal levels of melatonin have been associated with many psychotic illness including Seasonal Affective Disorder (SAD) and bipolar depression [42]. In normal women with stable mood, the level of Trp in the plasma increases in the first 2 days post labour. However it has been found that the levels remain continuously low in women with post-partum blues and that there is an increased degradation in post-partum blues [35, 40]. The plasma concentrations have been associated with obesity. It was found that in obese patients, the plasma Trp concentration and the ratio of Trp: other large amino acid are both low [41]. From this it has been predicted that the consequent Trp uptake and serotonin production may lead to abnormally low concentrations of serotonin. This was found by measuring levels in the plasma throughout 24 hour periods [41]. Trp is typically measured by HPLC with UV detection [36], with typical plasma reference ranges of 20 – 95 μmol/L [9].

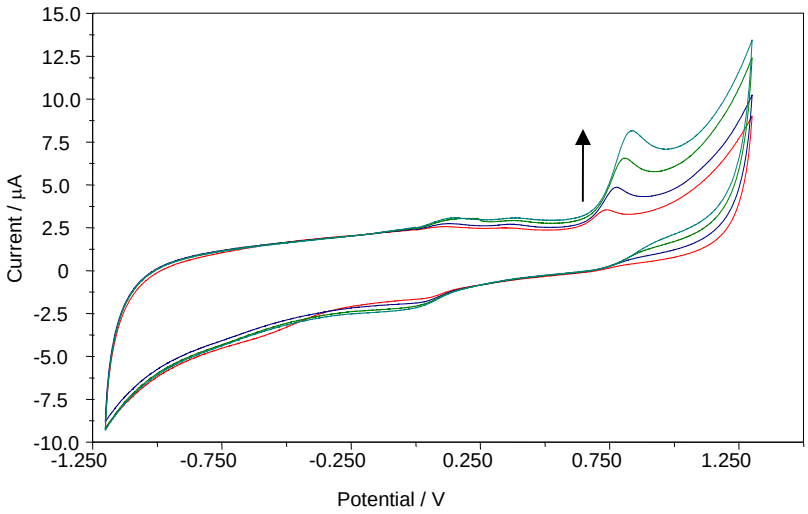

Figure 3.10. Cyclic voltammograms of increasing concentrations of tryptophan (100 to 400 µM) recorded at a glassy carbon electrode in pH 7 buffer. Scan Rate: 50mV/s

The voltammograms recorded for the response of Trp, Figure 3.10, leads initially to an oxidation peak at +0.84V. Although the primary oxidation, this produces a tryptophan radical, which form as polymeric deposit on the electrode surface, resulting in the reversible redox peaks at +0.10 and -0.05V. Whilst the primary oxidation of tryptophan does increase linearly with concentration increase, the polymeric product provides much smaller peaks and may not increase proportionally. On initial inspection it can be suggested that tryptophan, by possessing a relatively large oxidation potential, would fall short of being considered as probe for the pH studies. The emergence of the secondary redox processes however could provide a versatile handle through which to monitor pH as they lie in the centre of voltammetric window and thus liable to lie within the region where most other species appear to be oxidised, as evidenced by the majority of the voltammetric signatures investigated thus far. The unusual nature of this is studied further as a potential pH probe later in the next chapter.

3.4.7 **Tyrosine**

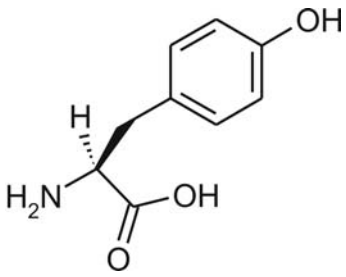

Figure 3.11. Tyrosine

Tyrosine (Tyr), Figure 3.11, can be oxidised to dityrosine [43]. It is usually a non-essential amino acid which is required for protein synthesis and is an intermediate in the synthesis of catecholamines (norepinephrine and epinephrine) thyroxine and melanin [9]. Although it can be absorbed from the diet Tyr is usually non-essential as tyrosine is also synthesised by the hydroxylation of phenylalanine. Phenylketonuria (PKU) is an IEM where this conversion does not occur due to an enzyme deficiency [44]. This results in too much phenylalanine and no tyrosine production, in this occurrence tyrosine becomes an essential amino acid and must be provided by the diet to prevent associated problems [45]. The measurement of tyrosine is used in the diagnosis of tyrosinemia, which has many forms (all of which express tyrosinuria and phenolic aciduria) and in the monitoring of PKU [9, 46].

There are many methods which can be used for measurement of tyrosine, the most commonly used is HPLC with UV detection, but it may also be measured by fluorometry and spectrophotometry [47]. It is important to monitor maternal phenylalanine and tyrosine in maternal PKU as a low concentration of tyrosine can be a factor in foetal damage [45]. Urine reference ranges vary but an example is 25 – 191 μmol/day [9], but can be up to double this in neonates [48].

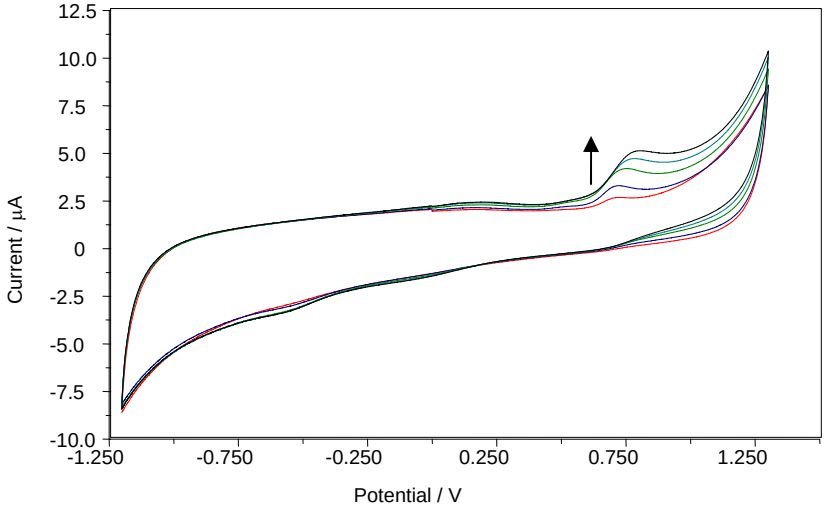

Figure 3.12. Cyclic voltammograms of increasing concentrations of tyrosine (100 to 500 μM) recorded at a glassy carbon electrode in pH 7 buffer. Scan Rate: 50mV/s

The voltammetric profile for increasing additions of tyrosine (100 to 500μM) is highlighted in Figure 3.12. In common with many of the physiological markers observed thus far, it leads to a broad oxidation peak at +0.76V through conversion to dityrosine. The situation is slightly more complex in that the oxidation leads to the deposition of polymeric material on the electrode. This is similar to the response obtained with tryptophan but in this instance there are no secondary redox peaks observable on subsequent voltammetric scans. This can be attributed to the fact that, in contrast to the conducting nature of the poly(indole) type films to characteristic of tryptophan oxidation, the polyphenylene oxide films to which tyrosine belongs are wholly non conducting, passive films.

3.4.8 **Uric Acid / Urate**

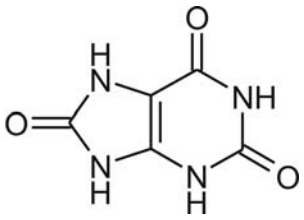

Figure 3.13. Urate

Uric acid (UA) can be oxidised to allantoin and is produced by the catabolism of purine nucleosides: adenosine and guanosine. These purines may be obtained directly from dietary sources, but the bulk of excreted UA is from degradation of endogenous nucleic acids. UA is typically found in the urate form at physiological pH and approximately 75% of the uric acid produced is lost in the urine with the majority of the remainder secreted into the gastrointestinal tract [9]. The condition most associated with abnormal uric acid levels, certainly with hyperuricaemia, is gout. This is a condition caused by excessive UA in the blood and fluid surrounding the joints which may crystallise as monosodium urate monohydrate in the synovial fluid and sometimes the surrounding tissue [49]. This causes the swelling and pain associated with gout. However, a high measurement of UA is not diagnostic of gout, it is commonly associated, instead the only true diagnostic test for gout is the identification of monosodium urate monohydrate crystals in the synovial fluid of the affected joint. In gout, a treatment such as alloprinol may be required to reduce the UA concentrations [50] in addition to dietary changes.

There are certain commonly reported risk factors associated with the development of gout, previously associated with excessive 'good living', these include: obesity, high purine diet (meat, seafood, alcohol) hypertension and other factors which cannot be altered e.g. sex and age [50]. Hyperuricaemia can lead to renal disease and UA is measured for the diagnosis and monitoring of pre-eclampsia and in patients receiving chemotherapy [44,51]. Hyperuricaemia may arise due to either increased formation or decreased excretion of uric acid [44]. UA is commonly measured in urine and serum by the uricase methods [9]. The reference ranges are method dependant. However for the commonly used uricase method, which is routinely automated, the following apply; Urine: 1.5 – 4.5 mmol/24h collection, Serum: Male 200 – 420 μmol/L, Female 150 – 350 μmol/L.

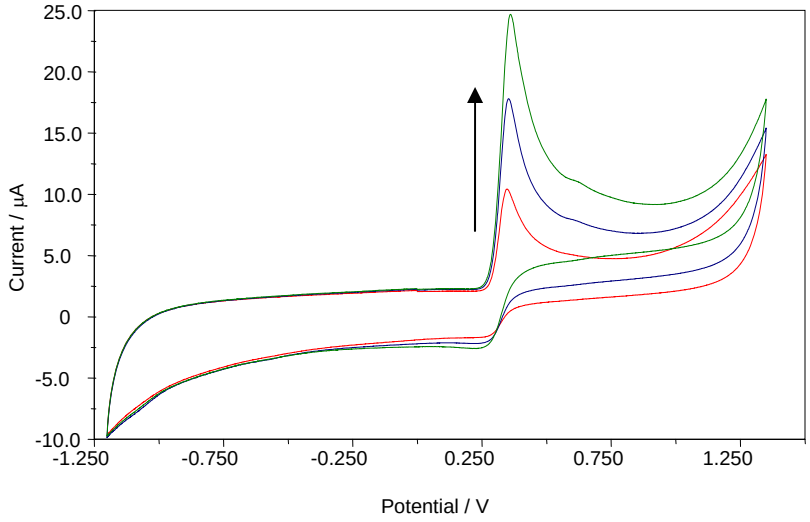

Figure 3.14. Cyclic voltammograms of increasing concentrations of uric acid (100 to 300 μM) recorded at a glassy carbon electrode in pH 7 buffer. Scan Rate: 50mV/s

The cyclic voltammograms recorded at a glassy carbon electrode in the presence of increasing concentrations of UA are detailed in Figure 3.14. In contrast to the majority of the voltammograms investigated thus far, the oxidation of UA produces a sharp signal with a magnitude far greater than previous biomolecules. The sharp oxidation peak at +0.37V is attributed to the transformation of UA to a quinone-imine intermediate. This process is quasi reversible with a back-peak due to partial reduction of the oxidation product observed +0.29V, particularly at high urate concentrations. The oxidation peak

heights increase proportionally with increasing concentrations. There are number of points to note from the voltammograms detailed in Figure 3.14. First is the fact that the position of the peak is significantly lower than the other biomolecules and second, the intensity of the oxidation process. The latter can be ascribed in part to an adsorption effect. The planar nature of the purine and the multitude of functionality with alternating polarity may favour hydrogen bonding with other polar groups on the carbon surface. The possibility is explored in subsequent chapters but it is clear that the relatively large abundance of urate and favourable electrochemical properties would appear to place this molecule as a candidate for further investigation as a potential pH probe.

3.4.9 **Xanthine**

Xanthine, Figure 3.15, is a key player in the same metabolic pathway as UA (catabolism of purines) and can be oxidised to UA. Xanthine is produced after inosine nucleic acids are converted to hypoxanthine by Purine Nucleoside Phosphorylase (PNP). The hypoxanthine is subsequently converted to xanthine by xanthine oxidase, the same enzyme that further converts xanthine to UA [9]. Xanthine is therefore a precursor of UA and one which is normally present in low concentrations [52] in comparison to UA and can be attributed to the latter being effectively the end product of purine catabolism.

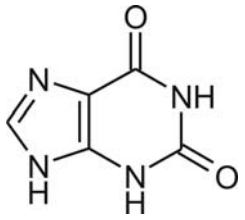

Figure 3.15. Xanthine

The cause of clinically raised levels of xanthine is usually a hereditary xanthinuria (xanthine in the urine) which are extremely rare set of hereditary diseases causing a defect in the purine metabolism. These are caused by a deficiency in one of the enzymes involved in the pathway, typically *xanthine oxidase* [53, 54]. As this enzyme is involved in the conversion of hypoxanthine to xanthine initially, a deficiency of this enzyme often causes very high levels of hypoxanthine in the urine; this can cause problems due to its low solubility and may therefore cause renal stones and subsequent haematuria and can lead to acute or chronic renal failure [46]. Xanthine concentrations can be measured in serum, urine, amniotic fluid and CSF by HPLC, GC-MS and enzymatically [52], with

reference ranges for: urine: <0.03 mmol / mmol of creatinine and plasma: 0.3 – 3.0 μmol/L.

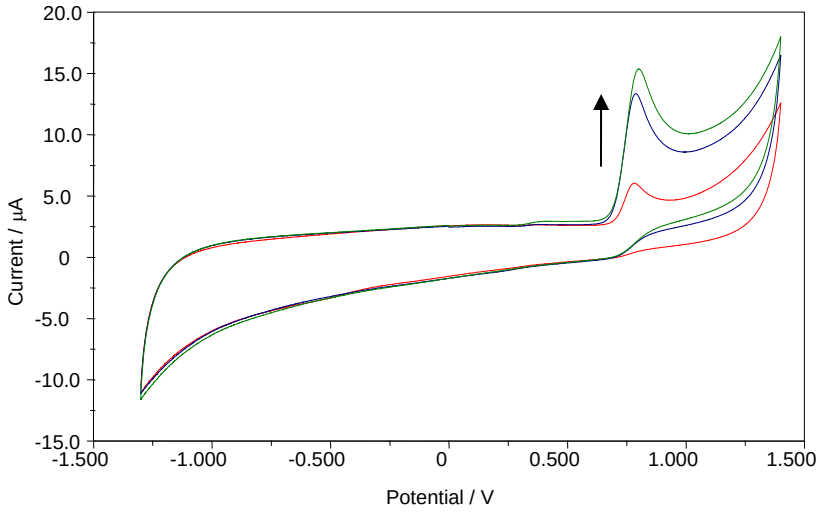

Figure 3.16. Cyclic voltammograms of increasing concentrations of xanthine (100 to 300 μM) recorded at a glassy carbon electrode in pH 7 buffer. Scan Rate: 50mV/s

Upon initial inspection, the voltammograms of xanthine look similar to those of urate and this could be expected, at least in part, due to the planar-polar nature of the purine. A single sharp peak is observed which has an adsorptive character. The main difference however lies in the relative peak positions. The oxidation of xanthine is more difficult to achieve than that of urate as evidenced by the oxidation peak at +0.80V. It could be anticipated that attempting to utilise this biomarker would be problematic despite the sensitivity of the peak. The latter would almost certainly be compromised by the presence of a multitude of other species that also undergo oxidation at such high potentials – many of which have been examined in this section.

3.5 Conclusions

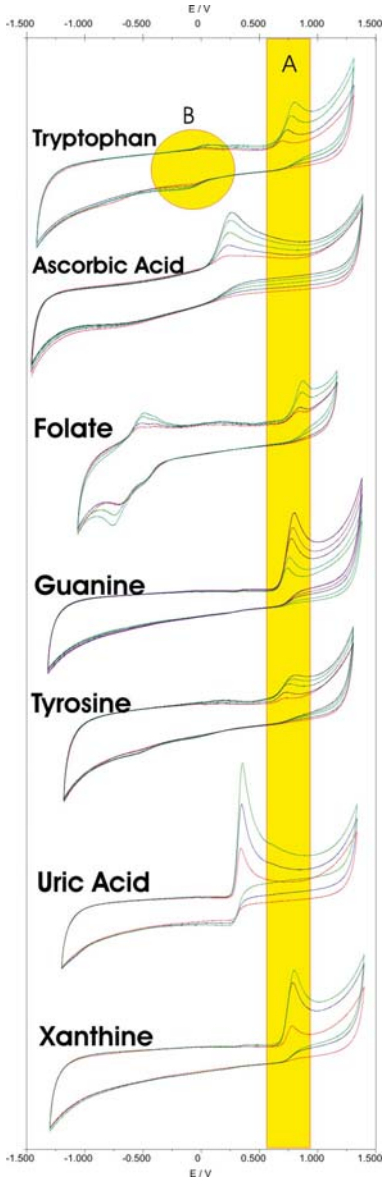

Figure 3.17. Comparison of oxidation peaks of 7 endogenous compounds (A) and the observation of the polymer oxidation/reduction (B) recorded at a conventional glassy carbon electrode. Scan Rate: 50mV/s

Due to the presence of such a wide variety of biological compounds that are able to undergo electrochemical interactions, the choice of the marker is of upmost importance as an *in situ* sensor would be safer and generally cheaper with no modification or just a physical modification (rather than chemical modification). These results obtained for the candidate probes highlight that fact that many overlap with each other. This is highlighted when the voltammograms are compared (**Figure 3.17**). The highlighted region (**A**) shows the overlap of many species, however, there are certain interactions which fall outside this common region. Importantly, Trp has a reversible interaction at +0.05V and -0.1V (highlighted **B**), this could be highly significant given the apparent lack of any interference at these potentials. The presence of this reversible redox interaction due to polymerisation of the Trp onto the sensor surface. A critical factor in choosing a marker is the physiological concentrations, whilst tryptophan is typically as very low concentrations, the ability to pre-concentrate via polymerisation on the electrode surface may allow sufficient peak magnitudes to be observed, a feature unique to Trp of the available biomolecules. Other potential probes include AA and UA, both of which have oxidation potentials outside of the common overlap region. However these both occur as similar oxidation potentials and therefore electrode modification would be required. AA is typically found in lower concentrations than UA, additionally the physical modification to remove the UA peak is difficult therefore, an alternative approach to the Trp polymerisation is the detection of UA. The next stage is to assess how they behave when the pH is variable and under simulated wound conditions.

3.6 References

1. Chai, JK. The pH value of granulating wound and skin graft in burn patients. *Chinese Journal of Plastic Surgery and Burns* 1992;8(3):177-8
2. Schneider, LA, Korber A, Grabbe D, Dissemond J. Influence of pH on wound-healing: a new perspective for wound-therapy? *Archive of Dermatological Research* 2007;298(9):413-20
3. Shukla, VK, Shukla, D, Timary, SK, Agrawal, S, Rastogi A. Evaluation of pH measurement as a method of wound assessment. *Journal of Wound Care* 2007;16(7):291-4
4. Mousa, HA. Aerobic, anaerobic and fungal burns wound infections. *Journal of Hospital Infection* 1997;37:317-23
5. Dissemond J, Witthoff M, Brauns, TC, Goos M. pH values in chronic wounds. Evaluation during modern wound therapy (in German). *Hautarzt* 2003;54(10):959-65
6. Prissanaroon-Ouajai W, Pigram PJ, Jones R, Sirivat A. A novel pH sensor based on hydroquinone monosulfonate-doped conducting polypyrrole. *Sensors and Actuators B: Chemical* 2008;135:366-74
7. Pandey PC, Singh G. Tetraphenylborate doped polyaniline based novel pH sensor and solid-state urea biosensor. *Talanta* 2001;55:773-82
8. Zeng W, Martinuzzi F, MacGregor A. Development and application of a novel UV method for the analysis of ascorbic acid. *Journal of Pharmacological and Biomedical Analysis* 2005;36:1107-11
9. Burtis CA, Ashwood ER, Bruns DE. Tietz textbook of Clinical Chemistry 4th edition 2006. Elsevier Saunders, Missouri USA.
10. Liu H, Xiang B, Qu L. Structure analysis of ascorbic acid using near-infrared spectroscopy and generalized two-dimensional correlation spectroscopy. *Journal of molecular structure* 2006;794:12-7
11. Hodges RE, Hood J, Canham J, Sauberlich, HE, Baker EM. Clinical manifestation of ascorbic acid deficiency in man. *American Journal of Clinical Nutrition* 1971;24:432-443.
12. Lee W, Davis K, Rettmer RL, Labbe RF. Ascorbic acid status: biochemical and clinical considerations. *American Journal of Clinical Nutrition* 1988;48:286-90
13. Muskiet FAJ. The importance of (early) folate status to primary and secondary coronary artery disease prevention. *Reproductive Toxicology* 2005;20:403-10.
14. Ueland PM, Vollset SE. Homocysteine and folate in pregnancy. *Clinical Chemistry* 2004;50(8):1293-5
15. Charles D, Ness AR, Campbell D, Smith GD, Hall MH. Taking folate in pregnancy and risk of maternal breast cancer. *British Medical Journal* 2004;329:1375-6
16. Shane B, Tamura T, Stokstad ELR. Folate assay: A comparison of radioassay and microbilogical methods. *Clinica Chimica Acta* 1980: 13-9
17. Kubasik NP, Graham M, Sine HE. Storage and stability of folate and vitamin B-12 in plasma and blood samples. *Clinica Chimica Acta* 1979:147-9

18. Thorp HH. Cutting out the middleman: DNA biosensors based on electrochemical oxidation. *TIBTECH* 1998;16
19. Ishibashi T, Hayakawa H, Sekiguchi M. A novel mechanism for preventing mutations caused by oxidation of guanine nucleotides. *European Molecular Biology Organization Reports* 2003;4(5):479-83
20. Davidson VL, Sittman DB, editors. *Biochemistry 3rd Edition* 1994. Harwal Publishing Company, Philadelphia, USA.
21. Sherley JL. Guanine nucleotide biosynthesis is regulated by the cellular p53 concentration. *The Journal of Biological Chemistry* 1991;266(36):24815-28
22. Vidotto C, Fousert D, Akkermann M, Griesmacher, A, Muller MM. Purine and pyrimidine metabolites in children's urine. *Clinica Chimica Acta* 2003;335:27-32
23. Pogson CI. Guanine nucleotides and their significance in biochemical processes. *The American Journal of Clinical Nutrition* 1974;27:380-402
24. Edenbrandt CM, Murphy S. Adenine and guanine nucleotide metabolism during platelet storage at 22°C. *Blood* 1990;76:1884-92
25. Wang HS, Ju HX, Chen HY. Simultaneous determination of guanine and adenine in DNA using an electrochemically pretreated glassy carbon electrode. *Analytica Chimica Acta* 2002;461:243-50
26. Todd B, Zhao J, Fleet G. HPLC measurement of guanine for the determination of nucleic acids (RNA) in yeasts. *Journal of Microbiological Methods* 1995;22:1-10
27. Varga I. Iodine determination in dietary supplement products by TXRF and ICP-AES spectrometry. *Microchemical Journal* 2007;85(1):127-31
28. Davidson VL, Sittman DB. Biochemistry 3rd Edition 1994. Harwal Publishing Company, Philadelphia, USA.
29. Bjergegaard C, Moller P, Sorensen H. Determination of thiocyanate, iodide, nitrate and nitrite in biological samples by Micellar Electrokinetic capillary chromatography. *Journal of Chromatography A* 1995;717:409-14
30. Demers LM, Spencer CA editors. National Academy of Clinical Biochemistry laboratory medicine practice guidelines. Laboratory support for the diagnosis of thyroid disease, Section III 2002;13:76-81 The National Academy of Clinical Biochemistry Washington. .
31. Kleinbongard P, Dejam A, Lauer T, Rassaf T, Schindler A, Picker O *et al.* Plasma nitrite reflects constitutive nitric oxide synthase activity in mammals. *Free radical Biology and Medicine* 2003;35(7):790-6
32. Gaspar A, Juhasz P, Bagyi K. Application of capillary zone electrophoresis to the analysis and to a stability study of nitrite and nitrate in saliva. *Journal of Chromatography A* 2005;1065:327–31
33. Tsikas D, Fuchs I, Gutzki FM, Frolich JC. Measurement of nitrite and nitrate in plasma, serum and urine of humans by high performance liquid-chromatography, the Griess assay,

chemiluminescence and gas chromatography-mass spectrometry: Interferences by biogenic amines and NG-nitro-L-arginine analogs. *Journal of Chromatogrpahy B* 1998;715:441-4

34. Pelletier MM, Kleinbongard P, Ringwood L, Hito R, Hunter CJ, Schechter AN *et al*. The measurement of blood and plasma nitrite by chemiluminescence: pitfalls and solutions. *Free Radical Biology and Medicine* 2006;41:541-8.
35. Porter RJ, Mulder RT, Joyce PR, Luty SE. Tryptophan and tyrosine availability and response to antidepressant treatment in major depression. *Journal of Affective Disorders* 2005;86:129-34
36. Birmes P, Coppin D, Schmitt L, Lauque D. Serotonin syndrome: a brief review. *Canadian Medical Association Journal* 2003;168 (11):1439-42
37. Laich A, Neurauter G, Widner B, Fuchs D. More rapid method for simultaneous measurement of tryptophan and kynurenine by HPLC. *Clinical Chemistry* 2002;48(3):579-81
38. Breum L, Rasmussen MH, Hilsted J, Fernstone JD. Twenty-four-hour plasma tryptophan concentrations and ratios are below normal in obese subjects and are not normalized by substantial weight reduction. *The American Journal of Clinical Nutrition* 2003;77:1112-8
39. Hazlerigg DG. What is the role of melatonin within the anterior pituitary? *Journal of Endocrinology* 2001;170:493-501.
40. Kohl C, Walch T, Huber R, Kemmler G, Neurauter G, Fuchs D *et al*. Measurement of tryptophan, kynurenine and neopterin in women with and without postpartum blues. *Journal of Affective Disorders* 2005;86:135-42.
41. Pacchierotti C, Iapichino S, Bossini L, Pieraccini F, Castrogiovanni P. Melatonin in psychiatric disorders: a review on the melatonin involvement in psychiatry. *Frontiers in Neuroendocrinology* 2001;22:18-32
42. Yound SN. Use of tryptophan in combination with other antidepressant treatments: a review. *Journal of Psychiatric Neuroscience* 1991:16(5):241-246
43. Tien M. Myeloperoxidase-catalysed oxidation of tyrosine. *Archives of Biochemistry and Biophysics* 1999;367(1):61-6
44. Dale Y, Mackay V, Mushi R, Nyanda A, Maleque M, Ike J. Simultaneous measurement of phenylalanine and tyrosine in phenylketonuric plasma and dried blood by high-performance liquid chromatography. *Journal of Chromatography B* 2003'799(293):1-8
45. Rohr FJ, Lobbregt D, Levy HL. Tyrosine supplementation in the treatment of maternal phenylketonuria. *American Journal of Clinical Nutrition* 1998;67:473-6
46. Spierto FW, Whitfield W, Apetz M, Hannon WH. Liquid-chromatographic measurement of phenylalanine and tyrosine in Serum. *Clinical Chemistry*1982;28(11):2282-5
47. Ambrose JA. Fluorometric measurement of tyrosine in serum and plasma. *Clinical Chemistry* 1974;20(4):505-10
48. Shapwa E, Blitzer MG, Miller JB, Africk DK eds. Biochemical Genetics: a laboratory manual. Oxford, UK. Oxford University Press 1989: 96-7

49. Falasca GF. Metabolic diseases: Gout. *Clinics in Dermatology* 2006;24:498-508
50. Weaver AL. Case 3: Acute Gout – risk factors and inappropriate therapy. *The American Journal of Medicine* 2006;119(11A):S9-S12
51. Schakis RC. Hyperuricaemia and pre-eclampsia: is there a pathogenic link? *Medical Hypotheses* 2004;63:239-44
52. Shihabi ZK, Hinsdale ME, Bleyer AJ. Xanthine analysis in biological fluids by capillary electrophoresis. *Journal of Chromatography B* 1995;669:163-9
53. R. Zannolli, Micheli V, Mazzei MA, Sacco P, Piomboni, P,Bruni E *et al*. Hereditary xanthinuria type II associated with mental delay, autism, cortical renal cysts, nephrocalcinosis, osteopenia, and hair and teeth defects. *Journal of Medical Genetics* 2003; 40:e121
54. Shibutani Y, Ueo T, Yamamoto T, Takahashi S, Moriwaki Y, Higashino K. A case of classical xanthinuria (type I) with diabetes mellitus and hashimoto's thyroiditis. *Clinica Chimica Acta* 1999;285:183-9

Chapter 4

Development of a poly-tryptophan based pH sensor

Abstract

The ability to monitor pH in wound fluids is of clear benefit to a range of healthcare scenarios in terms of direct clinical and patient led wound management. Changes in pH have been associated with many important changes within the wound environment, prominently through healing progression or due to bacterial infections. The development of a novel electrochemical pH sensor is described for use within wound exudates using small and chemical-free sensing technologies. The new tryptophan-based sensor has been developed, whereby free-tryptophan is polymerised onto the electrode surface acting as a pre-concentration step. The electrochemical evaluation of this polymeric deposit is shown to allow the measurement of pH as a result of the potential shift of the peaks associated with the redox processes. This is a novel approach, not only in the use of an endogenous marker of pH but also the *in situ* sequestering of the target species to effectively allow preconcentration on a solid-phase sensor.

Work detailed in this chapter has been published in *The Journal of Chemistry and Physics of Solids* 2008; 69: 2932-2935.

4.1 Introduction

The introduction to pH sensing in wound environments was outlined in the previous chapter. A number of preliminary studies identified the possibility of exploiting the electrochemical polymerisation of tryptophan (to a polyindole type framework). The identification of this polymerisation warranted further evaluation to assess its suitability as a pH sensitive probe. The adoption of this approach stands in marked contrast to current strategies as rather than modifying the electrode surface prior to placing within the wound, this approach would exploit a physiological molecule endogenous to the actual wound fluid and thereby deftly obviate any issues associated with biocompatibility.

The relatively small size of tryptophan (Trp) allows simple diffusion through capillary leakage that forms the wound exudate, only larger molecules such as albumin, are inhibited (partially) from the exudate. While the concentrations of Trp in biofluids are typically very low, the reference range is 20-95μM in human plasma [1]. The aforementioned polymerisation onto the electrode surface could, in principle, allow for more sensitive measurements than for the Trp monomer itself especially as the redox peaks attributed to the polymeric deposit reside within a region where there are few competing processes. The polymerisation of Trp has previously been investigated, but the exact mechanism of the polymeric product is believed to be multifaceted. It mainly relies upon the nucleophilic attack by water on the highly electrophilic (i.e. reactive) methylene-imine product of the primary oxidation [2] although numerous other intermediates and products can result and influence the final composition of the film. The exact mechanism or structure of the polymeric film deposited have not been rationalised and, as such, the polymeric product will be referred to simply as poly-Trp herein. As Trp has acid:base properties derived from the carboxyl groups, it is expected that the changing pH will alter the potentials required for redox transformations within the poly-Trp, as long as the carboxyl groups are maintained during polymerisation.

The modification of carbon substrates by amperometric anodisation of carbon fibre sensors is essential for their enhancing their sensitivity and specificity towards key biomolecular measurements. The surface of carbon can be modified by mechanical [3-5],

electrochemical [6-13], chemical [13-20] or thermal [21] means. There are typically three different levels of surface modification: alteration of the functionalities already present on the surface; the covalent attachment of hitherto exogenous species onto the electrode surface and, in the last level, the intercalation of species between the graphene layers of the base substrate. Altering the surface composition is amongst the more facile and can usually be achieved through the electrochemical pre-treatment/fracturing of the carbon substrate [6,11,16] as indicated in **Figure 4.1**.

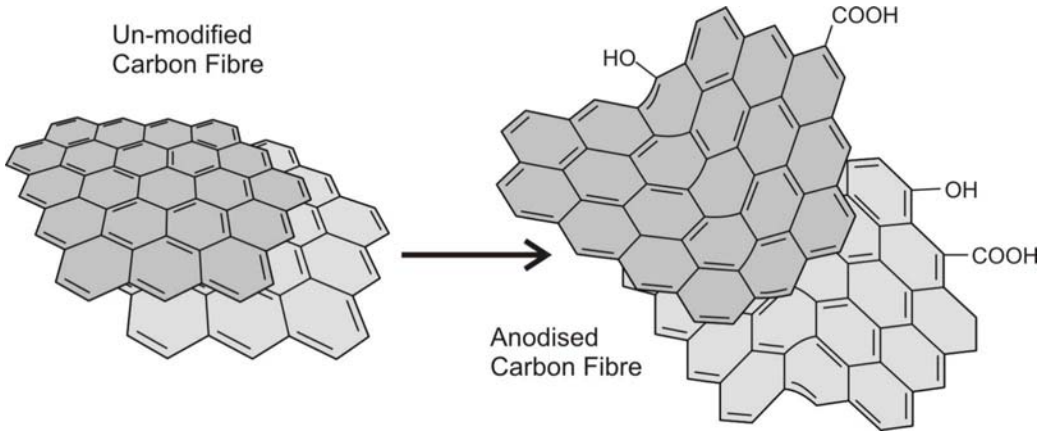

Figure 4.1. Schematic of the anodisation process

This typically involves the electro-oxidation of the carbon surface by applying a fixed anodic or cyclic potential. The oxidation increases the proportion of oxygen species such as hydroxyl, carbonyl, carboxyl and quinones at the electrode surface [13]. These are well known to influence the wettability, surface reactivity, porosity and conductivity of the electrode [6,7,9,22]. It can also have the beneficial effect of increasing the availability of edge plane sites as a consequence of exfoliation / fracturing processes that can, as with edge plane pyrolytic graphite (EPPG) electrodes, serve to increase electrode sensitivity towards particular analytes.

The large variety of physical forms that carbon can take allows for considerable versatility in the design of the sensor substrates used in electroanalytical applications. Glassy carbon, aerogels, fibre, graphitic felts and pastes are but a few of the more common [22]. Highly orientated pyrolytic graphite (HOPG) offering edge plane (EPPG) and basal plane (BPPG) morphologies are frequently used to explore the more

fundamental side of electron transfer processes but have found increasing application in analytical contexts. The basal and edge plane possess different properties with the latter tending to exhibit considerably faster electrode kinetics and, as a consequence, possesses the potential for greater detection sensitivities [3,4,23,24].

Laser patterning of carbon encapsulated composites have been shown to provide a quick and versatile method of producing electrode sensor assemblies but the ability of the laser to positively influence the surface characteristics of the underlying fibre has yet to be evaluated. The adoption of the electrochemical anodisation approach requires the introduction of a separate/discrete step in the construction of the electrode sensor and it is clear that combining the patterning/activation process would represent a considerable simplification in the development process. As part of the development of a poly-Trp pH sensor, the use of laser ablation as a means of removing protective polymer encapsulates to expose and ***activate*** the sensor surface in a single step is assessed. The rationale is to develop a faster and automatable approach towards the anodisation of the carbon sensors and for the optimal activation of the carbon-polycarbonate sensing substrates.

4.2 Experimental Details

*Materials***:** All reagents were of the highest grade available and used without further purification. Stock solutions of UA, (typically 5mM) were prepared in 0.1M NaOH. All other solutions were prepared using pH 7 BR buffer. For the development of a suitable conditioning potential for electropolymerisation of the Trp polymer to allow SqWV analyses the potential and times were varied between +0.5V and +1.1V (at 0.1V increments) and at conditioning times of 1, 2, 5, 10, 30, 60 and 120 seconds. The final characterisation is performed using the optimal and efficient +1.0V for 5 seconds conditioning immediately prior to SqWV. Electrochemical measurements were conducted using a μAutolab type III computer controlled potentiostat (Eco-Chemie, Utrecht, The Netherlands) using a three electrode configuration consisting of a glassy carbon working electrode (3mm diameter, BAS Technicol, UK), a platinum wire counter electrode and a 3 M NaCl Ag | AgCl half cell reference electrode (BAS Technicol, UK). Modification of carbon fibre electrodes was investigated using a 30W CO_2 air-cooled

computer controlled laser-cutter (FB400 series CadCam Technology Ltd, Nottingham, UK). Directional control over the laser, raster/vector speed and output power was achieved by means of the proprietary software (ApS-Ethos). The resolution of the laser beam was 25 μm. Electrochemical anodisation of carbon fibres was conducted using the procedures described previously [25,26] and typically involved amperometric oxidation (+2V, 15 minutes) in 0.1M sodium hydroxide solution.

4.3 Results and Discussion

4.3.1. Optimisation of Electropolymerisation

Having conducted a preliminary investigation of the response of tryptophan with cyclic voltammetry using glassy carbon electrodes (GCEs) in a conventional three-electrode system it was observed that an oxidation/reduction cycle attributed to the electrogenerated poly-Trp film could be seen at approximately +0.13V and +0.02V respectively (**Figure 3.17**). The next stage was to evaluate the electropolymerisation and characterize the polymer growth processes by repetitive voltammetric scans. The first stage in this investigation was to assess whether the electropolymer growth was due to the number of scan replicates or concentration. A nominal concentration of 500 μM Trp was chosen for this preliminary experiment and cyclically scanned between -1.2V and +1.3V. **Figure 4.2** shows that while there is a difference in the primary oxidation peak (+0.8V) due to the deposition of oligomeric oxidative product there are no differences in the oxidation or reduction of the polymer (+0.21V and -0.02V respectively) itself thereby proving that the polymer does not grow with successive scans and is therefore likely to be redox polymer rather than a true conducting polymer (c.f. polypyrrole) capable of promoting its own growth. As such it is likely that it forms a tight layer that effectively serves as a diffusional barrier to its own monomer and thereby growth terminates after pin holes have been sealed.

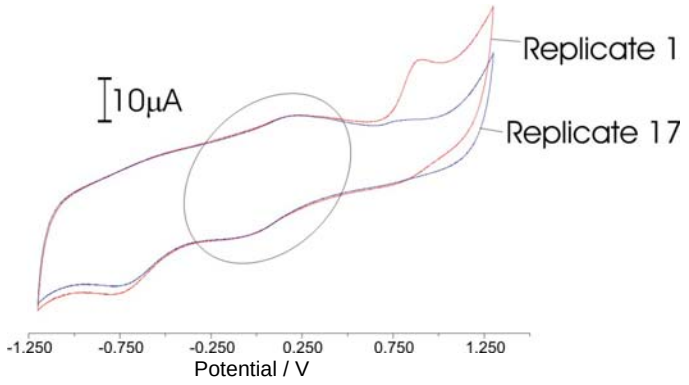

Figure 4.2. Cyclic voltammogram replicates from Trp. Scan Rate: 50mV/s

The availability of a distinct reduction process could be critical. In the previous investigations of the potential probe candidates – almost all exhibit oxidative processes – but none demonstrated any significant reduction process. The low potential observed with the poly Trp process is beneficial and in itself avoids many of those same electroactive interferes. Through selecting the reduction process – it was envisaged that this would secure the selectivity of the process. One possible issue is the reduction peak emanating from the reduction of urate given its quasi reversible characteristics. The only other issue would be molecular oxygen. As seen in **Figure 4.2**, the reduction of oxygen at -0.75V is apparent, but is distinct from the poly-Trp electrochemistry. Having established that the oxidation and reduction peaks do not change with scan replicates, the effect of concentration could then be assessed. Two sets of standards (0-170µM Trp) were used for the initial characterisation.

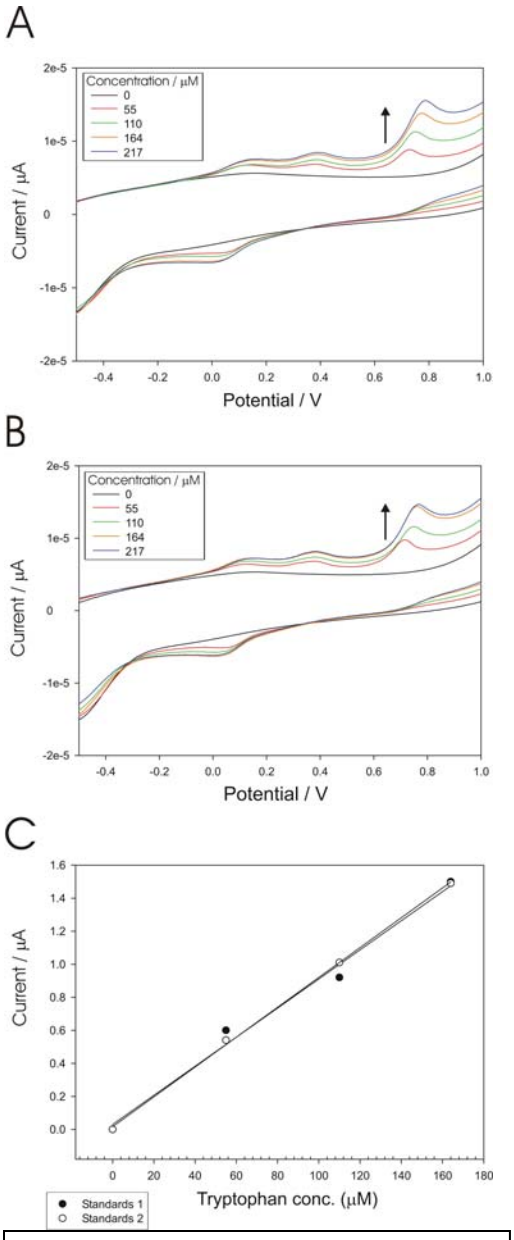

Figure 4.3:A, B; Detailed cyclic voltammograms for Tryptophan standards C; Standard plots obtained from A and B. Scan Rate: 50mV/s

This was selected on the basis of the concentration range expected within biofluids. The resulting voltammograms (**Figure 4.3A and 4.3B**) clearly show a proportional increase in peak height with increasing concentration and form linear standard plots (**Figure 4.3C**). In order to increase the sensitivity and ease of the measurements it was deemed an advantage to change from cyclic voltammetry to square wave voltammetry (Chapter 2) to further develop the analytical optimisation of the methodologies. In the previous instance, cyclic voltammetry was used to create the polymer during the **primary oxidation** of Trp, then using the return sweep to identify the redox process. In the case of square wave voltammetry – a single direction sweep is made and thus a suitable conditioning potential would be required prior to quantification by SqWV. The observation of the reduction peak (-0.02V) was chosen due to the previously stated factors as less endogenous electrochemically active compounds being reducible and of those tested there was no overlap with the reduction potential. There is also an extra oxidation peak observed at +0.39V, which could interfere with potential measurements.

A number of conditioning potentials (+0.5 - +1.1V) and times (1 - 120 seconds) were assessed to derive the optimal, most efficient electropolymerisation conditions (**Figure 4.4**). From this it was established that +1.0V was the most effective potential due to the greatest current being observed during the analysis of a 100μM standard (top of reference range). In order to allow for a more rapid measurement of Trp and to prevent electrode surface saturation with the poly-Trp at lower concentrations, a short conditioning period of 5 seconds was selected for further evaluation. Once the electropolymer had been deposited by the pre-measurement conditioning, the analytical step could be made by SqWV by scanning from +0.5V to -0.5V to observe the reduction

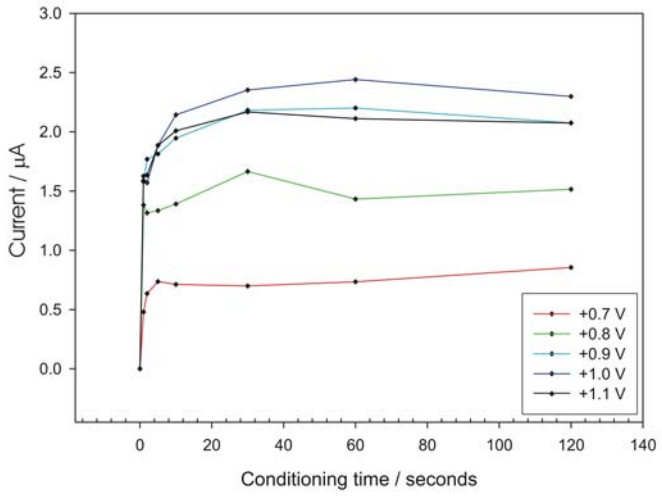

Figure 4.4; Assessment of conditioning potential and time on the reduction current for 100μM Trp measured by SqWV (+0.5V to -0.5V). Step height: 2mV, Amplitude: 10mV.

of the electrooxidation products. This scan range was utilised to prevent further electropolymerisation while allowing observation of the polymer reduction.

It is important to note that while this method is not primarily aimed at the quantification of the tryptophan in the wound exudate, the construction of low concentration standard plots (in buffered solution) is used mainly to highlight the sensitivity of the sensor system such that pH could be derived from the physiologically relevant concentrations.

When the pre-conditioned glassy carbon electrode was used to measure Trp in standard solutions within comparable concentrations to biofluids (i.e. 0-100μM) the electropolymerisation appeared to be saturated, as no increase in reduction current was observed. Therefore a lower standard range (0-17.5 μM) was assessed. **Figure 4.5A** details the square wave voltammograms for the nine standards measured and which were subsequently plotted to form a calibration plot **(Figure 4.5B)** with a clear linear correlation (r^2=0.994). It was anticipated that the sensitive nature of the poly-Trp detection, would ease the identification of pH promoted peak shifts in wound exudate.

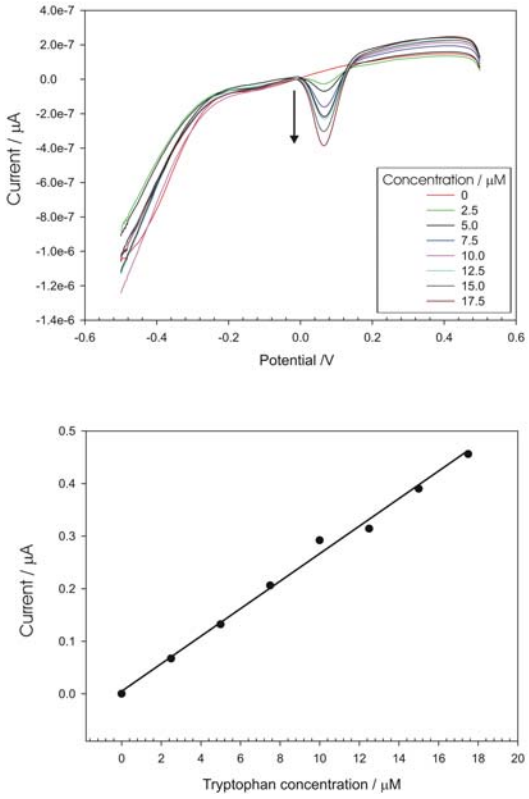

Figure 4.5:A). Square wave voltammograms of poly-Trp reduction from polymerized Trp standards. (B). Standard plot from current peaks obtained from A. Step height: 2mV, Amplitude: 10mV.

As the peak height is not of importance providing a clear and unambiguous signal is obtained, the necessity to maintain a linear calibration plot across the physiological range is largely irrelevant. Therefore, for the pH investigations, a polymerisation time of 30 seconds was used to ensure that a distinct peak was obtained at very low concentrations. Due to the small size of tryptophan it is anticipated that similar

concentrations would be observed in wound exudates to those of the peripheral circulatory system. There is little literature supporting the quantitative evaluation of tryptophan within wound exudates, however studies have found an average of 74μM in wound fluid (85% of serum concentration) over a 10 day study [27]. A concentration of 20μM was subsequently used for the assessment of pH sensitivity as this is well within the concentrations previously found and at the very bottom of the serum reference range. In this instance the use of SqWV was replaced with linear sweep voltammetry. The rationale for the change in experimental methodology reflects the fact that the latter would allow the introduction of a much simpler and hence cost effective electrochemical controller. The question that needed to be answered was whether or not such a change would unduly compromise the sensitivity of the measurement. While the initial work relied upon the use of a commercially available glassy carbon electrode, the development of small, flexible sensors suitable for encompassment within a wound dressing prompted the use of laminated carbon fibre matting electrodes as a further experimental refinement to the preliminary investigations. The challenge now is very much to attempt to move the sensor from a laboratory curiosity to something that could be transferred to a clinical setting.

The laminate electrodes, in their native unmodified form are largely unresponsive to bioconstituents. Anodisation (either chemical or by laser ablation) has been shown to sufficiently modify the electrode surface to enhance their electrochemical characteristics and allow their use for electroanalytical applications [26]**.**

4.3.2 *Carbon Fibre Matting*

This substrate was chosen for evaluation due to its reliability and ease of handling. The range pH 4 to pH 10 is generally accepted as spanning the desired remit for a smart-bandage application so as to exceed the actual clinical range observed in the studies reported in the Chapter One.

Initial testing by LSV (**Figure 4.6A**) lead to the construction of a linear calibration plot, **Figure 4.6B**, [reduction potential / V = -0.0423pH + 0.365, r ² 0.997], which clearly highlights the ability of this sensing system to monitor changing pH.

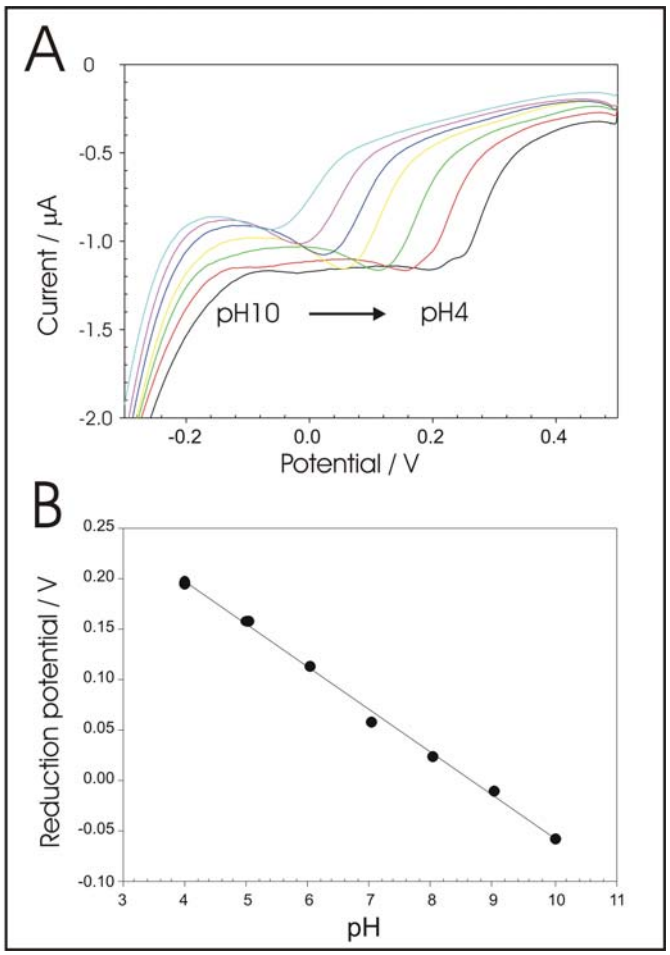

Figure 4.6.A) Linear sweep voltammetry poly-Trp reduction peak from polymerisation of 20µM Tryptophan in changing pH (4, 5, 6, 7, 8, 9, 10),
B). Calibration plot of reduction potential against pH.
Step potential; 1mV, Scan rate: 50mV/s.

Having proven that it can respond to changing pH, the influence of possible interferences needed to be assessed to ensure the system is analytically robust. As mentioned previously, the reduction of oxygen at the electrode surface is one possible interference. While it was found to be reduced at potentials significantly more negative potentials (-0.75V) than the poly-Trp peaks under fixed conditions at a glassy carbon electrode the same may not be true for the carbon fibre systems. It is also important to

remember that the peak will shift with pH – the basis of the measurement. **Figure 4.6B** highlights this fact with the peak position encroaching into the negative region as the pH is increased. The situation is further complicated by the possibility of oxygen concentration fluctuating within a wound environment. The presence and absence of oxygen must not mask or affect the peak position, and preferably size. The evaluation at a fixed concentration and pH both in the presence and absence of oxygen shows that there is no substantial difference between the scans (**Figure 4.7**) and therefore is not expected to affect reliability. The reduction of oxygen at the carbon fibre matting is still sufficiently negative to be inconsequential to the analysis of the poly Trp peaks.

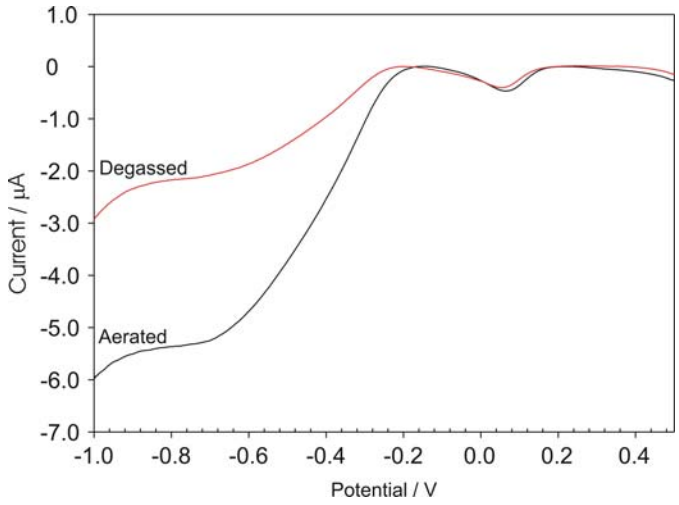

Figure 4.7. Linear sweep voltammetry of 20µM tryptophan in the presence (black) and absence (red) of oxygen. Step potential; 1mV, Scan rate: 50mV/s.

The reduction (back-peak) of the imine product of UA oxidation does however poses the possibility of interference with the measurements as previous experiments have shown that it can arise in a similar region. As UA also has acid:base properties, it would also be subject to shifting potentials with pH. A series of experiments were subsequently conducted using 500µM UA (physiological reference range 150-420µM) to assess the influence of this electrode process. Voltammograms showing the response to changing pH at fixed concentration of both Trp and UA are compared in **Figure 4.8** and offset for clarity. It is clear that a greater anodic shift is observed for the poly-Trp reduction peak, than the UA ion (quinone-imine) back-peak. The voltammetric profile becomes more

complicated as a consequence of the two electrode processes and could create a degree of ambiguity in terms of interpretation. However, the UA peak is always more positive than that of the poly trp irrespective of pH. The UA process is not so much a peak, as a large shoulder towards the end of the voltammetric range. Given that the scan commences from negative (left) to positive (right) – it could be anticipated that the first peak to be observed could be taken as the poly-Trp peak and hence the pH derived from that potential. One issue with this approach is that while UA can be negated. At low pH, another process is observed and is due to quinone groups present on the electrode surface. Inspection of the voltammograms recorded at pH 4 and pH 5 reveals that the first peak is not in fact the poly-Trp but the quinone artifact introduced by the electrode responding to the lower pH. This does create a seemingly irredeemable ambiguity as it opens the analysis to the dilemma of knowing when to ignore one peak but not another.

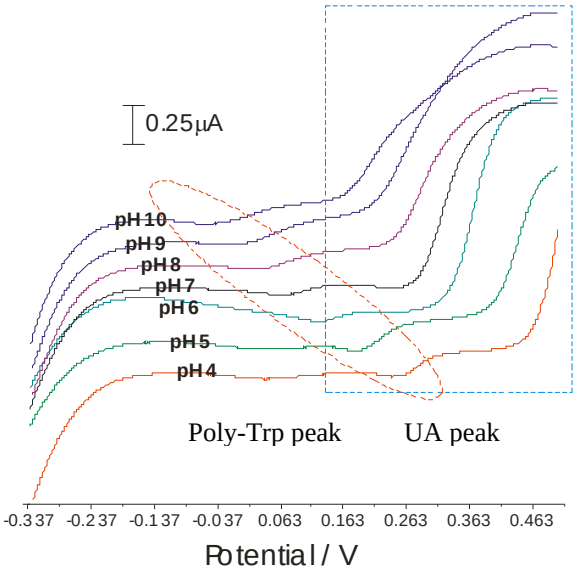

Figure 4.8. Linear sweep voltammetry of 20µM Tryptophan in changing pH (4-10) in the presence of urate (500uM). Step potential; 1mV, Scan rate: 50mV/s.

4.3.3 Alternative Sensor Substrates

As the peak shift in response to pH may, at least partially, rely upon the sensor matrix, alternative electrode substrates based on carbon-polycarbonate composite and gold were assessed. The use of carbon-polycarbonate composites for the electroanalytical determination of biomolecules has been studied. However the transfer of the approach towards the development of a pH sensor, especially the application to a smart-bandage / wound diagnostic, are all novel. Gold electrodes have widespread use without the need for pretreatments and would have the added advantage of being free from the endogenous quinone functionalities that are problematic in the previously observed fibre system (**Figure 4.8**).

4.3.4 Carbon – Polycarbonate Composites

Carbon loaded polycarbonate films were prepared by simply mixing appropriate ratios of carbon powder (1 micron diameter particles) with the corresponding weight of polycarbonate dissolved in dichloromethane. The resulting mixture was then cast on a planar surface and the solvent allowed to evaporate. The resulting film was then encapsulated within a laminate sheath in a process similar to that described for the carbon fibre matting. It was anticipated that the main issue would be the reduction in conductivity associated with the composite nature of the film – being essentially carbon islands distributed with a sea of insulating polymer. Anodisation has previously been shown to enhance the electrode properties but although easily accomplished with chemical means (sodium hydroxide) it was felt that would be insufficient to remove the polymeric binder.

What was needed was a process through which more carbon could be exposed. Laser ablation of surfaces to reveal underlying layers is a common process but it has not been used in the present context. There was also no guarantee that the resulting substrate would retain activity. A series of preliminary experiments were constructed with the aim of assessing the likely effects of the laser ablation on underlying carbon. The initial

experiments were conducted using carbon fibre rather than the composite. The rationale behind this choice was that the substrate is pure carbon and thus the influence of the laser irradiation could be more easily assessed without the ambiguity of interpolating the effects of inherent poor conductivity as a consequence of carbon particle distribution.

Carbon fibres were encapsulated within a polyester resin laminate as described previously. An electrode window was then created by rastering the laser across a pre-selected area of the polymer-fibre composite. This has the effect of removing the polymer and exposing the fibre which can, in principle, be used as the working electrode in a sensor assembly. Cyclic voltammograms detailing the response of unmodified and electrochemically anodised carbon fibres (of similar geometrical area) towards a model probe molecule (UA, 2 mM, pH 7) were then studied as a function of the laser activation. Initial studies focused on the assessing the performance of the fibre before and after electrochemical anodisation – activation. Cyclic voltammograms highlighting the results obtained are detailed in **Figure 4.9**. It can be seen that the oxidation of the purine (**I→II, Inset Figure 4.9**) at the unmodified fibre is barely visible and is characteristic of poor electron transfer kinetics at a substrate that is largely basal plane in structure. The voltammogram recorded at the electrochemically anodised fibre, in contrast, displays a well defined and easily quantifiable oxidation process. The change in profile is dramatic but is in keeping with previous work where electrochemical anodisation has been shown to aid both the resolution and the sensitivity of voltammetric processes [23,24]. The key question, however, is whether a similar effect could be achieved simply as a consequence of exposing the carbon surface to the laser.

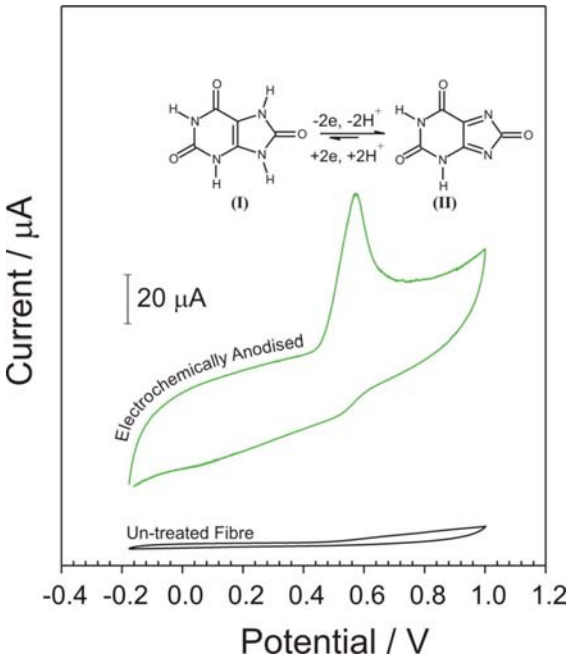

Figure 4.9. Cyclic voltammograms detailing the response of untreated and electrochemically anodised fibres towards 2mM uric acid (Inset).Scan rate: 50mV/s

Cyclic voltammograms highlighting the response of the laser etched carbon fibre structure towards urate (2 mM, pH 7, 50 mV/s) are detailed in **Figure 4.10**. In all cases, the area of polymer (0.03 cm^2) removed is the same. The only difference between the scans is the power applied to that defined area. The greater the laser intensity – the greater the magnitude of the apparent surface activation. The capacitive background current observed with the laser etched system is however significantly smaller than that obtained with the electrochemical pre-treatment and may reflect a greater propensity of the latter to introduce surface charge to the fibre through the generation of greater numbers of oxygen species.

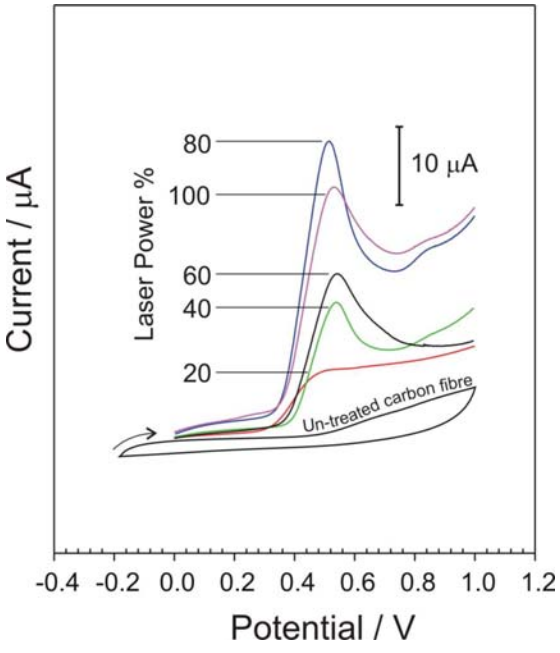

Figure 4.10. Linear sweep voltammograms detailing the influence of laser exposure on the activation (anodisation) of carbon fibre. Response to urate oxidation (2mM).Scan rate: 50mV/s

Application of the more extreme laser settings can however have a deleterious effect on the electrode surface and there is a sustained decrease in the peak height where either maximum power is applied or where multiple passes are used. This effect was further investigated with ferrocyanide as the model analyte. Cyclic voltammograms detailing the response of the various laser anodised (60 and 100%) fibres to ferrocyanide (2 mM, 50 mV/s) are compared in **Figure 4.11**. It can be seen that

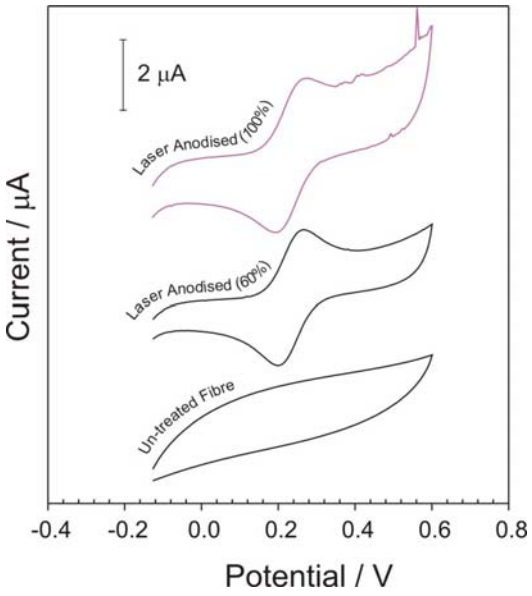

Figure 4.11. Cyclic voltammograms detailing the response of unmodified and laser anodised carbon fibres towards ferrocyanide (2 mM). Scan rate: 50mV/s

the unmodified fibre exhibits little response to the redox probe. Laser activation provides a superior response but the definition of the peak processes can be seen to degrade at the higher power setting with an increase in noise observed on the voltammetric trace.

It is clear that the response of the laser activated surface is similar to that observed after electrochemical anodisation and clearly provides an enhancement in performance over that attainable at the unmodified carbon. Scanning electron micrographs of the carbon fibre before and after laser treatment are detailed in **Figure 4.12A** and 4.**12B**. Exfoliation of the laser treated fibre can be observed even at moderate power settings (60%) and can be seen as striations along the fibre which will lead to a substantial increase in the electrode surface area – especially as a consequence of the nanofracturing at the surface.

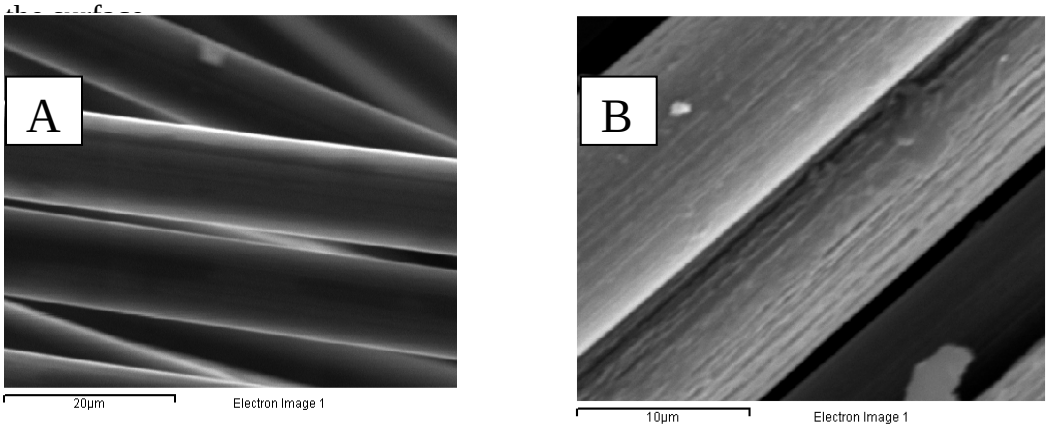

Figure 4.12. Scanning electron micrographs detailing the surface morphology of (**A**) untreated and (**B**) laser (power: 60%) anodised carbon fibres

This is seen more clearly in **Figure 4.13** where laser induced damage to the core fibre is observed at maximum power. It is important to note that the enhancement in peak resolution, however, is not simply a result of the increased area - as increasing the exposed and hence the "nominally active" area of the unmodified fibre did not lead to the behaviour exhibited by the either electrochemical or laser ablated fibres shown in Figures 4.10 and 4.11. The main difference between native and modified fibre lies in the relative population of the edge plane sites and oxygen functionalities. It is the increase in both

these features that would lead to the increase in electrode sensitivity and it can be seen from both the electrochemical and morphological characterisations that the laser option provides a viable alternative to the electrochemical process.

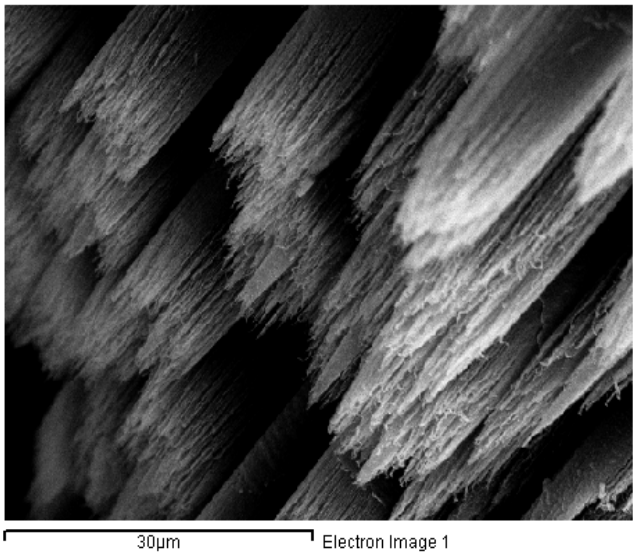

Figure 4.13. Scanning electron micrograph of carbon fibre after repeated exposure (2 passes) of the laser at full power

While these high laser anodisation powers are required for the extensive surface oxidation of carbon fibre substrates, much lower levels are needed when using carbon-polycarbonate electrodes. Electrode degradation can occur at much lower powers. The assessment of the differing laser powers using polycarbonate electrodes for poly-Trp monitoring and to enhance the sensitivity and peak separation through varying the anodisation of the composite sensor, LSV was used. The three laser anodisation powers (5, 10 and 15%) were compared (**Figure 4.14**), any greater anodisation led to structural weakening and damage to the substrate.

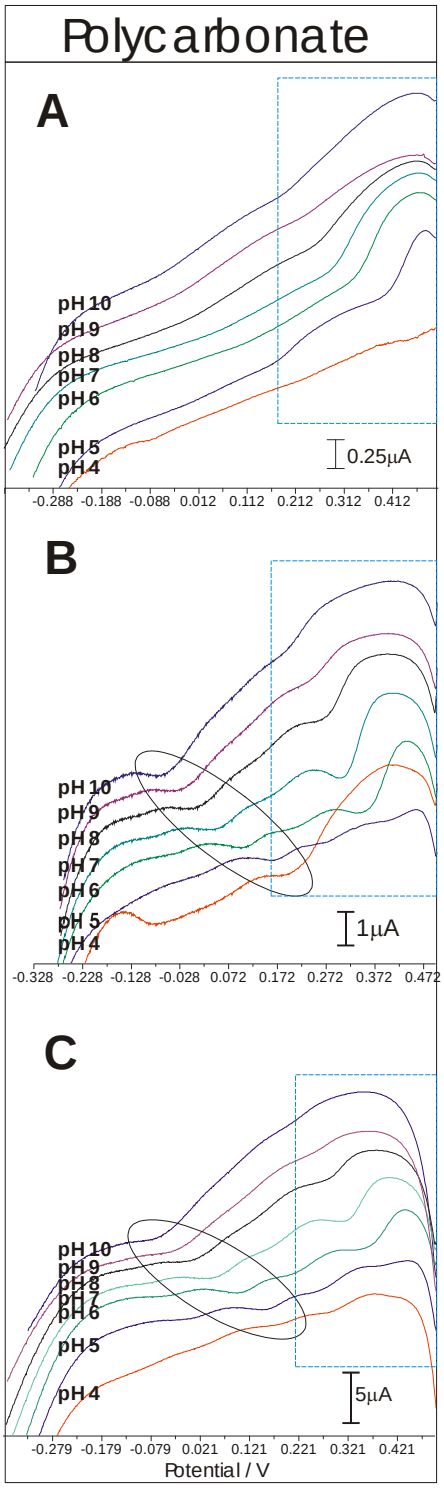

Figure 4.14. Linear sweep voltammetry of tryptophan (20µM) in the presence of uric acid (500µM) at changing pH (4-10) using carbon-polycarbonate electrode laser anodised using: (A) 5%, (B) 10% and (C) 15% laser power. Step potential; 1mV, Scan rate: 50mV/s.

There are a few small peaks in the 5% anodisation samples (**Figure 4.14A**), however, these are uniform throughout all pH samples and are attributed to the urate ion as proven in **Figure 4.14A**. Both the 10 and 15% laser settings produced small but, importantly, clearer poly-tryptophan reduction currents (**Figure 4.14B and 4.14C**). The 15% anodisation process however produced an enhanced peak separation allowing the poly-tryptophan peak to be clearly differentiated from the possible urate ion peaks in pH 5.

5%: no detectable peaks
10%: Reduction potential / V = -0.459 pH + 0.385, $r^2 = 0.982$
15%: Reduction potential / V = -0.0410 pH + 0.343, $r^2 = 0.994$

Unfortunately laser anodisation with 15% resulted in a loss of some peak definition and can be attributed to slightly more damage to the electrode surface. While the anodized carbon molecules were more active in the latter case, there were fewer in contact with the core substrate. As such, the use of 10% laser power anodisation was subsequently used. Testing of both the polycarbonate and gold electrodes in the presence of urate and tryptophan enabled the identification of the urate reduction peak as highlighted by the blue rectangle in **Figure 4.15**. For the polycarbonate electrode, the poly-Trp peak shift in the reduction potential was again found to cause overlap with the possible urate back-peak region. However, in contrast to the results observed with the carbon fibre matting, there is a substantial reduction in the magnitude of the peak process associated with the formation of quinone groups on the underlying substrate. Thus, in this case it could be possible to have an appropriate software algorithm that picks the first peak in the voltammetric scan as being the poly-Trp peak. The laser modified polycarbonate clearly provides a less ambiguous profile that simplifies interpretation and hence eases the derivation of the wound pH.

The use of gold electrodes were also assessed with the rationale being that these too would lack any quinoid groups that could interfere with the interpretation of the voltammetric scan. Gold is not however a simple system and its profile can be complicated by the presence of oxide redox processes formed as a consequence of the

actual analysis procedure. This was found in practice (**Figure 4.15**) and the large reduction potentials of the gold oxide were found to obscure the comparatively small poly-tryptophan interactions. As such, no difference could be inferred from the actual scan profile in the presence or absence of tryptophan.

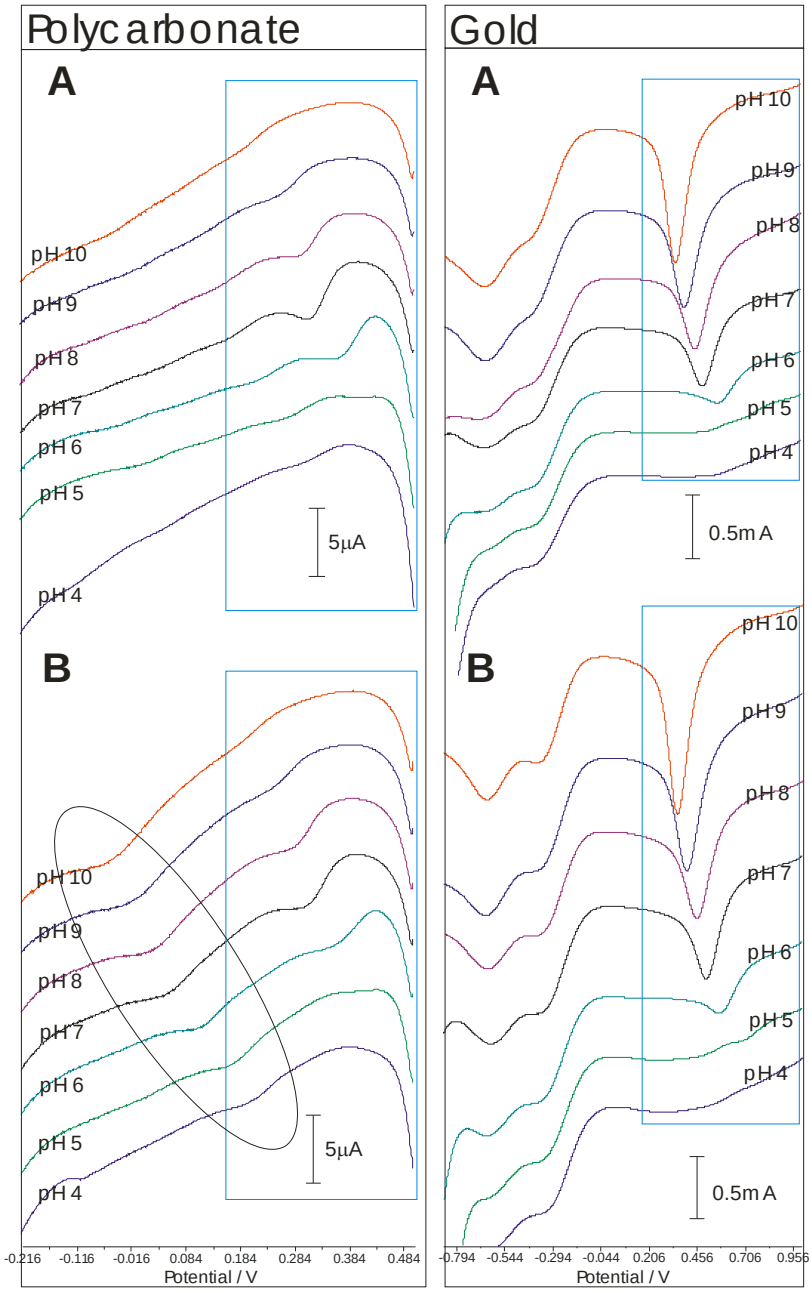

Figure 4.15. Linear sweep voltammetry of polycarbonate 10% laser anodisation and gold electrodes in (A) just uric acid (500µM) and (B) uric acid (500µM) and tryptophan (20µM). Step potential; 1mV, Scan rate: 50mV/s.

In a final attempt to enhance the peak separation and magnitude of the very small target reduction peaks in the polycarbonate voltammograms, the use of SqWV was reinstated using the same experimental setup. **Figure 4.16** details the responses in the presence of urate and tryptophan. In this instance there was no substantial improvement over the LSV method beyond a slight increase in peak definition.

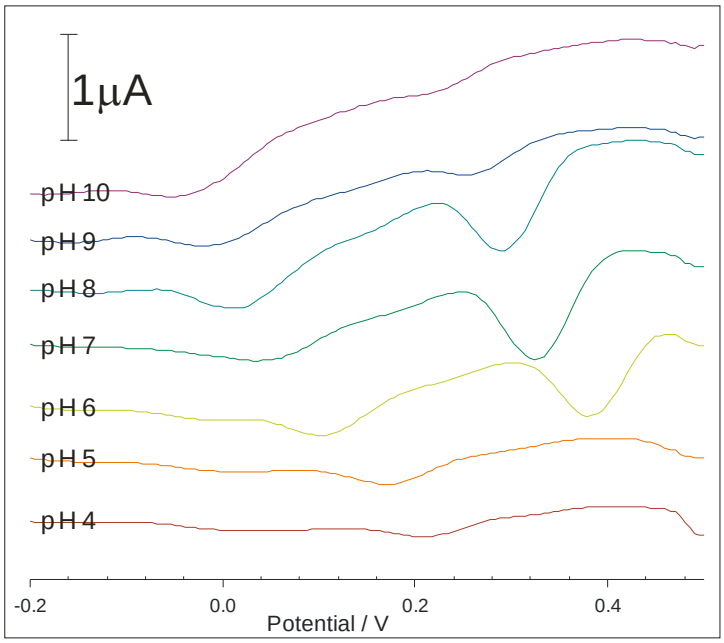

Figure 4.16. Square wave voltammograms recorded at a laser anodised polycarbonate electrode in the presence of 20µM tryptophan in the presence of uric acid (500µM). Step height: 2mV, Amplitude: 5mV.

[Square Wave Voltammetry: Reduction potential = -0.0446pH + 0.384, r ² 0.972]

While the results from both LSV and SqWV are sufficient to allow the monitoring of pH transformations in a wound exudate, the small peak heights are an obvious impediment but could be remedied by further refinement of the signal processing software. Optimisation of the scan parameter could also improve the response through reducing the capacitance background and thereby improving the signal to noise ratio. It could also be possible to investigate methods through which to remove the quinone

functionalities from the substrate and thereby clarify the scan even further. Such processes would however require a greater degree of chemical modification and optimization to ensure that the conductivity of the substrate was not compromised as a consequence of the manipulation. Such studies are certainly worthy but are out with the present scope of this project.

4.4 Conclusions

The sensor systems described enabled tryptophan to be polymerized onto the sensor surface. This polymeric product has been shown to provide a quantifiable shift in the position of the reduction process which can be used to evaluate the response to changing pH. While the sensor developments detailed within have shown good progress in the linear detection of pH solely relying on the endogenous probe, the interference of the urate oxidation product reduction peak was an obvious issue. It was found, however, that the use of a laser modified polycarbonate system provided a much cleaner voltammetric scan and that by appropriate application of signal processing data the signal could easily be used to determine pH. The latter has clear promise for use as wound sensor through adopting the novel features of the polycarbonate surface. More importantly it exploits the electrochemical manipulation of an endogenous biomolecule to create an immobilized product that is not only responsive to pH but whose signal can be extracted in a region free from interference.

4.5 References

1. Burtis CA, Ashwood ER, Bruns DE. Tietz textbook of Clinical Chemistry 4th edition 2006. Elsevier Saunders, Missouri USA.
2. Nguyen NT, Wrone MZ, Dryhurst G. Electrochemical oxidation of tryptophan. *Journal of Electroanalytical Chemistry* 1986;199(1):101-126
3. Lawrence J, Robinson KL, Lawrence NS. Electrochemical determination of sulfide at various carbon substrates: a comparative study. Analytical Sciences 2007;23:673-6
4. Banks CE, Compton RG. Edge plane pyrolytic graphite electrodes in electroanalysis: an overview Analytical Sciences 2005;21:1263-68
5. Krizkova S, Beklova M, Pikula J, Adam V, Horna A, Kizek R. Hazards of secondary bromadiolone intoxications evaluated using high-performance liquid chromatography with electrochemical detection. Sensors 2007;7:1271-86
6. Paixao TRLC, Kosminsky L, Bertotti M. Use of electrochemically pretreated glassy carbon electrodes as ph sensors in potentiometric titrations. Sensors and Actuators B 2002;87:41-6
7. Gu HY, Yu AM, Chen HT. Electrochemical behaviour and simultaneous detection of vitamin B-2, B-6 and C at electrochemically pretreated glassy carbon electrode. Analytical Letters 2001;34:2361-74
8. Liu S, Miller B, Chen A. Phenylboronic acid self-assembled monolayer on glassy carbon electrode for recognition of glycoprotein peroxidase. Electrochemistry Communications 2005;7:1232-6
9. Di J, Zhang F. Voltammetry detection of trace manganese with pretreatment glassy carbon electrode by linear sweep voltammetry. Talanta 2003;60:31-36
10. Florescu M, Brett CMA. Carbon film electrode for oxidase based enzyme sensors for food analysis. Talanta 2005;65:306-12
11. Farhadi K, Karimpour A. Electrochemical behaviour and determination of clozapine on a glassy carbon electrodes modified by electrochemical oxidation. Analytical Sciences 2007;23:479-83
12. Vakurov A, Simpson CE, Daly CL, Gibson TD, Millner PA. Acetylcholinesterase-based biosensor electrodes for organophosphate pesticide detection: I. Modification of carbon substrate for immobilization of acetylcholinesterase Biosensors and Bioelectronics 2004;20:1118-25
13. Tao Y, Lin ZJ, Chen XM, Chen XI, Wang XR. Tris(2,2 ‘-bipyridyl)ruthenium(II) electrochemiluminescence sensor based on carbon nanotube/organically modified silicate films. Analytica Chimica Acta 2007;594:169-74
14. Thorogood CA, Wildgoose GG, Crossley A, Jacobs RMJ, Jones JH, Compton RG. Differentiating between ortho- and para-quinone surface groups on graphite, glassy carbon and carbon nanotubes using organic and inorganic voltammetric and X-ray photoelectron spectroscopy labels. Chemistry of Materials 2007;19:4964-74

15. Chen S, Yuan R, Chai Y, Zhang L, Wang N, Li X. Amperometric third-generation hydrogen peroxide biosensors based on the immobilization of haemoglobin on multiwall carbon nanotubes and gold colloidal nanoparticles. Biosensors and Bioelectronics 2007;22:1268-74
16. Wang H, Zhang A, Cui H, Liu D, Liu R. Adsorptive stripping voltammetric detection of erythromycin at a pretreated glassy carbon electrode. Microchemical Journal 2000;64:67-71
17. Wang HS, Ju HX, Chen HY. Simultaneous determination of guanine and adenine in DNA using an electrochemically pretreated glassy carbon electrode. Analytica Chimica Acta 2002;461:243-50
18. Lin XQ, Jin GP, Monolayer modification of glassy carbon electrode by using propionylcholine for selective detection of uric acid. Electrochimica Acta 2005;50:3210-6
19. Li C, Wan Y, Sun C. Covalent modification of glassy carbon surface by electrochemical oxidation of r-aminobenzene sulfonic acid in aqueous solution. Journal of Electroanalytical Chemistry 2004;569:79-87
20. Kotkar RM, Desai PB, Srivastava AK. Behaviour of riboflavin on plain carbon paste and aza macrocycles based chemically modified electrodes. Sensors and Actuators B 2007;124:90-8
21. Morita K, Shimizu Y. Microhole array for oxygen electrode. Analytical Chemistry 1989;61:159-62
22. Friedrich JM, Ponce-de-León C , Reade GW, Walsh FC. Reticulated vitreous carbon as an electrode material. Journal of Electroanalytical Chemistry 2004;561:203-17
23. Banks CE, Compton RG. New electrode from old: from carbon nanotubes to edge plane pyrolytic graphite. Analyst 2006;131:15-21
24. Moore RR, Banks CE, Compton RG. Electrocatalytic detection of thiols using an edge plane pyrolytic graphite electrode. Analyst 2004;129:755-8
25. Sharp D, Davis J. Integrated urate sensors for detecting wound infection. Electrochemistry Communications 2008;10(5):709-13
26. Dutt JSN, Cardosi MF, Wilkins S, Livingstone C, Davis J. Characterisation of carbon fibre composites for decentralised biomedical testing. Materials Chemistry Physics 2006;97:267-272
27. Caldwell MD. The temporal change in amino acid concentration within wouind fluid –a putative rationale. *Clinical and Experimental Approaches to Dermal and Epidermal Repair: Normal and Chronic Wounds* 1991;365:205-22

Chapter 5

Development of a urate-based pH sensor

Abstract

Urate is present in all biofluids and at much higher concentrations than the previously studied tryptophan and, as such, has been investigated as an alternative system with which to develop a pH sensor. The new sensors developed within exhibit both high specificity and sensitivity, with the ability to detect urate in biological fluids - an essential step towards the urate-pH sensing system. The reagent-free sensors have been printed onto flexible bandage material and shown excellent linearity across a wide pH range (pH 4-10) and therefore are flexible enough and have a sufficient range, respectively, to allow their use within the proposed application. The chemical-free basis of the sensors for detection of urate is an important factor in the development of safe technologies. The sensor system is suggested as a substantial advancement in smart-bandage technology with direct applicability towards healthcare and a novel approach for *in situ* pH monitoring.

Due to the novel, potentially beneficial and viable nature of this sensing system the work detailed within the present chapter is subject to patent-approval.

5.1 Introduction

As outlined in the introduction to **Chapter 3**, the development of a small, flexible and cost-effective pH sensor is sought for use within wound dressings. The prototypes reported herein have the notable advantage of avoiding the need for exogenous chemicals and, as such, can be regarded as being effectively reagentless. The proposed urate (UA) based pH sensor takes advantage of urate as an endogenous chemical probe and hence avoids many of the issues of biocompatibility that would plague most approaches to chemically modified electrode systems. The key requirement in this instance is the physical modification of the bare sensor substrate to optimise the detection of the marker compound directly within the wound fluid such that an analytically significant signal can be obtained. UA is found in all bodily fluids and substantial quantities have been found in wound exudates (**Table 5.1**), with little difference between some serum and burn blister fluid concentrations. Burn blister fluid is essentially plasma which has been filtered through vessel walls (via capillary leakage), reducing the concentration of large molecules e.g. albumin. UA is relatively small (168Da) and, as such passes, through vessel wall easily and is ubiquitous within wound fluid [1].

Table 1. Urate concentrations found in biological fluids

Sample	**Range (μM)**	**Reference**
Normal serum reference range	150-420	[2]
	120-450	[3]
Normal urine reference range	1500-4500μmol/24h	[2]
	1480-4430μmol/24h	[3]
	Mean (μM) +/- SD	
Normal CSF	25 +/- 1 μM	[4]
	14 +/- 2 μM	[5]
	Mean (μM) (Range)	
Normal saliva	136 (81-176)	[6]
Tears		
Collection method 1	98.1 (54.8-194.4)	[7]
Collection method 2	116.5 (50.3-308.1)	
Collection method 3	166.0 (73.7-322.0)	
Acute wound fluid	232 (110-325)	[8]
Chronic (V.U.) wound fluid	166 (46-368)	
Corresponding plasma	295 (198-475)	
Burn blister fluid	342 (180.8-497.4)	[1]
Serum	335.4 (295.1-407.9)	

The electrochemical measurement of UA is well established for diagnostic purposes in which it is a key player to but it has yet to be evaluated as an indirect marker of pH and the present investigation represent a wholly novel application of the purine. In most cases, the electrochemical investigations have focused on reducing the influence of UA when attempting to detect other physiologically relevant species. Thus the prevalence of this proposed biomarker has been regarded as a complication in most previous studies, whereas it is clearly an advantageous asset in the present application. An important characteristic of electrochemical UA measurement is that the potential required to oxidise UA is related to the pH of the solution with well defined Nernstian behaviour. Due to the specificity of SqWV, the physically modified carbon sensors can allow the position of the oxidation peaks to be used as an indirect measurement of pH. The pH range targeted for this development focused on a range of pH 4 to 10. This significantly exceeds the "normal" clinical remit of pH 5.45 to pH 8.65 established in a recent study of chronic wounds [9].

The work focused on the development of carbon working electrodes for application towards pH sensing. The core rationale being the versatility of the latter and while initial investigations were carried out using carbon fibre electrode, transfer of the strategy to a printable but chemically analogous carbon system should be relatively easy. This provides some significant advantage over other electrode systems and offers easy adaptation to mass manufacture processing facilitating the production of cheap disposable sensors. In addition, the ability to rapid print the complete assembly onto a range of substrates common to wound pads or dressings and stands in contrast to the more technologically demanding requirement of photolithographic metal deposition.

The electrode assembly can be small – milli to centimetre total spatial dimension – and as such are inherently versatile across a range of formats or for large area rastering. The latter would ultimately allow profiling of the wound environment to highlight areas of localised infection rather than a simple yes / no. Advantages of pad-printing are the versatility this offers in terms of: ink composition, printed layer thickness, the size and shape of the electrode and the ability to print onto flexible and irregular substrates common to a variety dressing designs. The pad-printed electrodes investigated are

reagent-free, with long-term stability at room temperature and, due to the ease of construction and low cost of materials, are cheap and inherently disposable.

Chemical anodisation was used in this instance to improve sensor responses. While the laser technique was found to be advantageous for the polycarbonate systems detailed in Chapter 4, it was found to be incompatible with the printed systems. This is due to the thin film layers (50 micron) used in the printing process which are less than the penetration depth of the laser and thus substantially removed even at low laser powers. The anodisation procedure was pursued to enhance peak magnitude and optimize sharpness and can be attributed to the greater active surface area of the pressed carbon surface. We have demonstrated that physically modified carbon sensors are suitable for specific and sensitive detection of uric acid in biological and blister fluids. The research details investigates the applicability of this pH sensing system with preliminary assessments in buffer solutions through to final testing in Simulated Wound Fluid [10] before and after 24 hour bacterial growth of key organisms associated with wound infections (*Ps. aeruginosa, S. aureus, E. coli* and *K. pneumoniae).*

5.2 Experimental Details

Materials

All reagents used were of the highest grade available and used without further purification. Stock solutions of urate (typically 20mM) were prepared in 0.1M NaOH. All other solutions were made in the appropriate pH BR buffer. Simulated Wound Fluid (SWF) was prepared from 50% bovine serum (Sigma-Aldrich) and 50% maximum recovery diluent (1 g/L peptone, 8 g/L NaCl, autoclaved) and spiked with 200μM urate. Laminated carbon fibre matting electrodes were used as working electrodes.

Microorganisms

Stock bacterial cultures were used to inoculate 10mL of spiked SWF and grown at 37°C with shaking at 200 rpm for 18 hours (overnight). An aliquot (20μL) of the overnight culture was used to inoculate a fresh SWF (10mL) at the start of the experiments. After a

1.5mL sample aliquot had been collected at the starting point, the cultures were incubated as before for 24 hours. The samples were then stored at 4°C prior to analysis.

Instrumentation

Electrochemical measurements were conducted using a PalmSens Electrochemical Sensor Interface (Palm Instruments BV), controlled by a HP iPAQ Pocket PC. A three-electrode configuration was used consisting of a carbon fibre matting or printed carbon working electrode, a 3M NaCl Ag|AgCl half-cell reference electrode (BAS Technicol, UK) and a platinum wire counter electrode. The pH measurements were performed using an accumet® AP72 pH meter (Fisher Scientific)

5.3 Results and Discussion

5.3.1. Development and Optimisation of Sensors

The morphology of the laser patterned laminate – carbon composite was examined using scanning electron microscopy with the interface between the exposed fibre substructure and the insulating laminate detailed in **Figure 5.1**. The sensing element is effectively a random assembly of discrete and amalgamated fibres presenting a large 3-dimensional network and is in marked contrast to the planar designs found in conventional macro or micro sized urate sensor formats [11,12]. The initial analytical characterisation of the applicability of the network towards the sensing of UA was conducted in buffered solution – containing up to 500 μM ascorbic acid (AA). The addition of the latter is significant in that it is ubiquitous within biofluids and easily electro-oxidised at potentials not dissimilar to those required for UA detection. Square

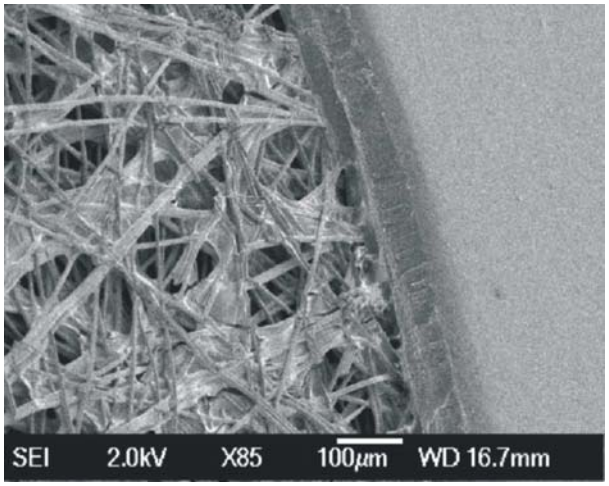

Figure 5.1. Scanning electron micrograph of the carbon fibre mesh / laminate composite.

wave voltammograms detailing the response of the carbon network to equimolar UA and AA are detailed in **Figure 5.2** (dashed line). A single, broad peak is observed with no resolution between the two compounds. Pre-treatment of the carbon fibre sensor through oxidation in 0.1M sodium hydroxide (+2V, 10 min.) yielded a very different response. A single sharp peak is observed at +0.23V which is attributed solely to the oxidation of urate. It has been previously shown that the anodic fracturing of the carbon substrate as a consequence of such pre-treatment gives superior resolution between AA and UA and markedly reduces the electron transfer kinetics of the former such that, under normal physiological concentrations, it provides a negligible contribution to the voltammetric profile. The anodizing of the carbon fibre created a substantial gain (~14x) in the magnitude of the UA peak as detailed in **Figure 5.2**.

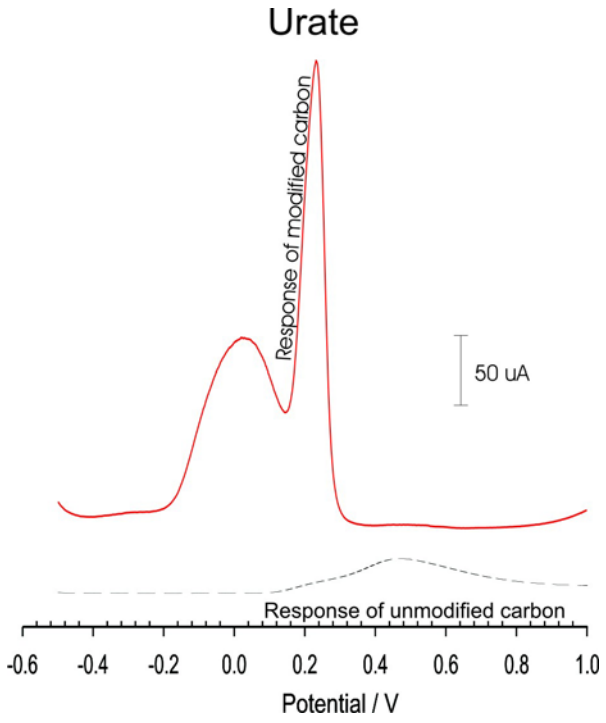

Figure 5.2. Square wave voltammogram comparing the response of an untreated carbon fibre in equimolar 100 μM UA and AA, with an anodized electrode in 100 μM UA and 2.2 mM AA (pH 7.0). Step height: 2mV, Amplitude: 10mV.

Confirmation that the sharp peak at +0.23V is indeed UA with no contribution from AA was provided by repeating the experiment but with a markedly increased concentration of AA. Square wave voltammograms detailing the response to 100 μM urate in the presence of AA (2.2 mM) are shown in **Figure 5.2** solid line. The ascorbate emerges as a broad peak (+0.03V) to the left of the sharp UA process. This highlights the fact that even in the presence of massive AA concentration – it is still possible to obtain an unambiguous assessment of UA concentration and is in marked contrast to the result obtained with the un-modified carbon fibre (**Figure 5.2 –** dashed line). The influence of real biofluids on the sensor response was again assessed using SqWV. The responses of the untreated and modified fibre sensors assemblies to whole blood are detailed in **Figure 5.3A**. Whole blood was selected as the test medium as it is

likely to be the toughest matrix that any sensor designed for physiological monitoring is liable to experience given that it contains everything; protein, fats, carbohydrates, and various small molecular weight species. It will also contain a whole variety of cells, all of which can interact and influence the sensing characteristics of the electrode. In this instance, 100μL of untreated blood was applied directly to the sensing surface and the measurement conducted almost immediately. The response of the un-modified fibre sensor shows effectively no discrimination between the different physiological components with a single broad peak found at +0.69V.

The pre-anodised sensor, however, displays a peak profile similar to that observed in the control buffer solution (**Figure 5.2 –** solid line). The magnitude of the peaks could be enhanced through increasing the degree of surface pre-treatment prior to applying the blood. Thus, extending the pre-anodisation time to 30 minutes results in a markedly enhanced signal with three, clearly resolved peak processes. The first (-0.12V) is attributed to the redox groups within the fibre substructure, the second (+0.23V) is the UA and the third (+0.66V) is liable to be a combination of other, less easily oxidised biological components such as those outlined in Chapter 3, typically Tyrosine (Tyr), Tryptophan (Trp) as well as other purines. This was corroborated by

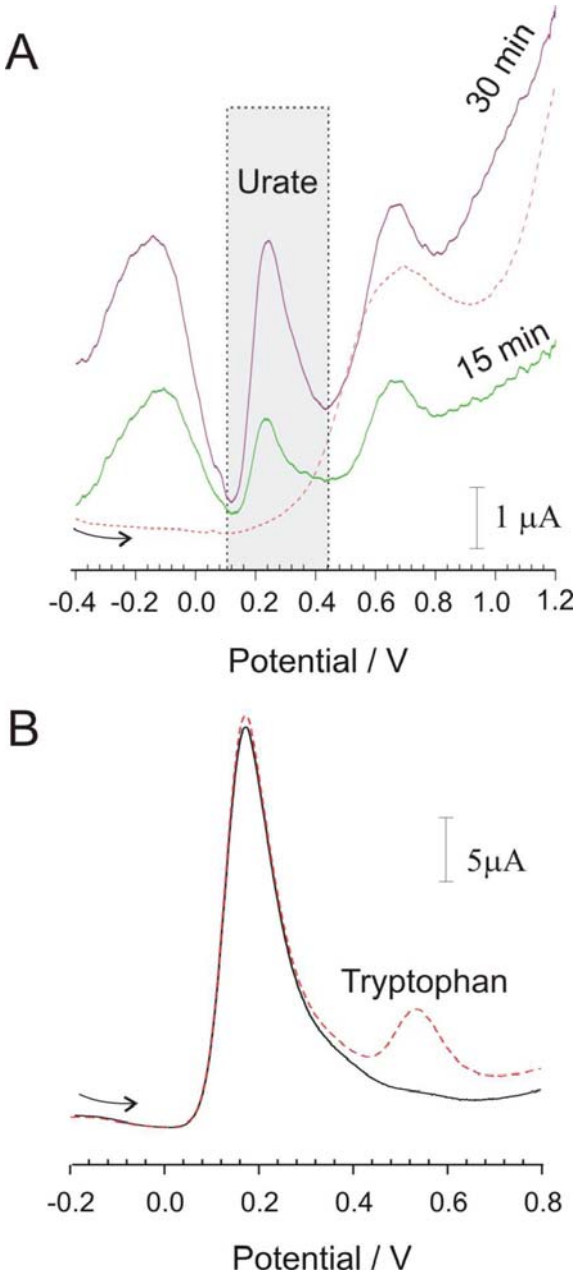

Figure 5.3. A) Square wave voltammograms detailing the response of the untreated carbon fibre (dashed line) and the anodized fibre (after 15 and 30 mins pre-treatment) towards whole blood. B) Response of 400 μM urate in the presence and absence of 100 μM tryptophan. Step height: 2mV, Amplitude: 10mV.

comparing the response to urate in the presence of tryptophan (**Figure 5.3B**). The emergence of a second peak at +0.53V is located in a similar position to that observed with the whole blood sample. Similar responses were observed with Tyr with near identical peak positions between Tyr and Trp highlighting both the limitation of the sensor for speciation in such complex fluids but, in the present instance, the supreme advantage of facilitating the almost unique discrimination of urate from the other blood constituents.

5.3.2 .Carbon Fibre Matting Electrodes for pH Measurements

The theoretical foundations that govern the relationship between the shift in the oxidation potential in response to changing hydrogen ion concentration is well established and were previously demonstrated in **Chapter 4**. A similar process was employed in this instance but rather than inducing the formation of a polymeric product – the electrode simply seeks to detect the presence of the urate biomarker alone. The concentration of 200μM UA was used throughout the reported results as this is a realistic physiological concentration as highlighted in **Chapter 3**.

A preliminary assessment of the of carbon fibre electrodes response towards changing pH shows the predicted linear shift in oxidation potential of urate, **Figure 5.4**, performed in buffered solutions. The oxidation peaks shift from ~0.44V to ~0.2V with increasing pH when measured by SqWV using a portable electrochemical controller (PalmSens). Analysis of the potentials lead to the formation of a linear calibration plot [Oxidation potential / V = -0.0549 pH + 0.708] with good agreement [r^2 = 0.995].

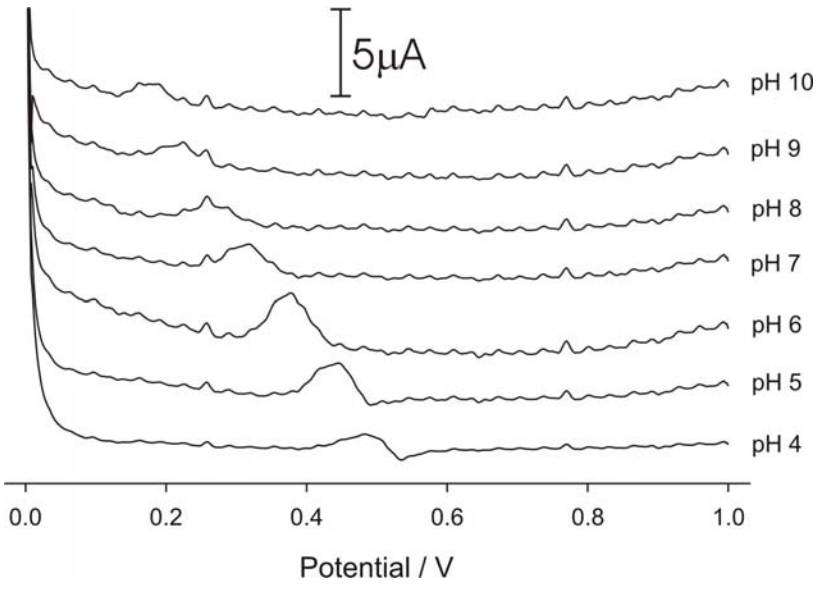

Figure 5.4. Square wave voltammetry of 200μM urate with carbon matting electrodes in changing pH buffer (4-10). Step height: 2mV, Amplitude: 10mV.

This preliminary work was the starting point for research towards small, flexible and inexpensive pH sensors for use in biofluid.

5.3.3. Pad Printed Electrodes for pH Measurement

In order to allow the production of more mass-producible sensors with greater versatility and flexibility, carbon sensors were pad-printed onto an ultra-flexible wound dressing backing material, this is commercially available and used in the manufacture of wound dressings (e.g. *Episil Absorbent* by Advancis Medical, UK). Printing sensors onto such flexible substrates is a novel step in the development of these sensors and could lead to the development of more integrated sensing systems. Previously, the sensors would be introduced as an additional, external component. The design of the sensors and the final print onto the dressing material are shown in **Figure 5.5.**

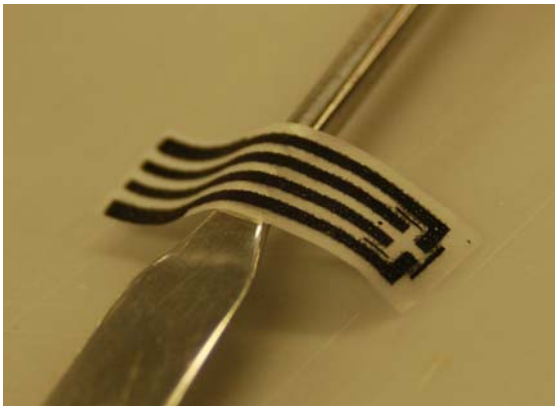

Figure 5.5.Pad printed sensors deposited on a typical wound dressing material.

The sensors were first characterised in buffered solution at a typical biofluid urate concentration of 200μM. Plain printed carbon sensors were first evaluated with a poor correlation to changing pH, **Figure 5.6** (filled dots), this was attributed to many factors, primarily, the very poor detection of urate, as highlighted by the small and broad oxidation currents observed in **Figure 5.7A**.

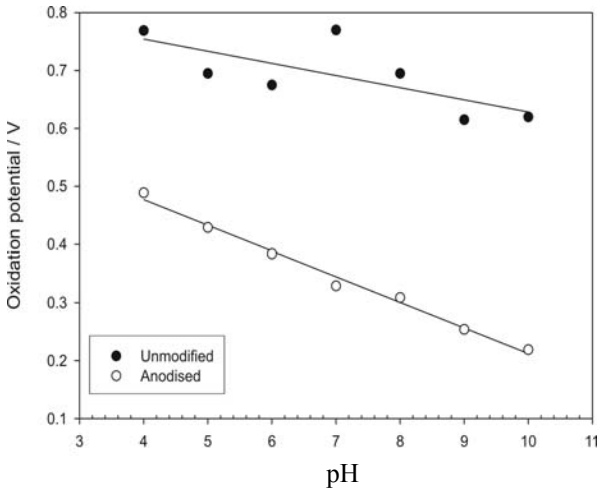

Figure 5.6. Urate oxidation potential shift with changing pH (4-10) buffered solutions for: unmodified pad printed electrodes (Filled circles) and anodised pad printed electrode (open circles)

An additional problem with the use of unmodified carbon electrodes for measuring UA as widely encountered with other sensor substrates in that there are many other biofluid constituents that oxidise at similar

potentials e.g. AA, Tyr and Trp, the use of an unmodified sensor in biofluids would incur these interference as well as the poor sensitivity of urate transformations. The broad oxidation peaks ~0.65V for plain carbon were attributed to UA oxidation in the buffered solutions tested, however, the signal to noise ratio was also very poor leading to error prone interpretation.

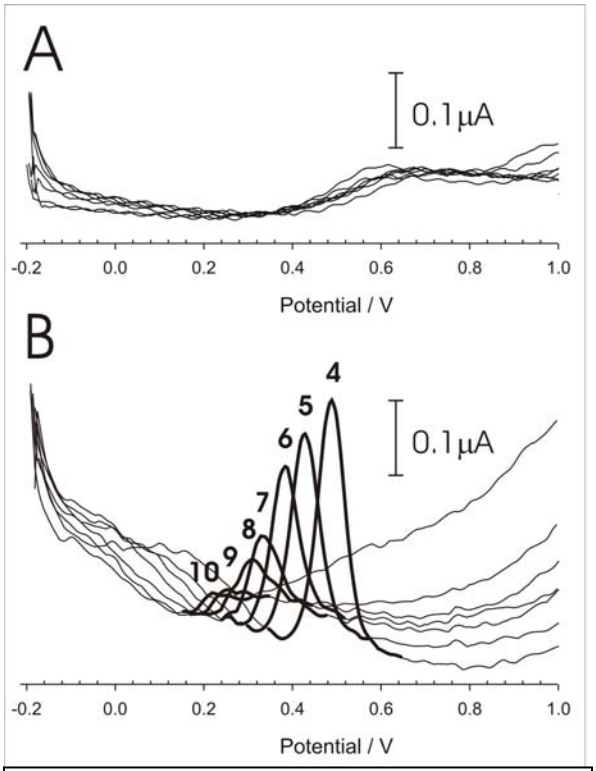

Figure 5.7. Square wave voltammetry of 200μM urate in changing pH (4-10) buffered solutions with pad printed electrodes: A). Unmodified and B). anodised. Step height: 2mV, Amplitude: 10mV.

As previously shown for carbon fibre matting electrodes, the anodisation of the carbon sensors creates a sharp, well-defined oxidation peak as shown in the voltammograms in **Figure 5.7B**, in agreement with previously published data [13] in that the peak magnitude is substantially increased and the peaks possess a Gaussian profile that allows better identification of the oxidation potential. While this makes interpretation much more accurate, the major advantages lie in the specificity imparted by the anodisation process. The oxidation occurs at notably lower potentials using anodised electrodes and this has been attributed to the increase presence of edge-plane sites and oxygen containing functional groups (e.g. carboxyl, hydroxyl, carbonyl) [15]. The most important difference between the unmodified and anodised electrodes is in the oxidation peak shift observed with changing pH. While the unmodified electrode does show a slight agreement (r^2=0.525), this is substantially increased by anodisation (r^2=0.990).

The calibration equation [Potential / V = -0.044 pH + 0.653, r^2 = 0.990] dictates that, on average, there is a 44mV shift per pH unit, this is in excess of the 29.55mV per pH unit (log H^+ change) as dictated by the Nernst equation (at 25 ^oC). The latter would be expected if the species were a simple solution based – freely diffusion based system. In the present case it is clear that there is an adsorption component – as evidenced by the

sharpness of the oxidation peak. It is likely that the interaction of the urate with the anodised carbon surface leads to a more stable configuration which can influence the native acid-base chemistry and thus account for the deviation from purely Nernstian behaviour. Regardless of these factors and underlying mechanisms - the increase in potential shift from a Nernstian 29.55mV/pH to 44mV/pH provides a serendipitous enhancement of the sensitivity of the pH sensor and is attributed to the increased functionality of the carbon substrate.

Having demonstrated the potential applicability of the pH sensor in buffered solution, the use in simulated wound fluid (SWF) was assessed. SWF has been used in the development of sensors and is readily used as a medium within which to grow microorganisms in a replicated wound environment. The key organisms associated with wound infection (*Ps. aeruginosa, S. aureus, E. coli* and *K. pneumoniae*) were grown in SWF spiked with a physiologically relevant concentration of UA for 24 hours. Samples were collected at the start and end of this incubation period were analysed by SqWV using anodized carbon printed electrodes. When the oxidation potential is compared with a pH measurement by a conventional laboratory glass-bulb pH meter (**Figure 5.8**), there is a good correlation (r^2=0.903) with a decrease in oxidation potential observed with increasing pH, highlighting the ability of the anodized printed carbon electrode to be used in biofluids for pH monitoring. These results however also highlight the ability to measure pH in complex biofluids and, importantly, in the presence of bacterial metabolites and byproducts. Overall the urate sensors developed are selective and have sufficient acid:base properties to enhance the oxidation shift of UA allowing more sensitive measurements of pH in the simulated biofluids.

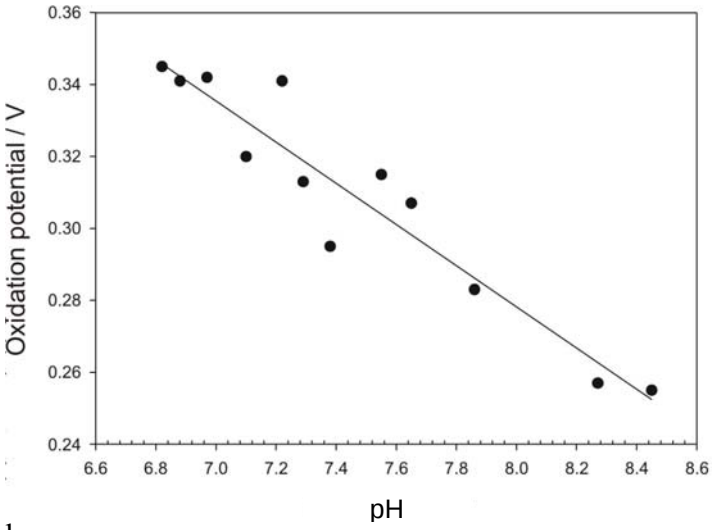

Figure 5.8. Urate oxidation peak shift due to pH change in simulated wound fluid as a result of bacterial growth

5.3.4. Effects of Temperature Change

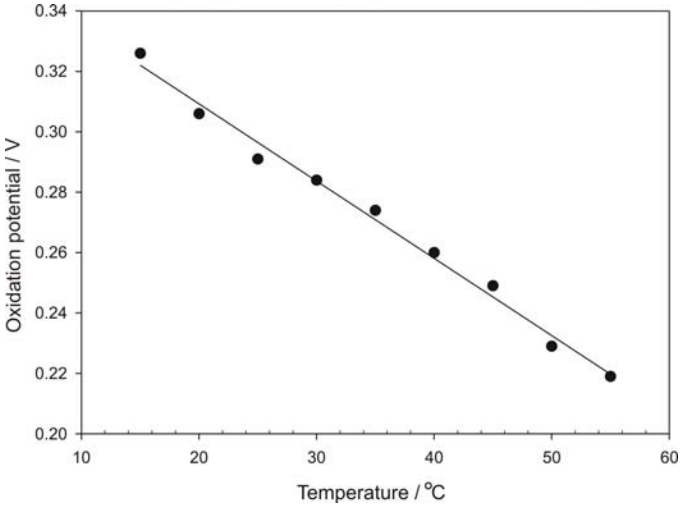

Figure 5.9. Effect of changing temperature on the oxidation potential of urate at an anodised pad printed electrode in simulated wound fluid

Given the temperature dependence of the potential (as per the Nernst equation outlined in Chapter 2), it was important to determine the extent to which this could affect the sensor performance for a given wound physiology. In the previous experiments the temperature was generally fixed at 25°C. The temperature of a pH 7.0 corrected SWF sample was controlled using a circulating water bath and passed through a jacketed cell. Square wave voltammograms were recorded as before after each temperature increment and the relationship between temperature and oxidation potential is highlighted in **Figure 5.9**. A linear response across a wide temperature range was observed [Oxidation potential /V = -0.00256pH+0.360, r^2=0.991]. A shift of 2.6mV/°C was found. The theoretical shift in oxidation potential derived from the Nernst equation is only ~0.1mV per °C, thus other factors contribute to the peak shift. These may include changes in interface kinetics at the sensor window, affects on biomolecular solubility or complexed-protein adhesion. Additionally these factors may affect the dissociation and effective functional groups through pKa shifts, normally observed through pH changes.

The temperature of a dressed wound can typically range between 25-35 °C [14]. Thus, the maximum shift that could be expected due to the temperature change is 26mV. When back calculated to a pH change using the calibration equation observed previously [Potential / V = -0.044pH + 0.653 (r2 = 0.990)], this equates 0.59 pH units. It can be anticipated that any temperature induced error would have little impact on the actual clinical assessment. Primarily this change is not too substantial, plus this larger range of temperatures reflects the extreme cases observed using different wound dressings. Under

normal circumstances, the temperature variation is likely to be minor due to the inherent physiological variation of pH within a wound and it is reported to be <3 $^{\circ}$C variation for the same dressing [14], i.e. <0.2pH units. While circulatory pH is under extremely close control, the stresses and factors in a wound environment would be much greater and not under systemic control. Given the changes documented in the literature,, these minor variations are likely to be of little significance. However, further work identifying the temperature variation within a dressed wound may provide a better understanding of the impact this may have on pH measurement.

5.4 Conclusions

The carbon based electrochemical sensors presented have proven ability to measure pH in simulated biofluids as a result of bacterial metabolism. The ability to measure the pH via UA oxidation transformations is novel and overcomes the main problem of size and flexibility of pH sensors to date. While the results are partially temperature dependant, the relatively small temperature range encountered in dressed wounds may still permit the clinical use of such a device. A linear response has been established across the range of pH4-10, far greater than that of biological exudates. The reagent-free and versatile system is proposed as a novel *in situ* sensor system to allow the simple measurement of pH using SqWV in a PoCT environment.

5.5 References:

1. Haycock, JW, Ralston DR, Morris B, Freedlander E, MacNeil S. Oxidative damage to protein and alternations to antioxidant levels in human cutaneous thermal injury. *Burns* 1998;23(7/8):533-40
2. *Diagnostic Services Handbook* (2005) Nottingham city Hospital NHS Trust, UK
3. Burtis CA, Ashwood ER and Bruns DE. Tietz textbook of Clinical Chemistry and Molecular Diagnostics 4th Edition. 2005; Elsevier Saunders, Missouri, USA.
4. Stover JF, Lowitzsch K, Kempski OS. Cerebrospinal fluid hypoxanthine and uric acid levels may reflect glutamate-mediated excitotoxicity in different neurological diseases. *Neuroscience Letters* 1997;238:25-8
5. Zamani A, Rezaei A, Khaeir R, Hooper CD. Serum and cerebrospinal fluid uric acid levels in multiple sclerosis patients. *Clinical neurology and neuroscience* 2008;110:642-3
6. Peréllo J, Sanchis P, Grases F. Determination of uric acid in urine, saliva and calcium oxalate renal calculi by high-performance liquid chromatography/mass spectrometry. *Journal of Chromatography B* 2005;824:175-80
7. Choy CKM, Cho P, Chung WY, Benzie IFF. Water-soluble antioxidants in human tears: effect of the collection method. *Investigative Ophthalmology & Visual Science* 2001;42(13):3130-4
8. James TJ, Hughes MA, Cheery GW, Taylor RP. Evidence of oxidative stress in chronic venous ulcers. *Wound Repair and Regeneration* 2003;11(3):172-6
9. Dissemond J, Witthoff M, Brauns TC, Goos M. pH values in chronic wounds. Evaluation during modern wound therapy (in German) *Hautarzt* 2003;54(10):959-65
10. Parsons D, Bowler PG, Myles V, Jones S. Silver antimicrobial dressings in wound management: a comparison of antibacterial, physical and chemical characteristics. *Wounds* 2005;17(8):222-32
11. Chen JC, Chung HH, Hsu CT, Tsai DM, Kumar AS, Zen JM. A disposable single-use electrochemical sensor for the detection of uric acid in human whole blood. *Sensors and Actuators B* 2005;110:364-9
12. Zen JM, Jou JJ, Hangovan G. Selective voltammetric method for uric acid detection using preanodized Nafion-coated glassy carbon electrodes. *Analyst* 1998;123;1345-50
13. Dutt JSN, Livingstone C, Cardosi MF, Wilkins SJ, Davis J. A clinical assessment of direct electrochemical urate measurements. *Talanta* 2006;68:1463-8
14. Ovington, L. Hanging wet-to-dry dressings out to dry. *Home Healthcare Nurse* 2001;19(8):477-84
15. Tao Y, Lin LZ, Chen XM, Chen XI, Wang XR. Tris(2,2′-bipyridyl)ruthenium(II) electrochemiluminescence sensor based on carbon nanotube/organically modified silicate films *Analytica Chimica Acta* 2007; 594: 169-174.

Chapter 6

Sensors to monitor urate metabolism by bacteria

Abstract

The applicability of employing a carbon fibre mesh as the sensing element within a smart-bandage for assessing urate transformations within wound exudates is evaluated and a novel strategy for the detection of bacterial contamination presented. While the urate developments in Chapter 5 investigated the potential shift as a result of pH, the actual quantification of urate is investigated as an alternative / complimentary sensing approach. The rapid and selective metabolism of urate by *Ps. aeruginosa*, the bacteria responsible for most adventitious wound infections, has been investigated. Due to the nature of the urate quantification by the novel electrochemical system, developments in surface modification to prevent biomolecular fouling have led to the successful application of a cellulose acetate perm-selective barrier. The sensors detailed enable the measurement of urate with the high level of accuracy and precision required for the proposed *in situ* application. A preliminary evaluation of the efficacy of utilizing the microbial response to endogenous wound urate as means of detecting the onset of infection is presented and its application critically appraised in simulated wound fluid.

Work detailed in this chapter has been published in *Electrochemistry Communication* 2008; 10: 709-713 and in *The Journal of Biochemistry* 2008; 144: 87-93

6.1 **Introduction**

The principal aim of the present chapter has been to investigate the use of an electrochemical sensing system that could facilitate the periodic monitoring of wound integrity with regard to the semi quantitative assessment of bacterial incursion. The underlying rationale has been to monitor the changes in the relative concentration of Urate (UA) within wound fluid. The purine has long been proffered as a possible biomarker for assessing oxidative stress processes whereby the severity of a particular clinical condition (i.e. hypertension) has been shown to be related to the relative variations in serum concentration [1]. The influence of oxidative stress processes on wound UA concentrations have also been the subject of considerable interest given the possible diagnostic value of the latter in assessing the progression of the healing process [2,3]. The core assumption in the present investigation is that should the bacteria be capable of selectively metabolising UA (either as a nitrogen source [4] or as a result of further enzymic conversion[5]) then a dramatic reduction in the concentration of the purine could then be attributed to the change in microbial activity within the wound fluid. Of prime importance would be change from the initial contamination to critical colonisation where the latter represents the danger point with regard to the development of infective complications.

Justification for the proposed detection strategy is based on the fact that while UA is the end product in purine metabolism within humans, microbial uricase will readily catabolise UA to allantoin [5]. Hence, under hitherto normal conditions (i.e. where the nominal microbial contamination common to ‘clean’ wound predominates) periodic monitoring of the wound should reveal a relatively stable urate concentration [2,3]. Upon the change from bacterial contamination to colonization, the growth of the bacterial colony will lead to a simultaneous increase in the expression of uricase. It could therefore be expected that a significant and sustained decrease in the wound urate concentration would be observed [5]. UA concentration will naturally vary from one person to another (within the reference range 150 - 420μM [1,6]), but the diagnostic remit of the proposed sensor lies not the extraction of an ***absolute*** urate concentration but rather on the ***relative***

change from the initial ‘clean’ condition to that where the bacterial growth has led to a substantial depletion of the biomarker.

The development of a sensor design that could allow the easily integration within a conventional bandage support has been investigated. A core objective was the periodic monitoring of urate directly within the fluids typical of wound environments, principally serum and blister fluid [7]. The change in urate concentration as a consequence of the presence of different bacteria (*S. aureus, Ps. aeruginosa and K. pneumoniae)* was assessed. These were selected on the basis of their differing Gram stain characteristics and, more importantly, their prevalence within burn wounds and their significance in causing infective complications and bacteraemia [7]. The results detailed herein rely on the use of carbon fibre matting as the sensing substrate. While the previous chapter has highlighted the greater versatility and mass-producibility of pad-printed carbon electrodes, it was thought that the greater sensitivity of the carbon fibre matting would be more advantageous for monitoring the peak heights and hence concentration.

In order to facilitate the use of the described sensors for quantification it was anticipated that there would be a need to prevent biomolecular fouling e.g. from proteins [8]. Electrode fouling is one of the main problems facing electrochemical analysis of biofluids and particularly where the electrode will be in contact with the fluid over a prolonged period. The main rationale was to improve the stability and reliability of the sensors and to facilitate more accurate and precise measurements. The sensors developed through the duration of this project are for periodical wound monitoring, the analytical stability is essential. The general impact of fouling in electrochemical systems results in a decrease in peak current magnitude and this is being used directly to relay the concentration of analyte within the fluid.

Electrode fouling is generally caused by the adsorption of non-electroactive compounds onto the electrode active surface. Proteins are the major source of electrode fouling [8] reducing the active-surface area with time, thereby reducing electrode sensitivity by inhibiting electron transfer reactions [9]. As the larger, higher molecular weight species (proteins and lipids) causing the electrode fouling it is possible to prevent these from interacting closely enough to allow adsorption to the electrode by applying a size-exclusion perm-selective barrier. An alternative approach is to apply an ion-selective

film, attracting species of the desired charge and repelling those of the unfavorable charge. This literature review contains the most commonly used modern electrode coatings and their uses, and assesses whether they may be of use in this application.

The different technologies that could be employed to aid the performance of the sensors were collated and a preliminary assessment of their relative merit to the current investigation conducted.

Poly (1,2 diaminobenzene)

Poly (1,2 diaminobenzene) can act as a size-exclusion membrane once electropolymerised onto the electrode surface. The membrane is used to allow only very small molecules to the electrode surface e.g. hydrogen peroxide and blocks most ascorbic acid and uric acid up to 2mM [11]. Its most common uses are in enzymic electrochemistry as an anti-interferent screen where small molecules are used for signalling and thus could be considered to be unsuitable for the direct detection of UA.

Polyphenol and Polypyrrole

These can both act as size-exclusion films, however they are also only suited to the electrochemistry of very small molecules e.g. the measurement of lactate via lactate dehydrogenase, where, like 1,2-diaminobenzene, they have served to block the interference by AA and UA [12].

Polymer of N,N-dimethylaniline (PDMA)

This cationic polymer has been the subject of many investigations over the past few years with many publications available. In 2003, the use of a PDMA modified glassy carbon electrode was shown to allow the detection of dopamine in the presence of AA [13]. Due to the polymer's hydrophobicity, it influences the voltammetric response of dopamine and AA and the film thickness can be altered by changing the concentration of DMA. Further work by Roy *et al.* [14] showed that the polymeric film of DMA has a

positive charge on the quaternary ammonium group in its backbone allowing the measurement of UA in the presence of AA by separating the oxidation peaks. This was observed due to the anionic nature of AA and UA at pH 7.0 and effectively ion exchanged into the cationic polymer so the oxidation potentials of these species were reduced. The use of this polymer allowed for UA and AA detection in the presence of physiologically important interfering species (e.g. glucose, purine, urea and citrate) although there was no mention of the effects of proteins. However, as albumin is anionic it could be anticipated that this may also be attracted towards the polymer. Given the relatively large size of albumin, the potential blocking effect could be considerable.

The applicability of the polymer was further extended through the incorporation of hexacyanoferrate as an electrocatalyst which was shown to improve oxidation peaks. It was shown to be stable in acidic, alkaline and neutral media and the polymer was shown to reduce electrode fouling caused by the oxidized products of AA. This polymer has also been applied to boron-doped diamond electrodes to allow the separation of serotonin and AA oxidation peak overlap [17]. While it could be envisaged that the system may be applicable to other electrode materials such as the carbon systems investigated in the present work, there are some issues relating to its deployment in a wound environment. Dimethylaniline has certain safety issues as the monomer is known to be highly toxic and a known carcinogen. It would be unwise to produce sensors in which it was used at the primary wound interface. The presence of unreacted monomer or the degradation or subsequent release of oligomeric products into the wound fluid may have far reaching consequences well beyond those that bacterial contamination could generate. While there is no doubt as to the favourable electrode characteristics that such a system could impart – the potential toxicological impact of a device failure would be too great to risk for an *in vivo* setting.

Poly(Phenylene oxide) (PPO)

A PPO film bearing oligoether groups can be deposited by electropolymerisation by controlling the potential and amount of current passed in much the same procedure as the previous polymers. The surface coating of PPO anodically forms from phenol with m-

$CH_3(OCH_2CH_2)_4O^-$ group found to be a useful tool for eliminating the adsorption of albumin on electrodes[18]. The main issue with the adoption of PPO in the present context is the low permeability of the resulting film. They tend to form highly compact layers that exclude most species and hence would be unsuitable for UA determination.

Nafion®

Using pre-anodized Nafion® coated electrodes, selective determination of uric acid in the presence of AA has been successful at pH 4 and 5 [19,20]. At this pH UA is **cationic** and the AA in **anionic**, thereby UA preferentially ion exchanges into the anionic Nafion® film and the AA is electrostatically repelled. The main problem with this application is that, for it to work, the AA and UA needs to have the differing charges to allow the ion-selective nature of the film to function. However at physiological pH 7.0, both the UA and AA are anionic and therefore would be repelled from the electrode and it was deemed that this electrode coating would be unsuitable for the condition likely to be experienced by the sensor.

Poly(4-vinylpyridine) (PVP)

Carbon paste electrodes coated in PVP have successfully been used to measure UA in the presence of AA by SqWV. However, this was also performed in a very acidic (pH 1.1) environment and is therefore unsuitable for the physiological pH of biofluids [21]. The toxicological properties possessed by the vinylpyridyl moieties would also factor against its adoption in the present application.

Poly (3-(3-pyridyl)acrylic acid

Zhang *et al.* [22] used of a poly (3-(3-pyridyl) acrylic acid modified glassy carbon electrode to facilitate the simultaneous detection of dopamine, AA and UA. The modified electrode provided sufficient peak separation due to the polymeric charge even at pH 7.0. However, the limited research into this method indicates that further development would

be required and clarification of the toxicological properties prior to its application in the present context.

2,2-bis (3-amino-4-hydroxyphenyl) hexafluoropropane (BAHHFP)

A BAHHFP modified glassy carbon electrode described by Milczarek [23] was shown to sufficiently suppress the ascorbic acid signal and shifts it towards the negative potential at pH 7.4. This could in principle allow better resolution of the urate signal but again with limited research the method may require further work for optimization and application in an *in vivo* context.

Dialysis Membranes

This represents a class of polymer material which is one of the simplest and most frequently used in electrode sensors designed for both *in vitro* and *in vivo* operation. The polymer is applied as a pre-cast or commercial dialysis membrane and can effectively prevent larger molecular weight species e.g. proteins and lipids and other cellular components from accessing the electrode surface. A few of the diverse examples include:

- The detection of the drug Clozapine using a horse-radish peroxidase and BSA carbon paste electrode covered with a dialysis membrane (12kDa m.w. cutoff) [24].
- Enzyme based UA measurement using phosphate and adenosine deaminase modified carbon electrode coated with self-cast dialysis membrane. This allowed detection in serum samples with no interference from proteins or oxidisable substances in serum [25].
- The measurement of chloride and bromide ions in serum by covering the electrode in 5kDa m.w.cut off dialysis membrane to prevent interference from proteins. [26]
- To form a diffusion layer in the detection of ascorbic acid or hydrogen peroxide a 12-14kDa pore size cellophane dialysis membrane has been used [27]

- For coating a Cd ion-selective electrode to prevent protein fouling using 12-16kDa membrane pulled over the end of an electrode and held in place with an o-ring. [28]
- Used in the construction of a microbial biosensor for the detection of 2,4-dichlorophenol, 12-14kDa m.w. cut off. [29]

These materials are one possibility that could be applied in the present context as the biocompatibility of the material is well established.

Cellulose acetate

Cellulose acetate films (CA) can be solvent cast from an ethanol solution onto the electrode surface and are widely used in biofluid electrochemistry as an effective size exclusion barrier. The basic premise is similar to the dialysis membrane but offers greater ease of manipulation in terms of solvent casting and coating. A successful CA film can be cast from 20% cellulose acetate, 60% acetic acid, 10% PEG 400 and 10% distilled water (% by weights). This was found to be the most effective cellulose acetate membrane for the rejection of Bovine Serum Albumin (BSA, 96%) and comparable to commercially available dialysis membranes[10]. As BSA has a molecular weight of 66kDa and Human Serum Albumin (HSA) is 67kDa, they are very similar in size. Given that the HSA is slightly larger, it could be anticipated that this membrane should serve as an effective screen that prevents fouling by species present in the wound environment. This approach could be ideal as the pores formed using a 1% cellulose acetate solution in 45:55 acetone to cyclohexanone have been shown to block proteins but allow smaller molecules to pass though and interact with the electrode surface. The ease with which the films could be incorporated into the present sensing strategy and the established biocompatibility was deemed to be further advantages and thus the accumulated evidence supported the adoption of this material in the present project.

6.2 Experimental Details

Materials

All reagents were of the highest grade available and used without further purification. Stock solutions of UA (typically 10mM) were prepared in 0.1M NaOH. All other solutions were prepared using pH 7 BR buffer. Electrochemical measurements were conducted using a μAutolab type III computer controlled potentiostat (Eco-Chemie, Utrecht, The Netherlands) using a two electrode configuration consisting of the carbon fibre assembly working electrode with a chloridised silver wire as the combined counter/reference electrode.

Microorganisms

Bacterial culture minimal medium was prepared according to the following composition (g/L): $MgSO_4.7H_2O$, 0.2; $FeSO_4.7H_2O$, 0.01; $CaCl_2$, 0.05; Glucose, 10.0; K_2HPO_4, 2.5; KH_2PO_4, 5.0 in distilled water. Aliquots of the broth were subsequently spiked to either 0.2mM uric acid or 0.2mM UA and 10mM urea prior to dilution. The media was then autoclaved. Bacterial growth was measured turbidimetrically (λ 600 nm) using a Jenway 6506 UV/Vis. spectrophotometer. Stock cultures were used to inoculate 10ml of TSB (MERCK 1.05459) and grown at 37°C with shaking at 200 rpm for 18 hours (overnight). Optical density measured (using 10 fold dilution in phosphate buffered saline, PBS). Prior to inoculation into chemically defined medium the bacteria were washed to remove TSB; 1.5mL of broth was centrifuged at 4500rpm for 5 minutes, supernatant aspirated and discarded, 1.5mL sterile PBS added, vortex mixed, centrifuged again and then these washing steps repeated twice before bacteria being finally suspended in 1.5mL sterile PBS. An aliquot, 100μL, of washed bacterial suspension used to inoculate 10mL of uric acid culture medium. Aliquots of this medium were taken at 4, 6 and 24 hours for measurement of optical density and then centrifuged to precipitate bacteria, supernatant could then be collected and stored at 4^oC for uric acid analysis, performed upon collection of 24 hour samples. The UA analysis was performed as before, with standards and controls being run at the start and controls repeated at the end.

6.3 Results and Discussion

Given that the urate sensors detailed in **Chapter 4** can clearly detect urate in a complex biofluid, the next issue to be addressed relates to whether or not it is indeed capable of monitoring urate beyond the initial scan. The intended application requires periodic scanning of the biofluid for differences in urate concentration and hence alert the patient / clinical staff to the possibility of wound colonisation. The rapid decline in the magnitude of the peak being used as evidence for the occurrence of the latter. Serum samples were used in this instance to avoid the complications of clotting and the need for exogenous agents to prevent such. This would allow replicate measurements on same sensor assemblies over a prolonged period and hence would mimic the conditions under which a prototype could be expected to operate.

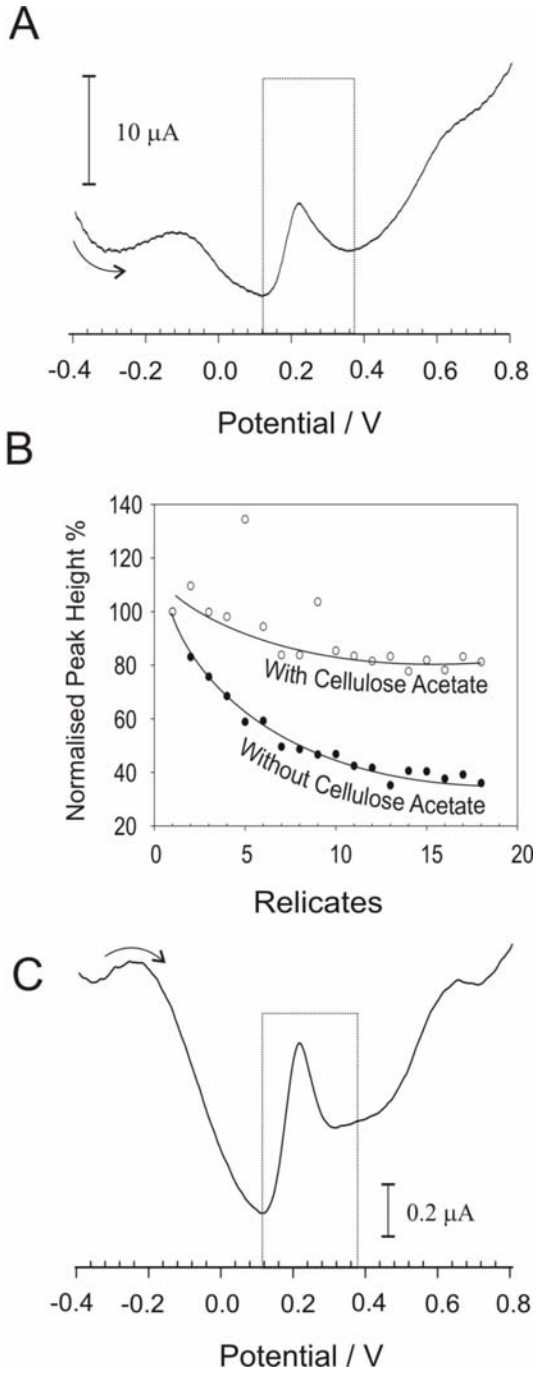

Figure 6.1. A) Square wave voltammograms detailing the response of an anodized carbon fibre sensing assembly towards human serum. B) Influence of cellulose acetate on the periodic response monitoring of urate in serum. C) Response of the pre-treated, cellulose acetate coated, sensor towards blister fluid. Step height: 2mV, Amplitude: 10mV.

A square wave voltammogram detailing the initial response to the application of the serum sample is shown in **Figure 6.1A**. The UA peak is again clearly resolved and is consistent with both the control UA solution and the responses observed in whole blood. The variation in peak height as a function of replicate scans (same sensor, same sample) is highlighted in

Figure 6.1B (solid circles). It can be seen that the peak height response decreases markedly with increasing measurements. It was envisaged that the sustained decay in the response could be attributed to the fouling of the electrode surface by the extra-cellular components, principally protein and fats, effectively reducing the active sensing area and hence the response. To counter this problem, the electrode surface was coated with cellulose acetate to act as a protective permselective barrier as selected from the literature review.

The response characteristics of this second modification have been included within **Figure 6.1B** (white circles) for comparison. There is an initial decay in response which is similar to that observed with the uncoated anodised fibre mesh but, in contrast to the latter, the response soon stabilises. It is possible that the initial responses are simply a consequence of the equilibration of the anodised fibre in the new medium. The difference in response characteristics (normalised to the peak height measured on the first scan) between the CA modified sensor and the uncoated, anodised, system is marked with only a minor loss in performance (~20%) observed with the former whereas the latter suffers significantly (>60% decrease).

The last hurdle in the preliminary assessment of the applicability of the sensing system was to determine whether or not it could detect UA in a blister wound, typical of the open wound liable to be subject to common bacterial infection. A square wave voltammogram detailing the response of the anodised sensor system towards the blister exudate (obtained from a human volunteer) is shown in **Figure 6.1C**. The profile is again similar to that found with the other biofluids and highlights the potential for applying the sensor system within a number of biomedical contexts where it may be necessary to monitor wound status.

The interaction between the bacteria inoculated within a medium containing 200 μM UA was monitored again using the carbon laminate sensor assembly. To ensure that accurate quantification of UA is possible, a series of standard curves were run throughout the investigation to cover the physiologically relevant range [0-500 μM, Peak Height [I_{pa}/μA] = 0.025 [Urate/μM] + 0.561, R^2 = 0.97]. Initial testing in the chemically defined minimal media for bacterial metabolism of UA for the three bacterial species as a function of incubation time is detailed in **Figure 6.2** along with the control (sterile

medium). It can be seen that the *Ps. aeruginosa* rapidly metabolised the exogenous UA and stands in marked contrast to parallel investigations with *S. aureus* and *K. pneumoniae.* An important point for consideration during the interpretation of these results is the fact that while all three organisms were sustained by the chemically defined broth, *Ps. aeruginosa* had the least growth (as measured by optical density). In this case, a period of 6.5 hours passed with no substantial increase in optical density being observed – which is in contrast to *S. aureus* and *K. pneumoniae* where an absorbance increase of 0.075 and 0.513 AU was observed respectively. Yet *Ps. aeruginosa* consistently exhibited the more rapid consumption of urate within the medium.

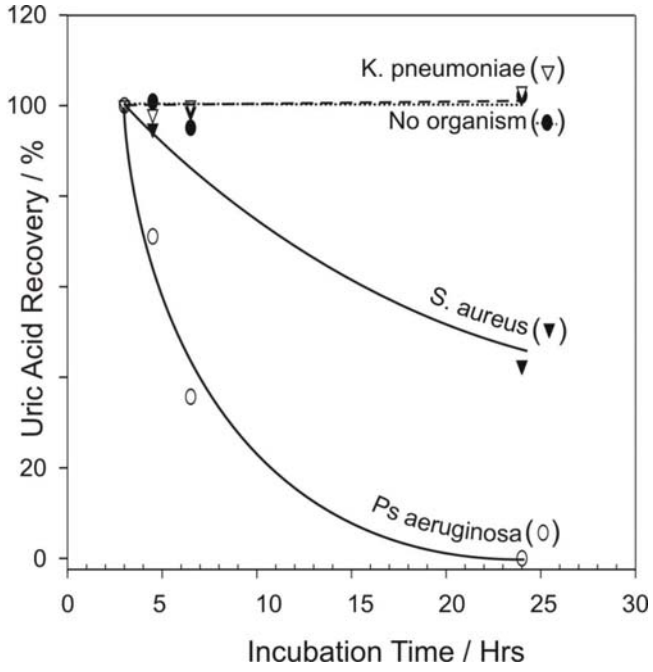

Figure 6.2. Influence of bacterial strain and incubation time on metabolism of exogenous urate (200 μM) compared with the sterile control (dotted line).

The differences in UA degradation cannot solely be attributed to the differences in bacterial multiplication (ie using UA as a nitrogen source), especially considering the 50 fold excess of urea (serving as an alternative nitrogen, carbon and energy source) present in the medium. It may be assumed that therefore that expression of uricase is largely responsible for the consumption of UA (especially in the case of *Ps. aeruginosa* [9, 10]) under the experimental conditions provided. The fact that the UA measurements were conducted using the carbon laminate sensor completes the final aspect of the investigation and demonstrates the capability of the assembly for monitoring urate both within common biofluids but also in the presence of bacterial moieties.

Having established that the UA sensors can monitor the substantial urate metabolism in a simple chemically defined media, the final step in the development of such a sensor towards smart-bandage application was testing the performance within biological fluids. Simulated Wound Fluid was again used (as Chapter 4), with bacterial

cultures inoculated into the SWF. The SWF was again spiked with 200μM UA and sample collected prior to and after 24 incubation. The sensors showed a linear relationship with UA concentration [Current / μA = 0.0173 urate concentration/μM + 0.754 (r^2 = 0.994)]. Upon testing the urate concentrations in the cultures, particularly after incubation, the peaks were still present but very variable with many indicating a much higher concentration than was initially added.

To assess the UA concentrations more accurately, the samples were analysed by a commercially available uricase based UV assay. Following calibration [Absorbance = 4.091 x 10^{-4} urate concetration / μM + 1.0389 x 10^{-5} (r^2 = 0.992)] the sample analysis showed that only small quantities of the added urate were metabolised (**Figure 6.3 black**) when the diluted bovine serum was used as media. Fresh cultures were setup again to assess the metabolism of UA by the organisms (**Figure 6.3 red**) but again, only small quantities of the urate were metabolised. When no organism was added 30 and 19μM UA degraded naturally and only slightly more UA degraded by the presence of most organisms tested, note that for *St. aureus* less UA is degraded, the exact mechanism leading to this is unknown. These experiments were performed by growing the organisms overnight and reaching the stationary phase of growth, so even in substantially higher bacterial loads than would be useful to detect in a wound, the UA is not metabolised. The main reasons ascribed to the difference between the minimal media and the SWF is the presence of a huge range of potential nitrogen source, which are evidently preferential over the production of urate oxidase (uricase) to make use of available UA.

Figure 6.3. Quantity of urate degraded after 24 hours incubation for 2 separate batches of bacterial cultures.

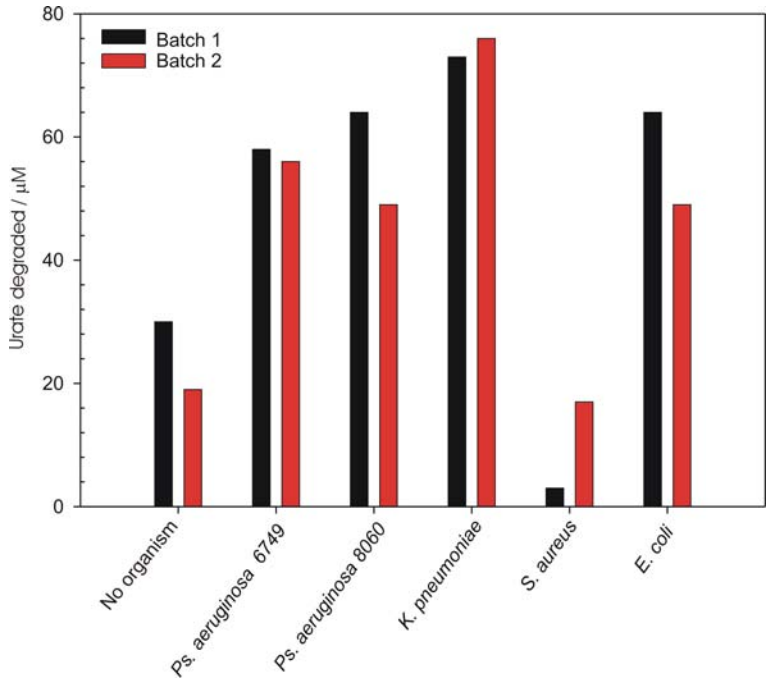

6.4 Conclusions

The carbon fibre sensing system has shown that periodical monitoring is feasible by the application of a CA permselective barrier and hence the system could facilitate short to medium term wound management. The ease with which the sensor can be fabricated, the unambiguous and sensitive nature of the signal is clearly an advantage over conventional UA measurement systems. While in chemically defined minimal media *Ps. aeruginosa* readily degrades exogenous urate and thereby allowing the depletion to be used as an early warning system, when tested in simulated wound fluid, the UA is not substantially depleted. As a result of these findings the UA sensor is not suitable for the proposed use due to the bacterial preference of using alternative nitrogen and carbon sources in physiological media. The stability of UA in the presence of huge bacterial loads of relevant opportunistic pathogens, however, adds to the pH sensor method robustness and therefore this Chapter is an essential follow up to **Chapter 4**.

6.5 References:

1. Verdecchia P, Schillarci G, Reboldi G, Santeusanio F, Porcellati C, Brunetti P. Relation between serum uric acid and the risk of cardiovascular disease in essential hypertension the PIUMA study. *Hypertension* 2000;36:1072-8
2. Coombes EJ, Shakespeare PG, Batstone GF. Observations on serum and urine alkaline ribonuclease-activity and urate after burn injury in man. *Clinica Chimica Acta* 1978;86:279-90
3. Haycock JW, Ralston DR, Morris B, Freedlander E, MacNeil S. Oxidative damage to protein and alteration to antioxidant levels in human cutaneous thermal injury. *Burns* 1997;23:533-40
4. Rouf MA, Lomprey RF. Degradation of uric acid by certain aerobic bacteria. *Journal of Bacteriology* 1968:617-22
5. Adámek V, Králová B, Suchová M, Valentova O, Demnerova K. Purification of microbial uricase. *Journal of Chromatography* 1989;497:268-75
6. Diagnostic Services Handbook (2005) Nottingham City Hospital NHS trust, UK
7. Ayton M. Wounds that won't heal. *Nursing Times* 1985;81:16-19
8. Geise RJ, Adams JM. Barone NJ, Yacynych AM. Electropolymerized Films to Prevent Interferences and Elctrode Fouling in Biosensors. *Biosensors and Bioelectronics* 1991;6:151-60
9. Alwarappan S, Butcher KSA, Wong DKY. Evaluation of hydrogenated physically small carbon electrode in resisting fouling during voltammetric detection of dopamine. *Sensors and Actuators B* 2007;128:299-305
10. Idris A, Lee KY, Hing HK. Preparation of cellulose acetate dialysis membrane for separation of bovine serum albumin. *Journal of Technology* 2005;42:35-46
11. Yao T, Koteqawa K. Simultaneous flow-injection of creatinine and creatine in serum by the combined use of a 16-way switching valve, some specific enzyme reactors and a highly selective hydrogen peroxide electrode. *Analytica Chimica Acta* 2002;463:283-91.
12. Krawcyzk TKY, Trojanowicz M. Lactate solid-state biosensor with multilayer of electrodeposited polymer for flow-injection clinical analysis. *Biosensors and Bioelectronics* 1996;11:1155-65
13. Roy PR, Okajima T, Ohsaka T. Simultaneous electroanalysis of dopamine and ascorbic acid using poly (N,N-dimethylaniline)-modified electrodes *Bioelectrochemistry* 2003;59(1-2):11-9
14. Roy PR, Okajima T, Ohsaka T. Simultaneous electrochemical detection of uric acid and ascorbic acid at a poly(N,N-dimethylaniline) film-coated GC electrode *Journal Of Electroanalytical Chemistry* 2004;561(1-2):75-82

15. Roy PR, Saha MS, Okajima T. Electrocatalytic oxidation of ascorbic acid by [Fe(CN)(6)](3-/4-) redox couple electrostatically trapped in cationic N,N-dimethylaniline polymer film electropolymerized on diamond electrode. *Electrochemica Acta* 2005;51(21):4447-54
16. Roy PR, Saha MS, Okajima T. Selective detection of dopamine and its metabolite, DOPAC, in the presence of ascorbic acid using diamond electrode modified by the polymer film *Electroanalysis* 2004;16(21):1777-84
17. Park SG, Park JE, Cho EL, Kwang JH, Ohsaka T. Electrochemical detection of ascorbic acid and serotonin at a boron-doped diamond electrode modified with poly(*N*,N-dimethylaniline) *Research on chemical intermediates* 2006; 32(5-6):595-601
18. Maede H, Okada T, Matsumoto Y, Katayama K, Yamauchi Y, Ohmori H. Electrochemical coating with poly(pheylene oxide) films bearing oligoether groups as a tool for elimination of protein adsorption to electrode surfaces. *Analytical sciences* 1999;15:633-9
19. Zen JM, Jou JJ, Ilangovan G. Selective voltammetric method for uric acid detection using pre-anodized Nafion-coated glassy carbon electrodes. *The Analyst* 1998;123:1345-50
20. Zen JM, Hsu CT. A selective voltammetric method for uric acid detection at Nafion ® -coated carbon paste electrodes. *Talanta* 1998;46:1363-9
21. Zen JM, Chen YJ, Hsu CT, Ting YS. Poly(4-vinylpyridine)-coated chemically modified electrode for the detection of uric acid in the presence of a high concentration of ascorbic acid. *Electroanalysis* 1997;9(13):1009-13
22. Zhang YH, Su S, Pan Y, Zhang LP, Cai YJ. Poly (3-(3-pyridyl) acrylic acid) modified glassy carbon electrode for simultaneous determination of dopamine, ascorbic acid and uric acid. *Annali Di Chimica* 2007;197(8):665-74
23. Milczarek G, Ciszewski A. 2,2-bis(3-amino-4-hydroxyphenyl)hexafluoropropane modified glassy carbon electrodes as selective and sensitive voltammetric sensors. Selective detection of dopamine and uric acid *Electroanalysis* 2004;16(23):1977-83
24. Blankert B, Dominquez O, Ayyas WEL, Arcos J, Kauffman JM. *Analytical Letters* 2003;37(5):903-13
25. Kinoshita H, Yoshida D, Miki K, Usui T, Ikeda T. An amperometric-enzymic method for assay of inorganic phosphate and adenosine deaminase in serum based on the measurement of uric acid with dialysis membrane-covered carbon electrode. *Analytica Chimica Acta* 1995;303:301-7
26. Arai K, Kusu F, Noguchi N, Takamura K, Osawa H. Selective determination of Chloride and Bromide ions in serum by cyclic voltammetry. *Analytical Biochemistry* 1996;240:109-13
27. Takatsy A, Csoka B, Nagy L, Nagy G. Periodically interrupted amperometry at membrane coated electrodes: a simplified pulsed amperometry. Talanta 2006;69:281-5
28. Fish SF, Brassard P. Dialysis membrane to prevent cadmium ion specific electrode fouling. *Talanta* 1997;44:939-45

29. Jantra J, Zilouei H, Liu J, Guieysse B, Tharvarungkul P, Kanatharana P, Mattiasson B. Microbial Biosensor for the Analysis of 2,4-Dichlorophenol, *Analytical Letters: Biosensors* 2005;38:1071-83

Chapter 7

The Development of a Pyocyanin Sensor

Abstract

Pyocyanin is produced by *Ps. aeruginosa* as a result of quorum sensing during wound colonisation increasing bacterial virulence and damaging host physiology both of which contribute to an increased risk of infection. The novel use of a photoreactor for the enhanced synthesis of pyocyanin through the photooxidation of phenazine methosulfate was evaluated. Prototype sensor assemblies based on carbon fibre tow for a smart-bandage application have been developed and response characteristics towards pyocyanin are detailed. The sensitive and linear quantification of pyocyanin is presented (r^2=0.998) across the biomedically relevant concentration range (1-100μM). Electrochemical measurements of pyocyanin by square wave voltammetry were established using carbon fibre assemblies (coefficient of variance =1.2 and 1.4 % for 10 and 50 μM pyocyanin, respectively). Further testing of the sensors in bacterial cultures demonstrated the potential applicability of the sensors for monitoring pyocyanin production by *Ps. aeruginosa* and validated using an established chloroform-acid/photometric method. The small and inexpensive sensor assembly is suggested for use in monitoring *Ps. aeruginosa* growth and may offer a new approach in infection diagnostics and smart-technologies.

The work detailed in this chapter has been published in *Bioelectrochemistry* 2009- in press.

7.1 Introduction

The opportunistic pathogen *Ps. aeruginosa* is the cause of many infections, compromised patients are particularly susceptible, e.g. pulmonary infection in cystic fibrosis (CFib) patients, surgical wound infections and burns wound infections. This coupled with the high incidence of antibiotic-resistant *Ps. aeruginosa* strains [1,2] prompts the necessity to develop new strategies for both detection and treatment, with the early implementation of the former clearly facilitating the latter. The ability to detect *Ps. aeruginosa* infections early could not only reduce the time spent in hospital and reduce patients' pharmaceutical requirements but also to improve patient morbidity and mortality and help curtail the financial burden of wound infections. *Ps. aeruginosa* uses many complex quorum sensing (QS) systems enabling the bacteria to make collective decisions with respect to the expression of specific gene sets controlling virulence [3]. An additional role of this QS system, proposed by Christensen *et al.* [4] has shown (in a mouse model) that it plays a vital role in the bacterial resistance to the innate immune system. This backs up previous work by Schaber *et al.* [5] which also details the vitality of quorum sensing in the infection of thermally injured mice.

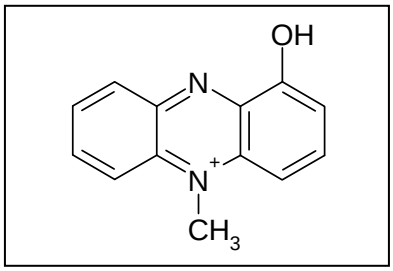

Figure 7.1. Structure of pyocyanin

One such virulence factor is pyocyanin (1-hydroxy-*N*-methylphenazine, Figure 7.1) which is a blue coloured redox-active dye and a member of a large family of tricyclic compounds known as phenazines. Reyes et al found that pyocyanin was synthesized *de novo* by 96% of the 835 *Ps. aeruginosa* strains tested within an overnight incubation and by 98% within 48 hours) [6]. As this dye is specifically synthesised by *Ps. aeruginosa,* the detection of pyocyanin is both organism specific and produced by most strains. Due to the low molecular weight of pyocyanin (210Da) it is readily diffusible and can easily permeate cell membranes [7,8]. Upon entry into cells, pyocyanin can be reduced by NAD(P)H and can subsequently reduce molecular oxygen to superoxide anion. This in turn dismutates to hydrogen peroxide and thereby induces oxidative stress in endothelial and epithelial cells through the generation of these reactive oxygen radicals [8]. As well as direct

cellular and molecular effects, these reactive oxygen species and the associated oxidative stress can be inhibitory to cell growth in bacteria, fungi and mammalian cells. Work using manganoporphyrin (a superoxide scavenger) showed it could partially inhibit the effects of pyocyanin on the human cell growth, again indicating the role of superoxide [8].

The effects of pyocyanin are of importance not only through virulence determination within the *Ps. aeruginosa* QS systems, but also for the direct physiological consequences (oxidative or not) on host tissues, which may allow more serious infections to initiate. The treatment of endothelial cells with 1-50μM pyocyanin results in a dose-dependant formation of hydrogen peroxide, this causes a decrease in the antioxidant soluble thiol - glutathione, demonstrating that pyocyanin exposes endothelial cells to oxidative stress [9,10]. Pyocyanin has been shown to slow human nasal ciliary beat frequency (CBF) and lead to the disruption of the epithelium in a reversible manner with the reduction attributed to a substantial decrease in intracellular cAMP (90%) and ATP (66%) [11]. If this bacterially derived molecule can cause epithelial damage within intact epithelium, it is reasonable to assume that it will cause widespread damage and prevent the healing within a wound environment. Pyocyanin has also been shown to arrest cell growth even at low concentrations (5-10μM) and the resulting cells developed a phenotype consistent with cellular senescence. It was also demonstrated that 25μM pyocyanin was sufficient to directly induce apoptosis [8].

Therefore the production of pyocyanin by *Ps. aeruginosa* may alone be degradatory on wound healing, by preventing cell growth in addition to the potential to induce apoptosis at higher concentrations, especially when considering that the concentrations within CFib patient's sputa have been detected as high as 130 μM [12]. Usher *et al.* [13] reported that pyocyanin induced a time and concentration dependant acceleration of neutrophil apoptosis at concentrations found in CFib patient's sputum. Additionally it was suggested that pyocyanin-induced apoptosis was associated with rapid and sustained generation of ROS and subsequent reduction of intracellular cAMP, concluding that affects on the neutrophil apoptosis may be a clinically important mechanism of persistence of *Ps. aeruginosa* in human tissue (e.g. chronic infections in CFib patients), however the same rationale may be true for wound infections [13]. Pyocyanin production by *Ps. aeruginosa* suppresses the acute inflammatory response by

pathogen-driven acceleration of neutrophil apoptosis and reducing local inflammation is advantageous for bacterial survival. This was assessed by Allen *et al.* in 2005 [14] comparing pulmonary infection clearing in mice with wild type and pyocyanin-deficient mutant strains of *Ps. aeruginosa*. During *Ps. aeruginosa* infections of the lungs in CFib patients, pyocyanin can inactivate many anti-oxidative stress mechanisms (e.g. catalase and the GSH redox cycle) again relating to the ROS / oxidative stress induced mechanisms of cellular dysfunction [15]. It has also acts antimicrobially towards other bacteria, e.g. *E. coli.*

There are few publications detailing the electrochemical determination of pyocyanin, however, using Adsorptive Stripping Voltammetry (AdSV) employing a hanging mercury drop electrode (HMDE) has enabled the measurement of pyocyanin at the nanomolar level [18]. In this instance the pyocyanin was effectively pre-concentrated on the HMDE prior to potential scanning. The use of the latter is not possible within a wound environment both in terms of instrumental operation and toxicological significance of exposing the wound to mercury. One interesting aspect is the fact that the analysis process results in the production of the oxidised form of pyocyanin which has negligible contribution to virulence. Thus the analysis procedure could, in principle, diminish the cytotoxic and infective characteristics of the metabolite. Therefore, if the pyocyanin concentration is reduced this may have a beneficial effect of reducing the virulence of the *Ps. aeruginosa* infection as the QS derived factors have been found directly affect the virulence [19] and the host's response to the infection.

The inhibition of quorum sensing as an anti-pathogenic treatment of *Ps aeruginosa* infection is not a new topic. The effects of QS inhibitors on the bacterial load of pulmonary infection in mice was discussed by Rasmussen and Givskov [3]. They reported that the use of QS inhibitors induced a faster clearing of the infection and therefore the degradation of the QS molecules may be of importance in *Ps. aeruginosa* infections whether pulmonary or epidermal. The degradation of the pyocyanin virulence factor by the actual detection may have direct antibacterial advantages and may be facilitated further by the use of large surface area sensors not only increasing sensitivity, but increasing the amount of pyocyanin oxidised.

The foundations of the pyocyanin sensor reported herein rely upon the properties of carbon fibre tow as a combined detection element and transduction conduit. Recent developments have seen the use of graphite rods as electrodes for monitoring the response to quorum sensing inhibition through pyocyanin detection [20]. Greater linearity and sensitivity are sought to allow the use of solid phase but flexible sensors with SqWV for infection diagnostics. The periodic *in situ* analysis of wound exudates may allow the early detection of pyocyanin production by *Ps. aeruginosa* thereby alerting the patient or clinical staff to the likelihood of progression from contamination to colonisation. This would also allow early instigation of antibiotic therapies as the infection initiates and this may be prior to the appearance of a clinical infection. While it is impossible to establish a reference range for pyocyanin production through *Ps. aeruginosa* infection, the concentration range of 0-100μM has been investigated as this covers the concentrations liable to be encountered [8-10] and the diagnostically relevant range that has been observed in other biofluids [12].

The applicability of this sensitive pyocyanin sensor is not limited to that of a smart-bandage within the biomedical context. Due to the potential severity and associated problems of *Ps. aeruginosa* infection within CFib patients, a point of care testing (PoCT) device enabling self/home monitoring of pyocyanin within the patient sputa, using the proposed assembly, could enable early detection of lung colonisation or the monitoring of chronic infections helping patient outcomes.

7.2 Methodology

A critical issue with the present investigation was the availability of pyocyanin that could be used for the quantitative evaluations. The bacterial metabolite is not readily commercially available. As pyocyanin is produced by *Ps. aeruginosa* infection, the purification of pyocyanin from this source is a well established albeit crude method. While this may be a cheap method for synthetic application and manipulation, the further refinement of the purification for analytical purpose as in this context would have been extremely problematic especially given the range of metabolites that can arise from bacterial culture. Purification from broth culture is widespread and many broth

compositions have been studied. Pyocyanin production is enhanced through the presence of magnesium chloride, potassium sulfate, glycerol and iron, but notably a low phosphate concentration all of which are important when considering the buffering agents of culture media. The details of the varying methodologies are available [22-25], however the enhanced production is not the primary problems with this approach. Unlike the chemical synthesis methods, many other bacterial phenazine and by-products must be removed from the crude pyocyanin. The pyocyanin can be extracted by chloroform washes (pyocyanin is soluble in chloroform) and many other methods have been established for the subsequence purification e.g. Watson *et al*. 1986 [26] using chloroform and petroleum ether precipitation and HPLC with UV detection.

Debate has arisen over the best method of purification from the crude bacterial pyocyanin produced. An overview of the commonly used methods is collated and critically assessed and include:

DCM/Hexane (1:2) Precipitation

This was used for purification of pyocyanin from liquid cultures after dichloromethane (DCM) extraction and column chromatography. The semipure residue was dissolved in 1mL DCM and precipitated with 2mL hexane. After standing on ice for 5 minutes, the mixture was centrifuged 14,000 rpm at 4 °C for 1 minute, forming a pellet of blue material, the solvent was aspirated off and the procedure repeated five times [29].

Multi-step Extraction

This was used for the extraction and purification of pyocyanin from bacterial broth cultures. Pyocyanin was extracted into chloroform from the incubation mixture supernatant and then re-extracted into 0.2 M HCI. A solution of 0.4 M borate-NaOH buffer (pH 10) was added to the deep red acid solution until the colour changed to blue and the pyocyanin again extracted into chloroform. This cycle was repeated 2 or 3 times, resulting in a clear solution of pyocyanin in chloroform. The latter was evaporated to a

small volume (ca. 1 mL) in a stream of cold air and then chromatographed on Whatman no. 4 in a solvent composed of n-butanol-acetic acid-water, 13:4:7 (v/v). Pyocyanin was eluted from the chromatogram with 0.2 N HCl and extracted into chloroform after treatment with borate buffer, as above. The chloroform solution was then re-chromatographed in an isopropanol-water, 4:1 (v/v) mixture. Again, the pigment was eluted with 0.2 N HCl and samples of the resulting solution used for the determination of concentration and for purity [24].

Chloroform and Aqueous Acid Re-extraction

This procedure has been used for the purification from bacterial cultures. Pyocyanin was obtained by growing *Ps. aeruginosa* strain PAO1 (ATCC 15692) in glycerol-alanine minimal medium [13] for 30 hours. The bacteria were removed from the dark blue medium by centrifugation, and three consecutive extractions of the medium with chloroform (1 to 0.2 ratio) removed most of the blue pigment. The purification of pyocyanin [16] involved both alternate extractions of the red, acid form of pyocyanin from the chloroform layers with acidified water and repeated chloroform extractions of the blue pyocyanin from neutralized water layers. After five base-to-acid conversions, the pyocyanin was concentrated in a 3-mL volume of slightly acidified water. This was done so that the pH of the isolated water layer could be adjusted to pH 7.5 with a minimum volume of 0.1 M NaOH. Needlelike crystals formed in the chilled solution over the following 2 h. These were trapped on a 0.45 μm (pore size) filter (Nuclepore Corp.), washed with water, dried under vacuum, and weighed [22,32,33].

Chloroform – Acid Water Extraction

This procedure was specified for the extraction and purification of pyocyanin from broth cultures. Pyocyanin was extracted from the broth culture of *Ps. aeruginosa* as previously described [23]. *Ps. aeruginosa* strain PAO1 (ATCC 15692) was grown in glycerol- alanine medium. The bacteria were removed by centrifugation. The culture supernatant was mixed with chloroform to remove most non pyocyanin pigments. The

blue pigments in chloroform were extracted by 10 mM HCl followed by neutral water. This process was repeated at least five times. The purity of the pyocyanin solution was confirmed by HPLC using a Beckman System Gold apparatus and a reverse phase C18 column. (Microsorb-MV-C18, 250x4.6 mm; Varian, Walnut Creek, CA). The solvent system consisted of 0.05% trifluoracetic acid (TFA) in water and 0.05% TFA in acetonitrile using 25 to 30 min runs [25].

It is clear that the combination of long incubation periods and the time consuming purification processes would be prohibitive and the yield could be highly variable in terms of quantity but also in purity. In most cases the chromatographic analysis is largely qualitative. The electrochemical characterisation however could easily be affected by the presence of even minor impurities and lead to ambiguities in the interpretation of the resulting voltammograms. Pursuing the bacterial production route was viewed as a last resort while alternative procedures were investigated.

The most viable alternative to both custom synthesis and bacterial production was thought to lie with the photooxidation of phenazine methosulfate (PMS). This was viewed as a cheaper option to commercial/custom synthesis and should be procedurally simpler to purify than the bacterial route. A variety of conditions have been described in the literature [27, 28] but typically involve a 0.5mg/mL solution of PMS subjected to illumination at room temperature under high intensity cool white fluorescent lights for 4 days. The photo-oxidation of PMS offers a relatively low cost with substantially fewer side products/contaminant and thus considerably easier purification. The main drawback however is the long incubation period required. To counter this problem, a novel approach to the photooxidation was investigated to allow faster and hence enhanced pyocyanin production. This revolved around the use of a custom-built photoreactor **(Figure 7.2)** to enhance the photooxidation production leading to an increased yield within 6 hours incubation compared with the previously reported 4 day reaction period.

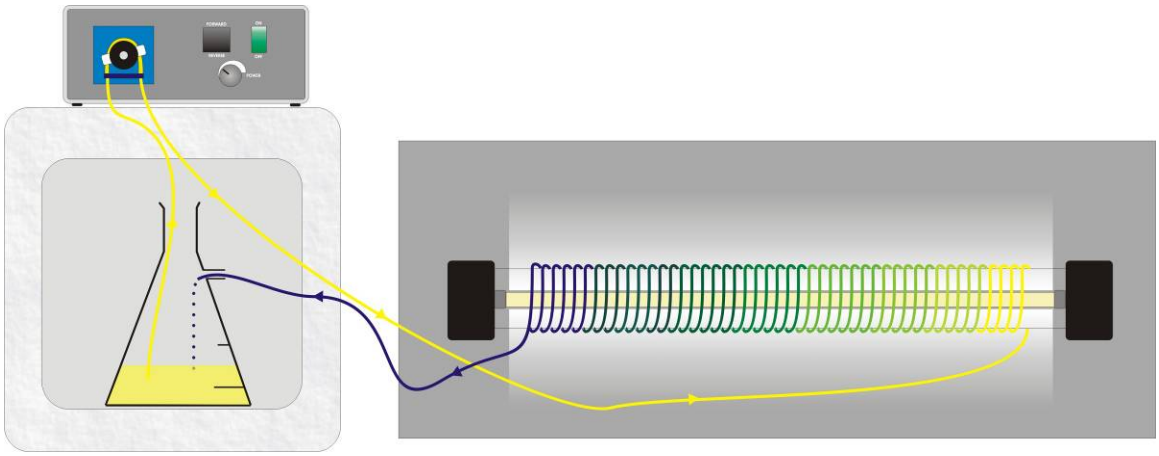

Figure 7.2. Photoreactor setup for enhanced photooxidation of phenazine methosulfate

The development of a robust production facility that could provide pyocyanin in high yield and of sufficient purity (as verified by uv, TLC and nmr) on demand was critical to the subsequent investigations.

7.3 Experimental Details

Pyocyanin synthesis

7.3.1 Standard Photooxidation [28,30]

A 0.5mg/mL solution of phenazine methosulfate (in pH 7.0 Britton-Robinson buffer) was illuminated under a cool white light for 96 hours. The blue solution was lyophilized and the residue dissolved in 2mL methanol. The methanol solution adsorbed onto silica gel 60 column (2.5x82cm) that had previously been equilibrated with 1% methanol in chloroform. Elution was accomplished with 15% methanol in chloroform, yellow and then red-coloured side products appeared in the eluate, followed by the blue pyocyanin. A yellow-green material remained adsorbed to the silica gel. A 60% yield of Pyocyanin (20mg) was obtained after removal of solvents from the pyocyanin-containing fractions in a rotary evaporator and subsequent lyophilization. The product co-migrated with

authentic pyocyanin by TLC in solvent systems A, B and C (A: standard solvent system 15% Methanol: Chloroform, B: Chloroform and methanol 1:1, C: Ethyl acetate, glacial acetic acid and water 3:2:1 [28,31] and crystals from chloroform exhibited a melting point of 133 °C.

7.3.2. Enhanced Photoreactor Photooxidation

Pyocyanin was synthesised by photochemical degradation of 0.5g/L phenazine methosulfate, PMS, (Sigma-Aldrich) [7] in Britton-Robinson buffer (pH 7.0). The photochemical reactor used (**Figure 1**) consists of 8m HPLC grade 1.5mm I.D. clear tubing wound around a commercially available aluminium fluorescent light (Kengo lighting TCF13, 13W lamp), PMS solution was circulated for 6 hours at 5 mL/min using a peristaltic pump (Gilson (USA) MINIPULS3). This yielded a strong blue coloured solution, the crude pyocyanin was extracted in three volumes of chloroform, dried with magnesium sulphate and filtered (Whatman No. 42) prior to rotary-evaporation in a 70°C waterbath, under vacuum, onto chromatography silica gel (40-63u 60A FLUOROCHEM UK). Crude pyocyanin was purified by column chromatography (50 x 5cm column) using 15:85 methanol: chloroform, collecting the blue portion and rotary-evaporated to dryness under vacuum. Purity was assessed in accordance with previous studies [28].

7.3.3. Crystallisation

Pyocyanin crystallisation was performed on the crude pyocyanin from the enhanced photoreactor synthesis. The synthesis was performed identically, but after the initial rotary evaporation of the pyocyanin fraction was crystallised instead of passing through a column. The crystallisation method used is based upon that used by Angell et al 2006, whereby their semi-pure pyocyanin residue was dissolved and precipitated in a 1:2 ratio DCM to Hexane on ice and filtered, this process was repeated 5 times. Instead of this, the same 1:2 ratio of DCM: hexane was used (typically 5:10 mL) but the sample was placed in a -20 °C freezer for precipitation overnight. After precipitation, the sample was filtered under vacuum prior to purity assessments.

7.3.4 Photometric pyocyanin analysis

1.5 mL of broth culture was centrifuged at 14,000rpm for 5 minutes, 1mL of supernatant was mixed with 1.5mL of chloroform and left to separate. The blue organic layer was mixed with 1mL of 0.2M HCl, whereby the blue mixture turns red and the red form of pyocyanin moves into the aqueous layer. This was re-centrifuged prior to measuring the absorbance at 520 nm and calculating the concentration (2460 M^{-1} cm^{-1})

7.3.5 Microbiology

Stock cultures were inoculation into *Pseudomonas aeruginosa* Broth (PAB) for pyocyanin measurements. *Pseudomonas aeruginosa* Broth (PAB) composition (g/L): glycerol 10.0, peptone 20.0, magnesium chloride 1.4, potassium sulfate 10.0, adjusted to pH 7.0 through the addition of sodium hydroxide. Broth cultures were incubated at 37^{o}C with orbital mixing at 150 rpm.

7.3.6 Instrumentation

Electrochemical measurements were conducted using a PalmSens Electrochemical Sensor Interface (Palm Instruments BV), controlled by a HP iPAQ Pocket PC using a three electrode configuration consisting of a glassy carbon electrode (3mm diameter; BAS Technicol. UK) or carbon fibre tow laminate working electrode, a 3M NaCl Ag|AgCl half cell reference electrode (BAS Technicol. UK) and platinum wire counter electrode. Cyclic voltammetry parameters: step potential 1mV, scan rate 50mV/s. Square wave voltammetry parameters: step potential 2mV, amplification 5mV, frequency 25Hz). Photometric measurements were performed using a Jenway (UK) 6715 UV/Vis. Spectrophotometer. Atomic force microscopy was performed using a NanoSurf® EasyScan AFM system.

7.4 Results and Discussion

7.4.1 Pyocyanin Synthesis and Purification

The initial synthesis was performed using a previously published method [28,30], whereby a 96 hours incubation is required to allow sufficient photooxidation of phenazine methosulfate. After the requisite chloroform extractions to collect only the chloroform soluble products (including pyocyanin) and rotary evaporation under vacuum, the solution was subject to column chromatography for purification as described in the experimental section.

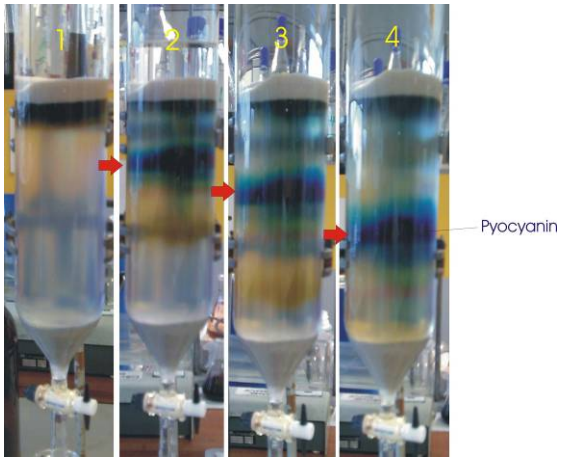

Figure 7.3. Column separation of crude pyocyanin

Figure 7.3 highlights the pyocyanin band observed by column chromatography and the other commonly observed by-products, firstly yellow and then red coloured side products appear, followed by the pyocyanin. A yellow-green material remains adsorbed to the silica gel. After collection, the pyocyanin fraction was again rotary evaporated to dryness under vacuum. The purity of this residue was assessed using TLC, melting point and UV analyses. TLC was performed using the three solvent systems described in the experimental section with the standard system **A**. (elution solvent 15% methanol in chloroform) gives a very narrow, concentrated pyocyanin band, allowing the slight reddish band just above to be observed. However, a previous group used other solvent ratios [28], **B**. Chloroform: Methanol (1:1) rf 0.60 and **C**. Ethyl acetate, glacial acetic acid, water (3:2:1) rf 0.23. However, under examination these both result in a much broader, diffuse pyocyanin band which covers the second band above thereby insufficiently determining purity. The use of column chromatography, as tested, produced a ~60% yield after 96 hours incubation.

In order to facilitate a more rapid photooxidation of PMS the photoreactor outlined in Section 7.2, **Figure 7.2** was assessed whereby the PMS solution is continuously pumped through a narrow diameter HPLC tubing in very close proximity to a cool light source. The interaction of the phenazine methosulfate molecules with light is increased substantially creating up to a ~40% yield within 6 hours. This affectively allows the synthesis and column purification of an acceptable yield within one working day which was a significant advantage over previously reported procedures. The additional benefits of this enhanced photooxidation is that it gives less time for the pyocyanin to degrade (e.g. to hydroxyphenazine) and can allow the on-demand synthesis of pyocyanin cheaply and efficiently.

Having developed a more efficient method of photo-oxidising PMS to pyocyanin, this still required the time consuming column chromatography to purify so an alternative was sought. Amongst the alternative methods described in the literature review, the simple precipitation of pyocyanin in a mixed solvent stood out as a simple and cheap method to evaluate. Pyocyanin, synthesized as previously described using the photoreactor, was precipitated overnight in the freezer in a 1:2 ratio of DCM: chloroform, prior to filtration. A yield of 17% was achieved using this method (compared with up to 40% by column chromatography). While it is a simple method of purification, it is was not as efficient as column chromatography due to the pyocyanin retained (and hence lost) in the solvent layer.

Table 7.1. Effect of pH on pyocyanin yield

pH	Yield (%)
3.0	**17.2**
5.0	**30.6**
7.0	**32.4**
9.0	**13.0**

The majority of reported methods for pyocyanin synthesis obtained through the photooxidation of phenazine methosulfate are performed in pH7 buffered solutions. The influence of varying pH on the subsequent yield was also assessed to ensure that the optimal conditions are used. **Table 7.1** shows the percentage yield observed with each pH.

There is little difference in yields between pH 5 and 7, however the yields using pH 3 and 9 are substantially smaller. Given the maximum yield was obtained at pH 7, these conditions were retained for all subsequent pyocyanin syntheses.

7.4.2 Electrochemical Monitoring of the Reaction Progression

The conversion of the yellow phenazine methosulfate to blue pyocyanin is visible, but a more accurate and less subjective approach was sought. Prior to the full development of a disposable pyocyanin sensor, initial use of a conventional glassy carbon electrode provided an easy way of monitoring of the conversion of PMS to pyocyanin by crude product analysis from the enhanced photoreactor setup. Cyclic voltammetry was used and the resulting voltammogram (**Figure 7.4**) clearly show the decreasing phenazine methosulfate oxidation peaks between -0.05V and +0.150V and the increasing pyocyanin oxidation peaks at -0.25V and +0.8V as a function of time.

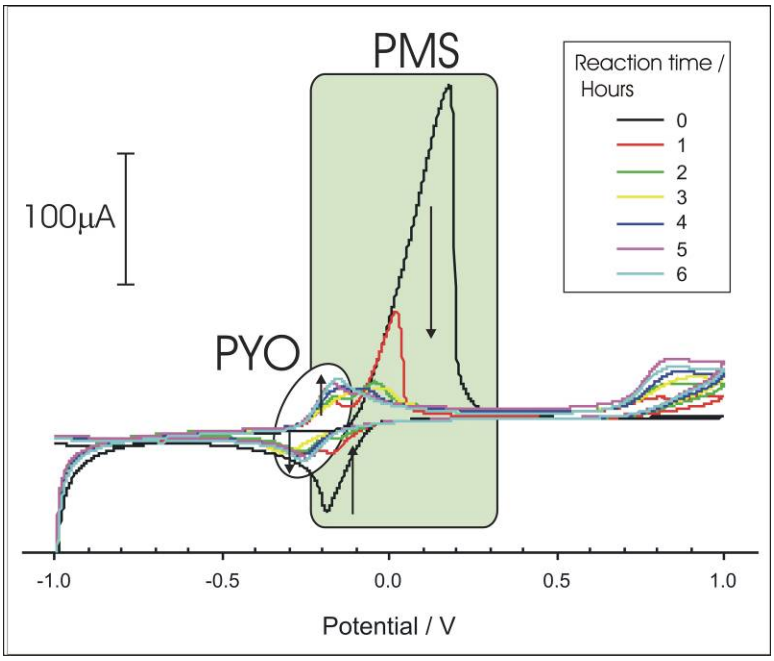

Figure 7.4, Cyclic voltammograms of the photooxidation of phenazine methosulfate to pyocyanin in the crude product of an enhanced photoreactor synthesis, from 1-6 hours. Scan rate: 50mV/s.

7.4.3 Pyocyanin sensor development and characterisation

The preliminary assessment of pyocyanin electrochemistry using cyclic voltammetry at carbon fibre electrodes shows both reversible phenazine transformations at -0.18V and -0.25V and a non-reversible phenolic oxidation of pyocyanin (I) at +0.85V (**Figure 7.5A**). The phenolic oxidation is responsible for the polymerisation of pyocyanin leading to increasing peaks heights observed with increasing scan cycles for both the phenazine oxidation and reduction. This is due to the cycling between the two polymeric forms (II) and (III) formed by the phenolic oxidation induced polymerisation.

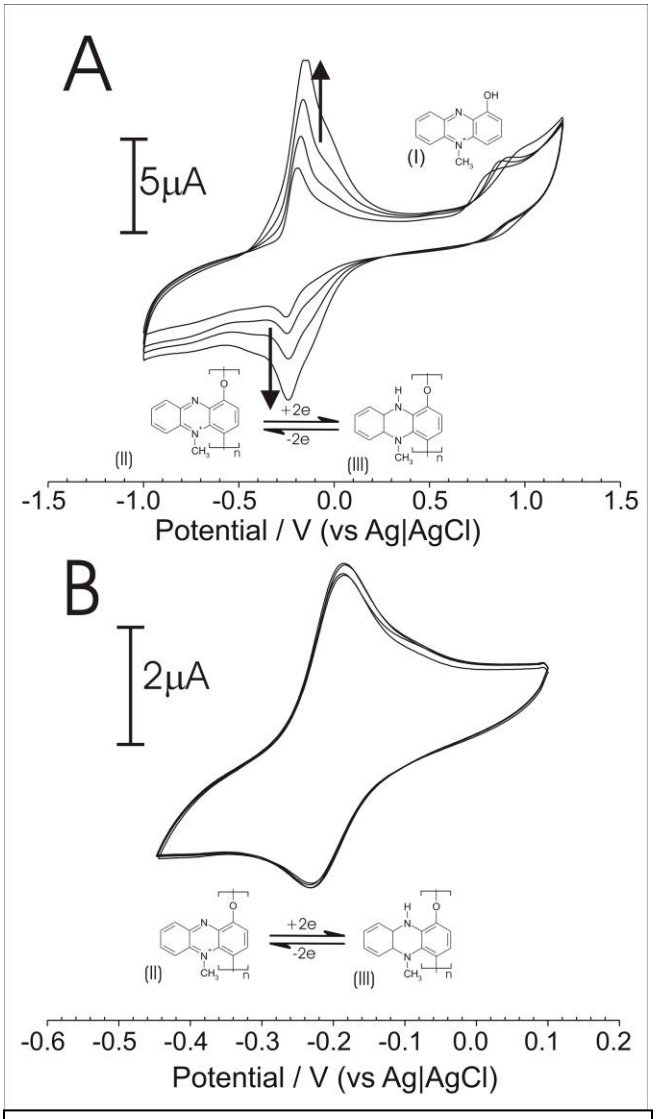

Figure 7.5. Assessing the suitability of carbon fibre assemblies for pyocyanin oxidation. Scan rate: 50mV/s
(A) Cyclic voltammetry of pyocyanin polymerisation due to high anodic potentials at 0, 10, 20 and 30 cycles
(B) Cyclic voltammetry of pyocyanin preventing polymerisation by limited scan range to -0.45V to +0.1V for 0, 10, 20 and 30 cycles

Limiting the anodic scan range to a maximum of +0.1V, the polymerisation is avoided and thus the oxidation observed at -0.017V is solely due to pyocyanin *in solution* as highlighted by **Figure 7.5B.** In contrast to the voltammograms exhibited in **Figure 7.5A**, the limited scan range provides a constant response upon repetitive scanning where the oxidation peak is solely derived from the 2 electron oxidation of solution based pyocyanin (I) to the oxidised form (IV). While the polymerisation of pyocyanin onto an electrode could be envisaged as a pre-concentration

phase, this is not suitable for a sensor system designed for periodical measurements as this would not only prevent repeated use of each electrode, but also allow the co-polymerisation of biofluid constituents, e.g. tryptophan. Pyocyanin was electropolymerised onto a gold slide electrode (necessary to ensure surface flat enough) and assessed by Atomic Force Microscopy (AFM). The morphological features of the resulting film are presented in **Figure 7.6**. The electrode surface after polymerisation (B) shows much greater surface roughness than the plain electrode (A), confirming that electropolymerisation of pyocyanin onto the electrode occurs as indicated by the voltammograms detailed in **Figure 7.5A**. The deposit is not however coherent and would appear to form through the gradual nucleation of oligomeric material.

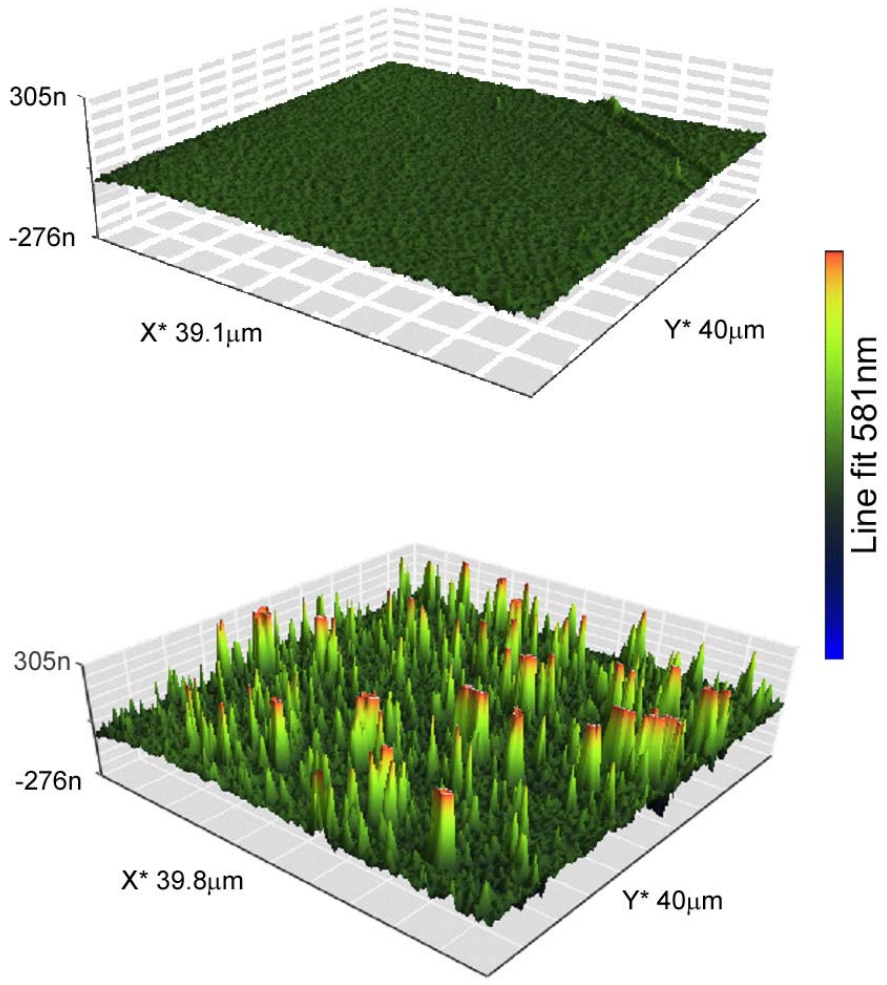

Figure 7.6. AFM of plain (A) and electropolymerised pyocyanin (B) on gold splutter coated slide electrodes.

Having established a suitable scan range, the response to different carbon substrates was assessed. SqWV enabled comparison of the more versatile carbon fibre tow, both plain (1) and anodised (2) along with the glassy carbon electrode (3) as a reference system. The resulting peak magnitude data are compared in **Figure 7.7A**. The anodised tow has a substantially greater response at lower concentrations and appeared to be more adept to biomarker monitoring and could be attributed to the anodic fracturing previously observed following anodisation [25]. The response was however found to exhibit non-linear dynamics as a result of the modifications and tended to saturate at much lower concentration than those required to be quantified in a biomedical scenario and is therefore unsuitable. Plain carbon fibre in contrast provides a linear response up to 100μM and thus was selected for further evaluations and used solely from herein. SqWV with plain carbon fibre gave rise to a single sharp oxidation peak observed at -0.17V, attributed solely to the oxidation of pyocyanin (**Figure 7.7B**).

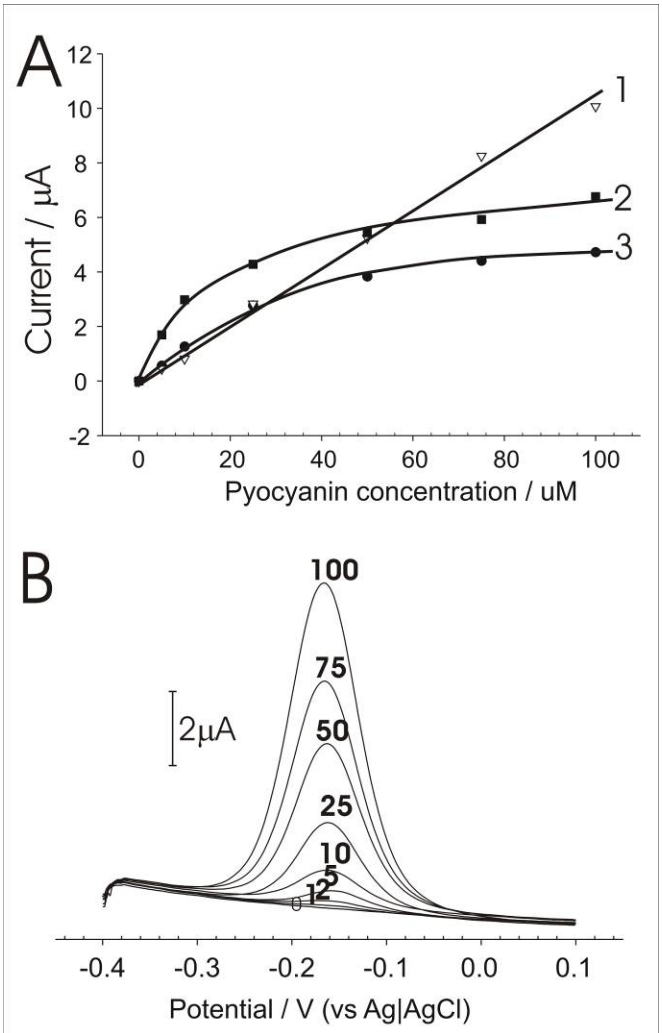

Figure 7.7 Assessing the suitability of carbon fibre assemblies for pyocyanin oxidation. Step height: 2mV, Amplitude: 10mV.
(A) Modified and plain carbon fibre sensors in comparison with glassy carbon electrode for pyocyanin quantification by square wave voltammetry (1. plain carbon tow, 2. anodised tow, 3. glassy carbon electrode).
(B) Square wave voltammograms of pyocyanin standards using a plain carbon fibre sensor (1-100μM)

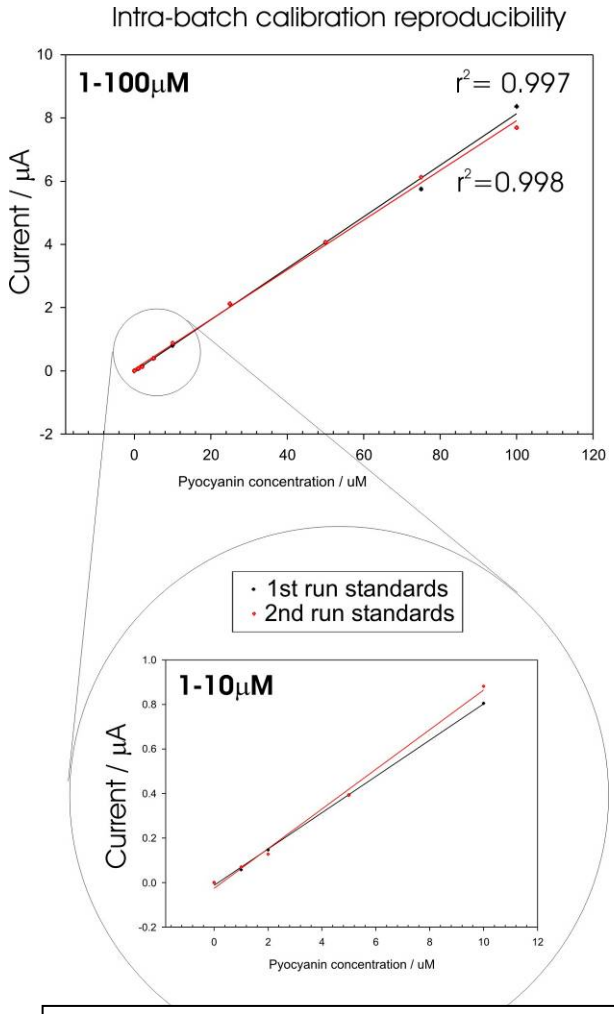

Figure 7.8. Calibration plots for pyocyanin measurements using carbon fibre electrodes

The plain carbon fibre electrode enabled linear quantification from 1μM to 100μM in buffered solutions (peak height/μA = 0.0814[Pyocyanin conc. /μM] -0.015, n = 9, R^2 = 0.998) indicating suitability for the proposed applications. The limit of detection of 0.030μM (LOD=3s/b) is beneficial to biomedical applications where sensitive detection of pyocyanin would enable the early detection of quorum sensing *Ps. aeruginosa*. **Figure 7.8** shows both a normal standard plot (1- 100μM), but also the lowered section 1-10μM to highlight the linearity at the very lower micromolar concentrations.

Given that the plan is for implementation within a smart bandage systems, it is important that the sensor is capable of reliably measuring pyocyanin concentrations beyond the initial measurements and ideally over a prolonged period. While this may not be an issue for certain applications (e.g. single scan outpatient detection of pyocyanin in sputa of cystic fibrosis patients), it is for the applications where continuous sampling is required. The use of pyocyanin sensors within wound environments would require periodic scanning to allow the early detection of pyocyanin. Two concentrations (10 and 50μM) were used for intra-batch precision assessment through 20 periodic replicates

using the plain carbon fibre assembly. The pyocyanin oxidation results in clearly visible and sharp peaks (**Figure 7.9** inlay) with no drift in oxidation potential. After the requisite equilibration / preactivation scans (not shown), the height of pyocyanin oxidation peaks are presented as a percentage of the mean (**Figure 7.9)**. The coefficient of variance (C_v) for the 10μM and 50μM populations are 1.2% and 1.4% respectively with no deviation greater than 2.6% for either concentration, thus demonstrating the quantitative precision of the electrode.

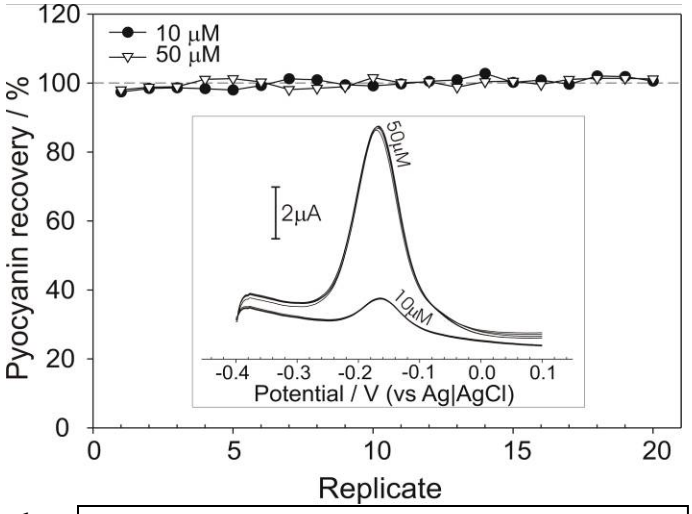

Figure 7.9. Assessing intra-batch precision of pyocyanin sensors. Pyocyanin recoveries across multiple replicates in 10 and 50μM pyocyanin. Inlay: square wave voltammograms during intra-batch precision assessment (scans 2, 6, 10, 14, 18. Step height: 2mV, amplitude 10mV.

The ability of *Ps. aeruginosa* to thrive in aerobic and anaerobic environments dictates the importance of a sensor to perform equally in both. The measurement of standards in both normally aerated and deoxygenated standards lead to the formation of two linear calibration plots (Oxygen present: Peak height/μA = 0.0764[Pyocyanin conc./ μM] + 0.0378, n=7, R^2=0.999 and oxygen absent: Peak height /μA = 0.0779[Pyocyanin conc./ μM] + 0.0961, n=7, R^2= 0.998), with no substantial difference between the two indicating suitable versatility. The negative potentials and narrow scan range limits the possible interfering endogenous compounds. Folate is the only biomarker considered electro-active within this potential range at an appreciable concentration in biofluids, (reference range of up to 0.028μM in adult serum [26]). High folate concentrations were found to have no observable effect on the pyocyanin oxidation peak (10μM pyocyanin standard) even at equimolar concentrations - over 300x the top of the adult folate reference range.

Following testing in buffered solutions, the use of the carbon fibre assembly for monitoring bacterially derived pyocyanin in broth cultures was evaluated. *Pseudomonas aeruginosa* Broth (PAB) was used due to its simplicity and previous observations of this media enabling pyocyanin production. Calibrations performed in PAB medium to ensure accuracy of measurements, again showing good linearity (Peak height/μA = 0.0350[Pyocyanin conc/ μM] + 0.0249, n=8, R^2=0.999). Three stock *Ps. aeruginosa* strains (*Ps. aeruginosa* NCTC 6749, *Ps. aeruginosa* NCTC 8060 and *Ps. aeruginosa* NCTC 8602) were used for the comparison between SqWV and chloroform-acid UV quantifications. The increasing pyocyanin concentrations during the incubation period, detailed in **Figure 7.10**, show that the trend of pyocyanin production is similar for both the methods used, highlighting the agreement between the point of care electrochemical measurement and

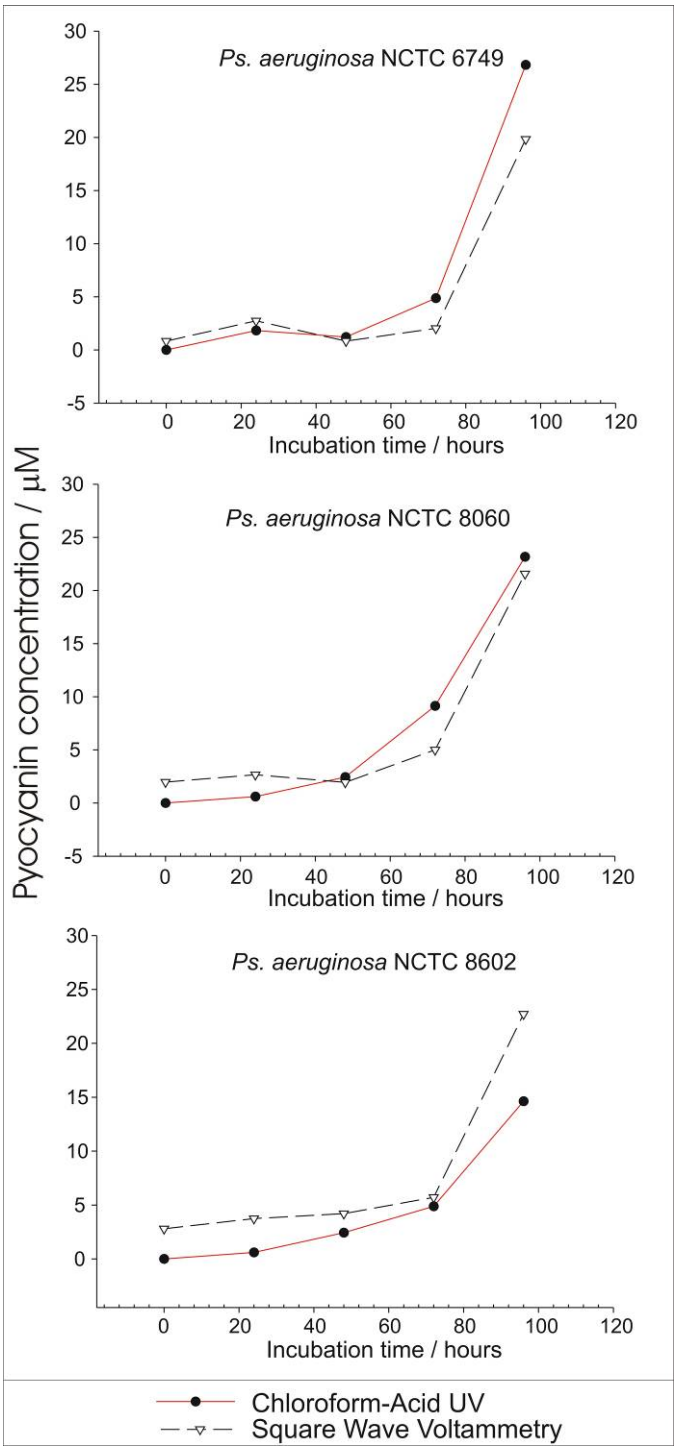

Figure 7.10. Detecting pyocyanin in bacterial broth cultures. Comparison of monitoring pyocyanin production by three stock strains of *Ps, aeruginosa* (NCTC 6749, 8060 and 8602) in *Pseudomonas aeruginosa* Broth (PAB), between chloroform-acid photometric method and the square wave voltammetry using a carbon fibre assembly.

the laboratory based extracted-UV method. The use of the carbon fibre assemblies has further advantages over the UV method: it is reagent free (no chlorinated waste from extraction); can be performed by non-specialists and the consumable electrodes are inexpensive. In addition, the successful use of the sensor in bacterial cultures shows the specificity towards pyocyanin oxidation, as the results are not affected by any of the other bacterially derived pigments or metabolites, e.g. *Ps. aeruginosa* NCTC 6749 produced pyomelanin (brown pigment).

7.5 Conclusions

The use of laminated carbon fibre tow electrodes has allowed the sensitive and precise quantification of pyocyanin at biologically relevant concentrations. Additionally, no interference is observed with high concentrations of folate or the presence or absence of oxygen, indicating applicability within biofluids and anywhere between aerobic and anaerobic environments. The electrode prototypes detailed have been shown to possess considerable potential for incorporation into a future ‘smart-bandage’ assembly to allow the early detection of *Ps. aeruginosa* colonisation of wounds. The sensor is also suggested as a potential PoCT for the early detection and monitoring of pulmonary infections in CFib patients.

7.6 References

1. Pirnay JP, De Vos D, Cochez C, Bilocq F, Pirson J, Struelens M *et al.* Molecular epidemiology of Peudomonas aeruginosa colonisation in a burn unit: persistence of a multidrug resistant clone and a silver-sulfadiazine-resistant clone. *Journal of Clinical Microbiology* 2003;41:1192-202
2. Cardo D, Horan T, Andrus M, Dembinski M, Edwards J, Peavy G, Tolson J, Wagner D, Special Article – National Nosocomial Infection Surveillance System report. *American Journal of Infection Control* 2004;32:470-85
3. Rasmussen TB, Givskov M. Quorum sensing inhibitors: a bargain of effects, *Microbiology-Socitey for General Microbiology* 2006;152:895-904
4. Christensen LD, Moser C, Jensen PO, Rasmussen TB, Christophersen L, Kjelleberg S *et al.* Impact of Pseudomonas aeruginosa quorum sensing on biofilm persistence in an in vivo intraperitoneal foreign-body infection model. *Microbiology* 2007;153:2312-20
5. Schaber JA, Carty NL, McDonald NA, Graham ED, Cheluvapa R, Griswold JA, Hamood AN. analysis of quorum sensing-deficient clinical isolates of Pseudomonas aeruginosa. *Journal of Medidical Microbiology*(2004;53:841-53
6. Reyes EAP, Bale MJ, Cannon WH, Matsen JM. Identification of Pseudomonas aeruginosa by Pyocyanin production on Tech agar. *Journal of Clinical Microbiology* 1981;13:456-8
7. Witson D, MacDermot J, Cole PJ, Taylor GW. Purification and structural analysis of pyocyanin and 1-hydroxyphenazine. *European Journal of Biochemistry* 1986;150:309-13
8. Muller M. Premature cellular senescence induced by pyocyanin, a redox active Pseudmonas aeruginosa toxin. *Free Radical Biology & Medicine* 2006;41:1670-7
9. Muller M. Pyocyanin induces oxidative stress in human epithelial cells and modulates the glutathione redox cycle. *Free Radical Biology & Medicine* 2002;33:1527-33
10. O'Malley YQ, Reszka KJ, Spitz DR, Denning GM, Britigan BE. Pseudomonas aeruginosa pyocyanin directly oxidizes glutathione and decreases levels in airway epithelial cells. *America Journal of Physiology- Lung, Cellular and Molecular Physiology* 2004;287:L94-103
11. Kanthankumar K, Taylor G, Tsang KWT, Cundell DR, Rutman A, Smith S *et al*. Mechanisms of action of Pseudomonas aeruginosa pyocyanin on human ciliary beat in vitro. *Infection and Immunity* 1993;61:2848-53
12. Wilson R, Sykes DA, Watson D, Rutman A, Taylor GW, Cole PJ. Measurement of Pseudomonas aeruginosa phenazine in sputum and assessment of their contribution to sputum sol toxicity for respiratory epithelium. Infection and Immunity 1988;56:2515-7
13. Usher LR, Lawson RA, Geary I, Taylor CJ, Bingle CD, Taylor GW, Whyte MKB. Induction of neutrophil apoptosis by the Pseudomonas aeruginosa exotoxin pyocyanin: a potential mechanism of persistent infection. *The Journal of Immunology* 2002;168:1861-8

14. Allen L, Dockrell DH, Pattery T, Lee DG, Cornelis P. Hellewell PG, Whyte MKB. Pyocyanin production by Pseudomonas aeruginosa induces neutrophil apoptosis and impairs neutrophil-mediated host defences in vivo. *The journal of Immunology* 2005;174:3643-9
15. Lau GW, Hassett DJ, Ran H, Kong F. The role of pyocyanin in Pseudomonas aeruginosa infection, *Trends in Molecular Micrbiology* 2004;10:599-606
16. Kerr JR, Taylor GW, Rutman A. Pseudomonas aeruginosa pyocyanin and 1-hydroxyphenazine inhibit fungal growth. *Journal of Clinical Pathology* 1996;52(5):385-7
17. Hassett DJ, Charniga L, Bean K, Ohman DE, Cohen MS. Response of Pseudomonas aeruginosa to Pyocyanin: Mechanisms of Resistance, Antioxidant Defences and Demonstration of Magnesium-Cofactored Superoxide Dismutase. *Infection and Immunity* 1992;60:328-36
18. Vukomanovik DV, Zoutman DE, Marks GS, Brien JF, van Loon GW, Nakatsu K. Analysis of pyocyanin from pseudomonas aeruginosa by adsorptive stripping voltammetry. *Journal of Pharmacology & Toxicology Methods* 1996;36:97-102
19. Smith RS, Iglewski BH. Pseudomonas aeruginosa quorum-sensing systems and virulence. *Current Opinions in Microbiology*2003;6(1):56-60
20. Bukelman O, Amara N, Mashiach R, Krief P, Meijlet MM, Alfonta L. Electrochemical Analysis of Quorum Sensing Inhibition, *Chemistry Communications* 2009;20:2836-8
21. Ezekiel HB, Sharp D, Villalba MM, Davis J. Laser-anodised carbon fibre: coupled patterning and activation of sensor substrates. *Journal of Physics and Chemistry of Solids* 2008;69(11):2932-5
22. Cox CD. Role of Pyocyanin in the Acquisition of Iron form Transferrin. Infection and Immunity 1986;52:263-70
23. Hassett DJ, Charniga L, Bean K, Ohman DE, Cohen MS. Response of Pseudomonas aeruginosa to Pyocyanin: Mechanisms of Resistance, Antioxidant Defences and Demonstration of Magnesium-Cofactored Superoxide Dismutase. Infection and Immunity 1992;60:328-36
24. Frank LH, DeMoss RD. On the Biosynthesis of Pyocyanine. *Journal of Bacteriology* 1959;77:776-82
25. O'Malley YQ, Reszka KJ, Spitz DR, Denning GM, Britigan BE. Pseudomonas aeruginosa pyocyanin directly oxidizes glutathione and decreases levels in airway epithelial cells. American Journal of Physiology – Lung, cellular and molecular physiology 2004;287:L94-103
26. Watson D, MacDermot J, Cole PJ, Taylor GW. Purification and structural analysis of pyocyanin and 1-hydroxyphenazine. *European Journal of Biochemistry* 1986;150:309-13
27. Usher LR, Lawson RA, Geary I, Taylor CJ, Bingle CD, Taylor GW, Whyte MKB. Induction of Neutrophil Apoptosis by the Pseudomonas aeruginosa Exotoxin Pyocyanin: A potential Mechanism of Persistent Infection. *The Journal of Immunology* 2002;168:1861-68
28. Knight M, Hartman PE, Hartman Z, Young VMA. A New Method of Preparation of Pyocyanin and Demonstration of an unusual Bacterial Sensitivity. *Analytical Biochemistry* 1979;95:19-23

29. Angell S, Bench BJ, Williams H, Watanabe CMH. Pyocyanin isolated from a marine microbial population: Synergistic production between two distinct bacterial species and mode of action. *Chemistry & Biology* 2006;13(12):1349-59
30. McIlwain H, The Phenazine Series Part VI: Reactions of, Journal of The Chemistry Society 1937;2:1704-10
31. Vukomanovik DV, Zoutman DE, Marks GS, Brien JF, van Loon GW, Nakatsu K. Analysis of pyocyanin from pseudomonas aeruginosa by adsorptive stripping voltammetry. *Journal of Pharmacology & Toxicology Methods* 1996;36:97-102
32. Friedheim E, Michaelis L. Potentiometric study of pyocyanine. *Journal of Biological Chemistry* 1931;91:355-68
33. Reszka KJ, O'Malley Y, McCormick ML, Denning GM, Britigan BE. Oxidation of pyocyanin, a cytotoxic product from Pseudomonas aeruginosa, by microperoxidase 11 and hydrogen peroxide. Free Radical Biology and Medicine 2004;36(11):1448-59

Chapter 8

Prevention of bacterial biofouling: An overview of current technologies

Abstract

Bacterial biofouling of biomedical devices, including sensors, is a widespread problem and one that is a key opponent in the development of *in situ* sensing systems. In addition to the use of silver impregnated materials to halt bacterial growth, a novel approach using the local generation of Reactive Oxygen Species (ROS) at an electrode surface is suggested. While ROS generation commonly relies on the use of a photosensitizer e.g. porphyrin, the photoactivation of such species leading to the generation of singlet oxygen, a powerful oxidizing agent, is a logistical problem for *in vivo* applications. The details of singlet oxygen and the difficult task of its detection are contained and the alternative approach of assessing electrochemically reducing oxygen into ROS is introduced. To aid the many studies of singlet oxygen and its production a novel electrochemical method for quantifying singlet oxygen has been developed, through the electrochemical oxidation of diphenylisobenzofuran, a singlet oxygen sensitive dye. The advantages of the electrochemical technique have been highlighted through the fact that much higher concentrations of photosensitizer could be used without interference. The effectiveness of this new method was highlighted using the photosensitizer tetraphenylporphyrin, widely for the production of singlet oxygen.

Work detailed in this chapter has been published in *Electroanalysis* 2009 – *in press.*

8.1 Introduction to Bacterial Biofouling

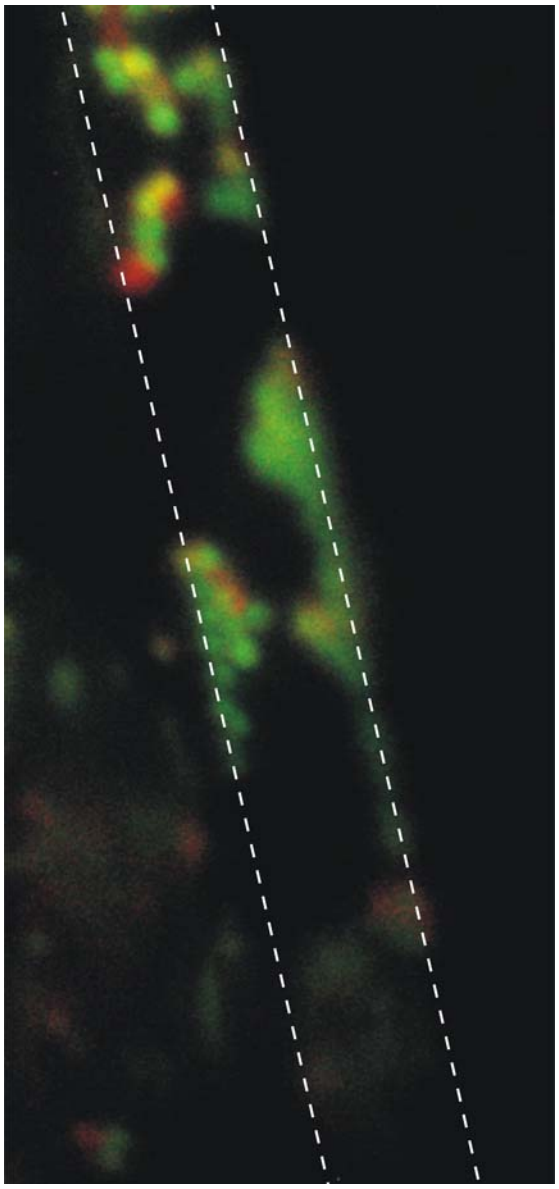

Figure 8.1. Fluorescence microscopy of staphylococcus aureus biofilm formed on the surface of a carbon fibre tow electrode. Dashed lines show edges of a 10μm thick carbon fibre. Stained with BacLight LIVE/DEAD kit, green = live cells, red = deads cells.

Biofouling of electrodes is a major problem when considering the *in vivo* use of electrochemical systems. Electrode fouling can result from the adsorption of endogenous macromolecules such as proteins, fats, carbohydrates and other cellular debris. This issue became apparent in Chapter 5 where the fouling of the electrodes with albumin was initially found to be problematic but later solved by the addition of size exclusion membrane coatings to the sensor surface. A more significant problem can arise where bacteria such as *S. aureus, Ps. aeruginosa* etc produce a biofilm.

Bacterial biofilms are complex aggregations of bacteria that adhere to a surface through the generation of an extensive protective and adhesive macromolecular matrix. The growth and spreading of these biofilms would effectively block the electrode surface potentially leading to erroneous results. The propensity for forming such a layer in the present context was demonstrated by applying a growing culture of *S. aureus* to the surface of a carbon fibre electrode (as used throughout this project). The colonization of the fibre and initiation of biofilm formation was assessed using fluorescence microscopy. Even after only a few hours, bacterial adhesion was apparent as indicated in **Figure 8.1**. The bright green cocci indicate living organisms and a large area of the electrode substrate is clearly blocked by the organisms

and demonstrates the potential problem that bacterial adhesion can bring to the deployment of any sensor designed for mid to long term monitoring applications. The detailed mechanisms of biofilm formation were detailed in Chapter 1. Given the problems that a biofilm can present for an electrochemical probe, it is necessary to have some strategies that can either prevent the biofilm formation from occurring at the device interface or at the very least a mechanism through which to minimize its effects. Antimicrobial coatings and surfaces are commonly exploited and advertised in consumer products but their efficacy remains contentious and it is important to note the they are an invariably not designed for applications in contact with broken skin or wound exudates. There is a marked difference between the requirements for an antimicrobial coating for a keyboard or a food preparation board and those necessary for the safe functioning of a wound dressing or implantable sensor. The potential for leaching of the antimicrobial is an ever present problem in the latter and it is vital to consider the potential toxicological properties of the respective material within a wound environment. Nevertheless, there are a number of options that have been investigated and could have application within the present context.

Chief amongst those are the photosensitisers which generate reactive oxygen species. A substantial literature base has emerged which covers a great deal of the chemistry that underpins their action but also examines their application within a clinical perspective. The main requirement is the selection of a molecular species that is capable of generating reactive oxygen species in sufficient quantities that can overwhelm the bacterial defences and hence provide a bactericidal action. A porphyrin derivative was chosen to act as our model system to assess the potential applicability of the system and the results are reported within this chapter. However, in order to place the results in context, a brief literature review of those reports pertinent to photosensitisers and their application has been collated and critically appraised first

8.1.1 Strategies for Preventing Biofilm Formation

In order to allow the electrode to function reliably and over an extended time period there must be an inhibition of the biofilm formation. Suggested methods include the use of silver or nano-silver coated particles as the production of silver cations is well known to be antibacterial. There are three main problems with the use of this: silver is an expensive substrate, it limits the electrode material and may interfere with electrochemical measurements.

The electrode could be coated with an antimicrobial agent, however the immobilization of such species onto the electrode may reduce or preclude its antibacterial mechanism of action. An alternative option would be to have a slow release of the antimicrobial as is employed in a number of antimicrobial polymers and similar in mechanism to the silver dissolution. This would also be a less than ideal option where the core rationale in the smart bandage design pursued here has been to minimize the possibility of material leaching in an uncontrolled manner into the wound environment.

Ideally the antibacterial agents should be able to be produced at the electrode surface upon demand and have a very localized effect principally at the device wound-interface. It was thought that the production of reactive oxygen species (ROS) could be a potential solution to this issue. The local production of ROS would be ideal as the half lives of such species are generally very short giving rise to a limited range of applicability and hence inducing only a very small zone of inhibition. ROS are generally defined as molecules or ions initially formed by the incomplete one-electron reduction of oxygen and can include many species: singlet oxygen ($^1O_2$), superoxide anion radical ($O_2\cdot^-$), peroxide (H_2O_2) and hydroxyl radical ($\cdot OH$). The use of ROS is of great interest currently in a variety of research fields including: life science, food chemistry and organic synthesis as well as possessing numerous oncological and microbiological roles [2].

One particular ROS that has been extensively studied for its generation and antibacterial efficacy is singlet oxygen. Singlet oxygen is used to name the two metastable states of molecular oxygen with higher energy than the ground state triplet, produced by rearrangement of the electron spins of the two unpaired electrons in the

highest occupied orbitals of molecular oxygen. Singlet oxygen can be produced by photosensitisers, by energy transfer from dye molecules to molecular oxygen and is a powerful oxidising agent (one of the most active intermediates in chemical and biological reactions) [2]. Upon application of singlet oxygen to biological systems singlet oxygen can act as a strong cytotoxic agent and may chemically modify proteins, nucleic acids and lipid membrane leading to the organelle damage and ultimately apotosis. Singlet oxygen activity is not only exogenously derived but can be produced endogenously in neutrophil phagosomes and is the major oxidative antibacterial in neutrophils [3].

This singlet oxygen-bacterial attack occurs through:

- Interaction with bacterial cytoplasmic membrane
- Damage to bacterial respiratory enzymes
- Suppression of ATP formation
- Damage to bacterial DNA especially guanine [4].

The majority of recent studies have focused on the *in situ* generation of ROS for use in photodynamic therapy (PDT). The latter involves the use of a photosensitizer which upon irradiation with visible light undergoes a photochemical reaction and produces reactive compounds typically ROS. The term PDT is usually associated with oncology [5] and is currently used in the treatment of certain cancers since there is a preferential accumulation of certain photosensitizer species in malignant tissue [6]. Consequently when the photosensitizer is exposed to the light source it produces ROS, which destroy the cancerous cells by either rapid necrosis or delayed apoptosis [7]. At present, the use of PDT in oncology is limited largely to oesophageal and certain lung cancers [5] but is being trialed in other areas of medicine such as in the treatment of age related macular degeneration and precancerous skin conditions [5].

Variants of photodynamic therapy have also been applied as antimicrobial treatments and work in much the same way. Photodynamic antimicrobial chemotherapy (PACT) involves the application of PDT for antimicrobial purposes in recognition of the chemotherapeutic essence of the technique. The use of photosensitizers in microbial

eradication can be traced back to before the age of chemotherapy [8]. However, the subsequent success of chemotherapeutic antimicrobials and the cost/use implications of the more accessible pharmaceutical preparation led to a premature decline in the interest of photosensitizers for healthcare application. In recent years there has been a resurgence in the use of PDT/PACT and are a number of more specialist applications to which the technique could be highly effective. One example is the use of PACT for blood disinfection in donated blood and its corresponding products [9]. An important factor to consider in the use of ROS generation as a therapeutic is that as singlet oxygen has very short half life. Singlet oxygen may not have time to penetrate human cells sufficiently but can easily permeate through the smaller bacterial cells and therefore may kill these cells more effectively [10].

The use of PACT in the treatment of infections is normally to be restricted to localised superficial infections due to the requisite light supply. The current clinical applications being investigated are the mouth, stomach and skin (especially in burns patients and chronic non-healing wounds) [11-13]. It was also suggested that it could be useful for rinsing and sterilisation of the sinuses in sinusitis [14]. Numerous photosensitizers have shown an antimicrobial response to light; Chlorin E6, porphyrins, Rose Bengal, phenothiazinium and phthalocyanines are some of the more common [15-17]. Certain characteristics are required from a photosensitizer: it should produce reasonable quantities of singlet oxygen, possess photochemical stability and appropriate spectral characteristics for the application [18].

8.1.2 Porphyrins

Porphyrins are by the most common type of photosensitiser and have been widely used due to the commercial availability of general structures and their synthetic versatility for producing a large range of derivatives. The porphyrins are a group of tetrapyrroles which can be split into two categories: *endogenous* porphyrins, involved in the synthesis of heme [19] and synthetic porphyrins with molecular amendments to alter their characteristics.

In 1990 Malik *et al* [14] proposed a possible 5-point mechanism of bacterial photoinactivation by porphyrins:

1. absorption of the porphyrin into bacterial cell wall,
2. binding of porphyrin to the inner bacterial cell wall,
3. binding may be carried out in dark and is non-toxic to cells,
4. possible translocation of porphyrin into cytoplasm and
5. photoinactivation by porphyrins in or associated with the bacterial cell.

Upon photoactivation of porphyrins two consequential reactions can occur:

Type I reactions, photoreactions without-oxygen, these reactions cause electron abstraction (e.g. of hydrogen) and redox reactions.

Type II reactions are oxygen dependant and produce ROS (importantly Singlet Oxygen), which mediates oxidations and peroxidations; it is this type of reaction we are concerned with regarding singlet oxygen production and antimicrobial efficacy [8,11].

Upon exposure to the correct wavelength of light, a porphyrin (or other photosensitizer) is excited to its triple state, this energy is passed onto molecular oxygen to produce ROS [11] as highlighted in **Figure 8.3:**

Figure 8.3. The excitation of porphyrins and mechanism of singlet oxygen production

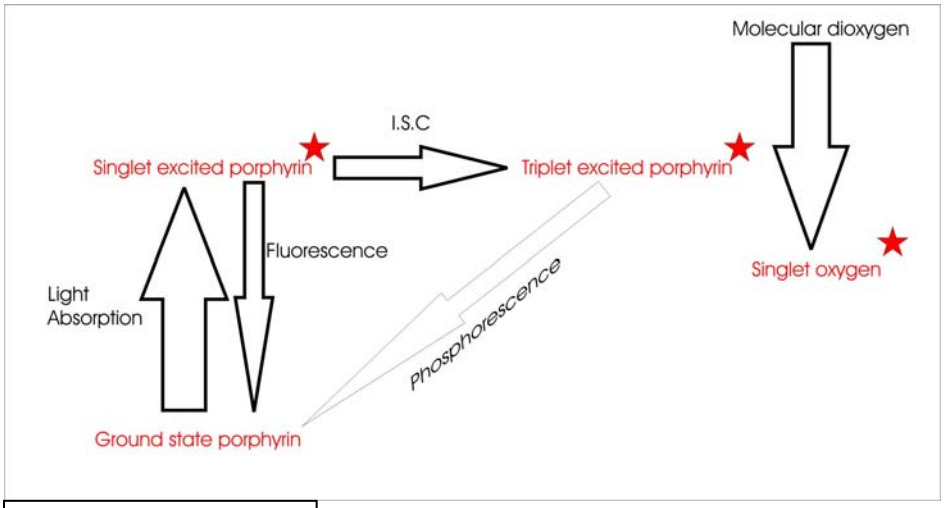

(I.S.C = Inter-System Crossing)

8.1.3 Singlet Oxygen

The chemistry of singlet oxygen and its cytotoxic properties was reviewed by Meisel and Kocher in 2005 [11]. Singlet oxygen may interact with bacterial cytoplasmic membranes and damage bacterial respiratory enzymes together with suppression of ATP formation [3]. In addition to the affects on cellular components, singlet oxygen can damage bacterial DNA [4]. Work by Li *et al.* [20] in 1997 demonstrated that photoactivation of porphyrins in the presence of DNA induced formation of "nicked" plasmid DNA, however it clear that the activity of porphyrins is not just dependant on DNA damage *in vitro*. Work performed during the same year by Chatterjee *et al.* [21] also found that photoactivation of porphyrins could damage plasmid DNA, but more specifically recognised singlet oxygen reacts predominantly with guanine in DNA

The very short half life of singlet oxygen in water (4μs) can be dramatically extended by using different solutions, namely ethanol (20μs) and chloroform (250μs) [11]. Furthermore, it has been reported by numerous research groups that the half life of singlet oxygen is extended significantly in buffer based upon D_2O rather than H_2O [18,22]. The half life is so short for singlet oxygen (particularly in water) this limits how far the singlet oxygen can diffuse to target areas of the bacterial cell to cause damage whilst still viable.

The activity of singlet oxygen is readily stopped by being quenched back to the ground state molecular oxygen. There are two fundamental types of singlet oxygen quenching: physical and chemical. In physical quenching the quencher enters an excited state (either vibrational or electronic) and may occur by triplet energy transfer or by simple catalysis of singlet oxygen to ground state oxygen [22]. Chemical quenching is when the quenchers combines with oxygen or is oxidized by the ROS. Therefore molecular oxygen acts as a physical quencher for the excited stated of the porphyrin taking the electronic energy to return the porphyrin to its ground state, and producing singlet oxygen as a consequence. The solvent quenching constant (kq) of a solution defines the lifetime of the singlet oxygen generated [23] and explains why singlet oxygen has a much longer lifetime in D_2O compared with H_2O. However, large discrepancies

have been observed for the lifetimes of singlet oxygen, which have been attributed to the impurities present in the quencher and from the inaccuracy of indirect detection methods [23]. A substantial number of singlet oxygen quenching compounds have been studied in recent years, both exogenous and endogenous. Exogenous singlet oxygen quenchers usually contain reactive Pi electrons or *n*-lone pairs of sufficiently low ionization energy. Some common examples include: olefins, aromatic and heteroaromatic compounds, amines, sulphur containing compounds and the commonly used azides [24]. There are many endogenous singlet oxygen quenchers thus confirming their importance in nature to protect cells from the genotoxic and cytotoxic effects of singlet oxygen. These quenchers are typically antioxidants. Ascorbate, carotenoids and tocopherols are the most common antioxidants and efficient singlet oxygen quenchers [11,25-29]. Beta-carotene has an important role as a singlet oxygen quencher whereby it may act as an anti-cancer agent [26]. It has also been found to be a particularly efficient singlet oxygen quencher in the cellular environment and therefore can be used as a treatment of photodermatoses [26]. Tocopherol (Vitamin E) is a biological antioxidant which can function as an effective scavenger of singlet oxygen operating through both physical and chemical quenching mechanisms [27,28]. Among the many other biological compounds which have a quenching ability are:

- Sulphur containing compounds such as glutathione have a pronounced ability to protect cells against the oxidative damage caused by singlet oxygen [25].

- Iodine, singlet oxygen may be quenched by iodine by the endothermic electronic energy transfer to produce a triplet state of Iodine and molecular oxygen [30].

- Dissolved oxygen may itself also act as a quencher of singlet oxygen [7]. Although necessary for its generation, high concentrations can also inhibit singlet oxygen activity.

- Fatty acids and lipids may also quench singlet oxygen through chemical oxidation [31].

8.1.4 *Singlet Oxygen Detection Strategies*

In order to assess and compare the efficiencies of singlet oxygen generation, many methods have been developed to measure the photoinduced yield. The largest problem facing their development and implementation however is the very short half-life of singlet oxygen [11]. Finding the most efficient and cost-effective method for detecting singlet oxygen is essential to enable the identification of the most effective singlet oxygen production methods. The half-life of singlet oxygen is massively affected by the solvent used: water 4μs, ethanol 20μs, chloroform 250μs and benzene 24μs. Therefore to enable a more sensitive detection of singlet oxygen the use of ethanol or chloroform may be beneficial due to the delayed degradation of the singlet oxygen. It is important to note that while he use of such solvents are clearly inappropriate for use in a smart bandage application – their relevance lies in the selection of a photosensitising material that could subsequently be incorporated. The main rationale being that the differing characteristics of the solvents can be used to assess the relative efficiencies of the ROS generators.

In order to be able to compare the different techniques available and to decide which would be most suitable, the methods of singlet oxygen detection were investigated and form two groups: direct and indirect.

Direct Methods

Direct detection of singlet oxygen was facilitated by development of near infra-red (NIR) sensitive photomultipliers, allowing direct observations of singlet oxygen by its weak near-infrared phosphorescence around 1270-80 nm [7,18] the measurement at this wavelength is the monomeric measurement, which is required for detection of low concentrations of singlet oxygen. The direct measurement of singlet oxygen is also possible at 634 nm and is related to the simultaneous deactivation of two singlet oxygen molecules upon collision, detection of the dimol is therefore disadvantaged by requiring a high concentration of singlet oxygen to enable sufficient molecules to collide [2,32]. Direct methods are currently the most reliable way of measuring singlet oxygen and used

to assess singlet oxygen production in many applications. These include photoactivation of sugar-pendant fullerene derivatives, in liposomes, in industrial dyes, in cells *in vitro* and tissues *in vivo* and in keratinocytes [33,34].

Indirect Methods

Indirect detection methods typically utilise chemical markers that are modified upon exposure to singlet oxygen. The products of the subsequent reaction are, measured – typically by a change in absorbance at particular wavelengths. The chemical markers used have been split into the following groups:

Tetrafulvalene derived compounds:

- Tetrathiafulvalene-anthracene dyad with two tetrethylene glycol units, measured by chemiluminescence with a detection limit of 1.0 μM. However due to its poor solubility in water the assay is performed in water/methanol mixture [35].

- 4,4'(5')-Bis [2-(9-anthryloxy)ethylthio] tetrafulvalene, BAET, also measured by chemiluminescence, but found to have a detection limit of 50nM and has been used to measure singlet oxygen in saliva in the salivary defence system [36].

Pyrrole containing compounds:

- DanePy (dansyl-2,2,5,5,-tetramethyl-2,5-dihydro-1H-pyrrole) is converted to a nitroxide radical (DanePyO) which can be measured spectrofluorimetrically as the nitroxide induces fluorescence quenching. This has been used in plant leaves for the determination of singlet oxygen production during photoinhibition and photosynthesis [37].

- BTMPC and BMPC (*tert*-butyl-3,4,5-trimethylpyrrolecarboxylate and N-benzyl-3-methoxypyrrole-2-*tert*-carboxylase respectively) are oxidised by singlet oxygen, which can be measured by a decrease in absorbance at 280 and 252 nm. This has been used in HPLC systems as a postcolumn reaction/detection system

and also in a post capillary electrochromatography separation and it has been, used in PDT drug development and assessment [38,39].

Pyrazole containing compounds:

- 4,4'-Bis(1-p-carboxyphenyl-3-methyl-5-hydroxyl)-pyrazole measured by electron spin resonance spectroscopy [40].

- Terbium (III) chelate fluorescence. (*N,N,N', N'*-[2,6-bis(3'-aminomethyl-1'-pyrazole)-4-(9'anthryl)pyridine] tetrakis (acetate)-Tb^{3+} (PATA-Tb^{3+}) These are water soluble markers of singlet oxygen production and utilise fluorescence detection with a detection limit of 10.8 nM [41].

Furan containing compounds:

- 2,5-Dimethylfuran (2,5-DMF) is degraded to hydrogen peroxide by singlet oxygen in the presence of methanol and sulphuric acid which may be measured fluorometrically. Detection limit in methanol was 0.1μM [42].

- 1,3-Diphenylisobenzofuran (DPBF) a quencher of singlet oxygen, whose oxidation can be measured spectrophotometrically as a decrease in absorbance at 410 nm or 442 nm. This is used to evaluate the reactions of singlet oxygen with various substrates e.g. anti-inflammatory drugs piroxicam and tenoxicam. It is also used in the comparison of different solvents for the lifetimes of singlet oxygen and the effect of porphyrin modifications on the yield of singlet oxygen [43,44].

Miscellaneous Markers:

- Luminol (5-amino-2,3-dihydro-phthalazine-1,4-dione) measured by chemiluminescence, has been used to determine the antioxidative activity of various compounds against singlet oxygen [45].

- 4,4'-Dichlorobiphenyl and three other commercially available polychlorinated biphenyls: Aroclors 1242, 1248 and 1254. Detection limits varied from 3.0 nM for 4,4DBP up to 50 nM for some of the Aroclors. These have also been used as postcolumn reaction detection in HPLC systems [46].

- The Iodide method. Iodide (I^-) is oxidised to Triiodide (I_3^-) - the increase in the latter being spectrophotometrically measured at 287 nm and 351 nm [18,20]. However work by Mosinger *et al.* [47] showed that once a critical concentration of Triiodide is produced, singlet oxygen production stops as the triple states within aggregates are quenched by fast relaxational processes

The two most commonly used methods are the photobleaching of 1,3-DPBF and the iodide method [18,20,32,48]. Given the greater sensitivity of the 1,3-DPBF bleaching, this method has been chosen for use in the present project. The major disadvantage of the DPBF photobleaching method when used with certain photosensitizers, is that the soret peak of e.g. tetraphenylporphyrin directly overlaps the 412nm transmission used for monitoring of singlet oxygen production thus leading to much higher and error prone photometric measurements. As such, a new electrochemical detection method was developed and is outlined in the following sections.

8.1.5 Porphyrins Against Bacteria

An advantage of using PACT, regarding the safety to human cells, is that the active compounds (ROS) are required to diffuse through the cell to the more sensitive intracellular location (e.g. DNA). Given that human cells are much larger than bacterial cells, the ROS are more likely to intercepted before attacking the more sensitive components [10]. The use of porphyrins as photosensitizers for bactericidal and bacteriostatic control is common and there has been extensive research into the use of both hitherto endogenous and the purely synthetic porphyrin variants in an attempt to optimise their antimicrobial affects [48,49]. Use of synthetic or modified endogenous porphyrins are believed to be beneficial as they are not present in surrounding tissues.

Thus, the impostion of wavelength specific irradiation could be used to activate specific moieties improving selectivity and avoiding unwanted photoreactions from those photosensiters that may be in healthy cells and tissue [8].

The initial problem found with the application of porphyrins as photosensitizers was that Gram negative bacteria were found to be relatively resistant to the believed cytotoxic effects induced by ROS production. This was demonstrated by Malik *et al.* in 1990 [14] whereby the Gram positive bacteria e.g. *S. aureus, Streptococcus pyogenes* and *B. subtilis* all exhibited considerable sensitivity to a haematoporphyrin derivative. Gram negative bacteria: *E. coli, Ps. aeruginosa* and *K. pneumoniae*, in contrast, were all resistant. It was deduced that this behaviour arose as a consequence of the structural differences between the two classifications of bacteria (i.e. Gram negative and positive). Gram-negative bacteria have a more complex outer barrier with two lipid bilayers as indicated in Chapter 1. Gram-positive bacteria possess a single lipid bilayer and a more permeable outer coat, and this is believed to account for the difference in sensitivity to porphyrin photoinactivation [49].

At present, the use of porphyrins as antimicrobials covers a variety of pathogens for oral infections, e.g. Gram negative anaerobic oral pathogen *Porphromonas* [16]. Also *Helicobacter pylori*, another Gram negative bacterium, is known to contribute to peptic ulcers and it was found that porphyrin treated *H. pylori* is killed upon illumination even with low levels of visible light [13]. Banfi et al [15] compared the bactericidal effects of various porphyrins with markedly different properties. It was confirmed that positive charges on the periphery of diffusable porphyrins is essential for the porphyrin to act effectively as a photosensitizer on both Gram-positive and Gram-negative bacteria. In addition, it was reported that "*a moderate degree of lipophilicity may improve photosensitizer efficiency.*" [15]. Conversely, it had been reported that the outer membrane of Gram negative bacteria has a high permeability to hydrophilic molecules up to a certain size and depends on the size of the porin channels. In contrast to the work by Banfi, it has been found that they exhibited a very low permeability to lipophilic molecules [50].

Many studies have been performed using porphyrins with various substituent groups attached to them. Sol *et al.* for instance [51] tested 24 amino-porphyrins,

discovering that porphyrin derivatives with two attached polyamines (spermine and spermidine) were able to effectively inhibit the growth of *St. aureus* and *E. coli*. Another series of investigations found that HpD (A mixture of haematoporphyrin (HP), protoporphyrin (PP) and hydroxyethylvinyldeuterporphyrin (HVD)) alone has little or no affect on the growth of many Gram negative bacteria. However, when HpD is coupled to arginine, the porphyrin derivatives became far more effective against many Gram negative organisms, including *Ps. aeruginosa, E. coli* and *K. pneumoniae* [50]. In keeping with illustrating the benefits of added amino groups to porphyrin derivatives, it was proven that an addition of pentlysine to Chlorin E6 (a porphyrin derivative) increased its efficacy against Gram positive bacteria and allowed it to inhibit Gram-negative bacteria [16]. The benefit of these modifications appears to be directly involved with their entrance into the bacterial cells. In addition to differing groups and molecules that have been attached to porphyrins to enable them to prevent growth of Gram negative bacteria, agents to aid the penetration of porphyrins into Gram negative cell have also been utilised. For example Colistin-"nonepeptide" can facilitate porphyrin activity on Gram negative bacteria [14].

The porphyrins are not always required to actually penetrate the bacteria in order to deliver an antimicrobial charge of ROS. Therefore the characteristics which are usually required for cell penetration of the porphyrin have no importance, as long as the porphyrin can produce sufficient single oxygen to inhibit the growth of bacteria. This feature is arguably of more relevance to smart bandage development as outlined in the introduction, the provision of leachable species would need to be precluded and have the photogenerator firmly anchored to either the dressing or the sensor. It has been found that three distinctly different synthetic porphyrins, possessing varying antimicrobial activities, all produce a very similar quantity of singlet oxygen [48]. Therefore porphyrins which excel in the penetrative kill may have no additional benefit in the immobilised experiments. The effects of porphyrins as photosensitizers is generally bactericidal rather than just bacteriostatic. This may appear apparent from the structure and functional damage caused by the singlet oxygen. However, it has been demonstrated that by incubating the porphyrin-inactivated bacteria for a second time in the dark that growth is unregulated [52].

Various groups have studied the effects of the growth phase of bacterial cells on efficacy of porphyrins as photosensitizers. Early work by Malik *et al.* [14] in 1990 suggested that (for HPD against *St. aureus*) the porphyrin effectively inhibited bacterial growth during the logarithmic growth phase, but not during the lag phase. However, later work by Banfi *et al.* [15] in 2006 reports that bacterial susceptibility to photosensitizers is independent from the growth phase. The contradictory nature of these results indicates the necessity to check this for each specific bacterial strain and porphyrin pairing.

Methicillin Resistant Staphylococcus aureus (MSRA) and antibiotic resistant strains of *Ps. aeruginosa* are extensive problems in healthcare as nosocomial infections. An advantageous characteristic of PACT is that drug resistant stains have no greater resistance to its affects. The singlet oxygen toxicity is not affected by methicilin resistance in *S. aureus* [53] nor the drug resistant strains in *Ps. aeruginosa* [50].

Development of bacterial resistance to treatments can occur by the following routes:

- **Bacterial target mutations**, usually by acquisition of new genes from plasmids or transposons
- **Alteration in efflux pump balance** i.e. either decreased influx or increased efflux
- **Actively disabling the drug,** usually by hydrolysis or modification
  [17,54]

Due to the nature of the photoactivation, a likely mechanism of developing resistance to PACT is by hindering the correct wavelengths of light from reaching the porphyrins. Such shielding could be plausible for certain bacterial strains which are pigmented whereby the latter absorbs the requisite light needed for activation of a particular porphyrin. Importantly *Ps. aeruginosa* may be pigmented [17]. Additionally the endogenous dyes of certain bacteria may be associated with quenchers [11] which may lead to a different form of resistance to photoinactivation. Bacteria can protect

themselves from the toxic effects of singlet oxygen by the up-regulation of various metabolic pathways that lead to the production of anti-oxidant species such as the carotenoids which effectively quench singlet oxygen [55]. Therefore bacterial strains which contain significant quantities of carotenoids are innately more resistant to the singlet oxygen and this is a potential resistance mechanism. The human body uses a larger array of antioxidants to protect against the reactive oxygen species for examples; beta-carotene, lycopene, ascorbic acid, alpha-tocopherol, uric acid, albumin and bilirubin and host of enzymatic process that offer additional protection from singlet oxygen [26,56].

The lighting conditions are fundamental to the success of photoactivation of porphyrins. Clearly the shorter and more efficient exposures are better. For the porphyrins to produce the ROS, the light which is applied needs to contain the correct wavelength as described by *The Grottus-Draper law*: 'The light used must be of an appropriate wavelength because only absorbed light can trigger a photochemical reaction' [11]. Porphyrins tend to be converted to their excited triplet state by absorption of light possessing wavelengths between 600-650 nm [8] and 600-690 nm [17]. Throughout experimental research into the photoactivation of porphyrins different types and strengths of lighting have been used, however white light and tungsten bulbs seems to be the most common. However, specific wavelength lasers and fibre optics have also been used [5,14,15,18,20,52]

Certain porphyrins illuminated by white light will efficiently kill *E. coli* and *Ps. aeruginosa* after 60 minutes exposure [15]. However, other porphyrin derivatives have shown that even shorter incubation times typically in the order of a few minutes are sufficient to kill *S. aureus* and *E. coli* [53]. It would be advantageous when considering the clinical application of these techniques to use those porphyrins with rapid effects. It is important to establish that the photoinactivation was not purely due to over heating of bacteria by the light source. This can be tested by using a bacterial control exposed to light in the absence of photosensitizer [48] and the use of cooling systems to prevent colony overheating.

8.1.6 Immobilised Porphyrins

Photoactivation of a photosensitizing agent can be toxic to the cell if it occurs intracellularly or extracellularly providing the ROS are generated within its immediate vicinity [17]. The latter is being increasingly adopted for use in new generation antibacterial materials and surfaces but could obviously possess the potential for transfer to sensing surfaces or fabrics used for wound dressings. This has been investigated in a recent study by Mosinger *et al.* [18] where 5,10,15,20-tetraphenylporphyrin was attached to a nanofabric and found to prevent the growth of *E. coli* . It was demonstrated that the porphyrins did not leach out from the nanofabric into the media and provides further evidence that sufficient singlet oxygen can be produced extracellularly to kill the bacteria.

One potential disadvantage of using immobilised porphyrins is that the cationic porphyrins, used more popularly due to their greater efficacy, may lose their advantage. Cationic porphyrins bind to anionic DNA and therefore cause greater damage to DNA upon illumination [20]. Only those porphyrins that are efficient at generating ROS can be considered for immobilization. There is no longer a need for specific structural adaptations that facilitate penetration of the bacterial cell, instead the emphasis is now placed on the functionalities that allow the porphyrin to be attached to a surface and ensure it is optimized for singlet oxygen generation. Using extracellular production of singlet oxygen in an attempt to inhibit bacterial growth was tried by Valduga *et al.* in 1993 [57] by keeping an air layer between the photosensitizer and the bacteria. It was found that this successfully killed Gram positive bacteria *Strep. faecium* and Tris-EDTA-treated *E. coli* but not untreated *E. coli*. Therefore further research into the use of extracellular singlet oxygen production is required. This would determine whether it is feasible, and whether specifically designed synthetic porphyrins may provide the answer. This may be by gross singlet oxygen production or by a complimentary release of an agent which may disrupt the outer cell membrane of the Gram negative cells allowing a quicker penetration of the singlet oxygen.

If porphyrins species were used in an *in*-situ dressing, toxicity of porphyrin derivatives should pose no threat to a patients' wellbeing if they are to be incorporated into some form of wound bandage, as some porphyrins e.g. HpDs are even used intravenously in anti-cancer therapy [50]. Hence they should be fine for a topical interaction, especially considering porphyrins have proven to not leach off a fabric into the wound surface [18]. However it has been reported that ROS can have various local effects on a wound and is associated with amino acid/protein modification and many oxidised protein by-products [58].

8.1.7 Proposed Methodology

Scheme 8.1. Reaction sequence for assessing singlet oxygen generated from tetraphenylporphyrin using diphenylisobenzofuran (I) as a quencher.

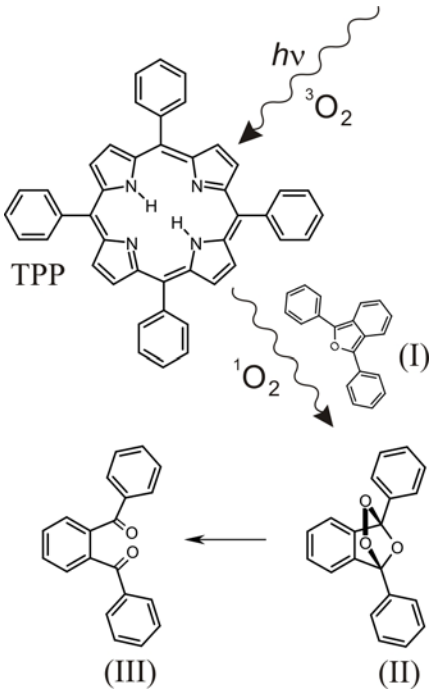

A porphyrin derivative was selected as a photosensitizing agent with the aim of assessing the production of singlet oxygen. The central rationale being that it could be utilized as part of a smart bandage application providing that it possessed demonstrable bactericidal activity. The photometric monitoring of diphenylisobenzofuran (DPBF) degradation is commonly used to detect and assess the efficiency of singlet oxygen production from photosensitisers. [15-18]. The predominance of the latter and the well developed knowledge base for its application was the principal reason behind taking this as the model quencher. The core rationale that underpins the process is outlined in **Scheme 8.1**. The irradiation of the photosensitizer (i.e. TPP) in the presence of dissolved oxygen results in the formation of singlet oxygen, whose subsequent interaction with DPBF (I) results in the endoperoxide (II) and ultimately producing 1,2-dibenzoylbenzene (III). The degradation of the endoperoxide to the corresponding di-ketone (III) is accompanied with a proportionate decrease in the

magnitude of the parent DPBF absorption band (λmax = 420nm) and it is this decrease that forms the basis of the spectroscopic method.

The efficacy of the porphyrin was assessed by an indirect route involving the Dibenzylisofuran derivative with follow up experiments involving microbial cultures. The results are reported and a critical appraisal of the potential suitability of the system for use in a smart bandage is provided in the following sections.

In order to counter the matrix effects, more restrictive concentrations (< 2 μM for TPP [15, 17]) have needed to be employed which may be appropriate in PDT – single cell type investigations but may be inappropriate where it could be envisaged that a higher loading may be required in PACT to combat biofilm formation and bacterial colonisation. The development of an electrochemical method to replace this would enable quicker experiments as higher concentrations of photosensitizer can be used, but also more reliable and accurate measurements of the DPBF marker. The main issues to be addressed in the present investigation were whether or not the proposed detection method would be a suitably sensitive method for the determination of changes in DPBF to allow the preliminary screening of suitable photosensitizers.

8.2 Experimental Details

*Methods and Materials***:** All reagents were of the highest grade available and used without further purification. Stock solutions of tetraphenylporphyrin and diphenylisobenzofuran were prepared in dimethylformamide (DMF) containing LiCl as supporting electrolyte. Typical working solutions of 50 μM tetraphenylporphyrin (TPP) and 200 μM DPBF (1,3 diphenylisobenzofuran) were used unless otherwise stated. DMF is used due to the solubility of DPBF and photosensitizers and the increased half-life of singlet oxygen in comparison to aqueous solutions. Prior to use, the glassy carbon electrode was polished using aluminium oxide nanoparticles and ultrasonicated in deionised water from an ElgaStat (Elga, UK) Test solution was put into a filtered light compartment, **Figure 8.2**, whereby all light entering the compartment passed through a HOYA Orange G filter, to prevent the photodegradation of DPBF by white light [18].

Figure 8.2 Filtered light compartment and analytical setup

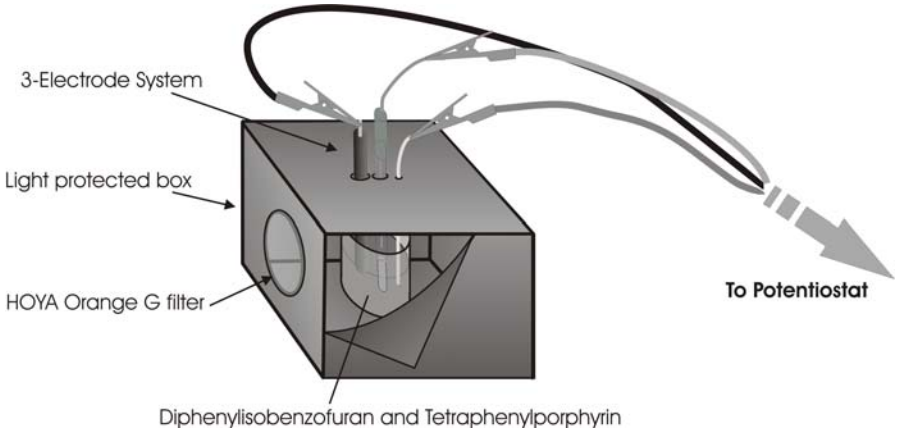

Illumination was performed using a desktop spot lamp with a 60W (Soft Light) bulb, kept 25 cm from the compartment (30 cm from reaction vessel) to ensure no heating of the sample.

*Instrumentation***:** Electrochemical measurements were conducted using a μAutolab type III computer controlled potentiostat (Eco-Chemie, Utrecht, The Netherlands). A 3-electrode configuration was used consisting of a Glassy Carbon Electrode (3mm diameter, BAS Technicol), an Ag|AgCl (3M KCl, BAS Technicol) half-cell reference electrode and a platinum wire counter electrode. (Square Wave Voltammetry parameters: ΔE_s 2mV, E_{sw} 5mV, f 25Hz)

8.3 Results and Discussion

Square wave voltammograms recorded a glassy carbon electrode detailing the oxidation of increasing concentrations of DPBF (50 μM additions) are shown in **Figure 8.3**. The resulting voltammograms show clearly defined oxidation peaks at +0.69 V, solely derived from the oxidation of DPBF (neither intermediate nor product are electrochemically active within the potential window examined). Calibrations performed in triplicate produced a linear range up to 250 μM (Peak height / μA = 4.44 x 10^{-3} [DPBF conc. / μM] + 7.524 x 10^{-3}, N = 6, R^2 = 0.997) allowing the simple electrochemical monitoring of DPBF degradation over the aforementioned concentration range.

Figure 8.3 Square wave voltammograms detailing the oxidation of increasing concentrations (50mM additions) of diphenylisobenzofuran (DPBF) at a glassy carbon electrode (DMF/LiCl).

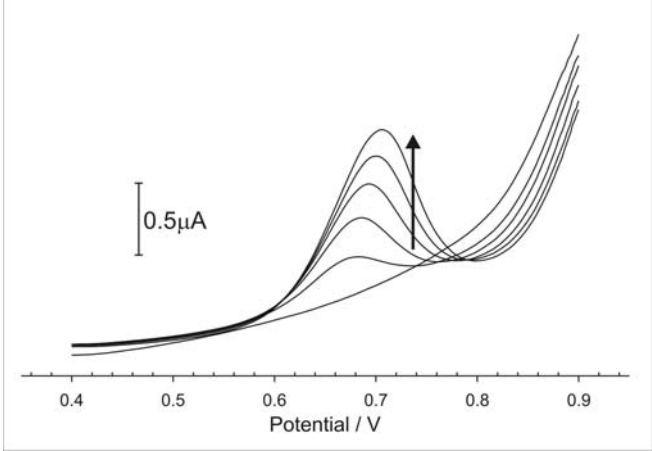

After the preliminary assessments, a concentration of 200μM DPBF and 50μM of TPP was chosen provide both an easily measurable response but which is also at least 25 fold higher concentrations than those limited in the spectroscopic methods [15,17]. Upon exposure to singlet oxygen, the electrochemically active DPBF degrades to 1,2-dibenzoylbenzene. Square wave voltammetry was performed on DPBF standards to assess the accuracy of the electrochemical oxidation using a conventional glassy carbon electrode. The next stage in the development and characterisation of this method was to test the ability to monitor singlet oxygen production using the widely used standard photosensitizer tetraphenylporphyrin (TPP) [16]. **Figure 8.4** shows the resulting DPBF concentrations at two minute intervals for both control and test experiments performed in the filtered light compartment (**Figure 8.2**) utilising a HOYA Orange (G) photography filter to prevent photodegradation.

Figure 8.4 Response comparison towards 200 μM DPBF within the light compartment in the absence (circles, illuminated) and presence (Squares, illuminated; triangles, dark) of 50 μM tetraphenylporphyrin.

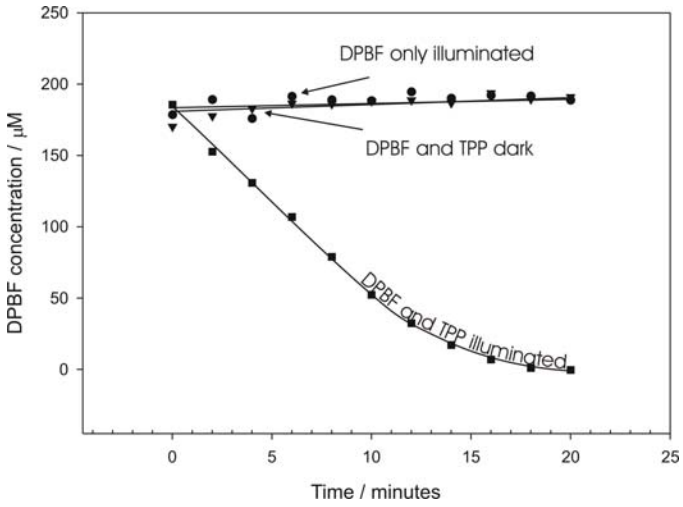

In the case of 'DPBF only illuminated' and 'DPBF and TPP dark', no changes in DPBF concentration were observed (**Figure 8.4**, circles and triangles, respectively). The absence of change in the control with no TPP proves the efficiency of the filtered light compartment to prevent photodegradation by white light. The second control 'DPBF and TPP dark' proves that no dark-reactions occur between the two compounds and thus any change observed in the test experiment is solely derived from the presence of both TPP and light, i.e. due to singlet oxygen production. When DPBF and TPP are both present *and* illuminated, a rapid degradation of DPBF is observed indicating the removal of the parent DPBF within 20 minutes (**Figure 8.4**, squares). This stands in marked contrast with the control experiments where no diminution of the signal was observed and clearly highlighting the ability of DPBF as potent candidate marker of singlet oxygen production. In addition to showing this new detection technique for singlet oxygen, it also highlights the necessity of light for singlet oxygen production, but porphyrins. If a wound bandage had porphyrins incorporated into it in the antimicrobial context, a problem could be getting light to the porphyrins. It is not appropriate to remove the bandage for the porphyrins to be illuminated due to increasing the risk of bacterial and fungal contamination. Recent research by Lee *et al.* [5] proved that porphyrins can be stimulated into singlet oxygen production by using a fibre optical coupled device, in this instance it was used for its anti-cancer properties in rats. While the methods used to illuminate are universal, there implementation is far form trivial and could be counter to the main requirement of producing an inexpensive and disposable device. The expense and impracticality of running fibre optics into a dressings from a light source and it use by non expert staff are likely to inhibit its uptake in the present context. A further problem, highlighted by Miskoski *et al* [59], is that singlet oxygen can

mediate photo-oxidation of tetracyclines. Tetracyclines, a group of broad spectrum antibiotics, are used extensively in medicine and photo-oxidation reduces their antimicrobial capabilities. This occurs in the presence of visible light, but has a greater effect at alkaline pH than at a physiological pH. However, it would be essential to consider this prior to its use so as not to interfere with current antibiotic use, especially as for example burns wounds could be the target for the tetracycline antibiotic therapy as it has been found that certain strains of partially resistant *Ps. aeruginosa* are susceptible to tetracycline [12].

8.4 Conclusions

The application of electrochemical measurements to monitor DPBF degradation as a consequence of singlet oxygen production by photosensitizers has been studied. Square wave voltammetry has proven to linearly quantify DPBF with accuracy and precision and free from interference from electroactive biofluid components. The successful use of this technique is detailed with the standard photosensitizer, tetraphenylporphyrin and deftly overcomes the common problem with the optical measurements where absorbance of the exogenous photosensitizer and indeed, matrix, invariably requires looking at minute absorbance changes that can fail to pick up small fluxes of reactive oxygen species. The electrochemical approach proposed is independent of matrix colour and is shown to be a quick, simple and sensitive method allowing greater flexibility for assessing photosensitiser efficacy.

8.5 References

1. Monroe D. Looking for chinks in the Armor of Bacterial Biofilms, *PLoS Biology* 2007;5(11):e304-7
2. Lu C, Song G, Lin JM. Reactive oxygen species and their chemiluminescence-detection methods. *TrAC-Trends in Analytical Chemistry* 2006;25(10): 985-95.
3. Tatsuzawa H, Maruyama T, Misawa N, Fujimori K, Hori K, Sano Y, Kambayashi Y, Nakano M. Inactivation of bacterial respiratory chain enzymes by singlet oxygen. *Febs Letters* 1998;439(3):329-33.
4. Nir, U, Ladan H, Malik Z, Nitzan Y. Invivo Effects of Porphyrins on Bacterial-DNA. *Journal of Photochemistry and Photobiology B-Biology* 1991;11(3-4):295-306.
5. Lee S, Vu DH, Hinds MF, Davis SJ, Hasan T, Khachemoune A, Rice W, Sznycer-Taub NR. Detection of singlet oxygen production for PDT treatments both in vitro and in vivo using a diode laser-based singlet oxygen monitor. *Optical Methods for Tumor Treatment and Detection: Mechanisms and Techniques in Photodynamic Therapy XV Biomedical Optics Symposium* 2006.
6. Alvarez M, Prucca C, Milanesio ME, Durantini EN, Rivarola V. Photodynamic activity of a new sensitizer derived from porphyrin-C-60 dyad and its biological consequences in a human carcinoma cell line. *International Journal of Biochemistry & Cell Biology* 2006;38(12):2092-101.
7. Dedic R, Korinek M, Molnár A, Svoboda A, Hála J. Singlet oxygen quenching by oxygen in tetraphenyl-porphyrin solutions. *Journal of Luminescence* 2006;119:209-13.
8. Wainwright M. Photodynamic antimicrobial chemotherapy (PACT). *Journal of Antimicrobial Chemotherapy* 1998;42(1):13-28.
9. Wainwright M. The emerging chemistry of blood product disinfection. *Chemical Society Reviews* 2002;31(2):128-36.
10. Soukos NS, Ximenez-Fyvie LA, Hamblin MR, Socransky SS, Hasan T. Targeted antimicrobial photochemotherapy. *Antimicrobial Agents and Chemotherapy* 1998;42(10):2595-601
11. Meisel P, Kocher T. Photodynamic therapy for periodontal diseases: State of the art. *Journal of Photochemistry and Photobiology B-Biology* 2005;79(2):159-70.
12. Estahbanati HK, Kashani PP, Ghanaatpisheh F. Frequency of Pseudomonas aeruginosa serotypes in burn wound infections and their resistance to antibiotics. *Burns* 2002;28(4):340-8.
13. Hamblin MR, Viveiros J, Yang C,Ahmadi A, Ganz RA, Tolkoff5 MJ. Helicobacter pylori accumulates photoactive porphyrins and is killed by visible light. *Antimicrobial Agents and Chemotherapy* 2005;49(7):2822-7
14. Malik Z, Hanania J, Nitzan Y. Bactericidal Effects of Photoactivated Porphyrins - an Alternative Approach to Antimicrobial Drugs. *Journal of Photochemistry and Photobiology B-Biology* 1990;5(3-4):281-93.

15. Banfi S, Caruso E, Buccafurni L, Battini V, Zazzaron S, Barbieri P, Orlandi V. Antibacterial activity of tetraaryl-porphyrin photosensitizers: An in vitro study on Gram negative and Gram positive bacteria. *Journal of Photochemistry and Photobiology B-Biology* 2006;85(1):28-38
16. Rovaldi CR, Pievsky A, Sole NA, Friden PM, Rothstein DM, Spacciapoli P. Photoactive porphyrin derivative with broad-spectrum activity against oral pathogens in vitro. *Antimicrobial Agents and Chemotherapy* 2000;44(12):3364-7
17. Wainwright M, Crossley KB. Photosensitising agents - circumventing resistance and breaking down biofilms: a review. *International Biodeterioration & Biodegradation* 2004;53(2):119-26.
18. Mosinger J, Janoskova M, Kamil L, Pavel K. Light-induced aggregation of cationic porphyrins. *Journal of Photochemistry and Photobiology A-Chemistry* 2006;181(2-3):283-9.
19. Ajioka RS, Phillips JD, Kushner JP. Biosynthesis of heme in mammals. *Biochimica Et Biophysica Acta-Molecular Cell Research* 2006;1763(7):723-36.
20. Li HD, Fedorova OS, Grachev AN, Trumble WR, Bohach GA, Czuchajowski L. A series of meso-tris(N-methyl-pyridiniumyl)-(4-alkylamidophenyl)porphyrins: Synthesis, interaction with DNA and antibacterial activity. *Biochimica Et Biophysica Acta-Gene Structure and Expression* 1997;1354(3):252-60.
21. Chatterjee SR, Shetty SJ, Devasagayam TPA, Srivastava TS. Photocleavage of plasmid DNA by the prophyrin meso-tetrakis 4-(carboxymethyleneoxy)phenyl porphyrin. *Journal of Photochemistry and Photobiology B-Biology* 1997;41(1-2):128-35.
22. Macpherson AN, Telfer A, Barber J, Truscott TG. Direct-Detection of Singlet Oxygen from Isolated Photosystem-Ii Reaction Centers. *Biochimica Et Biophysica Acta* 1993 ;1143(3):301-9
23. Oelckers S, Hanke T, Röder B. Quenching of singlet oxygen in dimethylformamide. *Journal of Photochemistry and Photobiology a-Chemistry* 2000;132(1-2):29-32.
24. Methods in Enzymeology 319, Singlet oxygen, UA A and Ozone. (2000) Elsevier Saunders, Missouri USA.
25. Devasagayam TPA, Sundquist AR, Di Mascio P, Kaiser S, Sies H. Activity of Thiols as Singlet Molecular-Oxygen Quenchers. *Journal of Photochemistry and Photobiology B-Biology* 1991;9(1):105-16.
26. Bohm F, Haley J, Truscott TG, Schalch W. Cellular Bound Beta-Carotene Quenches Singlet Oxygen in Man. *Journal of Photochemistry and Photobiology B-Biology* 1993;21(2-3):219-21
27. Kruk J, Hollander-Czytko H, Oettmeier W, Trebst A. Tocopherol as singlet oxygen scavenger in photosystem II. *Journal of Plant Physiology* 2005;162(7):749-57.
28. Fukuzawa K, Matsuura K, Tokumura A, Suzuki A, Terao J. Kinetics and dynamics of singlet oxygen scavenging by alpha-tocopherol in phospholipid model membranes. *Free Radical Biology and Medicine* 1997;22(5):923-30
29. Bodannes RS, Chan PC. Ascorbic-Acid as a Scavenger of Singlet Oxygen. *Febs Letters* 1979;105(2):195-6.

30. Wilkinson F, Farmilo A. The Mechanism of Quenching of Singlet Oxygen O-2star(1-Delta-G) by Molecular-Iodine. *Journal of Photochemistry* 1984;25(2-4):153-60
31. Krasnovsky AA, Kagan VE, Minin AA. Quenching of Singlet Oxygen Luminescence by Fatty-Acids and Lipids - Contribution of Physical and Chemical Mechanisms. *Febs Letters* 1983;155(2): 233-6.
32. Gorman AA, Rodgers MAJ. Current Perspectives of Singlet Oxygen Detection in Biological Environments. *Journal of Photochemistry and Photobiology B-Biology* 1992;14(3):159-76
33. Niedre M, Patterson MS, Wilson BC. Direct near-infrared luminescence detection of singlet oxygen generated by photodynamic therapy in cells in vitro and tissues in vivo. *Photochemistry and Photobiology* 2002;75(4):382-91
34. Bilski P, Kukielczak BM, Chignell CF. Photoproduction and direct spectral detection of singlet molecular oxygen (O-1(2)) in keratinocytes stained with rose bengal. *Photochemistry and Photobiology* 1998;68(5):675-8.
35. Zheng XP, Sun S, Zhang D, Ma, H, Zhu D. A new chemiluminescence probe for singlet oxygen based on tetrathiafulvalene-anthracene dyad capable of performing detection in water/alcohol solution. *Analytica Chimica Acta* 2006;575(1):62-7
36. Li XH, Zhang GX, Ma H, Zhang D, Li J, Zhu D. 4,5-Dimethylthio-4'- 2-(9-anthryloxy)ethylthio tetrathiafulvalene, a highly selective and sensitive chemiluminescence probe for singlet oxygen. *Journal of the American Chemical Society* 2004;126(37):11543-8
37. Hideg E, Kálai T, Hideg K, Vass I. Photoinhibition of photosynthesis in vivo results in singlet oxygen production detection via nitroxide-induced fluorescence quenching in broad bean leaves. *Biochemistry* 1998;37(33):11405-11
38. Denham K, Milofsky RE. Photooxidation of 3-substituted pyrroles: A postcolumn reaction detection system for singlet molecular oxygen in HPLC. *Analytical Chemistry* 1998;70(19):4081-5
39. Dickson J, Odom M, Ducheneaux F,Murray J, Milofsky R. Coupling photochemical reaction detection based on singlet oxygen sensitization to capillary electrochromatography. *Analytical Chemistry* 2000;72(14):3038-42
40. Igarashi T, Sakurai K, Oi T, Obara H, Ohya H, Kamada H. New sensitive agents for detecting singlet oxygen by electron spin resonance spectroscopy. *Free Radical Biology and Medicine* 1999;26(9-10):1339-45
41. Tan MQ, Song B, Wang G, Yuan J. A new terbium(III) chelate as an efficient singlet oxygen fluorescence probe. *Free Radical Biology and Medicine* 2006;40(9):1644-53.
42. Kreitner M, Ebermann R, Alth G. Quantitative determination of singlet oxygen. Production by porphyrins. *Journal of Photochemistry and Photobiology B-Biology* 1996;36(2):109-11
43. Venkatesan R, Periasamy N, Srivastava TS. Singlet Molecular-Oxygen Quantum Yield Measurements of Some Porphyrins and Metalloporphyrins. *Proceedings of the Indian Academy of Sciences-Chemical Sciences* 1992;104(6):713-22

44. Figueiredo TLC, Johnstone RAW, SantAna Sørensen AMP, Burget D, Jacques P. Determination of fluorescence yields, singlet lifetimes and singlet oxygen yields of water-insoluble porphyrins and metalloporphyrins in organic solvents and in aqueous media. *Photochemistry and Photobiology* 1999;69(5):517-28
45. Miyamoto A, Nakamura K, Ohba Y, Kishikawa N, Nakashima K, Kuroda N. Sequential injection analysis with chemiluminescence detection for the antioxidative activity against singlet oxygen. *Analytical Sciences* 2006; 22(1):73-6
46. Milofsky R, Ward J, Shaw H,Klundt I. Post-column photochemical reaction detection in liquid chromatography based on photosensitized generation of singlet molecular oxygen: Study of reaction parameters and application to the determination of polychlorinated biphenyls. *Chromatographia* 2000;51(3-4):205-11
47. Mosinger J, Jirsak O, Kubat P, Lang K, Mosinger B. Bactericidal nanofabrics based on photoproduction of singlet oxygen. *Journal of Materials Chemistry* 2007;17(2):164-6.
48. Zhang, JY, Wu XJ, Cao X, Yang F, Wang J, Zhou X, Zhang XL. Synthesis and antibacterial study of 10, 15, 20-triphenyl-5-{4-hydroxy-3-(trimethylammonium)methyl}phenylporphyrin as models for combination of porphyrin and alkylating agent. *Bioorganic & Medicinal Chemistry Letters* 2003;13(6):1097-1100.
49. Demidova TN, Hamblin MR. Effect of cell-photo sensitizer binding and cell density on microbial photoinactivation. *Antimicrobial Agents and Chemotherapy* 2005;49(6):2329-35
50. Szpakowska M, Reiss J, Graczyka A, Szmigielski S, Lasocki K, Grzybowski J. Susceptibility of Pseudomonas aeruginosa to a photodynamic effect of the arginine hematoporphyrin derivative. *International Journal of Antimicrobial Agents* 1997;8(1):23-7
51. Sol V, Branland P, Chaleix V, Granet R, Guilloton M, Lamarche F, Verneuil B, Krausz P. Amino porphyrins as photoinhibitors of Gram-positive and -negative bacteria. *Bioorganic & Medicinal Chemistry Letters* 2004;14(16):4207-11
52. Krouit M, Granet R, Branland P, Verneuil B, Krausz P New photoantimicrobial films composed of porphyrinated lipophilic cellulose esters. *Bioorganic & Medicinal Chemistry Letters* 2006;16(6):1651-5
53. Maisch T, Bosl C, Szeimies RM, Lehn N, Abels C. Photodynamic effects of novel XF porphyrin derivatives on prokaryotic and eukaryotic cells. *Antimicrobial Agents and Chemotherapy* 2005;49(4):1542-52
54. Yoneyama H, Katsumata R. Antibiotic resistance in bacteria and its future for novel antibiotic development. *Bioscience Biotechnology and Biochemistry* 2006;70(5):1060-75
55. Tatsuzawa H, Maruyama T, Misawa N, Fujimori K, Nakano M. Quenching of singlet oxygen by carotenoids produced in Escherichia coli - attenuation of singlet oxygen-mediated bacterial killing by carotenoids. *Febs Letters* 2000;484(3):280-4

56. Wagner JR, Motchnik PA, Stocker R, Sies H, Ames BN. The Oxidation of Blood-Plasma and Low-Density-Lipoprotein Components by Chemically Generated Singlet Oxygen. *Journal of Biological Chemistry* 1993;268(25):18502-6
57. Valduga G, Bertoloni G, Reddi E, Jori G. Effect of Extracellularly Generated Singlet Oxygen on Gram-Positive and Gram-Negative Bacteria. *Journal of Photochemistry and Photobiology B-Biology* 2003;21(1):81-6.
58. Moseley R, Stewart JE, Stephens P, Waddington RJ, Thomas DW. Extracellular matrix metabolites as potential biomarkers of disease activity in wound fluid: lessons learned from other inflammatory diseases? *British Journal of Dermatology* 2004;150(3): 401-413.
59. Gulielmos V, Schueler S, Miskoski S, Sanchez E, Garavano M, Lopez M, Soltermann AT, Garcia NA. Singlet molecular oxygen-mediated photo-oxidation of tetracyclines: kinetics, mechanism and microbiological implications. *Journal of Photochemistry and Photobiology B-Biology* 1998;43(2):164-71
60. Pervaiz S. Reactive oxygen-dependent production of novel photochemotherapeutic agents. *Faseb Journal* 2001;15(3):612-7

Chapter 9

ROS- Electrochemical Generation and Detection

Abstract

To enable the protection of sensor surfaces from biofouling new surface treatments and coating are suggested, with the aforementioned idea of local production of ROS being introduced. The exploitation of the natural product plumbagin (5-hydroxy-1,4-naphthoquinone) as a monomer to produce polymer films that are capable of producing ROS on demand at an electrode interface is assessed. The efficacy of the native quinone to redox cycle and catalyse the reduction of oxygen to yield ROS has been evaluated through using ascorbate as anti-oxidant probe. The production and characterisation of the electropolymerised films along with its ability to produce reactive oxygen species has been investigated using cyclic voltammetry, spectrophotometry and electrochemical quartz crystal microbalance studies. Plumbagin coated electrodes have proven to produce ROS, more specifically, superoxide anion that dismutates to hydrogen peroxide – with known antimicrobial properties. Plumbagin coated electrodes are suggested as a possible mechanism to prevent bacterial biofouling and local growth, due to the antimicrobial mechanisms of these ROS, as discussed in the literature review (**Chapter 8**).

Work detailed in this chapter has been published in *New Journal of Chemistry – in press*

9.1 Introduction

The previous chapter examined the use of photosensitisers for the generation of reactive oxygen species (ROS) which is typically cytotoxic singlet oxygen. It was clear that the presence of a porphyrin under illumination could produce a significant yield of the latter. A number of issues arose in the course of those studies however which appeared to run counter to general aims of the project in terms of pushing forward the development of a disposable monitoring system. While the porphyrin photosensitiser could easily be immobilised onto the sensor or surrounding dressing material, such a procedure creates two problems. The first relates to the chemical modifications required to introduce and immobilise the porphyrin. The second relates to the fact that a light source is required to initiate the generation of ROS. The latter is by far the more pressing as it creates a level of complexity that is potentially incompatible with the general design ethos being pursued thus far. The sensors located within the bandage would be required to periodically scan to the wound fluid to indicate either a pH change (Chapters 4 and 5) or the release of bacterial metabolite (pyocyanin, Chapter 7). Accepting the need for mid to long term measurement then the periodic pulse of ROS would be required to maintain the integrity of the sensor surface. Given that the generation of ROS could be used to temporarily control bacterial colonisation, then the ability to control the duration over which the ROS is produced would also be advantages. In the case of the photosensitiser, the light source would need to permanently fixed to the bandage and it here that the level of instrument complexity, associated expense and need for expertise are inappropriate for the context in which the bandage is to be applied. An alternative method for control ling biofilm formation and, if possible, providing a sustained bactericidal action is clearly required.

The electrochemical reduction of dissolved oxygen to yield ROS (principally superoxide anion and peroxide) was investigated as one option that would address this issue. The latter has been widely exploited as a means through which to quantify oxygen content in various fluids but its adaptation to serve as a controlled source of potentially bactericidal ROS is a novel strategy. The following chapter details the results from a preliminary investigation into the use of the various “smart” films that could be

electrochemically stimulated to produce ROS. It could be envisaged that the modification of the design could be achieved with minimal additional complexity. The application of a voltammetric scan could simultaneously generate ROS and allow measurement of the biomarker previously investigated in Chapters 3-7. No additional instrumentation or electronics would be required and stands in marked contrast to the instrumental overhead necessary for the photodynamic production investigated in Chapter 8.

9.2 Proposed Methodology

Plumbagin (5-hydroxy-2-methyl-1,4-naphthoquinone) has been of widespread interest to the medical community in recent years and has long been an integral part of Siddha and Ayurveda practices [1-3]. It has been shown to engage in a multitude of biochemical roles and possesses cytotoxic properties that can be significantly disruptive to normal cellular function. It has however been suggested that, if appropriately targeted, it could offer a range of therapeutic benefits as it has been shown to modulate cellular proliferation/carcinogenesis [3-5] and possesses antimicrobial properties [6-10]. The primary mode of action in most cases has been ascribed to its ability to redox cycle – the generation of the semiquinone radical resulting in the production of ROS which subsequently attacks cellular physiology and ultimately initiates apoptosis (**Scheme 9.1A**) [3, 5]. The present investigation has primarily sought to examine the possibility of exploiting

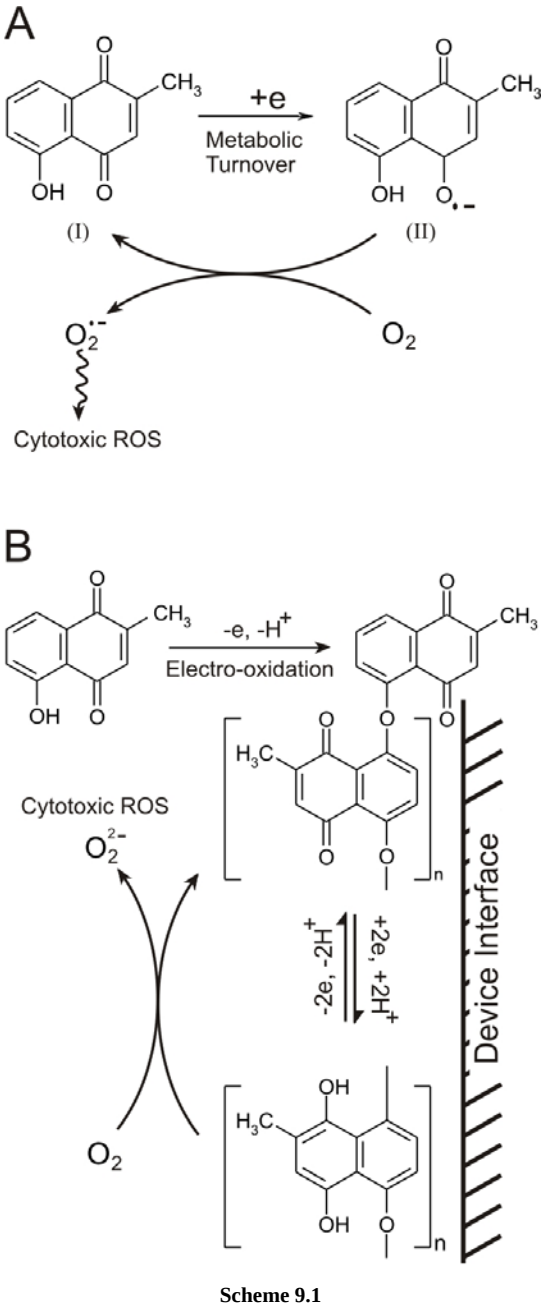

Scheme 9.1

Plumbagin whereby the electrochemical modulation of a film of the naphthoquinone serves as a controllable source of ROS to prevent biofouling.

Plumbagin has two core functionalities, the quinone redox centre responsible for the production of ROS and a phenolic group which could allow electropolymerisation and facilitate the production of a thin redox film [11,12]. Electrochemical oxidation of the phenol group should result in the production of a radical cation which can lead to the deposition of a thin film directly at the electrode surface [11,12]. The immobilised plumbagin is predicted to allow electrochemical cycling and that upon the imposition of a reducing potential the hydroxyl form should be generated which, in the presence of oxygen, should result in the production of ROS (superoxide anion radical or peroxide) (**Scheme 1B**)[3]. The redox cycling capability of plumbagin and its ability to form an electropolymerised film capable of generating ROS is considered.

9.3 Experimental Details

All reagents were of the highest grade available and used without further purification. Solutions of plumbagin (5 mM) were prepared in acetone. Stock glutathione and ascorbate solutions (typically 10 mM) were prepared in pH 7 BR buffer. Solutions of Ellman's reagent (1 mM) were prepared in pH 8 BR buffer. Electrochemical measurements were conducted using a μAutolab computer controlled potentiostat (Eco-Chemie, Utrecht, The Netherlands) using a three electrode configuration consisting of either a glassy carbon working electrode (3mm diameter, BAS Technicol, UK) or Platinum foil electrode (1cm^2). Platinum wire served as the counter electrode with a 3 M NaCl Ag | AgCl half cell reference electrode (BAS Technicol, UK) completing the cell assembly. The scan rate in all cases was 50 mV/s. Unless otherwise specified, all measurements were conducted at 22^oC ± 2^oC throughout. Electrochemical Quartz Crystal Microbalance (EQCM) measurements were obtained using a computer controlled Quartz Crystal Microbalance (Maxtek INC, USA) and polished 5 MHz Titanium / Gold crystals (Maxtek INC, USA).

9.4 Results and Discussion

Cyclic voltammograms detailing the response of plumbagin (0.8 mM, pH 7) at a glassy carbon electrode in the presence and absence of oxygen are detailed in **Figure 9.1**. Upon scanning towards negative potentials the quinone is reduced (-0.28 V) with the corresponding oxidation process observed at -0.03V. In the presence of oxygen, the magnitude of the reduction peak is significantly increased and can be attributed to the catalytic reduction of oxygen by the electro-reduced quinone (c.f. **Scheme 9.1B**). Confirmation of the latter was obtained by degassing the solution with nitrogen, here the peak height was found to be significantly decreased.

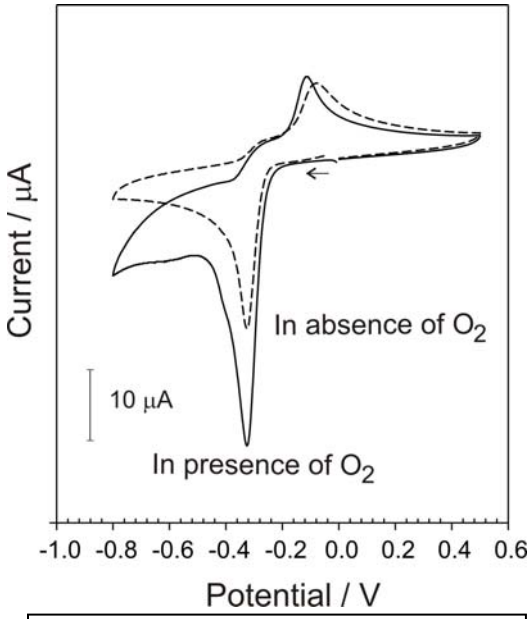

Figure 9.1. Cyclic voltammograms of Plumbagin (0.8 mM, pH 7) in the presence and absence of oxygen.

The system is clearly capable of catalysing the reduction of oxygen but its effectiveness as an interfacial ROS generator needed to be determined. A novel evaluation strategy was designed in which the interfacial concentration of an anti-oxidant probe would be used to estimate the production of ROS. Ascorbic acid served as our model probe. Its free-radical scavenging properties are well established and serves as one of the front line cellular defences against ROS and hence its relevance to the present investigation. It also possesses the key advantage of having a well defined redox signature which is sufficiently distinct from that of Plumbagin to allow its unambiguous quantification. It was our hypothesis that the ROS generated as a consequence of the electrochemically induced Plumbagin redox cycling would react with the AA (converting it to the electrochemically invisible de-hydroascorbate) and thereby leading to a visible decrease in AA concentrations. The advantage of this approach was that it would directly reflect the production of ROS at the electrode interface.

Five repetitive scan cyclic voltammograms detailing the response observed at a GCE to plumbagin (0.8 mM) and AA (0.4 mM) in pH7 buffer under nitrogen flow are highlighted in **Figure 9.2A**. Three distinct processes can be observed; the redox cycling of the quinone component of plumbagin (at -0.28V and -0.03V respectively) and the irreversible oxidation of the AA at +0.37V. The scans can be seen to be effectively stable but there is a gradual decrease in the magnitude of the AA. This can be attributed to the irreversible oxidation leading to a small but cumulative depletion of ascorbate at the electrode, the scan rate being too fast to allow complete diffusional replenishment of the interfacial concentration between cycles. The experiment was repeated in the presence of oxygen and the corresponding voltammograms detailed in **Figure 9.2B**. It can be seen that the magnitude of the quinone reduction peak process increases markedly while the AA peak diminishes much more rapidly than that observed under the degassed conditions. Given near identical conditions, bar the presence of oxygen, it is possible to draw the conclusion that the electrogeneration of ROS species at the interface results in the marked depletion of the AA probe.

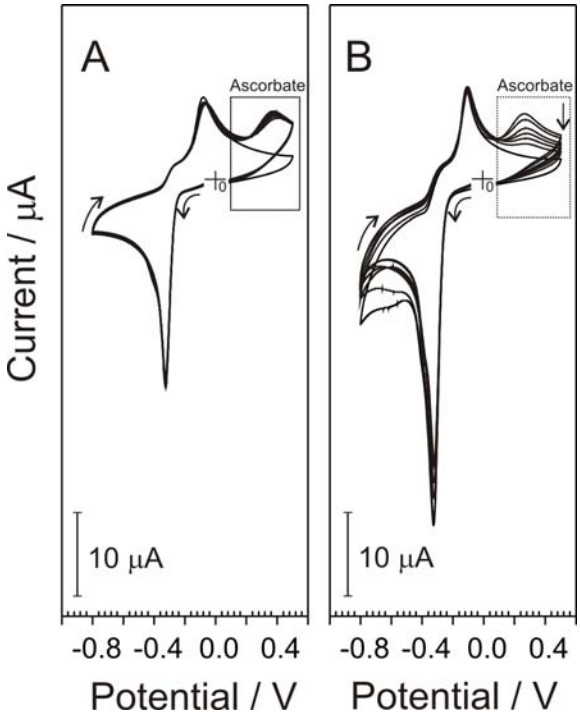

Figure 9.2. Cyclic voltammograms detailing the response of repetitive scanning on the influence of Plumbagin and Ascorbate (0.8 and 0.4 mM respectively) in the absence (A) and presence (B) of oxygen.

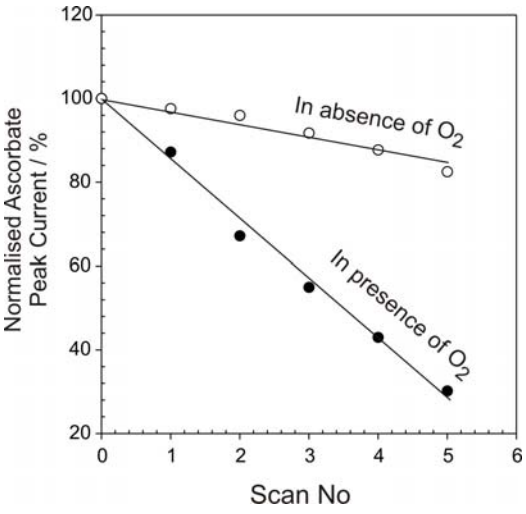

Figure 9.3. Ascorbate oxidation peak magnitude upon cycling in the presence of Plumbagin within oxygenated and nitrogen degassed solution

A more quantitative appraisal of the effect of repetitive cycle number on the removal of AA is shown in **Figure 9.3**. There is a depletion under degassed conditions but this can be ascribed to the diffusional artefact noted earlier and results in a 10% decrease over the experiment lifetime. In contrast, in the presence of oxygen the interfacial ascorbate is reduced by 70% and indicates clearly the efficacy of plumbagin redox cycling as a means of generating ROS.

Polymerisation of Plumbagin

Plumbagin film formation was attempted through the direct electro-oxidation of the 5-hydroxy functionality. It was anticipated that this would lead to polyphenylene oxide film formation consistent with conventional phenolic electro-oxidation [11,12]. Cyclic voltammograms detailing the response at a glassy carbon electrode are shown in **Figure 9.4**. The irreversible oxidation of the phenol was observed at +0.95 V and was found to decrease on successive scanning which is again consistent with formation of a phenol film. The profile of the quinone component changed markedly with scan number. On the first scan – prior to phenol oxidation - the reduction and oxidation processes are consistent with the standard

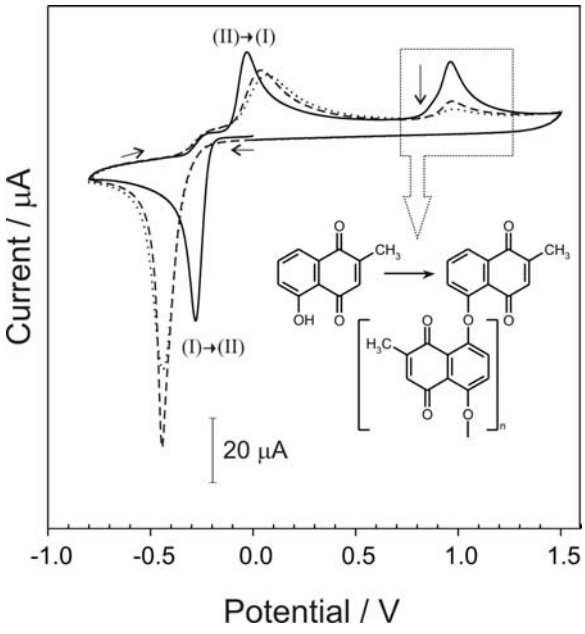

Figure 9.4. Repetitive scan cyclic voltammograms detailing the electropolymerisation of Plumbagin (0.8 mM, pH 7) at a glassy carbon electrode.

solution based monomer. After oxidation of the phenol had occurred the subsequent scans show a shift in the quinone reduction peak to more negative potentials, along with an increase in the magnitude and the sharpness of this peak. This can be rationalised on the basis of the formation of a surface immobilised redox species – consistent with the main aim.

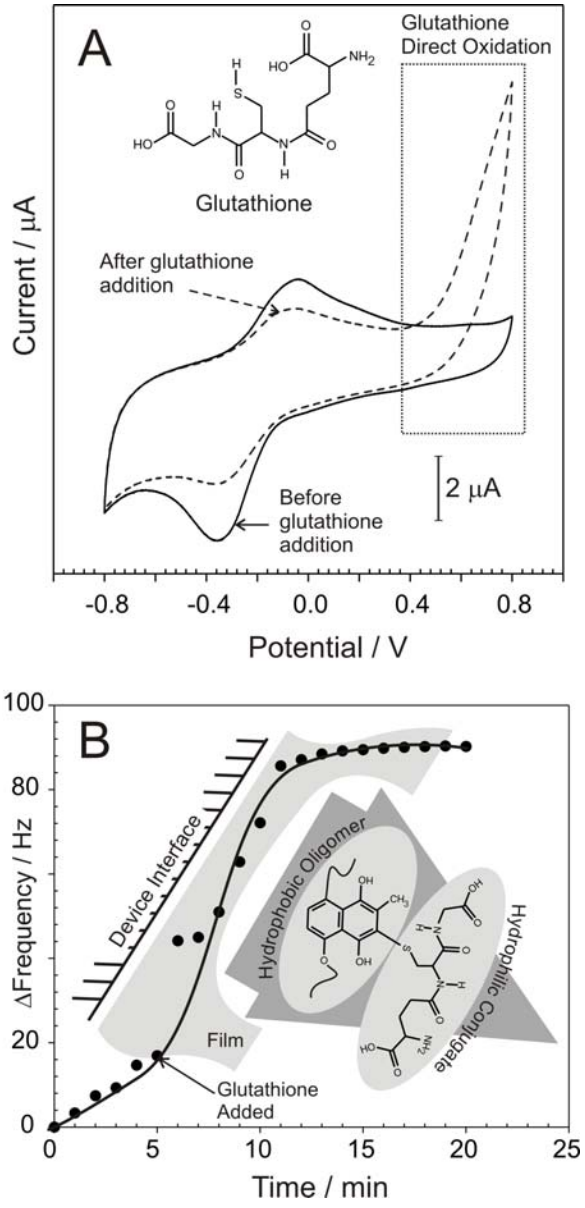

Figure 9.5. (**A**) Cyclic voltammograms detailing the response of a Plumbagin modified glassy carbon electrode towards glutathione (0.3 mM additions). (**B**) EQCM response of a Au-Plumbagin modified electrode before and after the addition of glutathione (0.385 mM).

Removal of the modified electrode and placement within fresh buffer – devoid of Plumbagin monomer – revealed that the activity of the quinone component was retained at the electrode surface. Cyclic voltammograms detailing the electrode response are shown in **Figure 9.5A**. The shape of the redox processes are broad and stand in contrast to the sharp processes observed in the initial polymerisation stages (**Figure 9.4**). This may reflect a more heterogeneous population of different redox species. The magnitude of the peak processes was found to be markedly smaller than expected and this is ascribed to formation and subsequent loss of oligomeric material during polymerisation and transfer. Thus, while sharp surface redox process were observed in **Figure 9.4** – these are now more likely to reflect particulate/oligomeric structure which are only loosely adhered to the electrode surface. The significance of the latter was corroborated through conducting EQCM studies (**Figure 9.5B**). The polymerisation process was repeated using a gold

patterned crystal (deposited from 10 mM Plumbagin dissolved in ethylacetate containing 0.05M tetrabutylammonium perchlorate as supporting electrolyte, 50 scans). Upon removing the crystal and placing in fresh pH 7 buffer devoid of the monomer, it can be seen that there is a gradual loss of material from the electrode surface (expressed as ΔFreq, 0-5 min) ascribed to the oligomers slowly diffusing into the solution. An interesting observation was found when glutathione (385 μM) was added to the solution. The latter is known to react with naphthoquinone to form water soluble conjugates (indicated in the inset schematic within **Figure 9.5B**) [13,14] and a similar effect was found in this instance with a dramatic increase in the rate of oligomer removal before attaining a stable plateau. This is again corroborated in **Figure 9.5A** where the polymer formed at the glassy carbon electrode is shown to degrade in the presence of glutathione (330 μM, pH 7). There is however an underlying layer of insoluble polymer. However, as the redox processes attributed to the poly-plumbagin are not removed completely, the reduction in the population of the poly-plumbagin will inevitably compromise the effectiveness the films ability to generate ROS.

Cyclic voltammograms detailing the response of the plumbagin modified GCE in buffer solution in the presence and absence of oxygen are detailed in **Figure 9.6**. The magnitude of the quinone reduction peak is significantly larger in the scan carried out in oxygen than what it is in the absence of oxygen. This data is consistent with the electrochemistry seen for the monomer solution highlighting that the quinone component of the molecule is retained and is accessible within the film enabling it to catalyse the reduction of oxygen. ROS are known to react with glutathione causing a decrease in there concentration. The poly-Plumbagin films ability to produce ROS was examined further with a spectrophotometric technique using

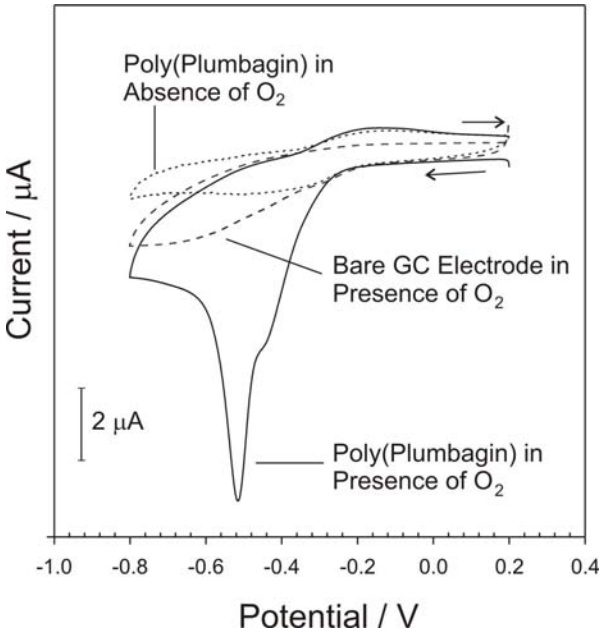

Figure 9.6. Cyclic Voltammograms detailing the response of a glassy carbon electrode in the presence of oxygen and a plumbagin modified glassy carbon electrode in the presence and absence of oxygen. Scan rate: 50 mV/s.

Ellman's reagent to monitor the changes in glutathione concentration due to the presence of the ROS produced by the film. The modified electrodes were placed into a solution containing glutathione (167μM) and held at a reduction potential (-1.2V) for 5 and 10 minutes. An aliquot of the electrolysis solution was reacted with a solution of Ellman's reagent allowing the glutathione concentration to be determined spectrophotometrically via a calibration graph. The glutathione concentration was seen to decrease by 56.9% and 88.9% respectively compared to the no change in concentration for the control solution (modified electrode placed in glutathione solution for 10 minutes with no reduction potential applied) this confirms that the poly-plumbagin film is able to catalyse the production of ROS.

A number of preliminary experiments were conducted to assess the ability of the poly(plumbagin) film to generate sufficient quantities of ROS that would provide a bactericidal action. The film was deposited onto a carbon mesh similar to that investigated in previous chapters. *Ps. aeruginosa* and *S. aureus* were used as a model bacterial species due to their importance in the wound environment and the key feature of producing biofilms. The modified electrodes were saturated in an overnight culture (grown in a conventional nutrient broth) of each test organism and incubated at 37°C. The electrode potential was held at -1V to reduce oxygen and thereby generate the ROS. The electrode was maintained at this potential for 120 minutes after which the bacteria were stained with the BacLight™ LIVE/DEAD® fluorescent stain system used into differentiate dead from live cells. While there were some evidence of dead cell the majority of the exposed culture were largely unaffected. While the film is clearly capable of generating ROS that deplete normal extracellular anti-oxidants, the penetration of the bacteria and subsequent bactericidal action appear inefficient. There could be three factors that account for this. The first being that the film is too thin and not enough ROS are being produced, second the plumbagin itself may not be an efficient producer of ROS and third the nature of ROS being generated is ineffective against the target bacteria. A more generic approach to the formation of the films was taken in an effort to counter the first two issues. In addition, the reaction products resulting from the reduction of oxygen was undertaken with a view to establishing the identity of the principal ROS species.

There is a potentially huge array of quinones that could be used to catalyse the reduction of oxygen but very few are capable of being directly immobilised onto an electrode. The possession of the phenolic functional group allowed an easy route to the polymerisation of the monomer but this grouping is fairly unusual in the majority of quinoid structures that are available through either commercial routes or from the purification of natural products. The availability of the labile proton at the 2 position is much more common and imparts the characteristic susceptibility of quinone to nucleophilic attack. The latter was exploited as the basis of a simple *in situ* immobilisation procedure. The aim was to generate a film containing sulphydryl functional groups which would subsequently acts as hook through which to anchor the quinone of choice. This would open up the vast number of potential analogues. The basic strategy is highlighted in **Scheme 9.2A.**

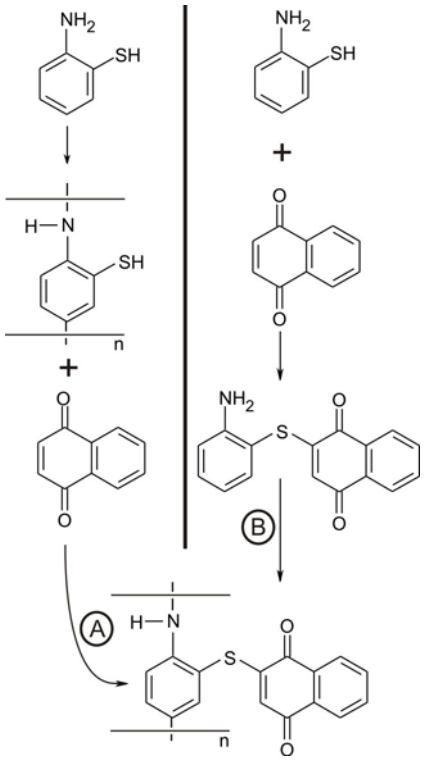

Scheme 9.2

Mercaptoaniline was selected on the basis that the monomer would follow as polymerisation path similar to conventional polyaniline systems. It was envisaged that this would contrast the phenol films in that the former is capable of electrochemically promoted growth and thus could result in a thicker film – thereby ultimately increasing the number of quinones sites. Naphthoquinone was used as the model system through which to produce the modified film. There were a number of issues with this approach – the main problem being the failure to generate a coherent base film. While it was possible to observe the oxidation of the monomer – there was no indication of any significant deposition – either voltammetrically or through observing mass change on a quartz crystal. It was thought that as the monomer is oxidised to the radical cation that the sulphydryl group acts as a scavenger resulting in the inhibition of the polymerisation process and the formation of the corresponding disulphide (R-S-S-R). It was also possible that the high oxidation potentials required to oxidise the amino

functionality on mercaptoaniline would have led to simultaneous oxidation of the sulphur group.

An alternative approach was then taken in which the quinone was reacted with the mercaptoaniline prior to electropolymerisation as indicated in **Scheme 9.2B**. The rationale behind this strategy was that the reaction would tie up the sulphur moiety thereby avoiding the self inhibition witnessed with the previous attempts to polymerise the unattached monomer. The addition of naphthoquinone to the solution containing mercaptoaniline was found to change colour (from straw to bright red) and is consistent with the formation of the corresponding quinone-thiol conjugate.

The imposition of an oxidising potential for 30 minutes at +1.2V led to the cumulative deposition of the polymer. This was confirmed through examining the frequency response of a quartz crystal microbalance in an equimolar solution (2mM) of mercaptoaniline / naphthoquinone buffered at pH 7. The response is detailed in Figure 9.7 where the decrease in frequency is associated with an increase in the weight of material deposited at the crystal. Removing the applied potential immediately terminates the polymerisation process and is again corroborated by the fact that there is no further change in the frequency.

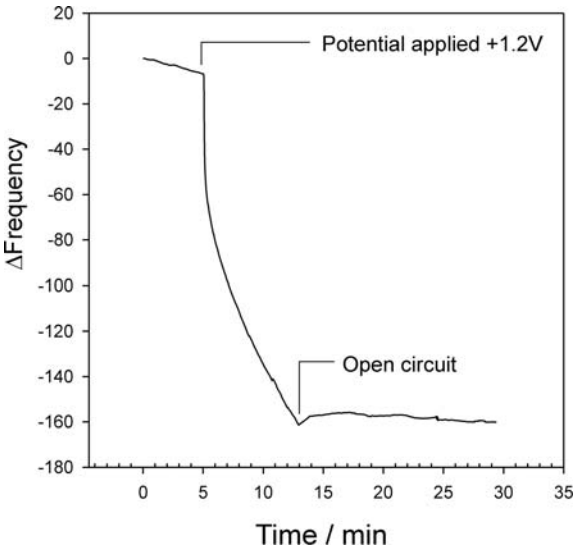

Figure 9.7. Response obtained at an EQCM crystal in the presence of mercaptoaniline and naphthoquinone.

Cyclic voltammograms detailing the response of the polymer deposited on a glassy carbon electrode and removed to a solution containing fresh pH 7 buffer are shown in Figure 9.8. In contrast to the plumbagin polymer, the redox transition of the quinone pendant groups are much broader. The voltammetric profiles of the polymer formatted in the presence of the naphthoqionine and the response to the mercaptoaniline after an analogous polymerisation procedure followed by exposure to the naphthoquione are compared in **Figure 9.8**. There is no electroactivity associated with the latter. It is clear that the sulphur functionality must be tied up before polymerisation.

The response to different scan rates was then assessed in the case of the pre-conjugated monomer. Cyclic voltammograms detailing the response are shown in **Figure 9.9** and highlight the fact that the magnitude of the peak processes vary in direct proportion to the scan rate and thus consistent with an immobilised species.

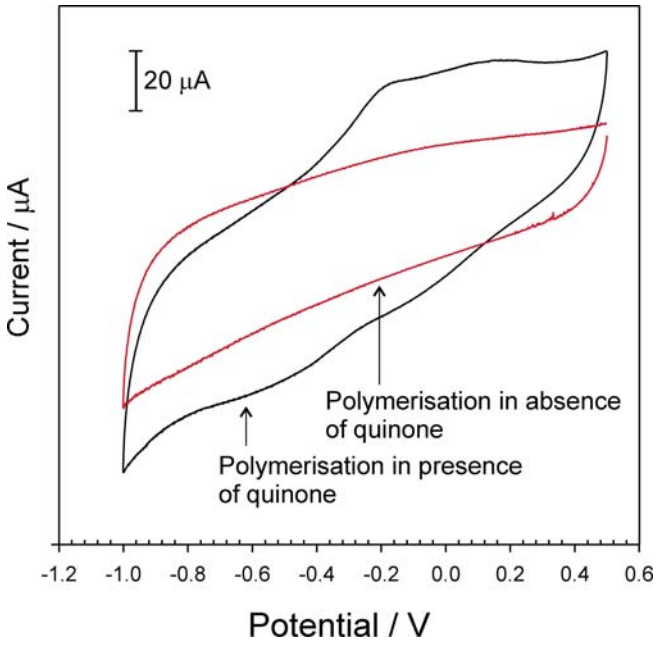

Figure 9.8. Cyclic voltammograms detailing the response of a glassy carbon electrode modified with the mercaptoaniline after being polymerised in the presence and absence of naphthoquinone. Solutions were degassed with nitrogen prior to measurement. Scan rate: 50 mV/s.

The main question to be answered however was whether or not the modified polymer would still be capable of catalysing the reduction of oxygen to produce ROS species. Cyclic voltammograms recorded at the polymer modified glassy carbon electrode in the presence and absence of oxygen are detailed in **Figure 9.10**. It can be seen that in the presence of oxygen, the reduction process is greatly enhanced in accordance with the electrocatalytic EC' mechanism. It is clear that the film is capable of reducing oxygen and would appear to provide a much greater response in terms of peak magnitude than that observed at the plumbagin modified electrode. The strategy highlighted in Scheme 9.2B

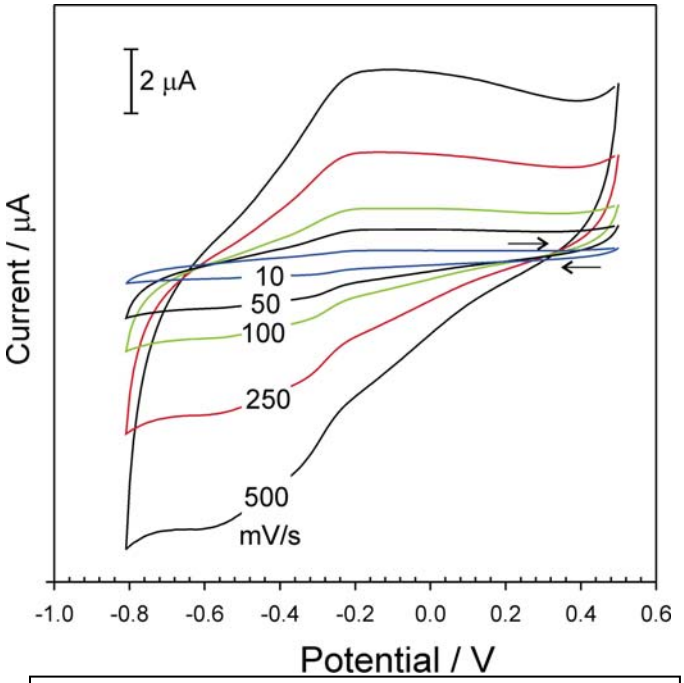

Figure 9.9. Cyclic voltammograms detailing the response of a glassy carbon electrode modified with the meracptoaniline-naphthoquinone film at various scan rates. Solution was degassed with nitrogen prior to measurement.

appears to offer a more generic approach as it is easy to conceive replacing the naphthoquinone with another quinone species. The main requirement being the possession of a C-H site at either the 2 or 3 position on the quinone moiety. The first two issues noted earlier have been addressed. Identification of nature of the ROS being produced was the last factor to be investigated. It is likely that upon the reduction oxygen to the superoxide anion ($O_2^{\cdot-}$) that it would dismutate to O_2^{2-} and thus produce peroxide. Evidence for the latter was required and therefore an assay was developed to test for the presence of electrogenerated peroxide.

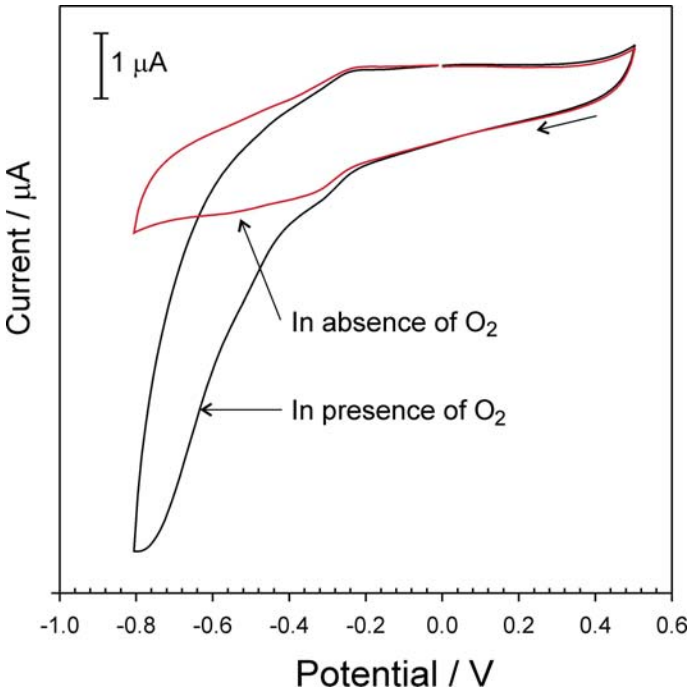

Figure 9.10. Cyclic voltammograms detailing the response of a mercaptoaniline-naphthoquinone modified glassy carbon electrode in the presence and absence of oxygen. Scan rate: 50 mV/s.

The basic approach revolved around the colorimetric response of an iron thiocyanate solution. In acidic solution, hydrogen peroxide in the sample oxidises ferrous ion (Fe^{2+}) to the ferric ion (Fe^{3+}). This reacts with ammonium thiocyanate to displace the ammonium ion to form the coloured ferric thiocyanate marker. This allows spectroscopic quantification (λmax 445nm). The reagent was prepared from ferrous ammonium sulfate (0.5%), sulfuric acid (0.5%), methanol (1.0%), ammonium thiocyanate (3.0%), glacial acetic acid (5.0%), deionised water (90.0%). The assay procedure was optimized to yield and assay protocol of Reagent to Sample of 1:50. This was mixed for 5 minutes prior to analysis.

Hydrogen peroxide calibration standards were prepared and ranged from 0.1 to 10ppm (prepared from 35% H_2O_2 solution in deionized water) and the subsequent spectra are

detailed in Figure 9.11. A non linear increase in the peak height was observed as indicated in the corresponding calibration graph detailed in **Figure 9.12**.

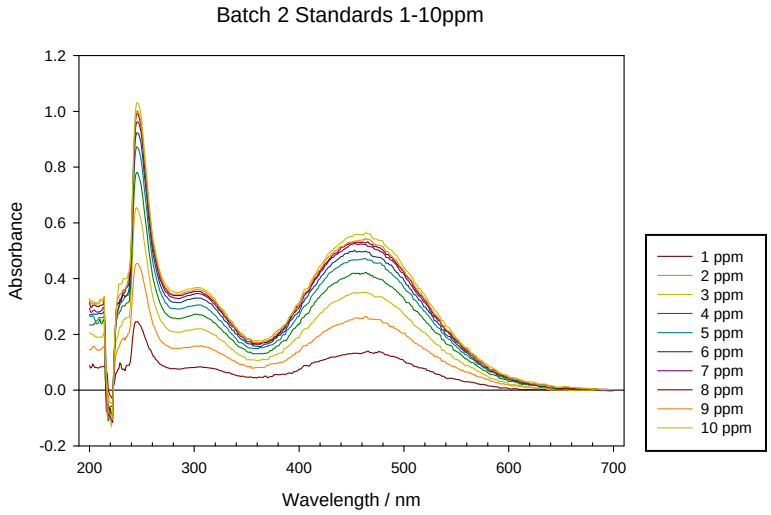

Figure 9.11. Spectra detailing the response of the ferrous-thiocyanate assy towards increasing concentration of peroxide.

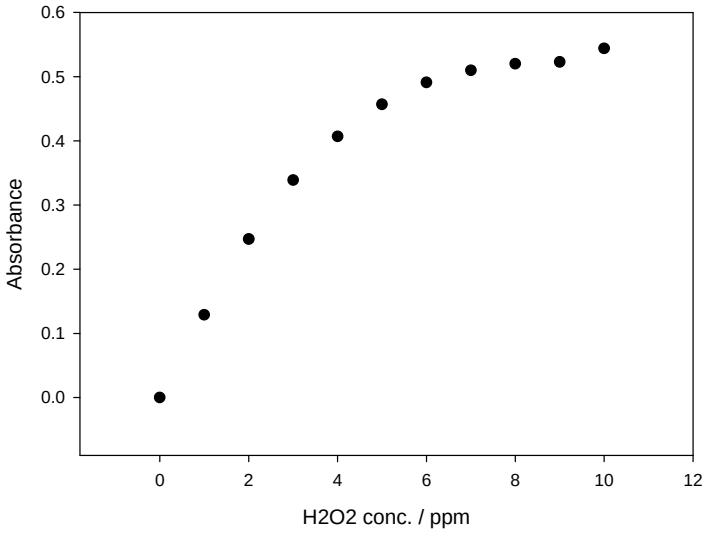

Figure 9.12. Calibration data detailing the response of the ferrous-thiocyanate assy towards increasing concentration of peroxide (λmax 445nm).

Inspection of the data reveals that there is a linear component to the graph observed at low (<2ppm) peroxide. The calibration run was repeated with a concentration from 0.1 to 1 ppm peroxide and the corresponding spectra and calibration data are detailed in **Figures 9.13A** and **9.13B** respectively.

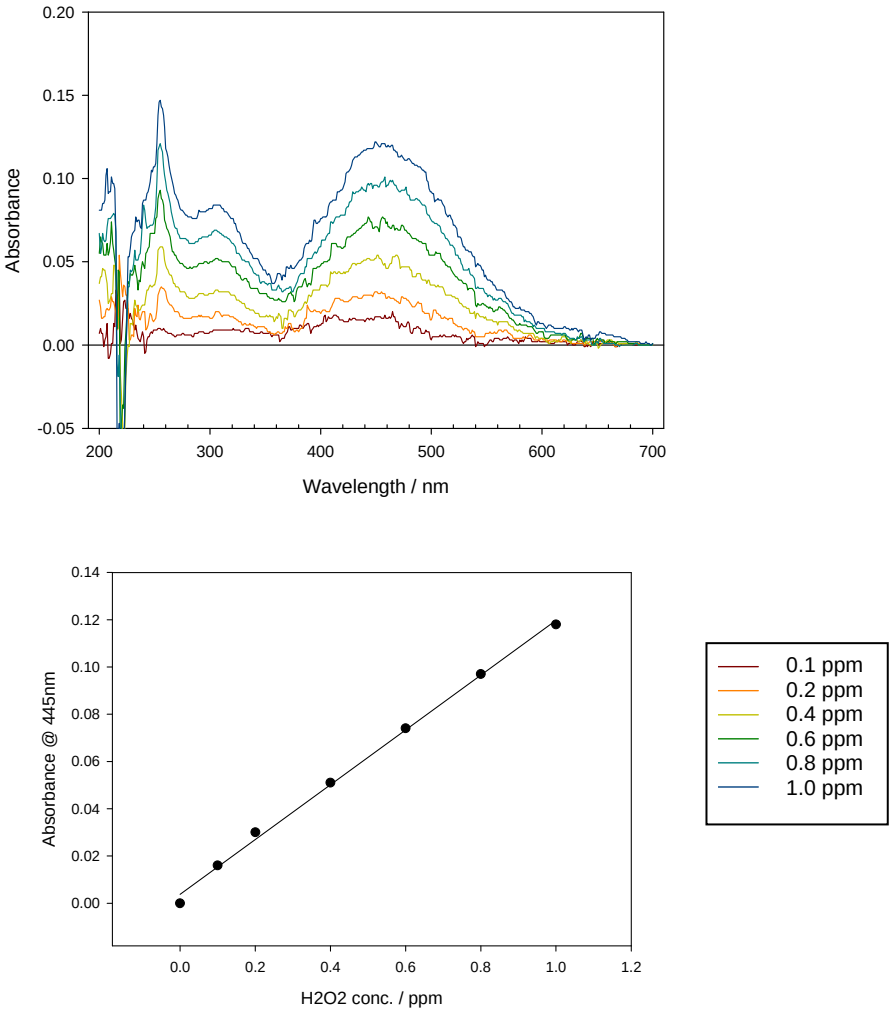

Figure 9.13. A) spectra detailing the response of the Fe^{2+}/SCN^- assay to peroxide. B) Corresponding calibration data (λmax 445nm).

In order to confirm the generic nature of the polymerisation process, the naphthoquinone was substituted with plumbagin. Plumbagin possess a methyl group at the 3 position and it may be possible to postulate that this might cause a degree of steric problems with regard to coupling with the thiol functionalities. In practice it has already

been observed that plumbagin will readily react through nucleophilic attack by thiols at the 3 position and hence should readily react with the mercaptoaniline. The addition of these two components led to a colour change analogous to that observed with the simpler naphthoquinone system and thus appeared to confirm the first step in the reaction was successful.

The conjugated monomer was electropolymerised on a large surface area carbon fibre matting using the same conditions as those mentioned previously. The modified electrode was removed, rinsed and placed a micro cuvette cell (total volume 1mL). The analysis solution consisted of 0.05M KCl. It was necessary to avoid the presence of complexing agents as phosphate was found to interfere with the assay through precipitating the iron reagent. The electrode was then held at -1V for 10 minutes in the presence of air. An aliquot was then removed and assayed as before. The process was then repeated using a plain, unmodified electrode as the control in order to assess the effectiveness of the new poly(plumbagin) system. The corresponding spectra are compared in **Figure 9.14**.

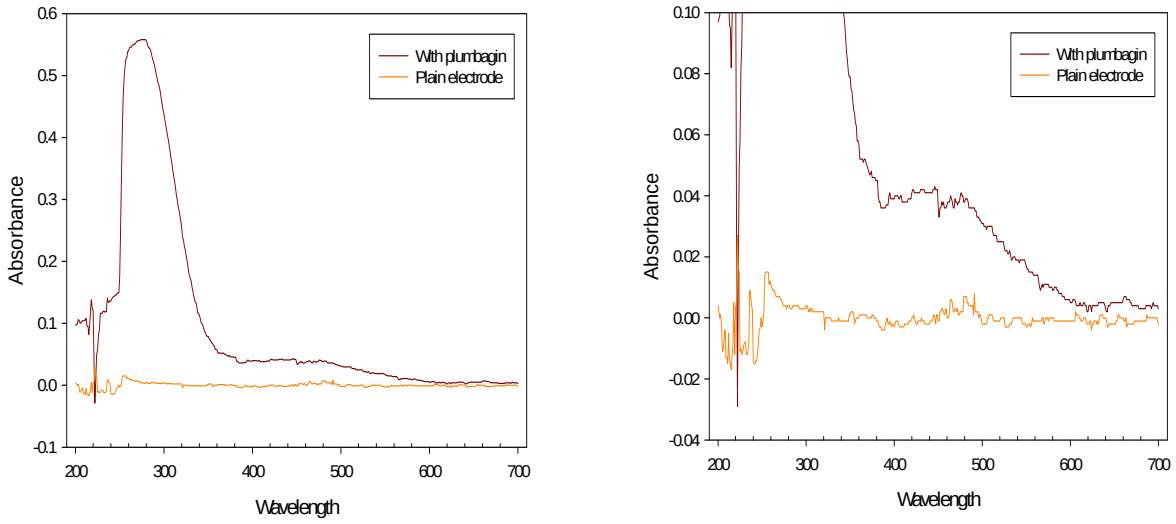

Figure 9.14. Spectra comparing the capacity of plumbagin modified and plain electrodes to generate peroxide – as measured by the Fe^{2+}/SCN^- assay

It can be seen that the modified plumbagin greatly enhances the reduction of oxygen and results in the production of peroxide. The response of the unmodified electrode under similar conditions yields essentially no peroxide. After 10 minutes the concentration of peroxide within the cell was found to increase to 0.33 ppm in the bulk solution. Given that the peroxide is generated at the electrode interface, the equivalent concentration of peroxide at the interface to a 100μm diffusion depth is 11ppm, 1.1ppm per minute. The electropolymerisation protocol proposed is clearly generic as evidenced by the ability to put different quinones onto the electrode. It is also of major benefit when considering the production of ROS. The production of peroxide is not the most severe of ROS but its production is significant and it could be enhanced through increasing the thickness of the film. There is also a possibility of using iron nanoparticles or complexes immobilised either at the electrode surface or within the film to generate Fenton effects whereby the peroxide is converted to OH radicals which are a much more potent ROS. This aspect is however beyond the scope of the present project but the work provided so far lays the foundation for a number of follow up investigations.

9.5 Conclusions

The ability of Plumbagin monomers and polymers to generate ROS at the electrode interface has been demonstrated and although the polymer is limited in terms of film thickness it has the potential to be used as a smart material in devices opening up a new avenue for exploration and adaptation. A generic polymerisation protocol has been developed and the identity of the electrogenerated ROS identified. The efficacy of exploiting the immobilised catalytic systems has also been highlighted and shown to be vital when considering the use of oxygen reduction as the source of the ROS.

9.6 References:

1. J.C. Tilak, S. Adhikari, T.P.A. Devasagayam, Redox Report, 9 (2004) 219
2. S. Sowmyalakshmi, M. Nur-e-Alam, M.A.Akbarsha, S.Thirugnanam, J. Rohr, D. Chendil, Planta, 220, (2005) 910
3. V. SivaKumar, R. Prakash, M.R. Murali,H. Devaraj, S.N. Devaraj, Drug and Chemical Toxicology, 28 (2005) 499
4. Y.L. Hsu, C.Y. Cho, P.L. Kuo, Y.T. Huang, C.C. Lin, Journal Pharmacology and Experimental Therapeutics, 318 (2006) 484
5. L.C. Lin, L.L. Yang, C.J. Chou, Phytochemistry, 62 (2003) 619
6. B.S. Park, H.K. Lee,S.E. Lee, X.L. Piao, G.R. Takeoka, R.Y. Wong, RY; Y.J. Ahn, Journal of Ethnopharmacology, 105 (2005) 255
7. J.W. Chen, C.M. Sun,W.L. Sheng, Y.C. Wang, W.J.Syu, Journal of Bacteriology, 188 (2006) 456
8. J.S. Mossa, F.S. El-Feraly, I Muhammad, Phytotherapy Research, 18 (2004) 934
9. Y.C. Wang, T.L. Huang, Journal of Chromatography A, 1094 (2005) 99
10. J.Q.Gu, T.N. Graf, D.H. Lee, H.B. Chai, Q.W. Mi, L.B.S. Kardono, F.M. Setyowati, R. Ismail, S. Riswan, N.R. Farnsworth, G.A. Cordell, J.M. Pezzuto,S.M. Swanson, D.J. Kroll,J.O. Falkinham, M.E. Wall, M.C. Wani, A.D. Kinghorn, N.H. Oberlies, Journal of Natural Products, 67 (2004) 1156
11. K.A. Marx, T.A. Zhou, D. McIntosh, S.J. Braunhut, Analytical Biochemistry, 384 (2009) 86
12. M. Ferreira, H. Varela, R.M. Torresi, G. Tremiliosi, Electrochimica Acta, 52 (2006) 434
13. I.A. Solsona, R.B. Smith, C. Livingstone, J. Davis, Journal of Colloid and Interface Science, 302 (2006) 698
14. R.B. Smith, C. Canton, N.S. Lawrence, C. Livingstone, J. Davis, New Journal of Chemistry, 30 (2006) 1718

Chapter 10

Conclusions

The ever-present risk of HAI, especially to major wounds, is a significant problem in modern healthcare. While some of these infections may be preventable by more stringent guidelines and the imposition of hygiene protocols, the presence of opportunistic pathogens in the normal flora can facilitate the infection of compromised patients. The development of new, rapid PoCT diagnostics is needed to allow the early detection of the non-preventable infection of wounds. In order to allow the development of a multiplexed sensor array that can offer indication of generic infections and those specific to key organisms, a variety of *in situ* sensors are required. The development of sensors suitable for incorporation and operation directly within a wound dressing is the most advantageous approach as this would reduce the need for wound re-dressing. The latter is problematic in that it both disturbs wound healing and offers an extra route to contamination.

Whereas previous research has focussed on the detection and identification of the bacteria themselves, the general presence of colonising bacteria can initiate an infection and have immediate effects on the local wound environment. The incursion of a wound infection is known to have many local effects, including those on physiological pathways and alter the local expression/concentrations of acute phase inflammatory proteins (e.g. C-reactive protein) and the levels of cytokines. The ability to simply detect the presence of the bacteria or their effects on the wound has been the primary focus of this research. The chemical transformations within the wound exudates can provide important diagnostic information which can be sufficient to assess wound condition without having

to implement the time consuming process of identification. In order to allow the development of sensor assemblies that are both small enough to be integrated seamlessly within a dressing and that are cost-effective enough to enable widespread use is a considerable challenge but the developments presented within go some way to addressing the core issues.

A variety of carbon based substrates, the majority of which could be suitable for transfer to a disposable format, have been developed and their applicability assessed throughout this project. A preliminary study of endogenous molecules of interest has been completed and serves as a functional library that categorises their various electrochemical properties. These served as the basis of subsequent experiments in which the central theme was to exploit endogenous biomarkers rather than introduce synthetic reagents and, as such, toxicological issues could be deftly avoided. Tryptophan and urate were selected for the investigation and while these have been extensively studied in the literature, a series of wholly novel sensing strategies have been developed and their potential exploitation critically evaluated.

A generic marker of both infection and of wound healing progression is the measurement of pH. The problems of size, cost and biocompatibility limit the use conventional pH sensing technologies. It was demonstrated that polymeric tryptophan species which are pH responsive can be formed on the surface of carbon electrodes from the reservoir of endogenous amino acid. The resulting film gives rise to a novel redox couple that is notably distinct from the other species present in typical biofluids and thereby gives rise to an unambiguous signal. The use of a voltammetric detection methodology represents a novel direction and contrasts the potentiometric approaches almost invariably encountered in pH measurements. In this case the acid:base properties of this polymeric deposit was exploited whereby altering the pH results in a predictable and measurable shift in the potential required to reduce the oxidised form of the polymer. A linear relationship was observed across a wide range of pHs (pH 4-10). The system was found to function even in instances where there is a very low concentration of tryptophan.

Importantly, this work formed the foundation of a wholly novel strategy of exploiting endogenous biological material to act as a molecular pH probes due to their

inherent pH dependent redox properties. The use of urate as an endogenous pH probe was also investigated and found to serve as an alternative and versatile probe due to its presence in high concentrations within biofluids. It was envisaged that this would provide a more sensitive indicator. Carbon fibre electrodes were developed allowing both the linear detection of urate in biofluids and the determination of pH. The underlying process was similar to that of the tryptophan but the exception of avoiding the need for the pre-conditioning – polymerisation step. The resulting by-product of the urate oxidation is allantoin which is a physiologically benign molecule and thus presents no toxicological issues. The applicability for this new pH sensing methodology were assessed in simulated wound fluid during colonisation by key bacteria and was shown to follow the trend in pH peak shift when compared with a conventional pH probe.

Many bacterial species, including those relevant to wound infections, can metabolise urate rapidly through the expression of the uricase enzyme. The production of uricase in a wound environment was assessed as it was envisaged that this would incur the rapid degradation of the urate within the wound environment. As such it could serve as an alternative approach to urate sensing technology whereby the rapid degradation of urate may indicate colonisation by a certain group of uricase expressing organisms. A number of prototype sensors were developed to provide quantitative evaluation of urate concentrations within biofluid over prolonged sensing times. It was found that bacterial colonisation will exhaustively metabolise urate, but only when in a limited (nutritionally minimal) environment. However, subsequent studies revealed that when the same bacteria were grown in a complex simulated wound fluid, alternative nitrogen sources are utilised preferentially leaving the urate essentially untouched. This prevents the use of the urate sensor for bacterial identification but it does however strengthen the viability of the urate as a pH sensor as it demonstrates that endogenous urate will be unaffected by normal biophysiological or bacterial processes within the wound.

An alternative strategy was investigated to allow the identification and quantification of specific bacterial species and centred on the measurement of a release of bacterial metabolite – pyocyanin. Infections caused by *Ps. aeruginosa* are widespread and problematic and therefore was the target for the development of a very sensitive, accurate and precise sensor for the detection of pyocyanin. This compound is a virulence

factor released during colonisation by the organism. Carbon fibre was again used as a sensing substrate due to its flexibility and cost-effective nature as well as the more important feature of its sensitivity towards pyocyanin. The technology was further extended and an additional application for use within sputa for the detection of chronic lung infection in cystic fibrosis patients was identified and suggested as a future avenue of investigation where it could be invaluable in community point of care testing devices.

In order to ensure reliability during medium to longer term monitoring scenarios, especially of the quantitative pyocyanin sensing, the final part of the project focused on the development of antimicrobial coatings, to prevent biofouling / biofilm formation on the electrode sensing window. The most studied conventional approach to antibacterial materials is the slow release of silver ions into the local environment. While this is a useful principle, the inherent adaptability of pathogenic organisms and the protective exopolysaccharide of even very early stage biofilms meant alternative routes were sought. The generation of ROS has proven antimicrobial properties through a variety of cellular interactions. It was anticipated that the localised generation of ROS may be ideal due to the very powerful oxidative effects, but the very limited half-life of the radical species affecting only very close targets, principally bacteria at the sensor interface which are liable to initiate biofilm formation. A substantial literature review revealed that the most studied route of ROS generation is the photogeneration of singlet oxygen, by photosensitizing species. The immobilisation of photosensitizers may be possible on the electrode surface, but implementation would require photoactivation through clear dressings or the introduction of fibre optics. Neither approach was found to be applicable to a disposable wound dressing and would increase costs associated with the material, instrumentation and expertise required to operate and maintain the devices. A new approach through coating the electrodes with an immobilised polymeric coating to enhance the electrochemical reduction of oxygen to superoxide anion and subsequently to peroxide was found to be a more viable route. The general principles required to form the film were investigated a new approach developed that allows the speedy production of custom films optimised. The ability of the films to produce ROS on demand was demonstrated and the identity of the ROS confirmed through spectroelectrochemical assays. The ability of the resulting ROS to provide a localised oxidative action was also

studied and the depletion of anti-oxidants commonly employed as cellular defences was found to be rapid. Further work is needed to enhance these sufficiently to allow an antimicrobial effect but the initial studies clearly lay the foundations for a new approach to the protection of remote / implantable sensing.

In conclusion, new sensor technologies have been developed that may allow both generic and species specific detection of infection, with a possibility of monitoring healing progression through the use of small, carbon-based electrochemical sensors. Smart, controllable coating technologies have been developed and have been successfully applied to prevent macromolecular fouling and a tentative demonstration of oxidative power through the local production of reactive oxygen species. Subsequent work which may follow on from these developments includes the clinical testing of the sensors assemblies for a final assessment of their clinical applicability and the enhancement of radical generation to allow long-term monitoring.

Appendix 1

Publications

Carbon Fibre Composites: Integrated Electrochemical Sensors for Wound Management
Duncan Sharp, Stephen Forsythe, James Davis. *The Journal of Biochemistry* 144, 87-93 (2008)

Integrated Urate Sensors for Detecting Wound Infection
Duncan Sharp, James Davis.
Electrochemistry Communications 10, 709-713 (2008)

Laser Anodised Carbon Fibre – Coupled Activation and Patterning of Sensor Substrates.
Henry Bukola Ezekiel, **Duncan Sharp**, Maria Marti Villalba, James Davis.
The Journal of Chemistry and Physics of Solids 69, 2932-2935 (2008)

Electrochemical Detection of Singlet Oxygen
Duncan Sharp, James Davis.
Electroanalysis 2009 *in press*

Approaching Intelligent Wound Management: Carbon Fibre Sensor for Pyocyanin Detection
Duncan Sharp, Patience Gladstone, Robert Smith, Stephen Forsythe, James Davis.
Bioelectroanalysis 2009 *in press*

Plumbagin: A Natural Product for Smart Materials
Laura A.A. Newton, Emma Cowham, **Duncan Sharp**, Ray Leslie and James Davis
New Journal of Chemistry – in press

Appendix 2

Conference contributions

Oral Presentations:

14th Biodetection Technologies conference (2009), Baltimore, USA,
‘Intelligent Wound Management: In-situ Sensors to Detect Infection’

Robin Hood Interdisciplinary Network for Electrochemistry (RHINE) (2009), Hull, UK
‘Towards smart bandages: Carbon Fibre Sensor for Electrochemical Pyocyanin Detection’

Nottingham Trent University, Science and Technology Conference (2009).
‘Towards Smart Bandages’

Selected Posters:

Robin Hood Interdisciplinary Network for Electrochemistry (RHINE) 2009, Hull, UK.
‘Biofilm resistant coatings for smart implants’

Biosensors 2008, Shanghai, China
‘Integrated Urate sensors for detecting wound infection’

EuroAnalysis XIV (2007), Antwerp, Belgium.
‘Carbon Fibre Composites: Integrated electrochemical sensors for wound management’